www.csiro.au

Overview of aquitard and geological fault simulation approaches in regional scale assessments of coal seam gas extraction impacts

Chris Turnadge, Dirk Mallants and Luk Peeters

CSIRO Land and Water

This report was commissioned by the Department of the Environment and Energy and was prepared by CSIRO.

2018

Citation

This report should be cited as:

Turnadge C, Mallants D and Peeters L (2018) Overview of aquitard and geological fault simulation approaches in regional scale assessments of coal seam gas extraction impacts, prepared by the Commonwealth Scientific and Industrial Research Organisation (CSIRO), Canberra.

Table of Contents

Figures

Tables

Abbreviations

Abbreviation	Description
API	American Petroleum Institute
AEM	Airborne ElectroMagnetic (survey)
APLNG	Australia Pacific Liquefied Natural Gas (project)
BME	Bayesian Maximum Entropy
CMA	Cumulative Management Authority (Queensland)
CoA	Commonwealth of Australia
CSG	Coal Seam Gas
CSIRO	Commonwealth Scientific and Industrial Research Organisation (Australia)
DFN	Discrete Fracture Network
DNRM	Department of Natural Resources and Mines (Queensland)
EIS	Environmental Impact Statement
FEFLOW	Finite Element groundwater FLOW (model)
GEM	Generalised Equation of state Model
GRACE	Gravity Recovery And Climate Experiment (satellites)
HSU	HydroStratigraphic Unit
MC	Monte Carlo (sampling methodology)
mD	milliDarcy
MODFLOW	MODular groundwater FLOW model
MPA	MegaPAscals
MPS	Multiple Point Statistics
µD	microDarcy
NSW	New South Wales
OGIA	Office of Groundwater Impact Assessment (Queensland)
PDF	Probability Density Function
QCLNG	Queensland Curtis Liquefied Natural Gas (project)
QGC	Queensland Gas Company
Qld	Queensland
QWC	Queensland Water Commission
SMOS	Soil Moisture and Ocean Salinity (satellite mission)
SWS	Schlumberger Water Services
US EPA	United States Environmental Protection Agency
USG	UnStructured Grid

Glossary

Term	Description
Aleatory uncertainty	Uncertainty characterised by inherent randomness or stochasticity of a system that cannot be reduced by further data collection
Anisotropy	A term used to describe the directional dependence of given properties; for example, the hydraulic properties of an aquifer (as opposed to isotropy, which denotes identical properties in all directions)
Aquifer	Rock or sediment in a formation, group of formations or part of a formation, which is saturated and sufficiently permeable to transmit quantities of water to wells and springs
Aquitard	A saturated geological unit that is less permeable than an aquifer and incapable of transmitting useful quantities of water. Aquitards often form a confining layer over aquifers
Auto-covariance	Function that gives the covariance of the process with itself at two points in space
Bimodal distribution	A statistical distribution featuring two distinct modes or maxima
Breccia	Rock consisting of angular fragments of stones cemented by finer calcareous material
Capillary pressure	The force necessary to squeeze a hydrocarbon droplet through a pore throat (works against the interfacial tension between oil and water phases)
Cataclasite	A cohesive fault rock with a random composition containing 10%–50% fragments in a finer grained matrix
Cauchy boundary condition	Also known as a third-type boundary condition, involves specification of both the value and the derivative that the solution of a differential equation needs to produce along the boundary of a model domain. Applicable to both numerical and analytical models
Clay smear	Process in which clay from the wall rock is incorporated in a fault zone
Cleats	Cleats are natural fractures in coal. They usually occur in two sets that are perpendicular to one another and perpendicular to bedding. The cleats in one direction form first and exhibit a high level of continuity. These are called “face cleats”. Cleats perpendicular to face cleats are called “butt cleats”
Coal measure	Geological strata of the Carboniferous or Permian periods usually containing sequences of coal seams
Coal seam	Individual layers containing mostly coal. Coal seams store both water and gas. Coal seams generally contain more salty groundwater than aquifers that are used for drinking water or agriculture
Coal seam gas	A form of natural gas (generally 95 to 97% pure methane, CH_4) typically extracted from permeable coal seams at depths of 300 to 1000 m. Also called coal seam methane (CSM) or coalbed methane (CBM)
Co-kriging	A form of kriging in which the distribution of a second, highly correlated variable (i.e. covariate) is used in addition to the primary variable to produce interpolated values. Co-kriging can improve interpolated estimates if the primary variable is difficult, impossible, or

Term	Description
	expensive to measure and/or if the secondary variable is sampled more intensely than the primary variable
Confined aquifer	An aquifer that is isolated from the atmosphere by an impermeable layer. Pressure in confined aquifers is generally greater than atmospheric pressure
Confining pressure	The combined hydrostatic stress and lithostatic stress; i.e. the total weight of the interstitial pore water and rock above a specified depth
Covariance	Covariance is a measure of how much two given variables vary together, as a function of either space or time
Darcy flow	Liquid flow that conforms to Darcy's law
Darcy's law	A constitutive equation that describes the flow of a fluid through a porous medium such as rock or soil
Depressurisation	The lowering of static groundwater levels through the partial extraction of available groundwater, usually by means of pumping from one or several groundwater bores or gas wells
Deterministic	A type of mathematical analysis that assumes no randomness in the input data. A deterministic model will thus always produce the same output from a given input data or initial state
Dewatering	The lowering of static groundwater levels through complete extraction of all readily available groundwater, usually by means of pumping from one or several groundwater bores or gas wells
Diffusion	The process by which ionic or molecular constituents move under the influence of their kinetic activity in the direction of their concentration gradient
Diffusion coefficient	The quantity of a substance that, in diffusing from one region to another, passes through each unit of cross section per unit of time when the volume-concentration gradient is unity
Dirichlet boundary condition	Also known as a first type boundary condition, involves specification of the value that the solution of a differential equation needs to produce along the boundary of a model domain. Applicable to both numerical and analytical models
Dispersion or hydrodynamic dispersion	The spread of solutes, colloids, particulate matter, or heat by the combined processes of diffusion and physical mixing of fluids along the path of groundwater flow. This leads to a reduction of concentration at the macroscopic scale
Drawdown	A lowering of the water table of an unconfined aquifer or of the potentiometric surface of a confined aquifer, typically caused by groundwater extraction
Drill stem test	A procedure to determine the productive capacity, pressure, permeability or extent (or a combination of these) of a hydrocarbon reservoir, involving the circulation of drilling fluids and the use of inflatable bladders ('packers') to isolate the vertical extent of the test
Dual permeability	In a dual-porosity porous medium (reservoir, aquifer, aquitard), fluid flow occurs in both primary and secondary porosity systems
Dual porosity	A feature of soil/rock whereby fluids may be present within porous matrix blocks (which possess a particular storage capacity or "primary porosity") or within the open fractures

Term	Description
	(which provide additional storage capacity or “secondary porosity”). Flow may occur in both the fractures and the matrix
Effective parameters	Parameters used in ensemble-averaged equations (e.g., effective hydraulic conductivity relating the ensemble average flux to the ensemble mean gradient). They are an intrinsic property of the homogenised domain and not a function of the particular boundary conditions imposed on the domain
Effective porosity	The fraction of pores that are connected to each other and contribute to flow. Materials with low or no primary porosity can become very permeable if a small number of highly connected fractures are present
Ensemble-averaging	Formed by averaging over multiple realisations (model runs) of a spatio-temporal process.
Environmental Impact Statement	A document or set of documents describing a proposed development or activity and disclosing the possible, probable, or certain effects of that proposal on the environment and other potential receptors
Epistemic uncertainty	Uncertainty which represents a lack of knowledge about the appropriate value to use for a quantity; this uncertainty can be reduced through increased understanding (research) or collecting more relevant data
Equifinality	A state in which many different models are capable of reproducing the observed behaviour of a given natural system; also referred to as ‘non-uniqueness’
Equivalent parameters	Equivalent parameters are derived from spatial averaging methods. They are based on numerical modelling and are therefore valid only for a specific set of imposed groundwater flow boundary conditions. Sometimes the terms block-average or volume-average are used
Facies	All lithological and palaeontological features of a particular sedimentary rock, from which the depositional environment may be inferred
Fault core	The fault core is composed of structural elements that accommodate the majority of fault displacement. The fault core is often represented by a low permeability, continuous clay smear or a deformation band shear
Fault displacement	The offset between two sections of the same geological formation caused by uplift during or following fault activation
Fault throw	The vertical displacement caused by fault activation
Fault zone	The complete volume of rock deformed when lithospheric stresses cause two tectonic blocks to move in relation to one another; commonly comprised of two architectural elements - a fault core and damage zone
Gas wetting	The process of gas intruding a medium that has a preference for water
Gaussian (probability distribution)	A continuous function that approximates the exact binomial distribution and which represents the statistical distribution of many random variables. This can be described using only two parameters: mean (i.e. central tendency) and variance (i.e. spread). Typically visualised as a symmetrical bell-shaped graph
Geomechanical	Relating to the movement/expansion/contraction of soil and rock
Groundwater	Water occurring naturally below ground level (whether in an aquifer or other low-permeability material), or water occurring at a place below ground that has been pumped,

Term	Description
	diverted or released to that place for storage. This does not include water held in underground tanks, pipes or other works
Groundwater dependent ecosystem	Ecosystems that partially or fully rely on groundwater. These include terrestrial vegetation, wetlands, estuarine and near shore marine systems, river base-flows, cave and aquifer ecosystems and terrestrial fauna
Groundwater (single phase) flow model	A numerical solution to a partial differential equation used to describe the flow of water in the subsurface. Groundwater flow models involve the flow simulation of a single fluid phase (i.e. water). Common parameters used in groundwater flow models are hydraulic conductivity, specific yield and specific storage
Hydraulic conductivity	A coefficient of proportionality describing the rate at which a fluid can move through a permeable medium
Hydraulic fracturing	Also known as 'fracking', 'fraccing' or 'fracture stimulation', is one process by which hydrocarbon (oil and gas) bearing geological formations are 'stimulated' to enhance the flow of hydrocarbons and other fluids towards the well. In most cases is only undertaken where the permeability of the formation is initially insufficient to support sustained flow of gas. The hydraulic fracturing process involves the injection of fluids, gas, proppant and other additives under high pressure into a geological formation to create a conductive fracture. The fracture extends from the well into the coal reservoir, creating a large surface area through which gas and water are produced and then transported to the well via the conductive propped fracture channel
Hydraulic gradient	The difference in hydraulic head between different locations within or between hydrostratigraphic units, as indicated by water levels observed in wells constructed in those units
Hydraulic head	The potential energy contained within groundwater as a result of elevation and pressure. It is indicated by the level to which water will rise within a bore constructed at a particular location and depth. For an unconfined aquifer, it will be largely subject to the elevation of the water table at that location. For a confined aquifer, it is a reflection of the pressure that the groundwater is subject to and will typically manifest in a bore as a water level above the top of the confined aquifer, and in some cases above ground level
Hydraulic pressure	The total pressure that water exerts on the materials comprising the aquifer. Also known as pore pressure
Hydrofacies	A homogeneous sedimentological unit or a homogeneous but not necessarily isotropic hydrogeological unit, formed under characteristic conditions which lead to characteristic hydraulic properties
Hydrostratigraphic unit	A formation, part of a formation, or group of formations of significant lateral extent that compose a unit of reasonably distinct (similar) hydrogeologic parameters and responses
Hysteresis	The difference between the paths followed with time during stress loading and unloading. Also used to describe different paths (1) during solute or gas adsorption and desorption and (2) wetting and drying of porous media
Imbibition	The process of absorbing a wetting phase into a porous rock. Spontaneous imbibition refers to the process of absorption with no pressure driving the phase into the rock
Interburden	Material of any nature that lies between two or more bedded ore zones or coal seams

Term	Description
Inter-cell hydraulic conductivity	Hydraulic conductivity computed at the interface of two neighbouring model cells by combining the hydraulic conductivities pertaining to neighbouring cell centres in various ways (typically harmonic mean), depending on flow conditions and on the manner in which hydraulic conductivity is assumed to vary between these cells
Inter-layer conductance	Inter-layer conductances quantify the ability to conduct flow between a pair of adjacent grid cells. The interlayer-layer conductance is calculated as the inter-layer hydraulic conductivity divided by the elevation difference between adjacent model layers
Intrinsic permeability	The permeability of a given medium independent of the type of fluid present
Inverse modelling	The process of calculating from a set of observations the causal factors that produced them. Typically involves multiple model runs or iterations, starting with an initial set of parameter values that are gradually updated during the subsequent model runs until model predictions adequately describe the observations. The final parameter set is considered to be the best-fit representation of the real parameter values at the scale of measurement
Isotherm	A function describing the adsorption/desorption path of solute or gas on solids (e.g. rocks, coal)
Isotropy	The condition in which the hydraulic properties of a hydrostratigraphic unit are equal in all directions
Kriging	A geostatistical method of spatial interpolation (i.e. prediction) using weighted averages of surrounding data points. The data are a set of observations with some spatial correlation present
Langmuir isotherm	A mathematical relationship describing the covering or adsorption of a substance (e.g. gas) to a solid surface in relation to gas pressure or substance concentration. In case of unconventional gas, the Langmuir adsorption isotherm assumes that the gas attaches to the surface of the coal or shale, and covers the surface as a single layer of gas. The release of adsorbed gas from coal or shale is commonly described by a pressure relationship called the Langmuir Isotherm
Lithospheric stress	Stress in the outer solid part of the Earth (lithosphere)
Lithological facies	A mappable subdivision of a stratigraphic unit that can be distinguished by its facies or lithology-the texture, mineralogy, grain size, and the depositional environment that produced it
Matrix (rock matrix)	The finer grained mass of rock material in which larger grains/crystals are embedded
Mode	Most frequent value of a frequency distribution
Monte Carlo sampling	The sampling of uncertain data for use in Monte Carlo risk analysis or simulation
Monte Carlo simulation	The use of Monte Carlo analysis techniques to estimate the most probable outcomes from a model with uncertain input data
Multi-Gaussian distribution	Also multivariate normal distribution, is a generalization of the one-dimensional (univariate) normal distribution to higher dimensions
Multi-phase flow	The simultaneous flow of multiple phases, e.g. liquid and gas
Multimodal distribution	A statistical distribution featuring more than two distinct modes or maxima

Term	Description
Neumann boundary condition	Also known as a second type boundary condition, involves specification of the derivative that the solution of a differential equation needs to produce along the boundary of a model domain. Applicable to both numerical and analytical models
Numerical realisation	A numerically generated sample (usually of model parameters) drawn from a probability distribution, used to run a model simulation
Palaeochannel	A remnant of an inactive river or stream channel that has been either filled or buried by younger sediment
Permeability	The measure of the ability of a rock, soil or sediment to yield or transmit a fluid. The magnitude of permeability depends largely on the porosity and the interconnectivity of pores and spaces in the ground
Petrophysical observations	Properties that pertain to fluid behaviour within the rock, such as lithology (grain size, composition and texture), porosity, capillary pressure, permeabilities, irreducible saturations or saturations.
Porosity	The proportion of the volume of rock consisting of pores, usually expressed as a percentage of the total rock or soil mass
Preferential flow	Preferential flow refers to the uneven and often rapid and short-circuiting movement of water and solutes through porous media characterised by small regions of enhanced flux (such as faults, fractures or other high permeability pathways), which contributes most of the flow, allowing much faster propagation of pressure differences and transport of solutes through that pathway
Probability density function	A function that describes the relative likelihood for a random variable to take on a given value
Protolith	Unmetamorphosed rock from which a given metamorphic rock is formed
Radioactive isotopes	Natural or artificially created isotope of a chemical element having an unstable nucleus that decays, emitting alpha, beta, or gamma rays until stability is reached.
Recharge	The process whereby surface water (such as from rainfall runoff or irrigation) percolates through the ground to the water table
Regional-scale groundwater models	Models that encompass an entire groundwater system, geological basin or other significant area of interest that extends well beyond the measurable influence of individual bores or borefields
Relative permeability	The permeability of a medium for a specific fluid relative to the intrinsic permeability for a porous medium containing more than a single fluid phase (e.g., air and water or oil, gas, and water)
Representative elementary volume (REV)	The smallest volume over which a measurement of a property can be made that will yield a value representative of the whole volume under investigation
Reservoir (hydrocarbon)	Porous or fractured rock formations that contain significant reserves of hydrocarbons. Naturally-occurring hydrocarbons such as crude oil or natural gas are typically trapped in source or host rocks by overlying low permeability formations
Reservoir (multiphase) flow model	A numerical solution to a partial differential equation used to describe the flow of hydrocarbons and other fluids in a hydrocarbon reservoir. Reservoir models typically involve the flow simulation of multiple fluid phases and the use of dual domain approaches

Term	Description
	to simulate matrix and fracture flow. Common parameters used in reservoir models are porosity, permeability and water saturation
Robustness (of model predictions)	Insensitivity of model predictions to data outliers or other small departures from assumptions required by a predictive model, including the types of parametric distributions assumed
Saturated flow	Flow through a porous medium (such as soil or rock) in which the void space within the porous medium is entirely occupied by water (as opposed to water and gas)
Single phase flow	The flow of a single phase, e.g. liquid or gas
Solute	The substance present in a solution in the smaller amount. However, for convenience, water is generally considered the solvent (not the solute) even in concentrated solutions with water molecules in the minority
Spatial correlation	Spatial dependency (or correlation) between samples
Spatial interpolation	The procedure of estimating the value of properties at unsampled sites within the area covered by existing observations
Specific storage	The volume of water released from a hydrostratigraphic unit under confined conditions due to a unit decrease in pressure head
Specific yield	The ratio of (a) the volume of water released from an hydrostratigraphic unit under unconfined conditions due to a unit decrease in pressure head to (b) the total volume of the hydrostratigraphic unit
Stochastic process	Process characterised by a random probability distribution or pattern that may be analysed statistically but may not be predicted precisely
Stochastic analysis	A type of mathematical analysis that can be used to assess the uncertainty associated with models. It estimates the probability distribution of potential outcomes by allowing for random variation in one or more input parameters
Storativity	The volume of water released from a hydrostratigraphic unit per unit surface area due to a unit decrease in pressure head. Under unconfined conditions, storativity is equal to specific yield. Under confined conditions, storativity is equal to the product of specific storage and the thickness of the hydrostratigraphic unit
Stratigraphy	An arrangement of sedimentary, metamorphic and/or igneous rocks
Subsidence	Usually refers to downward vertical displacement of a point at or below the ground surface. However, the subsidence process actually includes both vertical and horizontal displacements. These horizontal displacements, in cases where subsidence is small, can be greater than the vertical displacement. Subsidence is usually expressed in units of millimetres
Sustainable groundwater use	The groundwater extraction regime, measured over a specified planning timeframe, that allows acceptable levels of stress and protects dependent economic, social, and environmental values
Transmissibility	Synonym for transmissivity. The hydraulic conductivity of an aquifer multiplied by the thickness of that unit

Term	Description
Transmissibility multiplier	Transmissibility multipliers account for the reduced or increased permeability for each cross-fault connection
Transmissivity	The rate at which a fluid is transmitted through a unit width of a hydrostratigraphic unit under a hydraulic gradient
Unconfined aquifer	An aquifer in which there are no confining beds between the zone of saturation and land surface
Unconventional gas	Natural gas found in a very low permeability rock, such as coal seam gas, shale gas, and tight gas. Unconventional gas such as coal seam gas is trapped in coal beds by adsorption of the gas molecules to the internal surfaces of coal. It cannot migrate to a trap and form a conventional gas deposit. This distinguishes it from conventional gas resources, which occur as discrete accumulations in traps formed by folds and other structures in sedimentary layers
Unimodal distribution	A probability distribution which has a single mode
Unlithified rock	Soft sediments that have little strength and are readily deformed under pressure
Upscaling	Upscaling is the process of transforming the detailed description of hydraulic parameters in a grid constructed at measurement scale to a coarser grid with less detailed description. It replaces a heterogeneous domain with a homogeneous one in such a way that both domains produce the same response under some upscaled boundary conditions
Vadose zone	The part of the Earth located between the land surface and the top of the saturated zone; i.e., the position at which groundwater pore pressure is equal to atmospheric pressure
Variogram (also semi-variogram)	A function describing the spatial dependency (similarity) between observations of a variable. The shape of the variogram is typically function of the distance and direction separating observations at two locations; at short distances the semi-variance is small, and typically increases with increasing separation distance. The semi-variance is defined as the variance of the difference between two variables at two locations. At zero separation distance the semivariance is called nugget (-effect). The sill is the maximum semivariance or the plateau of the semi variogram; the correlation length or spatial range is the distance over which variables are spatially correlated
Vibrating wire piezometer	Absolute pressure transducers aimed to measure soil or rock pore pressure. Multiple piezometers can be connected along a string that allows multiple pressure measurements in a single borehole
Water wetting	The process of water intruding a medium that has a preference for gas
Well	Borehole in which a casing (e.g. steel piping) has been placed to restrict connection to specific ground horizons/depths

Symbols

Symbol	Brief description and unit of measurement (L = length, T = time)
η_e	effective porosity [$L^3.L^{-3}$]
η_f	fracture porosity [$L^3.L^{-3}$]
η_m	matrix porosity [$L^3.L^{-3}$]
k	permeability [L^2]
k_h	horizontal permeability [L^2]
k_v	vertical permeability [L^2]
K	hydraulic conductivity [$L.T^{-1}$]
K_e	effective hydraulic conductivity [$L.T^{-1}$]
K_f	fracture hydraulic conductivity [$L.T^{-1}$]
K_h , K_x , K_y	horizontal hydraulic conductivity [$L.T^{-1}$]
K_m	matrix hydraulic conductivity [$L.T^{-1}$]
K_v , K_z	vertical hydraulic conductivity [$L.T^{-1}$]
Q	volumetric fluid flux [$L^3.T^{-1}$]
v	linear fluid flux [$L.T^{-1}$]

Acknowledgements

The authors would like to acknowledge the Commonwealth Department of the Environment and Energy for funding the project “Research to improve treatment of faults and aquitards in Australian regional groundwater models to improve assessment of impacts of CSG extraction”. The report was subject to internal peer review processes during its development and benefitted from reviews undertaken by Dr. Ludovic Ricard (CSIRO Energy), Dr. Rodrigo Rojas (CSIRO Land and Water), Dr. Jim Underschultz (University of Queensland) and Dr. Catherine Moore (GNS Science, New Zealand). The authors also thank CDM Smith, the Office of Groundwater Impact Assessment (Qld), Origin Energy, the Queensland Gas Company, and Santos Ltd for their assistance in the preparation of those parts of this overview that relate to groundwater flow modelling of coal seam gas related activities in Australia.

Executive summary

The project "Research to improve treatment of faults and aquitards in Australian regional groundwater models to improve assessment of impacts of coal seam gas (CSG) extraction" focuses on identifying and assessing the risks associated with deep groundwater extraction and depressurisation from energy resource development. The project aims to develop methodologies and techniques that will improve the predictive capability of regional groundwater models used in this context, specifically with respect to the representation of faults and aquitards. The project has three components: 1) an examination of aquitards, 2) an examination of faults, and 3) an examination of the upscaling of aquitard and fault properties such that they can be adequately represented in regional groundwater flow models.

This report provides an overview of approaches to simulating the hydrological influence of aquitards and faults in regional groundwater models, and also includes a summary of the literature relating to the third component of the report, i.e. regional scale groundwater modelling approaches. The overview provides a framework that can be used to guide research into appropriate methodologies and procedures for aquitard and fault zone representation in regional groundwater models. Specifically this study:

- Provides an overview of sources of uncertainty (aleatory and epistemic) and discussed methods to quantify their impact on groundwater flow and chemical transport
- Discusses four key physical processes involved in coal seam gas extraction at a local scale: dual domain flow, gas desorption, dual phase flow, and geomechanical deformation
- Reviews hydraulic conductivity measurement methods across a range of spatial scales (core, bore, regional)
- Provides examples of how soft data (mostly of a qualitative nature but plentiful in either the horizontal or vertical plane) may be used to derive improved estimates of hard (but sparse) data such as hydraulic conductivity
- Discusses local and global upscaling methods and their advantages/disadvantages in a CSG impact assessment context
- Reviews simulation-based spatial interpolation methods, including Monte Carlo sampling, two-point statistics, multi-point statistics, and transition probability geostatistics
- Provides a review of structural features including geological faults and fractured zones, in particular fault architecture and distributions and processes that alter fault zone permeability; identified that representation of faults in groundwater flow models for CSG-related impact assessments in Australia is rare
- Discusses equivalent porous media approaches for representation of combined matrix and fracture flow in fractured zones, including dual domain and discrete fracture network approaches
- Analyses ten Australian CSG impact studies involving groundwater flow models for the Surat Basin and Bowen Basins (Queensland), Gunnedah Basin (New South Wales) and Gippsland Basin (Victoria). Models were summarised with respect to the key local scale physical processes and regional scale considerations identified in this report, including dual phase flow, parameter upscaling and regionalisation, and representations of faults and fracture zones.
- Highlights the highly simplified representation of such local scale processes and regional scale considerations in the majority of groundwater models used in those ten CSG impact studies. Simplifications involved adopting spatially uniform values of hydraulic conductivity and storativity for aquitards, thus neglecting the spatial heterogeneity. The lack of data with regards to fault architecture and fault hydraulic properties means their representation in groundwater flow models is also very simplified: the only two studies that had reported inclusion of faults did so by modifying the conductance between neighbouring model cells in order to represent barriers or conduits to flow. This approach cannot be used to represent complex anisotropic fault

conceptualisations (e.g., cross-fault barrier/along-fault conduit structure); also, fracture zones surrounding the fault core were not simulated in any of the models.

- Identifies key knowledge and data gaps in regards to developing simplified, but defensible, regional scale groundwater flow models incorporating fit-for-purpose representations of aquitards and faults. While use of simplified models is an undeniable necessity, given the limitations regarding computational resources and data coverage, simplifications must be justified and based on application of accepted methodologies such as deriving equivalent properties through robust upscaling. Often, however, there are insufficient data to derive meaningful equivalent properties in the first place. There is therefore a need for better data integration across multiple scales to maximise subsurface coverage with existing data; this will require better linkages between geological, geophysical, hydrological and hydrochemical information, thereby encompassing several spatial scales of heterogeneity.
- Identifies the need for a more systematic adoption of methods to test the validity of model simplifications, e.g. what degree of complexity is required or acceptable for representing geological complexity, including discontinuous geological units and structural discontinuities, such as geological faults. The answer to this question will necessarily depend on the objective the model has to fulfil; there is thus no unique solution. Some studies discussed here provide a benchmark example of how such testing can be undertaken; these involved comparison between single phase and dual phase simulations of depressurisation and the effect of different ways of upscaling geological layers exhibiting contrasting hydraulic properties such as coal beds and interburden.

The imposition of large hydraulic stresses associated with coal seam gas extraction has the potential to result in significant increases in magnitude of vertical hydraulic gradients across aquitards. In this context, the term “significant” may refer to changes that are sufficient to trigger legislative requirements. For example, for unconsolidated aquifers of the Surat Cumulative Management Area of Queensland, areas in which groundwater level drawdowns greater than two metres persist are classed as Immediately or Long-term Affected Areas. Changes in vertical hydraulic gradients may in turn affect the groundwater flow regime of aquifers overlying or underlying the target coal seam formations. Aquifers serve as a water source for purposes such as stock and domestic use, crop irrigation, or town water supplies. Changes to flow regimes in such aquifers may therefore impact upon the sustainable use of existing and future groundwater users. Due to the anisotropy of coal formations (which typically consist of alternating permeable fractured coal and less permeable interburden facies), groundwater extraction from coal seams will primarily induce horizontal flow within the seams. Vertical flows into coal seam formations during depressurisation for CSG extraction are typically further limited by overlying and/or underlying aquitard units that act as hydraulic seals. The relatively low hydraulic conductivity of these units restricts the vertical propagation of significant changes to hydraulic gradients induced by CSG production to remain mainly within the overlying and/or underlying aquitards; consequently, vertical flows through these units are limited. The desaturation of coal seams that occurs as gas flows replace water flows in the vicinity of CSG extraction wells can further restrict the propagation of hydraulic gradient impacts. However, the sealing capacity of aquitard units can potentially be compromised by the presence of preferential flow paths along geological faults and/or via fracture networks. Similarly, in locations where a confining aquitard is spatially discontinuous due to inconsistent deposition or erosion, vertical fluxes through a confining aquitard may increase. In a coal seam gas development context, Environmental Impact Statement obligations require risk-based assessments of potential deleterious impacts on groundwater resources. Regional scale numerical groundwater flow models are typically used to provide such predictions.

This report summarises approaches to the simulation of the impacts of CSG extraction in regional scale groundwater flow models. The need for regional scale groundwater models is due to the vast areas covered by the CSG well fields and the extent and complexity of geological formations that potentially become affected. Specifically, two aspects of the modelling process are examined in detail. First, appropriate strategies for model parameter upscaling and spatial interpolation are examined. Here, upscaling refers to a change in observation scale resulting in a commensurate change in the scale of hydraulic property representation. Spatial interpolation refers to the estimation of parameter values in space; in the present study the interpolation is undertaken over regional scales (e.g., tens to hundreds of kilometres). Upscaling and spatial interpolation methods vary in complexity and in the level of data support required. These range from simple

approaches based on statistical metrics or Darcy Law-based methods to complex approaches based on geostatistical characterisation and facies reconstruction methods.

Second, numerical representations of geological faults and fracture systems in groundwater flow models are identified. The effects of faults on hydraulic properties in the context of upscaling are discussed, which typically result in changes to the conceptualisation of faults and their flow properties. The common use of transmissibility multipliers to represent faults in reservoir models is discussed, in addition to more detailed approaches involving explicit representations of fault zone heterogeneity. For the simulation of groundwater flow in fractured porous media, three categories of methods are summarised, ranging in complexity from equivalent porous media approaches to discrete fracture network models.

A selective summary of various local scale processes (e.g., multi-phase flow, gas desorption) that affect the prediction of CSG impacts is also presented and methods by which to represent these processes are discussed. A large number of simulation codes have been assessed regarding their capability for handling such key processes. The report concludes with a summary of studies which have used numerical groundwater flow models to simulate the impacts of coal seam gas extraction in Australia. Throughout the report available methods for the quantification of model and prediction uncertainty are highlighted. It should be noted that the focus of the report is on groundwater flow and hydraulic responses; therefore the simulation of solute transport is not discussed.

The key finding presented in this report is that representations of aquitards and geological faults in groundwater flow models used to estimate potential impacts of coal seam gas production are often highly simplified. For aquitards, simplification typically involves neglecting the spatial heterogeneity of hydraulic conductivity and storativity by adopting spatially uniform values. The use of uniform values may be justified when equivalent properties are derived from robust upscaling methods, or when the support volume used to derive flow properties is large enough to produce scale-independent values. Often, however, there are insufficient data to derive meaningful equivalent properties in the first place. Clearly, there is a need for better data integration across multiple scales to maximise subsurface data coverage; this will require better linkages between geological, geophysical, hydrological and hydrochemical information, thereby encompassing several spatial scales of heterogeneity.

As far as the representation of geological faults and fault networks is concerned, there exists a paucity of data with regards to both fault architecture (e.g. orientation, location, size and frequency) and to the flow properties of faults. In addition, due to a lack of numerical capability in standard groundwater flow models, the implementation of faults is often not trivial. As for aquitards, the improved integration of different sources of information on the geometry and flow properties of fault zones is required to better conceptualise and represent faults in groundwater flow models. This conceptualisation, and the testing of the role of faults on local and regional groundwater flow systems, will benefit from improved numerical schemes that seamlessly merge fine-scale fault meshes with coarse-scale numerical grid blocks while avoiding computationally prohibitive model run times.

1. Introduction

The imposition of large hydraulic stresses on a groundwater flow system, such as those associated with coal seam gas production or groundwater abstraction for agriculture or domestic use, has the potential to result in significant changes to hydraulic gradients and thus to groundwater flow directions and, ultimately, to the groundwater mass balance. In particular, the cumulative impacts of multiple extractions in developed groundwater basins may present risks to the security of existing groundwater users. For example, the operation of coal seam gas extraction, mining and irrigated agriculture within the same region may generate cumulative impacts on groundwater and surface water resources that are in addition to the separate impacts of either agriculture or mining separately. Regional assessments require developing an estimate of the cumulative impacts of cross-sector interactions on water availability and use and their probabilities. The risk analysis is to consider both the likelihood and consequence of these impacts (Barret et al. 2013).

Due to the anisotropy of coal formations (which typically consist of alternating permeable fractured coal and less permeable interburden facies), groundwater extraction from coal seams will primarily induce horizontal flow within the seams. Vertical leakage into coal seam formations during depressurisation for CSG extraction is typically limited by the presence of overlying and/or underlying aquitard units with relatively low hydraulic conductivity that restricts the rate of vertical flow. The vertical propagation of large hydraulic gradients induced by CSG production is therefore limited. The desaturation of coal seams which occurs when gas flows replace water flows in the vicinity of CSG extraction wells can further restrict the propagation of hydraulic gradient impacts. However, the confining capability of aquitard units can be compromised by the presence of preferential flow paths due to geological faulting and/or fracture networks. Similarly, in locations where a confining aquitard is spatially discontinuous (due to inconsistent deposition or erosion) the connectivity between two aquifers, or between a coal seam and an aquifer, may be increased. A third mechanism which may compromise the integrity of a confining aquitard is inter-aquifer connectivity induced by (uncased) water bores, mineral exploration boreholes, leaky conventional oil and gas wells, and leaky abandoned CSG wells [e.g., (Hart et al., 2006; SKM, 2013; NSW chief scientist & engineer report, 2014)].

In this Chapter general principles of multiple aquifer-aquitard flow systems (Section 1.1) and groundwater flow models in risk-based CSG impact assessments (Section 1.2) are discussed.

1.1. Multiple aquifer–aquitard flow systems

For simple hydrogeological systems, the propagation of hydraulic stresses can be relatively straightforward to estimate. For example, consider the potential drawdown in an unconfined aquifer caused by extraction from an underlying confined aquifer separated by an aquitard (Figure 1a).

This problem requires the characterisation of two aquifers and one aquitard, all of which are near to land surface. In this case, analytical solutions may be employed [e.g., Hantush (1960); Neuman and Witherspoon (1969)] to provide a first order estimate of drawdown. In contrast, the simulation of flow in deep groundwater basins featuring multiple aquifers and aquitards (i.e., 'layer cake' stratigraphy) is not trivial, and becomes even more complex when considering heterogeneity. In such environments, the vertical propagation of hydraulic responses requires the characterisation of multiple aquifers and aquitards. Analytical approaches are thus unsuitable for the characterisation of relatively complex hydrostratigraphic systems. Instead, numerical or semi–analytical approaches are often used. For example, consider a groundwater flow system featuring an unconfined aquifer, a confined aquifer and a coal formation, each of which are separated by aquitards (Figure 1b). Depressurisation to an elevation equal to the top of the coal formation is proposed to enable the release of gas from the coal formation by desorption (see Section 2.2). If prior information regarding the hydraulic conductivity of the aquitards is poorly constrained, predictions of drawdown in the overlying unconfined aquifer resulting from extraction will also be poorly constrained. In other words, the model used will predict a wide range of equally probable solutions (a.k.a equifinality or non-uniqueness). In order to test the sensitivity of aquifer drawdown to

aquitard hydraulic conductivity, a semi-analytical groundwater flow code such as TTim (Bakker, 2013) may be employed, in which homogeneous hydraulic properties are assumed (Figure 2). Note that such simplifying assumptions may only be justified under certain conditions; e.g. when the hydrostratigraphic units simulated feature minimal spatial variability. Such limiting assumptions are often not appropriate for real world coal seam gas production contexts.

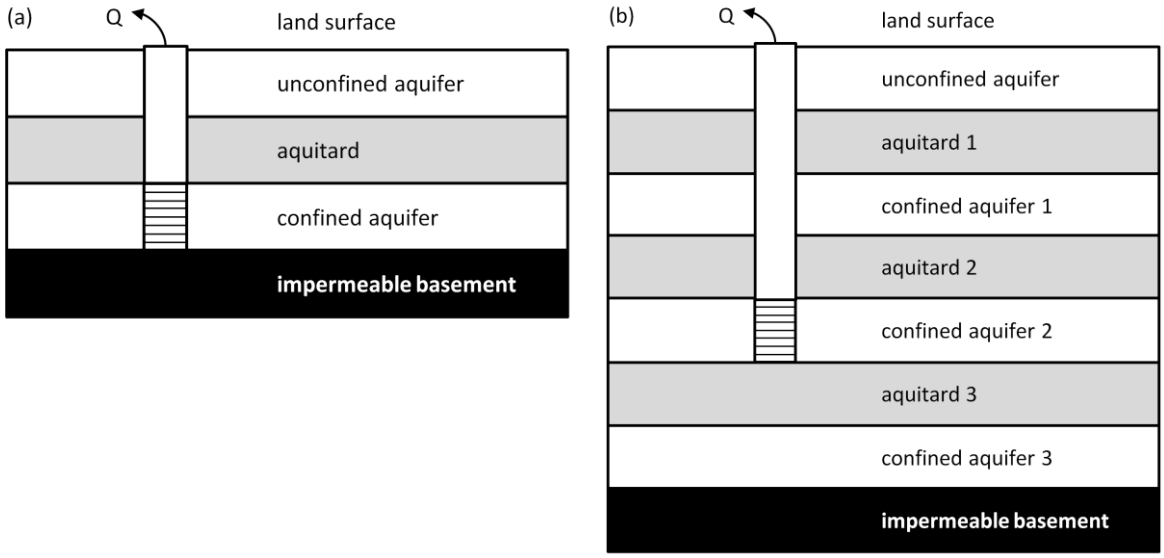

Figure 1. (a) Simple conceptual model of a shallow groundwater flow system featuring groundwater extraction from a confined aquifer overlain by an aquitard and an unconfined aquifer. (b) Simple conceptual model of a deep groundwater flow system featuring groundwater extraction from a confined aquifer (i.e., coal measure) overlain and underlain by multiple aquifer and aquitard types. For illustration purposes a fully penetrating well was used in both cases.

Using semi-analytical solutions enables the exploration of drawdown impacts of increasing differences between aquifer and aquitard hydraulic conductivities (Figure 2). For example, after 30 years of extraction, a maximum drawdown of nearly 24 metres in the unconfined aquifer occurs at 100 metres distance from the bore when the aquitard K_v value is specified as one tenth of the aquifer K_v value (i.e. 0.1 $m.d^{-1}$; red line). Conversely, an aquitard K_v value that is one thousandth of the aquifer K_v value (i.e. 0.001 $m.d^{-1}$; green line) results in a drawdown of 2 metres at 100 m distance from the bore. This is explained as follows: in the lowest aquitard K_v case (green), the upward vertical propagation of depressurisation toward the unconfined aquifer from underlying hydrostratigraphic units is severely restricted by the hydraulic conductivity of the two aquitards. Water is instead sourced from the confined production aquifer itself, resulting in increased drawdown of water levels in that aquifer. In comparison, in the highest aquitard K_v case (red), vertical flows through the two aquitards are greater and therefore the drawdown in the confined production aquifer is relatively smaller.

In practice, the prediction of hydraulic impacts from CSG operations involves the representation of much more complex geology than depicted in Figure 2, involving dipping strata, discontinuous units and/or structural features such as faults. In addition, the simulation of regional scale groundwater flow systems often requires the use of multiple boundary conditions of various types. For these reasons, numerical groundwater flow models are typically employed.

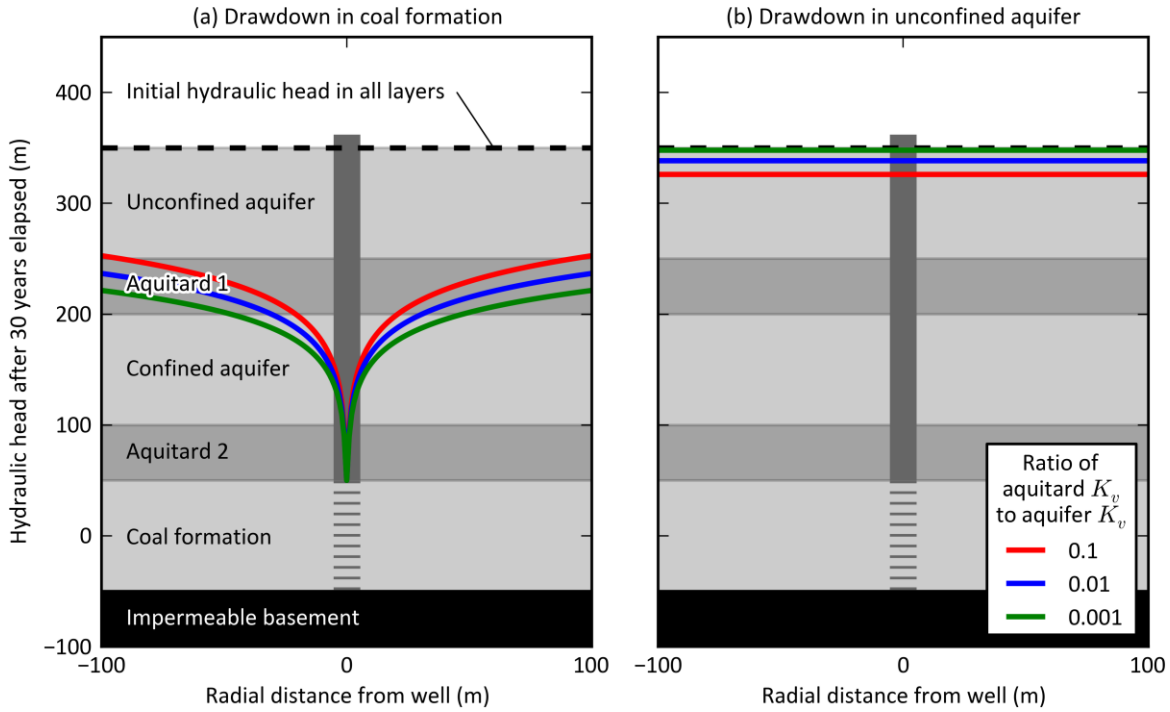

Figure 2. Sensitivity of drawdown in (a) coal formation and (b) unconfined aquifer due to groundwater extraction to simultaneous changes in the vertical hydraulic conductivity of both aquitards present.

1.2. Groundwater flow models in risk-based CSG impact assessments

1.2.1. Risk-based approach

In a coal seam gas development context, numerical groundwater flow models are typically used to provide predictions of groundwater-related consequences of proposed developments as part of Environmental Impact Statement (EIS) obligations [e.g., State of New South Wales (2015), State of Queensland (2014)]. Such predictions include the magnitude and spatial extent of changes in hydraulic head or groundwater level and changes in groundwater flow rates (e.g., discharge to surface water bodies) associated with a given impact (in some cases exposure) scenario (e.g. see Table 1 and associated text for discussion). The risk associated with a given scenario is calculated as the product of its probability of occurrence and the associated consequences. In practice, the probability of occurrence (or likelihood) may be difficult to quantify, although in some instances this quantification may be straightforward. An example of a difficult to quantify likelihood would be where the magnitude of an impact relies significantly on the possible presence of a difficult to detect a preferential flow pathway (e.g. conductive fault) between a coal seam target formation and a receptor in a beneficial aquifer (e.g. groundwater bore). In contrast, likelihoods would be straightforward to quantify where an established impact relationship already exists between a receptor of the impact (e.g. groundwater dependent ecosystem) and known stresses in a stressed groundwater system. Usually likelihoods are difficult to quantify, due to lack of knowledge and hence the uncertainty associated with a predicted consequence of interest must be estimated rather than quantified. Indeed, many of the values assigned to the parameters, initial conditions and boundary conditions (hereafter referred to collectively as parameters for brevity) used in numerical groundwater flow models are uncertain. Consequently, the predictions generated by such models are inherently uncertain. Predictions salient to the present report are the magnitude and spatial

extent of drawdown in productive, adjacent aquifers (confined and unconfined), as well as subsurface fluxes between a near-surface aquifer and underlying units.

A risk analysis combines the likelihood of occurrence of events with the severity of the consequences of those events to characterise the level of risk, often using a risk rating matrix (Figure 3). The risk rating matrix may be qualitative, semi-quantitative or quantitative depending on the degree of confidence in specifying events and their likelihood.

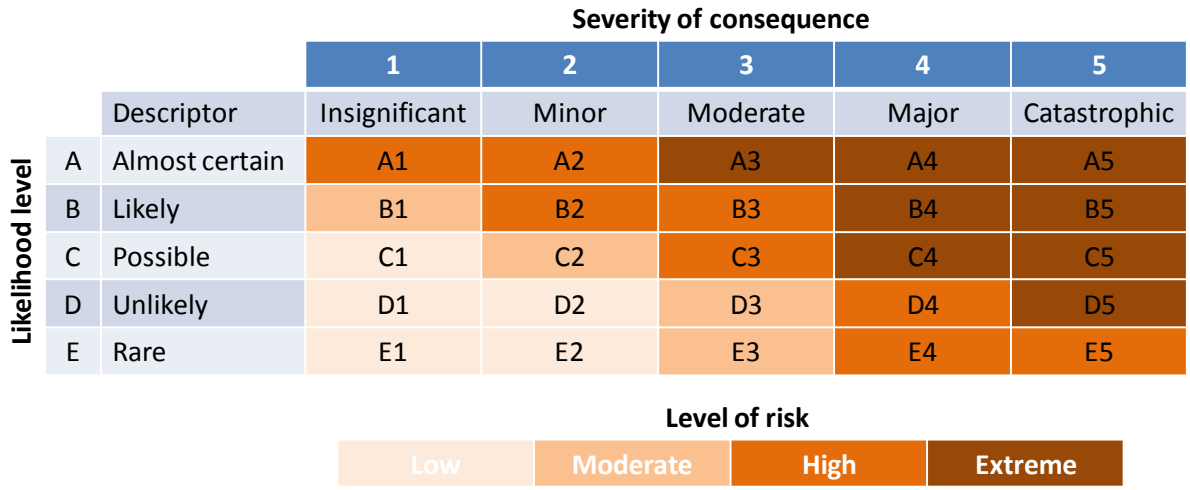

Figure 3. An example of a qualitative risk rating matrix where consequence ratings range from 'insignificant' (1) to 'catastrophic' (5) and likelihoods range from 'rare' (E) to 'almost certain' (A) (CoA, 2008).

Benefits of a risk analysis include:

1. providing quantitative estimates of impact, likelihood and risk within a logical scientific framework;
2. providing insights into where high value water assets (for example water dependent listed threatened species and State listed important water features) may face high risks; and,
3. identifying where risks may occur that have previously not been identified or have been underestimated.

1.2.2. Predictive uncertainty and likelihood

Where a model is used to simulate the potential impacts of a development, the likelihood associated with a certain consequence may be quantified. A consequence can be, e.g., a receptor response following exposure to chemical concentrations in receiving environments. Therefore in a risk-based context, where a model is used to assess impacts, model prediction uncertainty is analogous to likelihood.

Model prediction uncertainty can be quantified, for example, by considering multiple realisations of model evaluations yielding probabilities of exceeding certain consequences (i.e. Monte Carlo methods). Such realisations account for uncertainty in models and data. Linear approximations of predictive uncertainty may also be employed for computationally rapid assessments and are based on propagation of error formulae, and can be useful where model run times are long, as can occur in regional modelling contexts. Examples of such approximations include efficient sampling schemes (such as factorial, Latin Hypercube or bootstrapping approaches), as well as methods based on the Kalman Filter approach to data assimilation (Kalman 1960; for example, the PREDUNC tools that are part of the PEST suite of software; Doherty 2010). Hybrid methods such as Null Space Monte Carlo which combine some of the computationally thorough aspects of Monte Carlo methods with some of the computational expediency aspects of error propagation methods can also be used (Tonkin and Doherty, 2009).

Predictions generated by numerical groundwater models used in EIS studies are typically compared to regulatory (i.e., threshold) or baseline levels. In this sense, groundwater models are used to test hypotheses; i.e., to test whether a given model output will exceed a specified threshold value. The model output is typically some form of expected value (e.g., 50th, 90th or 95th percentile) which reflects the degree of prediction confidence desired (e.g., Figure 4a). Hypothesis testing then focuses on whether the error bounds associated with a given prediction metric (in addition to the value of the metric itself) exceed the threshold metric specified (e.g., Figure 4b).

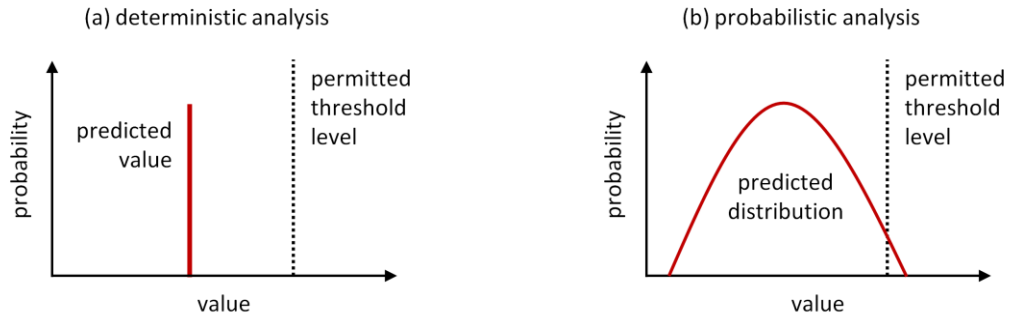

Figure 4. (a) Conceptual example of a deterministic approach to hypothesis testing of a threshold exceedance problem: a single value is predicted, which does not exceed the permitted threshold level. (b) Conceptual example of a probabilistic approach to hypothesis testing of a threshold exceedance problem: a statistical distribution of many predicted values is produced, from which a small (low probability) subset exceed the permitted threshold level.

In the Surat Cumulative Management Area, Queensland, maximum cumulative declines of two and five metres of hydraulic head have been prescribed for unconsolidated and consolidated aquifers respectively (QWC, 2012). In New South Wales, groundwater licenses for new developments such as CSG projects are granted on the basis that drawdowns at existing bores do not exceed cumulative or absolute threshold levels, depending upon aquifer type, productivity and location (NSW Office of Water, 2012) (Table 1). For confined aquifers, thresholds are generally assessed at the locations of existing water bores. For unconfined aquifers, thresholds are assessed at 40 metres distance from existing water bores. Maximum cumulative declines are calculated based on the period immediately following the commencement of the first water sharing plan for a given resource.

Table 1. Summary of various aquifer interference threshold metrics applied in New South Wales (NSW Office of Water, 2012).

			Unconfined		Confined	
			maximum cumulative decline	maximum absolute decline	maximum cumulative decline	maximum absolute decline
Aquifer type	Productivity	Location	(%)	(m)	(% or m)	(m)
Alluvial	high	Lower Murrumbidgee	10	2	40 %	3
	high	other	10	2	40 %	2
	low	any	10	2	40 %	2
Coastal sands	high	any	10	2	2 m	2
Porous rock	high	GAB – recharge areas	10	2	0.2 m	15
	high	GAB – other	N/A	2	0.2 m	30
	high	non–GAB	10	2	–	2
	low	any	10	2	–	2
Fractured rock	high	any	10	2	–	2
	low	any	10	2	–	2

1.2.3. Sources of uncertainty

Two types of uncertainties exist in groundwater flow and transport modelling: aleatory and epistemic uncertainty (Helton et al. 2008; Ross et al. 2009; Swiler et al. 2009). Epistemic uncertainty represents a lack of knowledge about the appropriate value to use for a quantity; this uncertainty can be reduced through increased understanding (research) or collecting more relevant data. The word epistemic derives from the Greek *episteme*, which means knowledge. Aleatory uncertainty is characterised by inherent randomness or stochasticity of a system that cannot be reduced by further data collection. The word aleatory derives from the Latin *alea*, which means the rolling of dice.

The advantage of separating the uncertainties into aleatory and epistemic is that we thereby make clear which uncertainties can be reduced and which uncertainties are less prone to reduction. This categorization helps us in allocation of resources and in developing assessment models. Furthermore, better understanding of the categorisation of uncertainties is essential in order to properly formulate risk problems (Der Kiureghian and Ditlevsen 2007).

Epistemic uncertainty can be subdivided into parametric and structural (model) uncertainty (Srinivasan et al. 2007). Parametric uncertainty, for instance, reflects our partial knowledge about the appropriate value to use for the spatially averaged hydraulic conductivity *K* in groundwater flow analysis; *K* has, by definition, a single value but this single "effective" value can never be known with certainty. Parameter uncertainties are strictly epistemic because the uncertainty in the estimation decreases and may asymptotically vanish with increasing quantity and quality of the available observational data. Model (structural, conceptual) uncertainty in groundwater modelling manifests itself on a multiplicity of scales, ranging from regional scale, to field scale, to laboratory scale, to pore scale. In groundwater modelling different conceptual models are typically based on different geological interpretations (Højberg and Refsgaard 2005; Rojas et al. 2010).

Indeed, the backbone of the conceptual groundwater model is a geological model consisting of a number of structural elements, typically derived from stratigraphical interpretation, and a strategy for how to handle the geological heterogeneity within such structural elements. Groundwater models typically have been constructed on the basis of a single geological model structure with the assumed best possible geological representation of the unknown reality. A commonly used approach is then to assume the existence of so-called effective parameter values characterizing the large-scale variation of the hydraulic properties, e.g., piece-wise constant values within the structural elements. These parameters are defined in such a way that, when optimized, they are expected to reproduce the average behaviour of the heterogeneous properties within the structural elements. Several studies have recognized that geological structural uncertainty often is the most important source of uncertainty (Bredehoeft 2005; Højberg and Refsgaard 2005; Refsgaard et al. 2012). The most commonly used approach to assess uncertainty of model predictions due to conceptual geological uncertainty is to run multiple geological models in a scenario modelling or multimodel approach (Neuman and Wierenga 2003; Rojas et al. 2010; Troldborg et al. 2007). By running an ensemble of relatively simple computer models, each of which represents an alternative conceptualization of the same system, the conceptual uncertainty (or model structural error) is quantified.

Højberg and Refsgaard (2005) analysed the importance of parameter uncertainty relative to conceptual geological uncertainty by constructing three alternative groundwater models on the basis of three different geological interpretations for their study area in Denmark. Inverse model calibrations against groundwater heads and streamflows revealed a similar performance by the three models. A Monte Carlo based parameter uncertainty analysis showed that the model parameter uncertainty was the dominating source of uncertainty for prediction of groundwater heads throughout the model area. However, the results illustrated that the conceptual model uncertainty became relatively more important for prediction of groundwater recharge and even more important for prediction of chemical concentrations in abstraction wells (Figure 5). Højberg and Refsgaard (2005) concluded that conceptual geological uncertainty will be more dominating than parameter uncertainty, the more the model predictions are extrapolations from the basis of model calibration (e.g. uncalibrated chemical velocities and concentrations).

Epistemic uncertainty may or may not be modelled probabilistically. Note that uncertainty about parameters in statistical models is almost invariably epistemic. Furthermore, the uncertainty in the data themselves is both aleatory, because they

are subject to random sampling or observation errors, and epistemic, because there are always unknown parameters to learn about.

In addition to probability theory, several alternatives exist that permit a less detailed representation of epistemic uncertainty than is possible with probability theory. As a result, these alternatives may more appropriately characterize epistemic uncertainty in the presence of limited information than probability theory. In particular, the use of probability to characterize epistemic uncertainty in the presence of limited information can imply the presence of more knowledge than is actually present.

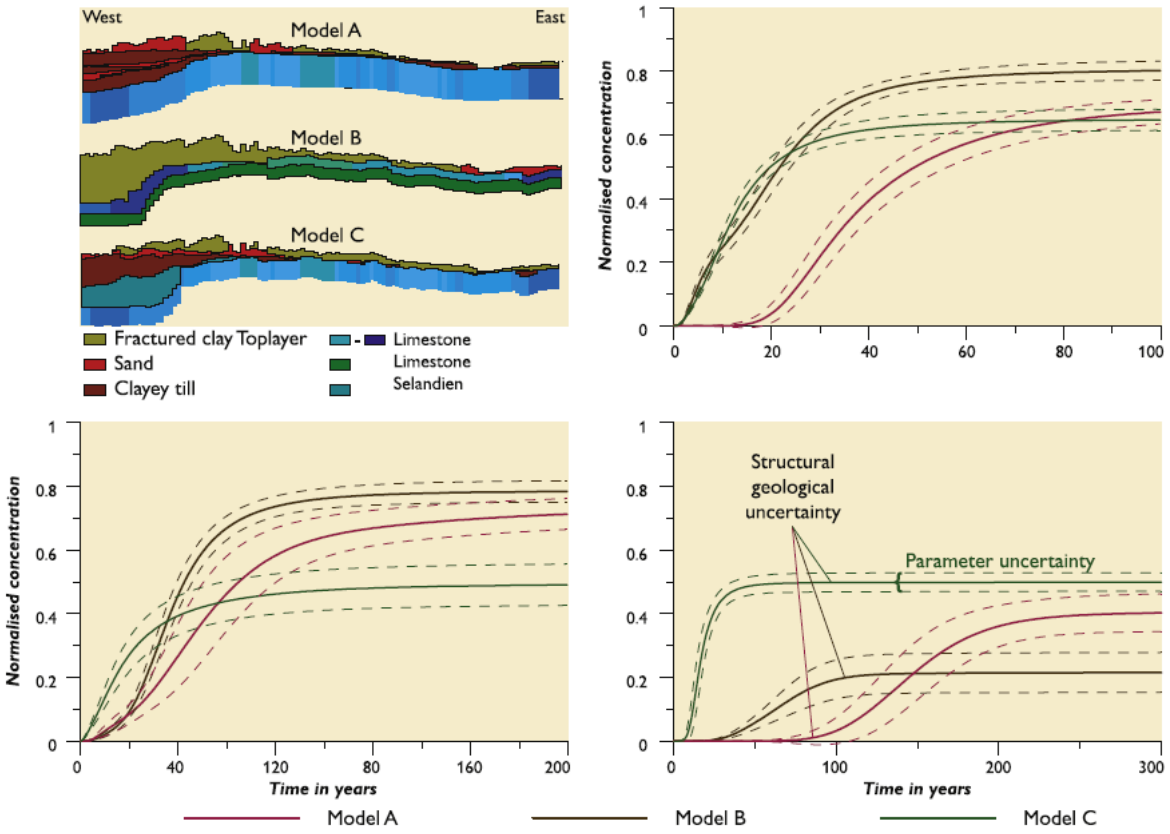

Figure 5 Simulated breakthrough in three selected abstraction wells for three models with different geological interpretations illustrated by the W–E cross-sections in the upper right corner. For each abstraction well the prediction uncertainty due to parameter uncertainty is shown with dashed lines for each of the three models (Højberg and Refsgaard 2005)

The simplest way to propagate epistemic uncertainty is through interval analysis. In interval analysis, it is assumed that nothing is known about the uncertain input variables except that they lie within certain intervals. That is, there is no particular structure on the possible values for the epistemic uncertain variables except that they lie within bounds. The problem of uncertainty propagation then becomes an interval analysis problem: given inputs that are defined within intervals, what is the corresponding interval on the outputs? A common approach to interval analysis is to sample from the uncertain interval inputs, and then take the maximum and minimum output values based on the sampling process as the estimate for the upper and lower output bounds. Usually a uniform distribution is assumed over the input intervals, although this is not necessary. Figure 6 shows how Monte Carlo sampling may be used to propagate epistemic uncertainty. The input distributions for the three model parameters x are all represented by intervals, and so is the output. Five samples are taken from each parameter, and the simulation model is run five times with these sets of input, resulting in 5 realizations of the output y shown on the right. Note, however, that one must be careful not to interpret the result with

any type of structure other than an interval on the output. Furthermore, while sampling is easy to implement, it may underestimate the true output interval (Swiler et al. 2009).

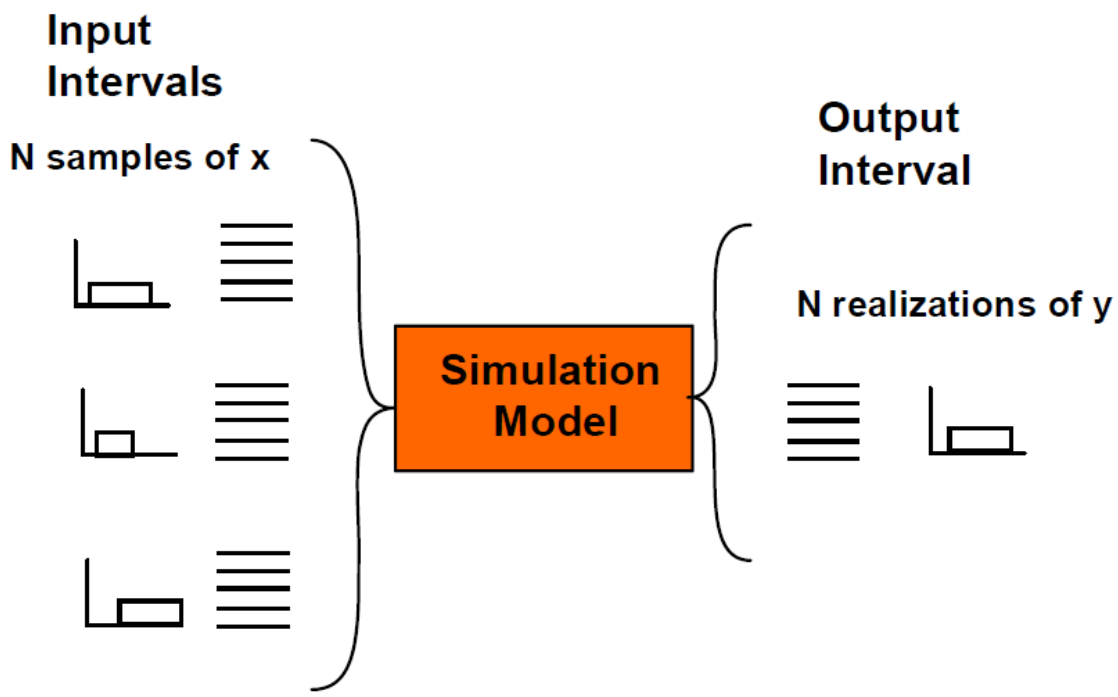

Figure 6 Monte Carlo sampling used for epistemic interval propagation (Swiler et al. 2009)

A second way to propagate epistemic uncertainty is by using Dempster-Shafer or evidence theory (Helton et al. 2004; Helton et al. 2008; Swiler et al. 2009). Evidence theory involves two specifications of likelihood, a belief and a plausibility. In Dempster-Shafer or evidence theory, the epistemic uncertain input variables are modelled as sets of intervals, and each variable may be defined by one or more intervals. The user assigns a basic probability assignment (BPA) to each interval, indicating how likely it is that the uncertain input falls within the interval. The BPAs for a particular uncertain input variable must sum to one. The intervals may be overlapping, contiguous, or have gaps. Dempster-Shafer has two measures of uncertainty - belief and plausibility. The intervals are propagated to calculate belief (a lower bound on a probability value that is consistent with the evidence) and plausibility (an upper bound on a probability value that is consistent with the evidence). Together, belief and plausibility define an interval-valued probability distribution, not a single probability distribution. The outcomes of an uncertainty analysis based on evidence theory can thus be represented with cumulative believe functions (CBFs), cumulative complementary believe functions (CCBFs), cumulative plausibility functions (CPFs), and cumulative complementary plausibility functions (CCPFs) (Figure 8). CBFs and CPFs are analogues to cumulative distribution functions (CDFs); the latter represent probability of non-exceedance, i.e. Prob ($X \leq x$): it defines the fraction of density or probability for a random variable X that falls below some particular value x (Figure 7). The CBF can be viewed as the minimum amount of likelihood that must be associated with an event; the CPF can be viewed as the maximum amount of likelihood that could be associated with an event. It can be shown that CBF (X) ≤ CDF (X) ≤ CPF (X) (Helton et al. 2004). Conversely, CCBFs and CCPFs are analogues to complementary cumulative distribution functions (CCDFs), where the latter represent probability of exceedance, i.e. Prob ($X > x$) = 1 - Prob ($X \leq x$) (Figure 7). It can be further shown that CCBF (X) ≤ CCDF (X) ≤ CCPF (X) (Helton et al. 2004).

CCDFs are commonly used to display the results of risk assessments for two reasons. First, CCDFs answer the question how likely is an outcome to be this large or larger, which is typically the question of interest in risk assessment. Second, CCDFs facilitate displaying small probabilities associated with large consequences.

The main method for calculating Dempster-Shafer intervals is computationally very expensive. Indeed, the propagation of uncertainty representations with less internal structure than probability theory through a model to obtain the resultant

uncertainty representations for model results can require more computation (i.e., model evaluations) than is the case when probability is used to represent uncertainty. Many hundreds of thousands of samples have to be taken over the space.

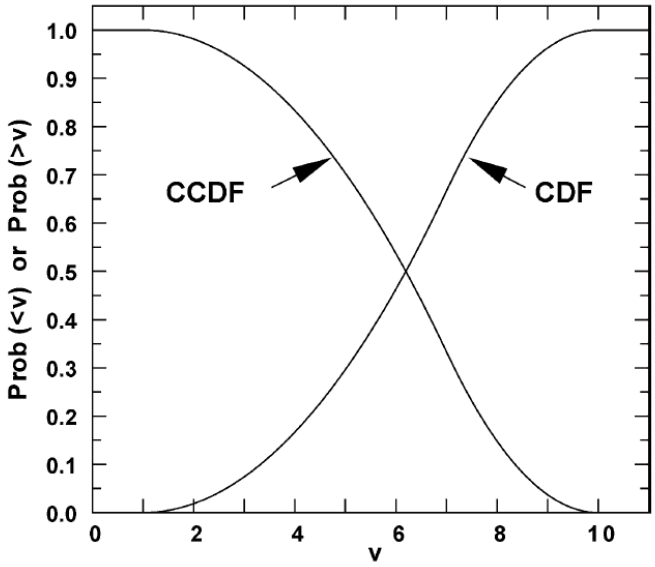

Figure 7 Cumulative distribution function (CDF) and complementary cumulative distribution function (CCDF) for variable v with a triangular distribution on [1, 10] and a mode at 7 (Helton et al. 2004).

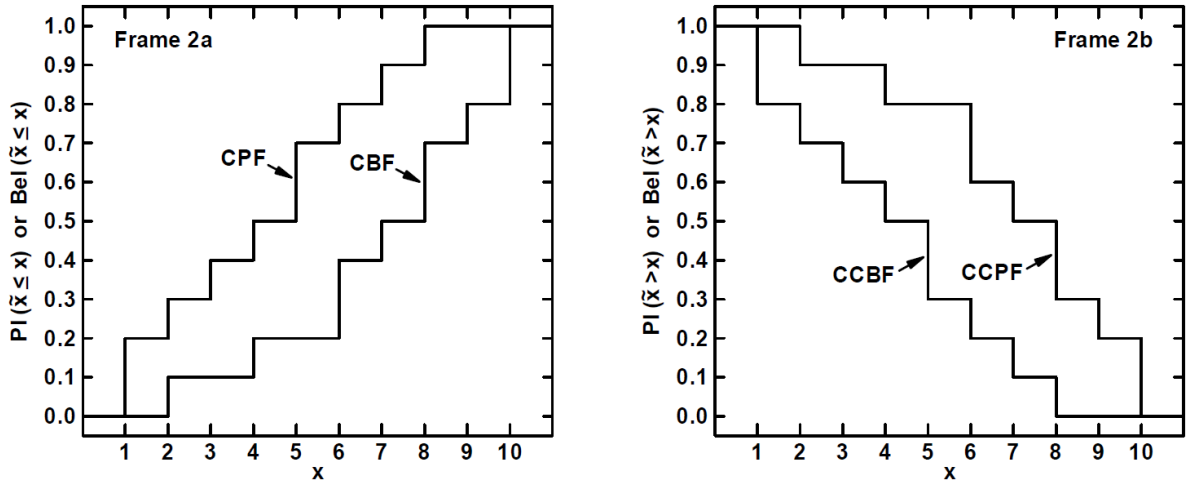

Figure 8 Plot of cumulative plausibility function (CPF), cumulative believe function (CBF), cumulative complementary plausibility function (CCPF) and cumulative complementary believe function (CCBF) (Helton et al. 2008).

Aleatory uncertainties are usually modelled with probability distributions (CDFs or CCDFs). Epistemic uncertainty leads to distributions of these functions. In other words, the outcome is a probabilistic characterization of the epistemic uncertainty associated with families of CDFs and CCDFs, which in turn are probabilistic characterizations of aleatory uncertainty. Figure 9 shows a Monte Carlo sampling approach that is often used to propagate aleatory uncertainty. In this case, one can interpret the resulting output samples probabilistically and fit an appropriate distribution.

Aleatory uncertainty is present in almost all data that we collect, due to random variability between the members of a population that is being sampled from, or to random measurement errors. The results of performance and risk analyses for complex systems are usually presented as CDFs and CCDFs that summarize the effects of aleatory uncertainty. In turn, the presence of epistemic uncertainty results in many possible values for these CDFs and CCDFs.

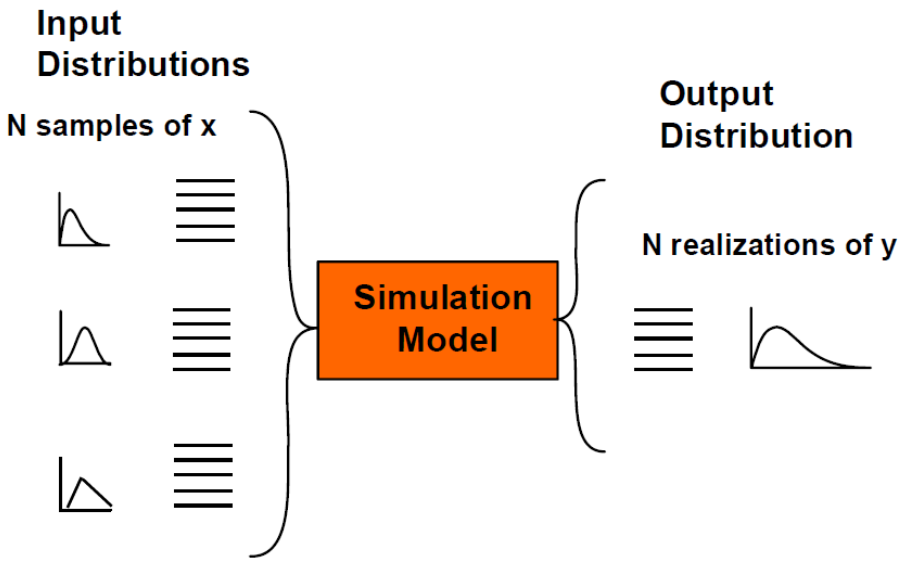

Figure 9 Monte Carlo sampling used for aleatory uncertainty propagation (Swiler et al. 2009)

1.2.4. Addressing uncertainty in groundwater models

In discussing uncertainty in the current report, the focus will be on structural and parameter uncertainty. Uncertainties in conceptual and numerical models are managed with specific procedures when selecting the models, datasets and computer codes in the impact assessments (Section 1.2.3). Furthermore, models should be fit for purpose. The selection of datasets (including input parameter values) is dependent on the mode of analysis, and whether deterministic or stochastic approaches are required. The most common approach has been deterministic assessments, whereby a so-called 'best estimate value', which represents the analyst's or expert's best judgement of what the (realistic) value of a given parameter should be under the conditions and assumptions of the scenario or assessment case, is selected (Mallants et al. 2009). Then, in addition, a 'high-end estimate' might be defined that represents a possible value, either higher or lower, but tending towards a value of the parameter that will have the effect of causing an overestimate of the impact, e.g., a higher hydraulic conductivity of an aquitard or a higher depressurisation boundary conditions.

In a stochastic analysis, frequency distributions or probability density functions (PDFs), or ranges of input parameters, need to be defined. If the aim is to investigate sensitivity, then often uniform or log-uniform PDFs can be defined that span the possible range of a parameter value. If, however, an estimate of risk and uncertainty analysis is required, then greater attention needs to be given to defining the limits and form of the PDF to represent the best available knowledge of the key input parameters (those parameters that have been identified through judgement and the results of sensitivity analysis).

Data or parameter uncertainty can be ascribed to a number of sources. Firstly, field and laboratory methods used to measure hydraulic properties directly are generally subject to uncertainty. While field-based observations may be conducted at a proper spatial scale to capture a reasonable amount of spatial heterogeneity of the subsurface, they are subject to the inability to control experimental conditions perfectly. Both initial and boundary conditions can be better controlled for laboratory-based observations, but such measurements are subject to the inability to replicate in-situ conditions perfectly and generally are conducted on small core samples that capture only part of the spatial heterogeneity (see further in Section 3.2). Secondly, when field or laboratory methods are used to estimate hydraulic properties indirectly by relating the prime variable of interest (e.g., hydraulic conductivity) to more easy to measure formation properties (e.g., porosity, grain size distribution, electrical or magnetic properties), the empirical relationships used to derive hydraulic properties are subject to uncertainty (Cronican and Gribb, 2004; Rogiers et al., 2012; Slater, 2007; Vienken and Dietrich, 2011). A third source of parameter uncertainty is associated with the upscaling of hydraulic properties. This is due to the scale dependency and heterogeneity of many hydraulic properties; e.g., the values of such properties can

increase with increasing scale (see Section 3.2) and are often heterogeneous. Note that upscaling techniques that fail to account for macro features that promote preferential flow paths may yield lower upscaled hydraulic properties. The magnitude of the increase due to scale dependency cannot be predicted *a priori*. White et al. (2014) discuss that failure to represent hydraulic conductivity heterogeneity during model calibration will lead to a misfit as the (single) incorrectly estimated hydraulic conductivity compensates for model structural error or conceptual uncertainty. A fourth source of parameter uncertainty is associated with the spatial interpolation of parameter values between an often limited number of measurement locations. Geostatistical approaches to spatial interpolation, such as ordinary kriging, include the quantification of interpolation uncertainty (Bissell and Aichele, 2004; Pucci and Murashige, 1987; Weber and Englund, 1992; Weber and Englund, 1994). Figure 10 displays three types of uncertainties often encountered in complex models of subsurface structures (geological models): type 1 - data imprecision and quality (e.g. imprecise interpretation of a geological formation boundary based on ill-defined input data); type 2 - inherent randomness (affecting extrapolation away from known points); and type 3 - incomplete knowledge (of structures such as geological faults) (Hall 2012; Wellman et al. 2010).

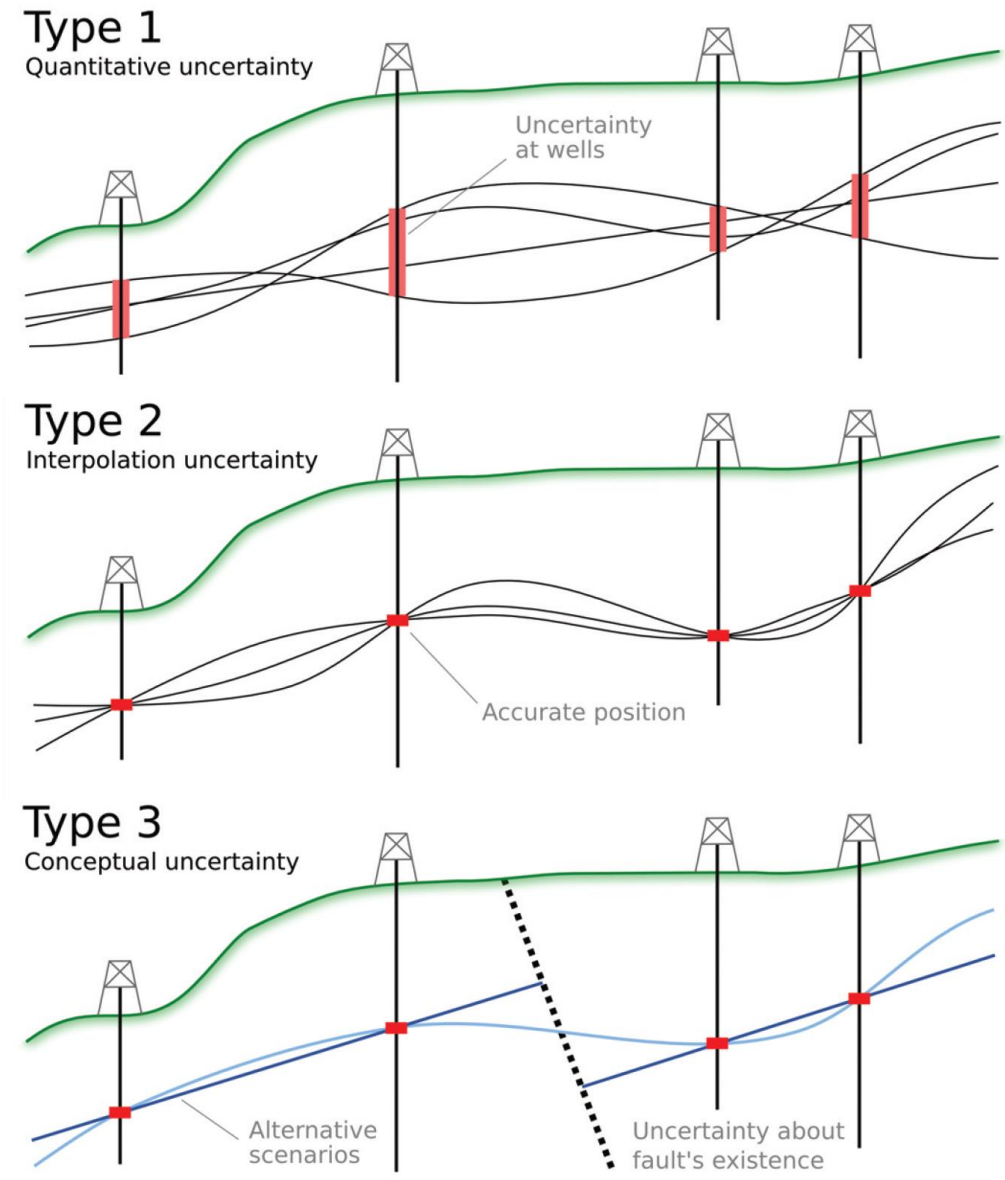

Figure 10 Classifications of the uncertainties in structural modelling; (top) interpretation of a geological formation boundary based on ill-defined input data points (i.e. where the contact position itself is uncertain) and resulting uncertainty in the interpreted boundary, (middle) uncertainty of interpolation between and extrapolation away from known data points, (bottom) incomplete knowledge of structures in the subsurface, e.g. does a fault exist or not (Modified by Hall 2012, after Wellman et al. 2010).

Reducing parameter uncertainty associated with spatial interpolation may be achieved by using co-kriging. Co-kriging methods are used to take advantage of the covariance between two or more regionalized variables that are related, and are appropriate when the main attribute of interest (e.g., well data) is sparse, but related secondary information (e.g., seismic data) is abundant. Rogiers et al. (2012), for example, used air permeameter data as secondary variable to improve predictions of laboratory based K_s measurements (primary variable). The performance increased from R^2=0.35 for ordinary kriging (laboratory Ks only) to R^2=0.61 for co-kriging. Geostatistical-data-integration methods yield more-reliable reservoir models because they capitalize on the strengths of both data types. The mutual spatial behaviour of regionalized variables is known as co-regionalization (Ahmed et al., 1991; Almeida and Frykman, 1994; Fegh et al., 2013; Xu et al., 1992). These approaches assume multi-Gaussian distributions; hence, only the first two moments (mean and standard deviation) are reported from the interpolation. Other techniques such as Bayesian Maximum Entropy – BME (Christakos 2000; Christakos et al., 2002) are able to report the full probability density function (PDF) at interpolation nodes, which is advantageous for obtaining confidence intervals for non-Gaussian PDFs.

In the absence of sufficient prior information to characterise a parameter's probability density function, the uncertainty associated with a given parameter can be described using a uniform statistical distribution (i.e., all values between A and B are equally likely), a triangular distribution (highest probability for the mean value) or using a normal statistical distribution (i.e., a mean value is most likely and other values between A and B are variably less likely, depending upon their proximity to the mean). Lognormal transformations are recommended when the measurement range spans several orders of magnitude. The bounds of these statistical distributions are typically informed by expert opinion (i.e., local hydrogeologists, database ranges, or textbook ranges). The type of statistical parameter distributions can be estimated directly through the collection of such data, which may result in a unimodal, bimodal, or even multimodal distribution (Beerten et al., 2009). Alternatively, parameter distributions can be estimated indirectly through model inversion, in which parameter values are adjusted in order to match model outputs to state observations. This is essentially Bayesian theory in practice: updating prior distributions by matching calculated to observed states to derive posterior distributions. Normal (Gaussian or bell-shaped) distributions are the single most important and frequently-used distribution in statistical analysis; many statistical tests are based on an assumption of normally-distributed or normal data. For PDFs whose shape deviates from a bell-shape distribution (hydraulic conductivity is typically log-normally distributed), the skewness and kurtosis parameter are typically used to quantify the degree of non-normality, together with non-parametric tests such as the Shapiro-Wilk test (Shapiro and Wilk, 1965). If the original data are not normally distributed, several data transformations can be explored to convert the original non-normal data to a transformed normally distributed data set (see e.g. Mallants et al., 1996). The logarithmic transformation is often used for positively skewed data; the lognormal distribution is also commonly used as a model for groundwater data (US EPA, 2009).

1.3. Report Structure

This report provides an overview of approaches to the simulation of aquitards and geological faults in regional scale groundwater flow models used to estimate the impacts of coal seam gas (CSG) extraction. Here regional scale is defined as 10^4–10^5 metres in the horizontal plane (Dagan, 1986). For example, groundwater flow in the Surat Basin, Queensland has been modelled by the Office of Groundwater Impact Assessment (Section 4.1.1); this basin features a spatial extent of 660 km × 550 km.

Two aspects of the modelling process are examined in detail, particularly with regards to representations of aquitard units and geological faults. First, appropriate strategies for model parameter upscaling and spatial interpolation are examined, with respect to the representation of aquitard units in particular. Here, upscaling refers to a change in observation scale, which is often defined using the Representative Elementary Volume (REV) concept (Bear, 1972). Spatial interpolation refers to the estimation of parameter values in space; in the present study the interpolation is undertaken over regional scales. Second, numerical representations of geological faults and fractured zones in groundwater flow models are identified. In addition, local scale processes (e.g., multi-phase flow, dual porosity) that affect the prediction of CSG impacts are summarised and means of their representation are discussed. Throughout the report, available methods for the quantification of model and prediction uncertainty are discussed. It should be noted that the focus of the report is on

groundwater flow; in particular, hydraulic responses to groundwater extraction for CSG production. Therefore, the simulation of solute transport is not discussed, nor are responses to the reinjection of co-produced water.

The structure of the present report is as follows. First, four key local scale processes are briefly discussed: dual domain permeability and porosity, gas desorption, dual phase flow, and geomechanical deformation (Chapter 2). These are significant in terms of the accurate characterisation of groundwater extraction rates for CSG production and also in terms of the accurate simulation of drawdown impacts in the immediate vicinity of CSG extraction wells. Two key regional scale considerations are then discussed: (1) the upscaling and regionalisation of groundwater flow model parameters; and (2) the representation of structural features in such models (Chapter 3). The latter includes geological faults and fracture networks, both of which may compromise the capacity of aquitard units to limit the vertical propagation of hydraulic gradients resulting from CSG production. For both (1) and (2), various methods of representation developed in academic literature are described and compared. The final section of the report provides a synopsis of all publicly documented numerical groundwater flow models used for CSG production impact simulation in Australia to date (Chapter 4). Approaches used to upscale and regionalise parameter values are summarised, as are methods of representing geological faults and fracture networks. A summary of findings is provided in Chapter 5.

2. Local scale considerations for CSG reservoir simulation

The focus of the present overview is on the implementation of parameter upscaling approaches and the representation of structural features in regional scale groundwater flow models. Here regional scale is defined as 10^4–10^5 metres in the horizontal plane (Dagan, 1986). However, local scale physical processes relevant to simulation of aquitards and geological faults in regional scale groundwater flow models used to estimate the impacts of coal seam gas must also be represented to ensure the robustness of impact predictions. The representation of these processes can significantly affect the hydraulic response calculated at a local scale, which is subsequently propagated at a regional scale, typically by a coupled reservoir-regional groundwater model. These processes were summarised by Moore (2012) and CoA (2014a). Four key physical processes involved in coal seam gas extraction at a local scale are:

1. **Dual domain flow:** the flow of fluids between domains of contrasting properties; e.g., matrix–to-cleats flow in coal seams or matrix–to-fracture flow in fractured rock aquifers;
2. **Gas desorption:** the removal of gas from the surface of coal cleats due to a reduction in hydrostatic pressure;
3. **Dual phase flow:** the simultaneous flow of constituents of various phases (i.e., water and gas in the case of hydrocarbon extraction) and the existence of unsaturated flow conditions; and,
4. **Geomechanical deformation:** changes in (a) rock permeability and porosity and (b) fluid permeability due to geomechanical deformation resulting from decreases in water pressure and subsequent increases in stresses carried by the coal matrix and the fluid contained therein.

Each of these processes is described in Sections 2.1 to 2.4. In addition to these four processes, it is noted that significant variations in the temperature and salinity of fluids mobilised during coal seam gas extraction may possibly lead to density driven flow. Density driven flow has been studied extensively in the context of seawater intrusion (Kolditz et al. 1998) or saltwater upconing (Motz 1992), but much less so in the context of coal seam gas extraction. At minimum, head measurements should be carried out in conjunction with measurements of electrical conductivity from which one can determine if density corrections of measured head to fresh water heads are required. Practical guidelines have been developed by Post et al. (2007) to determine quantitatively when variably-density effects on groundwater flow need to be taken into account or can be justifiably neglected.

2.1. Dual domain permeability and porosity

The flow of methane from coal matrix to CSG well occurs sequentially via three separate processes (Figure 14). First, methane is desorbed from surfaces within the coal matrix. Second, methane is transported through the connected pores of the coal matrix to cleats and fractures via diffusive processes. Third, once present in the cleats or fractures of a coal formation, methane is transported to a CSG well via Darcian flow processes. Therefore, describing fluid flow in coal seams requires a dual domain approaches to permeability and porosity to represent differences in hydraulic properties between cleats and the surrounding coal matrix.

Permeability is defined as the ability of a rock, soil or sediment to yield or transmit a fluid. The magnitude of permeability depends largely on the porosity and the interconnectivity of pores and spaces in the medium of interest. Permeability units are expressed hereafter in mD (milliDarcy). Permeability may also be expressed in SI units of m^2. Conversion from mD to m^2 is calculated according to the following relationship: 1 mD is equal to 9.869233×10^{-16} m^2. Saturated hydraulic conductivity (K, $m.s^{-1}$) is related to permeability (κ, m^2) as follows:

$$K = \kappa f = \kappa \frac{\rho g}{\eta} \quad (1)$$

where f ($m^{-1}.s^{-1}$) is the fluidity of the permeating liquid, ρ is fluid density (998.23 $kg.m^{-3}$ at 20°C), η is dynamic viscosity (10^{-3} $kg.m^{-1}.s^{-1}$ at 20°C), and g is acceleration of gravity (9.81 $m.s^{-2}$). The conversion between K and κ depends on the viscosity and density of the fluid at a given temperature. At 20°C, the fluidity f for water becomes 9.79×10^{6} $m^{-1}.s^{-1}$. In hydrogeological studies, where the focus is on the flow of groundwater, density and viscosity of the underground water are supposed to be known. Hence, hydrogeologists use K ($m.s^{-1}$) rather than permeability (mD), which is determined by pore space microstructure only. One milliDarcy is approximately equal to 10^{-8} $m.s^{-1}$ if water at 20°C is the saturating fluid.

Over the years, many models have been developed to describe preferential flow processes. Figure 11 provides a useful schematic of increasingly complex models that have been used to simulate preferential-flow processes through fractured rock. The **equivalent porous medium model** represents the domain with either fractures or rock matrix, and its flow properties are characterised by a single equivalent porous medium relative permeability curve. The relative permeability is the ratio of the effective permeability (permeability of one fluid in the presence of another fluid) of a fluid at a given saturation to some base permeability, typically the absolute permeability (see further Section 2.3.1). The total flow through this fracture-matrix system is assumed to be equivalent to flow through a composite porous medium that has hydraulic properties comprising both fracture and matrix properties. In contrast, the **dual-porosity model** allows flow only through the fracture continuum; a relative permeability curve is defined for the fracture only. Another alternative, the **dual-permeability model**, represents the fractures and matrix domain as separate continua. Each continuum has its own relative permeability curve, i.e. flow exists in both continua. If a different pressure exists between fracture and matrix, flow occurs between the two continua. In addition to the above continuum models that do not explicitly model fractures, **discrete fracture models** exist that include individual fractures and their hydraulic properties. In discrete fracture models, the rock matrix can be impermeable or alternatively has sufficient porosity to allow for flow.

In terms of how to model the representations of porous media depicted in Figure 11 featuring distinct contrasts in hydraulic properties, such as fractured rock, coal seams, and limestone aquifers, subsurface fluid flow can be conceptualised in one of three ways: uniform flow, dual porosity or dual permeability (Šimůnek et al., 2003; Šimůnek and van Genuchten, 2006) (Figure 12). In a uniform flow approach (Figure 12a), the combined flow through both matrix and fractured domains can be represented by equivalent hydraulic properties that are averaged over the representative elementary volume [REV; Bear (1972)] of interest (also see equivalent porous medium in Figure 11). Dual porosity approaches (Figure 12b and the dual porosity representation in Figure 11) primarily represent fracture flow (white) with flow to or from the matrix (grey) typically represented by a specified transfer rate. For example, Gerke and van Genuchten (1993a; 1993b) derived physically-based transfer rate coefficients for variably saturated dual porosity flow models. Dual permeability approaches Figure 12c and the dual permeability representation in Figure 11) represent both flow with fractures and within the matrix, with exchange of flow between the two domains driven by a pressure gradient or water saturation (Šimůnek et al., 2003).

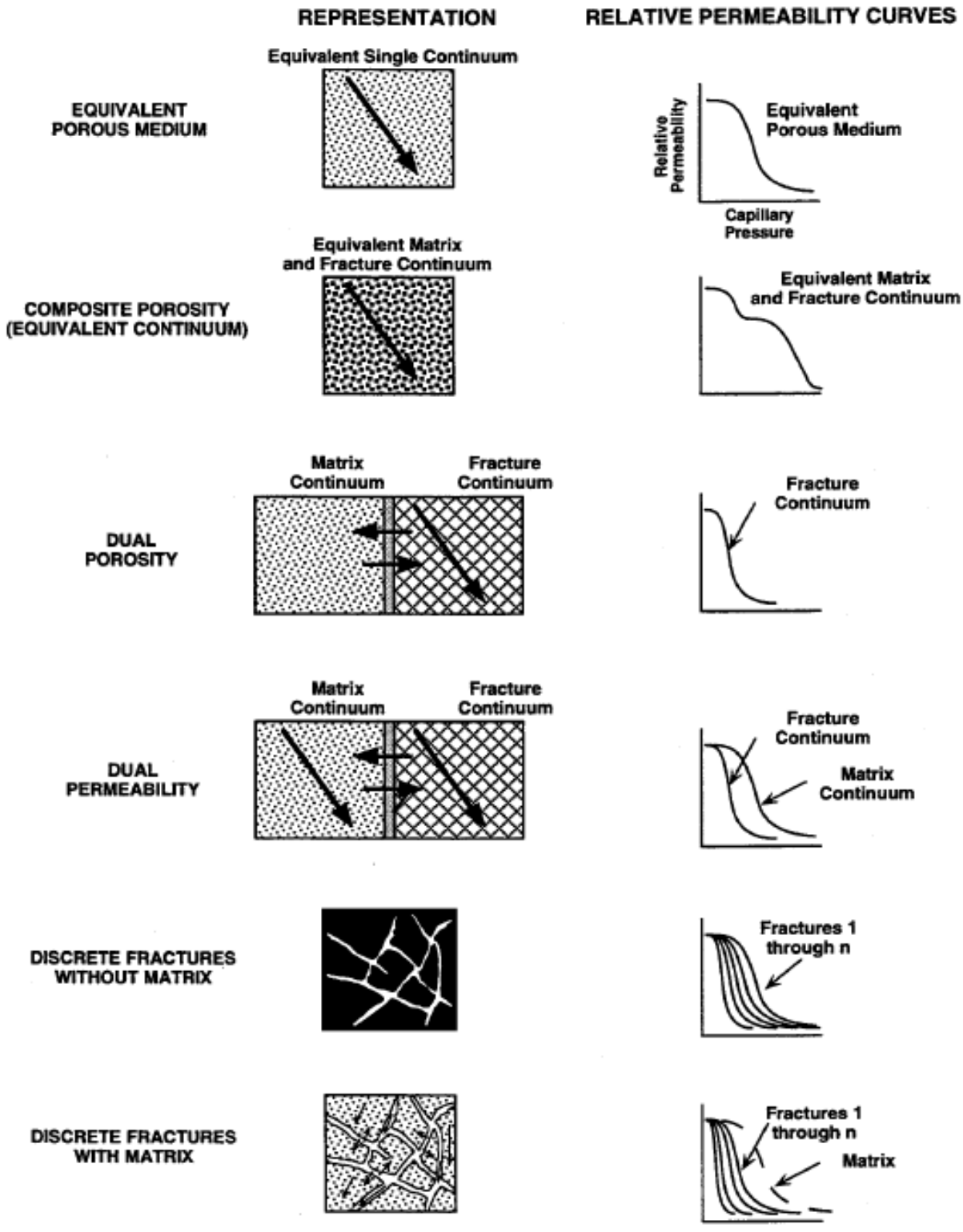

Figure 11. Conceptual models of flow through structured media (Altman et al., 1996).

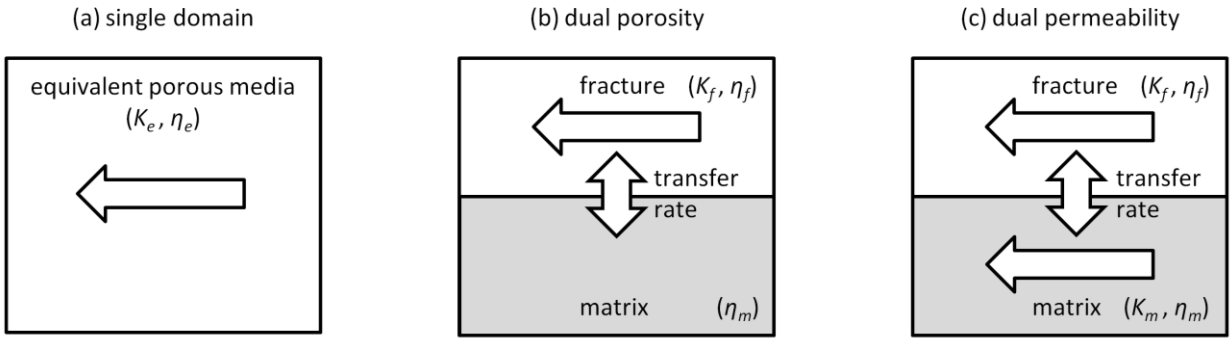

Figure 12. Comparison of (a) single domain, (b) dual porosity and (c) dual permeability approaches to groundwater flow [after Šimůnek and van Genuchten (2006)]. Symbols are defined as follows: K_e = equivalent hydraulic conductivity; η_e equivalent porosity; K_f = fracture conductivity; η_f = fracture porosity; η_m = matrix porosity; and K_m = matrix conductivity.

In order to simulate the simultaneous flow of water through both fractured and matrix domains, more complex dual-permeability models have been developed. Examples of dual-permeability models are given by (Gerke and van Genuchten, 1993a; 1993b; Jarvis, 1998; Liu et al., 1998; Liu et al., 2003; Pruess, 1991). These models all use different formulations for the water exchange between the fracture and matrix domains. A summary of various exchange (mass transfer) terms for dual-porosity and dual-permeability models is given by Šimůnek et al. (2003). Some descriptions of mass transfer for water are physically based, though approximate, while others are entirely empirical. The mass exchange for water can be based on water saturation (i.e., assumed to be proportional to the difference in effective water contents of the two regions) or pressure gradient (assumed to be proportional to the difference in pressure heads between the two pore regions). For porous media with well-defined geometries, the mass transfer coefficient can be defined by simple mathematical expressions (Gerke and van Genuchten, 1993a; 1993b). For rectangular domains, the mass transfer coefficient can be calculated as $3K_a/a^2$, where K_a is the effective hydraulic conductivity at or near the surface of the matrix–fracture interface and a is half the width of the matrix domain (Figure 13). It remains to be determined, however, whether these relationships are also applicable to coal.

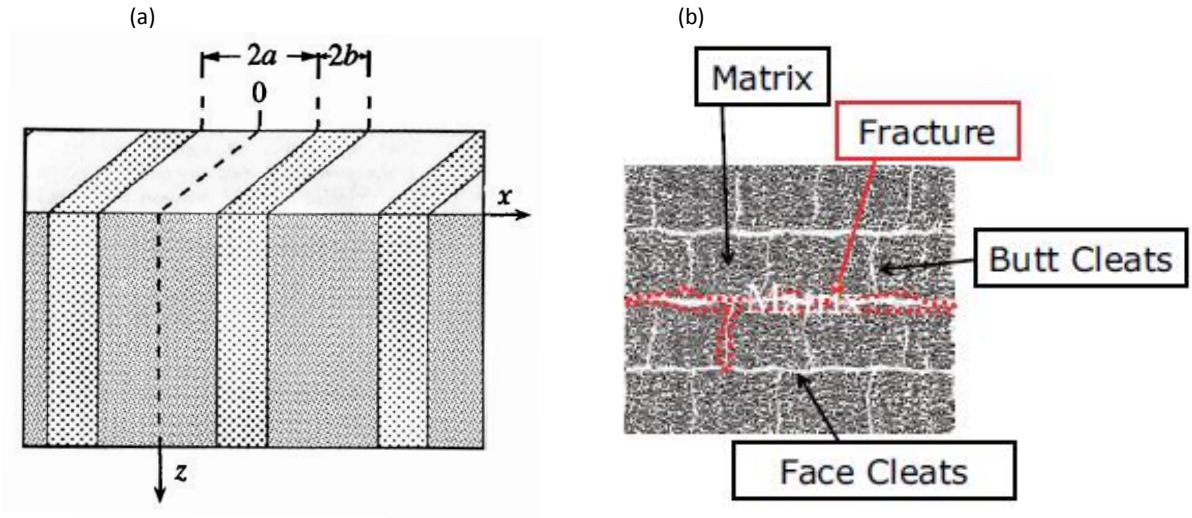

Figure 13. (a) Schematic illustration of rectangular parallel porous matrix blocks of width of 2a separated by fracture pore system of width 2b (Gerke and van Genuchten, 1993a; 1993b). (b) Schematic model of coal cleat and fracture system (Morad et al., 2008).

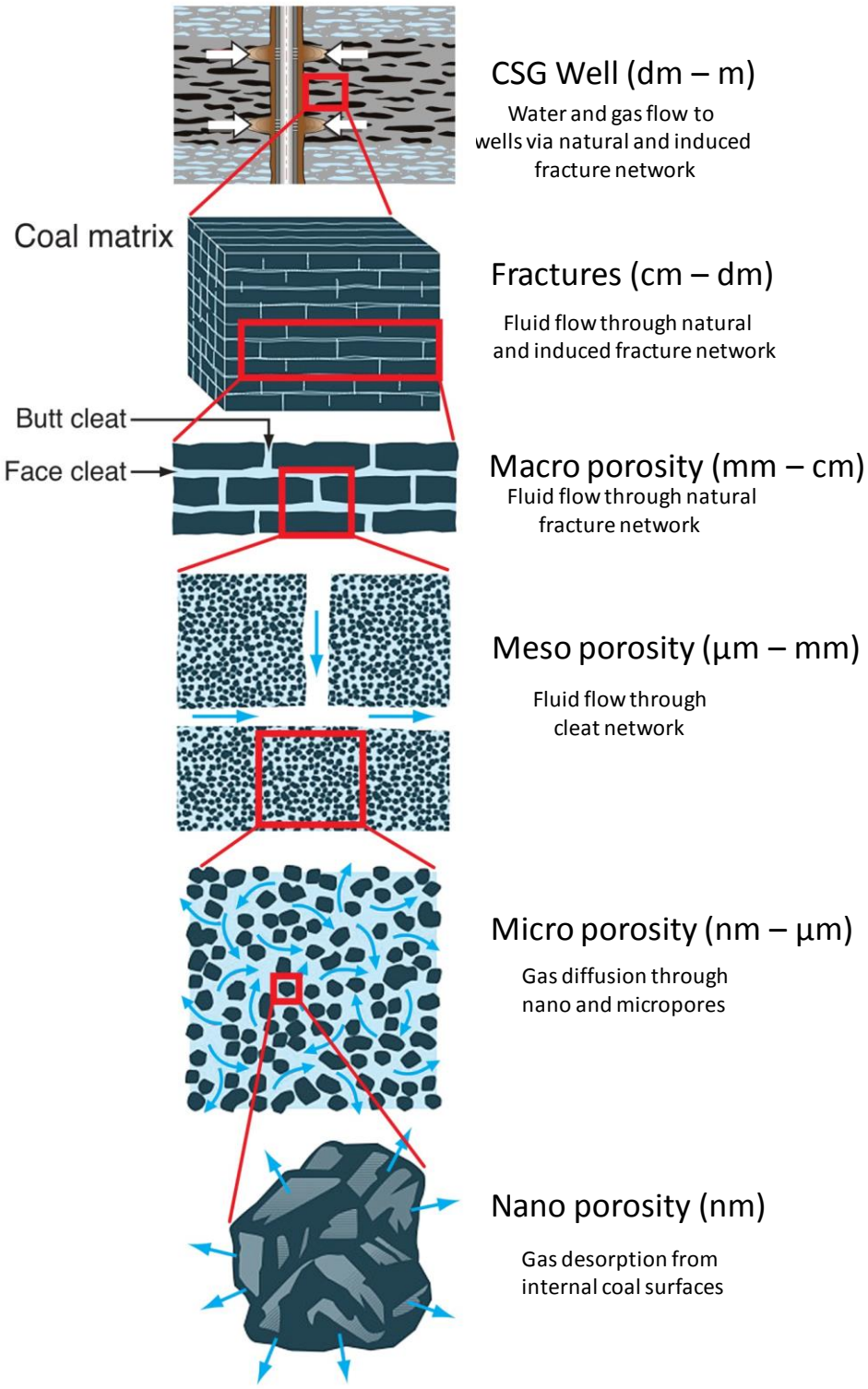

Figure 14. Multi-scale conceptualisation of methane gas liberation following depressurisation of the coal seam target formation. Methane desorbs from the surfaces and micropores of the coal matrix, then diffuses through the matrix, migrates into the cleats and fractures, and finally reaches the CSG well (adapted from Al-Jubori et al. 2009).

Coal seam gas reservoir models typically feature dual domain representations of hydraulic properties. Conversely, groundwater flow models used to propagate the effects of CSG depressurisation typically represent only matrix flow, although it should be recognised that the permeability of a coal cleat system will be higher than the matrix permeability of adjacent strata. Moore et al. (2014) compared the efficacy of reservoir and groundwater flow models for the representation of CSG extraction. They concluded that the coal and interburden components of coal measures should be

segregated, either explicitly (i.e., using discrete model layers) or implicitly, using a dual domain approach. Although relative permeability relationships were used, it should be noted that no distinction was made between the relative permeability of interburden and coal. This is important since, while coal is gas wetting, interburden material is water wetting (see Section 2.3.2 for a description of wettability).

With regards to the Australian context, the Queensland Gas Corporation GEN3 model (QGC, 2013) is an example of a dual porosity approach to the simulation of CSG-related groundwater extraction (see Section 4.1.4 for details). Uncertainty associated with dual domain approaches derives from a lack of knowledge of both the fraction of each domain present (relative distribution of n_f and n_m) and the value specified for the flow transfer rate. In addition, when the dual domain approach is applied to coal, an additional source of uncertainty is the rate of gas desorption from the coal matrix into the cleat.

In summary, the selection of an approach to representing dual domain water flow is dependent upon the aims of modelling and upon the availability and type of observation data. For accurate estimation of CSG groundwater extraction volumes and fluxes using local scale reservoir models, the use of a dual domain approach is crucial and commonplace. Conversely, when estimating the propagation of hydraulic responses incurred by CSG production over regional scales [i.e., 10^4–10^5 m; Dagan (1986)], a single domain equivalent porous medium approach may be appropriate. Examples exist, however, in which multiphase flow models have been applied at a regional scale (for example, the Queensland Gas Company's GEN3 model; see Section 4.1.4).

2.2. Gas desorption

Methane may be stored in coal seams in one of three states: free, absorbed or adsorbed. Free methane is present in open voids such as fractures (or as fluid located in the coal cleats) or in micropores unattached to the coal matrix. Absorbed methane is chemically held within the structure of coal material. Adsorbed methane is present on the surface of mainly micropores (as single or possibly double layers of molecules) within coal material (Moore, 2012). Coal seam gas refers to gas (typically methane) present in all of the above three states, but mainly adsorbed to the cleats of deep coal seams. Such gas reserves are retained in coal seams due to hydraulic pressure (Dallegge and Barker, 2000). Groundwater extraction leads to a reduction in reservoir pressure, thereby desorbing gas from the coal cleats. The rate at which gas desorption occurs with reducing pressure can be represented by a function known as an isotherm (Figure 15). The Langmuir isotherm (Langmuir, 1918) is the most commonly used isotherm for the simulation of coal seam gas production. Other isotherms include the Dubinin-Radushkevich model (Amankwah and Schwarz, 1995) and dual sorption model (Green and Selby, 1994). Desorbed gas replaces water and creates changes to coal seam permeability, as described by the relative permeability curves depicted in Figure 6. The simulation of simultaneous gas and water flow requires dual phase modelling approaches, as described in Section 2.3.

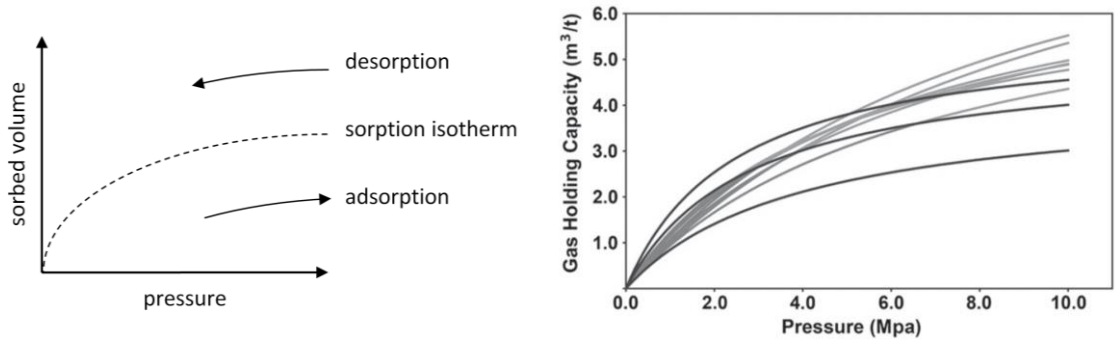

Figure 15. (left) Sorption processes as a function of hydrostatic pressure: sorption processes are described by a nonlinear isotherm (dashed line); adsorption (right arrow) of a constituent due to increased hydrostatic pressure results in an increased sorbed volume; conversely, desorption (left arrow) of a constituent due to reduced hydrostatic pressure results in a reduced sorbed volume [after Wang et al., (2014)]. (right) Nine adsorption isotherm test results from a single 5 m coal seams [Moore, 2012].

Uncertainties associated with the representation of gas adsorption processes primarily relate to sources of measurement error: handling procedures, incorrect moisture levels, methods used to compute gas density, and poor temperature and pressure calibration (Moore, 2012). Additional sources of uncertainty can be attributed to the heterogeneity within coal seams (Figure 15). Moore (2012) estimated the uncertainty of adsorption isotherms to range from 7 to 20%. However, it should also be noted that these isotherms typically describe the adsorption (rather than desorption) of gas molecules. It has been shown that gas sorption is a hysteretic process, much like the saturation–desaturation of porous media (Wang et al., 2014). In general, when an adsorption step follows a desorption step, the sorbed volume will be smaller than that initially present. Fully reversible hysteresis refers to cases where the shapes of adsorption and desorption isotherms may differ but the minimum adsorbed volume at minimum pressure is zero. Conversely, irreversible hysteresis refers to cases where the minimum adsorbed volume after desorption is nonzero. In an extensive review of methane data from 48 coal seams in 13 published studies, Wang et al. (2014) found that differences between adsorption and desorption isotherms were prevalent, illustrating the importance of hysteresis for coal seam gas recovery.

2.3. Dual phase flow

2.3.1. Relative permeability

Dual or two phase flow refers to the simultaneous flow of two fluid phases, typically water and either gas, oil or ice. In a coal seam gas context, dual phase flow refers specifically to the simultaneous flow of water and gas. If more than one fluid is present in the porous medium, the ability of the medium to transport one fluid depends on the amount of the other fluid. When two immiscible fluids (i.e., fluids that do not readily dissolve into one another) such as water and gas co-exist in a porous medium, their degree of saturation is expressed as S_l for liquid phase and S_g for gas phase, and $S_g + S_l = 1$ (or 100% if expressed as a percentage). For each phase (liquid or gas), a capillary pressure–relative saturation relationship exists (see Figure 16). To evaluate flow in such systems, both effective and relative permeability need to be considered (as described in Section 2.1). The effective permeability is a measure of the conductance of a porous medium for one fluid phase when the medium is saturated with more than one fluid. The relative permeability is the ratio of the effective permeability of a fluid at a given saturation to some base permeability, typically the absolute permeability (Amyx et al., 1960). The latter is the permeability of a porous medium saturated with a single fluid. If a single fluid is present in a rock, its relative permeability is 1. Absolute permeability is an intrinsic property of the rock, reflecting its internal structure; it does not depend on whether the fluid is oil or water (as long as the fluids are nonreactive with the rock). For gases the permeability is typically larger than the absolute permeability. Gas flow in pores is faster than liquid flow because liquids experience greater flow resistance at pore walls than do gases (Tanikawa and Shimamoto, 2006).

The absolute permeability of the rock is generally written as k. The effective permeability to a particular phase has subscripts as follows: k_w is effective permeability to water (units of milliDarcy, mD), and k_g is the effective permeability to gas (mD). Therefore, relative permeability to a particular phase is typically denoted with subscripts, where k_{rw} is relative permeability to water and k_{rg} relative permeability to gas.

In summary, the relative permeabilities to each of the two fluids water and gas can be written as (Amyx et al., 1960):

$$k_{r_w} = \frac{k_w}{k} \quad \text{and} \quad k_{r_g} = \frac{k_g}{k} \tag{2}$$

The sum of effective permeabilities is less than the absolute permeability because the fluids are immiscible, thus interfacial tension exists between the phases. The presence of more than one fluid in the same pores causes additional resistance to flow for both fluids.

The capillary pressure–relative saturation relationship for both water and gas flow depends on the direction of saturation change, which leads to the phenomena of hysteresis (Figure 16). Hysteresis will be explained here for water flow into and out of a conventional rock reservoir. The drainage curve is the relationship followed during dewatering of a conventional reservoir rock (the rock is considered water wet), i.e. we consider the displacement of water by a non-wetting fluid (gas or

oil or CO_2). Originally the rock was completely filled with water (water saturation of 100%). The non-wetting gas phase first enters the rock at entry pressure. As the capillary pressure increases, so does the gas saturation (and conversely, water saturation decreases). The arrows on the drainage curve show the direction of saturation change. By convention, because wetting-phase saturation is decreasing, it is called a drainage process. Water saturation continues to reduce until it reaches irreducible water saturation, S_{wi}.

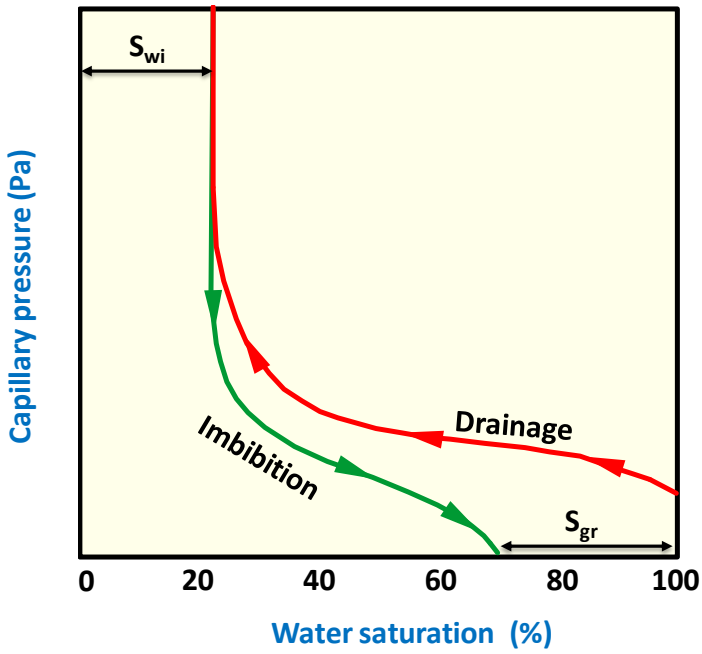

Figure 16. Hysteresis in capillary pressure for the water wet system. The primary drainage and imbibition curves bound the capillary-pressure relationship (S_{wi} = irreducible water saturation)

Assume next that the rock was at irreducible water saturation at the end of the water displacement phase. The imbibition curve is the path followed when water is now displacing the non-wetting fluid, starting at irreducible water saturation. In Figure 16, the arrows show the direction of saturation change. By convention, because wetting-phase saturation is increasing (water is being imbibed into the rock), the process is called imbibition. The imbibition curve terminates at water saturation less than 100% as not all the gas is displaced from the rock. The amount of gas trapped in an immobile state at the end of the imbibition process is the residual gas saturation, S_{gr}. The difference in paths between the drainage and imbibition curves is called hysteresis.

A somewhat similar hysteretic behaviour exists within the cleat system (where Darcy's law applies, see Figure 14) of coal seams, with characteristic capillary pressure – relative saturation curves. The hysteretic behaviour of capillary pressure – relative saturation curves and relative permeability curves (not shown) adds an additional level of complexity to the dual phase flow behaviour in coal formations. The determination of such relationships on coal and interburden and their incorporation in dual phase flow models remains a considerable challenge.

In coal seams that become depressurised due to removal of water, the gas which is adsorbed in the coal matrix begins to diffuse and enters the cleat/fracture system. Once the pressure drops in the cleat below the desorption pressure, gas begins to desorb and free methane gas saturation builds up within the cleat/fracture system. Two-phase flow now exists in the cleat system. As gas saturation continues to increase, water is displaced from the cleat space and the relative permeability of the coal to water and gas changes with gas impeding the passage of water. This type of behaviour is described by relative permeability curves shown in Figure 17. A typical example of a capillary pressure–liquid saturation curve and corresponding relative permeability curve is shown for a "water wet" clastic system in Figure 17(b).

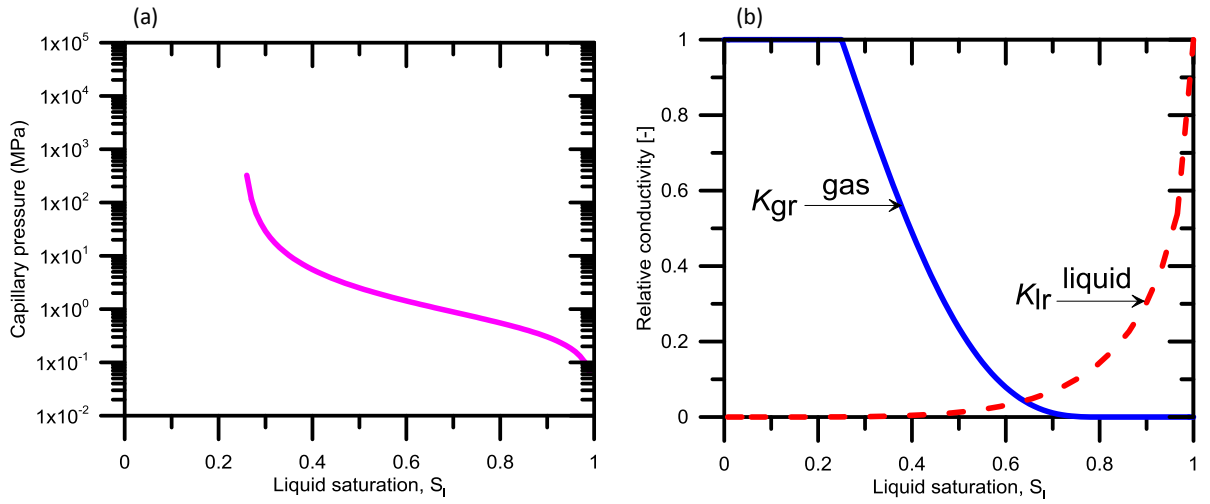

Figure 17. (a) Capillary pressure as function of water saturation, and (b) relative permeability for liquid (i.e. water) and gas of plastic Boom clay, Belgium as function of water saturation (Mallants et al., 2007). Clay is assumed to be water wetting. Mathematical models and parameters are defined in Table 2.

Reservoir models typically simulate dual phase flow while most groundwater flow models simulate single phase (i.e., water) flow only. A comprehensive summary of available multiphase flow models is presented in Appendix 1. Consideration of the gas phase can be important when calculating target pressures for coal seam depressurisation (OGIA pers. comm., 2015). The omission of dual phase effects in numerical flow modelling can result in significantly different impact predictions. In order to model the flow of gas, it is common practice to simulate a target pressure head equal to a hydraulic head of water located several tens of metres above the top of a target coal seam. However, in practice this pressure head will include both water and gas phases; therefore the required pressure head of water will be lower. The primary advantage of single phase models is their relatively lower computational requirements (and therefore short solution calculation times) in comparison to multiphase models. This is of particular benefit to models featuring large spatial extents and/or long hydraulic equilibration times. Low computational requirements are also of benefit to uncertainty quantification analyses, which often require the solution of 100s or 1000s of numerical models.

Table 2. Equations used to describe relative liquid and gas permeability and saturation for Figure 17 (ith., 2007). Parameter m was fitted to liquid saturation – capillary pressure data.

Parameter	Equation	Parameter values for plastic Boom clay, Belgium
Relative liquid permeability	$k_{rl} = \sqrt{S^*}\left\{1 - \left[1 - (S^*)^{1/m}\right]^m\right\}^2$	m = van Genuchten shape parameter (=0.5) S_l = liquid saturation
Relative gas permeability	$k_{rg} = \left(1 - \hat{S}\right)^2\left(1 - \hat{S}^2\right)$	S_{lr} = residual liquid saturation (=0.2)
Relative liquid saturation	$S^* = (S_l - S_{lr})/(S_{ls} - S_{lr})$	S_{ls} = saturated liquid saturation (=1.0)
Relative gas saturation	$\hat{S} = (S_1 - S_{lr})/\left(1 - S_{lr} - S_{gr}\right)$	S_{gr} = residual gas saturation (=0.15)

The water production curves in a CSG reservoir look similar to the production curves for a conventional productive aquifer. Maximum water production rates are achieved initially but decline thereafter through a combination of reservoir pressure decrease and decreasing relative permeability to water as the degree of gas desorption increases (Figure 18).

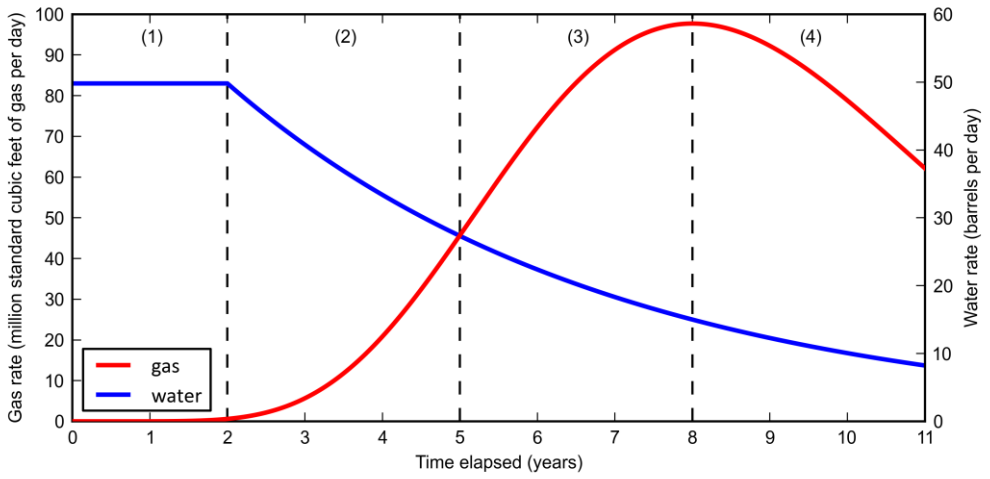

Figure 18. Example of a coal seam gas production profile, showing gas (red) and water (blue) production and highlighting four production phases: (1) constant water flow with negligible gas flow; (2) decreasing water flow with increasing gas flow, where water flow is dominant; (3) decreasing water flow with increasing gas flow, where gas flow is dominant; and (4) decreasing water flow with decreasing gas flow (after Morad et al., 2008).

From the discussion above it is clear that many factors confound the characterisation of relative permeability curves and their use in simulations of regional scale CSG impacts. Relative permeability relationships are not only inherently strongly nonlinear, they are also impacted by wetting considerations, hysteretic effects, and the heterogeneity of porous media. Relative permeability curves can be considered as spatially and temporally distributed relationships. This has important implications and challenges for deriving upscaled hydraulic properties that take account of dual phase processes for assessing CSG impacts. Despite this importance, examples in the literature on upscaling dual phase processes and hydraulic properties in the CSG context are scarce but include Moore et al. (2013; 2014a) and Herckenrath et al. (2015). Moore et al. (2014a) compared two methods of representing dual porosity effects in a single domain groundwater flow model used to assess regional impacts of CSG developments. A dual domain model was first implemented in the ECLIPSE simulator to explicitly represent coal and interburden facies of a coal measure, which then served as a yardstick for comparison with an upscaled single domain approach. Next, the effects of two different coal measure upscaling methods on relative permeability functions were investigated. The first method of simplification involved amalgamation of the coal and interburden facies, followed by property upscaling involving vertical averaging over both coal and interburden cells. A second method involved separating coal from interburden while preserving total coal and interburden thickness within any vertical grid column, yielding a small number of coal-only layers separated by correspondingly segregated interburden material. Upscaled properties were then calculated using a lithology specific vertically averaging process. While the former method was found to be completely unsuitable, the latter method was able to adequately reproduce the true nonlinear relative permeability versus saturation relationship.

Herckenrath et al. (2015) demonstrated use of the van Genuchten (1980) approximation of saturation-based permeability to simulate the hydraulic impacts of CSG extraction using a MODFLOW–USG model. Through comparisons to a multiphase reservoir simulation, the single phase model was found to simulate transient drawdown responses relatively accurately, despite errors in the approximation of saturation.

2.3.2. Wettability

An important rock property to consider in multi-phase flow (here the gas/water system) is wettability. The principles of wettability will be summarised here for the relatively well known system where the rock is the water-wetting phase. Wettability properties of coal seams and multi-phase flow in coal seams are much less well known and are the subject of ongoing research within the oil and gas industry. The current summary is necessarily simplified and limited, but provides basic processes that are relevant to coal seam multi-phase flow phenomena.

Wetting related forces can influence multi-phase fluid behaviour within aquifers in many ways, including desaturation-saturation history and relative permeability. Wettability describes the preference of a solid to be in contact with one fluid rather than another. A drop of a preferentially wetting fluid will displace another fluid on a rock surface; at the extreme it will spread over the entire surface. Conversely, if a non-wetting fluid is dropped onto a surface already covered by the wetting fluid it will bead up, minimizing its contact with the solid (rock). The balance of forces (surface tensions) in the hydrocarbon/water/rock system will result in a contact angle, Θ, between the fluids at the solid surface (Figure 19). The contact angle Θ is defined by the interfacial (boundary) tensions at the surface between different phases. When two or more fluids are present, there are at least three sets of forces acting on the fluids. The interfacial tensions used in Figure 19a are defined as: γ_{so} is the interfacial tension between rock surface and oil, γ_{sw} is the interfacial tension between the rock surface and water, and γ_{ow} is the interfacial tension between oil and water. The interfacial tensions are related through Young's equation:

$$\gamma_{SO} - \gamma_{SW} = \gamma_{WO} cos\theta \quad (3)$$

Note that (i) the contact angle Θ is always measured through the denser liquid phase (i.e. water in a water-oil or water-gas system), and (ii) oil is depicted in Figure 19a to represent the non-wetting phase.

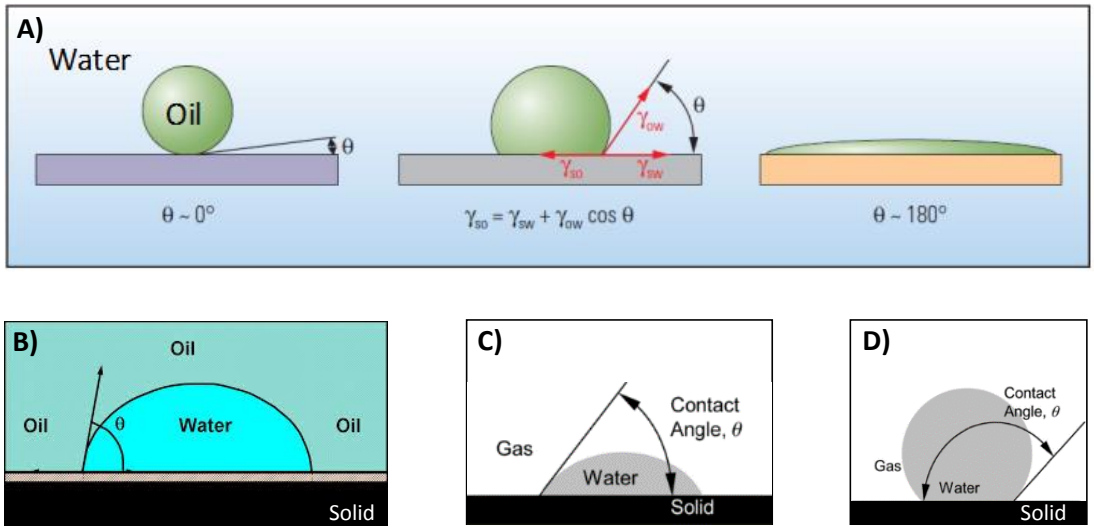

Figure 19. A) Principle of contact angle using oil as non-water wetting phase, surrounded by a water phase. An oil drop (green) surrounded by water (blue) on a water-wet surface (left) forms a bead. The contact angle Θ is approximately zero. On an oil-wet surface (right), the drop spreads, resulting in a contact angle of about 180°. An intermediate-wet surface (centre) also forms a bead, but the contact angle comes from a force balance among the interfacial tension terms, which are γ_{so} and γ_{sw} for the surface-oil and surface-water terms, respectively, and γ_{ow} for the oil-water term (Abdallah et al., 2007). B) Contact angle using water as the wetting phase, surrounded by an oil phase. C) Contact angle less than 90° for a water-gas system where water is the wetting phase. D) Contact angle greater than 90° for a water-gas system where water is the non-wetting phase.

In a homogeneous, porous material saturated with gas or oil and water, complete wetting (Θ = 0°) describes one end member of a continuum in which the rock surface strongly prefers contact with water (Figure 19b and c), i.e. water preferentially wets the rock surfaces (contact angle between rock and water is much less than 90°). This would likely occur in the siliciclastic rocks in between the coal seams. A strongly oil or gas-wetting surface prefers contact with oil or gas (this occurs at a contact angle greater than 90°, and would typically exist within the coal seams – see Figure 19d). Complete non-wetting occurs for Θ = 180°. Degrees of wetting apply along the continuum, and if the rock surface does not have a marked preference for one fluid over the other, its condition is termed intermediate wetting or neutral-wetting (a contact angle of approximately 90°) (see Iglauer et al. (2014) for wettability states and corresponding contact angles).

A non-wetting phase like oil or gas does not preferentially wet the rock surface. Repulsive forces between rock and fluid cause the non-wetting phase to preferentially occupy pores with larger pore throat radii (this could also end up being

larger pores but not always). Therefore, a non-wetting phase fluid is often the most mobile fluid, especially at large non-wetting phase saturations. Natural gas is never the wetting phase in hydrocarbon reservoirs.

Pore surfaces in low permeability reservoirs with a high organic content would most likely be gas-wet, whereas in the interburden pore surfaces are more likely to be water-wet, although transient changes in wettability also occurs. Laboratory experimentation indicates that as the saturation of the non-wetting phase increases with increasing capillary pressure then the wettability can shift where the initially non-wetting phase can become more wetting (Venkataramanan et al., 2014). This can then create a situation where the relative permeability is also transient.

2.4. Geomechanical deformation

The production of coal seam gas can impose geomechanical stresses upon a gas reservoir. Depending upon the geomechanical properties of the host rock, such stresses can potentially result in changes to the rock properties and thus relative permeabilities that affect dual phase flow behaviour in the reservoir. When changes in reservoir structure occur, this results in changes to the rate of dual phase flow to a CSG production bore. As gas is produced from a CSG reservoir, two distinct and opposing phenomena occur that can affect the absolute permeability of the cleat system (Morad et al., 2008):

- The decrease in reservoir pressure reduces the pressure in the cleats. Cleat net effective stress (which is the difference between overburden stress and pore pressure) can cause changes in cleat permeability. Depending upon the orientation of cleats relative to the in-situ stress orientation, cleat compression or dilation may result in either the reduction or enhancement of cleat permeability, respectively.
- Desorption of gas from the coal matrix results in shrinkage of the matrix. Shrinkage causes the space within the cleats to widen and the permeability of the cleats increases.

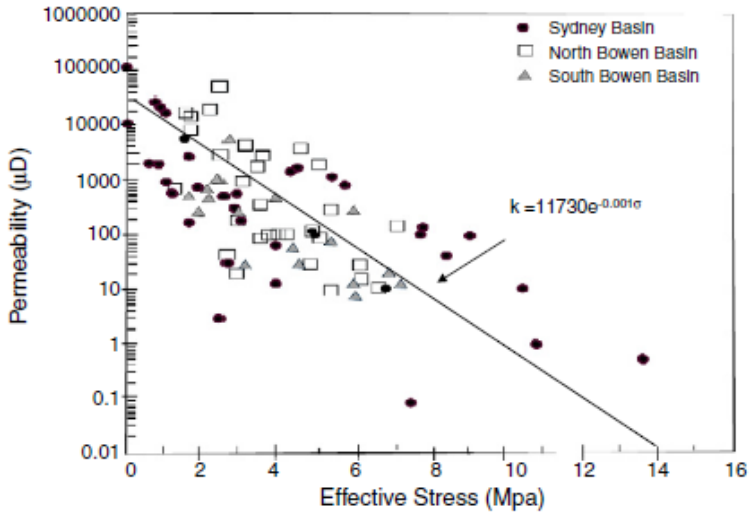

Figure 20. Coal seam permeability as a function of reservoir stress [Enever and Henning (1997) in Pan and Connell (2012)].

CoA (2014b) reviewed modelled predictions of subsidence produced for Environmental Impact Statement studies for future CSG projects in Australia. Land surface subsidence of up to 300 mm was predicted for Santos developments in the Bowen and Surat basins. The submission for the APLNG project predicted that subsidence was unlikely to be expressed at land surface as shallower consolidated and competent rock may operate as a "bridge" to restrict downward movement (CoA, 2014b). These predictions are currently limited by a lack of characterisation of rock geomechanical properties. The uncertainty of these types of predictions could, in future, be constrained significantly through the systematic investigation of such properties.

3. Considerations for regional scale groundwater flow modelling

Coal seam gas production processes occur at the local scale and result in the alteration of pressures within a coal formation. Coal measures are typically part of a larger groundwater basin comprising a sedimentary sequence of aquitards and aquifers. The potential propagation of CSG depressurisation impacts through such a sequence may occur at a broader (i.e., regional) scales, depending upon the size of one or a number of CSG developments. Here regional scale is defined as 10^4–10^5 metres in the horizontal plane (Dagan, 1986). Groundwater flow models used to simulate the potential for impacts from CSG extraction are developed at the regional scale; however, the parameterisation of such models is typically based (directly or indirectly) on data observed at much smaller scales. This is partly because regional scale observations are difficult or are the subject of current research and such methods have not yet become standard practice in a CSG context. For example, the use of environmental tracer data to assist the robust estimation of predictions has been demonstrated in a number of contexts. These include the estimation of regional scale groundwater connectivity, the derivation of flow velocities (and groundwater residence times), and the quantification of surface water-groundwater interactions. Potential exists for broader uptake of these methods in CSG impact assessments. Of the applications listed, the characterisation of surface water–groundwater connectivity is of particular relevance to CSG impact assessment, in order to estimate potential effects on surficial groundwater water ecosystems. Despite advances in regional scale observations, the majority of groundwater flow related properties will likely remain of a local-scale nature. For this reason, an upscaling process is required to translate parameter values between the two scales.

When upscaling hydraulic properties for inclusion in groundwater flow models, care should be taken to ensure that the scale of determination (by measurement or modelling) encompasses all heterogeneities relevant at the scale of the cellular numerical groundwater flow model. Methods to determine subsurface hydraulic properties, either directly or indirectly, range in scale from core scale (i.e., 10^{-1}–10^0 m) to regional scale (i.e., 10^4–10^5 m). Core scale observations may include permeametry testing of core scale permeability and porosity. Bore scale observations may include a range of hydraulic, geophysical and hydrochemical testing methods. Regional scale estimates of hydraulic properties may be obtained from environmental tracer observations or inverse numerical modelling.

As stated previously, the representation of aquitards and geological faults in numerical simulations of CSG impacts on groundwater resources is the primary focus of this report. In this context, two key points should be considered when developing a regional scale groundwater flow model to simulate the propagation of CSG impacts. The first point relates to the parameterisation of the model and involves a two-step approach (Tran, 1996). The first step relates to the method(s) by which small scale estimates of hydraulic properties may be upscaled to the scale of numerical model cells (typically 1 km × 1 km in horizontal extent) to obtain equivalent properties and their spatial statistics (e.g. probability density function and variogram). Equivalent properties such as hydraulic conductivity K are representative for larger model blocks and obtained by averaging a given property distribution over a finer grid. The spatial averaging method is typically based on numerical modelling; hence the equivalent properties are therefore valid only for a specific set of groundwater flow boundary conditions.

The second step involves the spatial interpolation of the upscaled hydraulic properties; the latter are typically available only at a limited number of locations. This involves the interpolation (i.e. estimation between observations) of hydraulic property values at a single scale, i.e. the regional modelling scale. Typically, for regional scale numerical groundwater flow models, this is undertaken in the areal plane on a layer-by-layer basis. Where a sufficient spatial distribution of hydraulic property observations exists, spatial interpolation is typically informed by the spatial correlation structure between the observations.

The second key point relates to the method(s) used to represent structural features (such as geological faults) in numerical groundwater flow models. In contexts featuring a high degree of past geological activity and deformation, such features

can have significant effects on a groundwater flow system (an overview of impacts of faults on regional groundwater flow systems is provided in Underschultz et al. (2016).

An ancillary point of consideration is that a single groundwater flow model typically is not the most effective way to simulate physical processes at both local and regional scales; one of the reasons being, apart from the scale issue, that groundwater models generally lack the specific capabilities to simulate CSG-specific processes such as gas desorption, dual-phase flow and dual porosity/permeability. For example, the volume of water extracted for CSG operations and the magnitude of the resulting depressurisation is typically estimated using a reservoir model such as ECLIPSE (Schlumberger, 2011) or GEM (Computer Modeling Group, 2003). These results are then used as input (i.e., boundary conditions) in a regional scale numerical groundwater flow model [e.g., using software such as MODFLOW (Harbaugh, 2005) or FEFLOW (Diersch, 2005)]. The means of coupling two such models is therefore a further key consideration when simulating the potential impacts of CSG production.

This Chapter includes a review of hydraulic conductivity measurement methods (Section 3.1), a discussion on parameter upscaling (Section 3.2) and structural features (faults and fractured zones) and their representation in groundwater models (Section 3.3).

3.1. Review of hydraulic conductivity measurement methods

It is important to recognise that various methods of measuring hydraulic conductivity are available, each of which correspond to a unique spatial scale. When characterising a groundwater flow system using multiple multi-scale observations, these require simultaneous upscaling and integration. For instance, hydraulic conductivity measurements may exist at each of the five spatial scales shown in Figure 21.

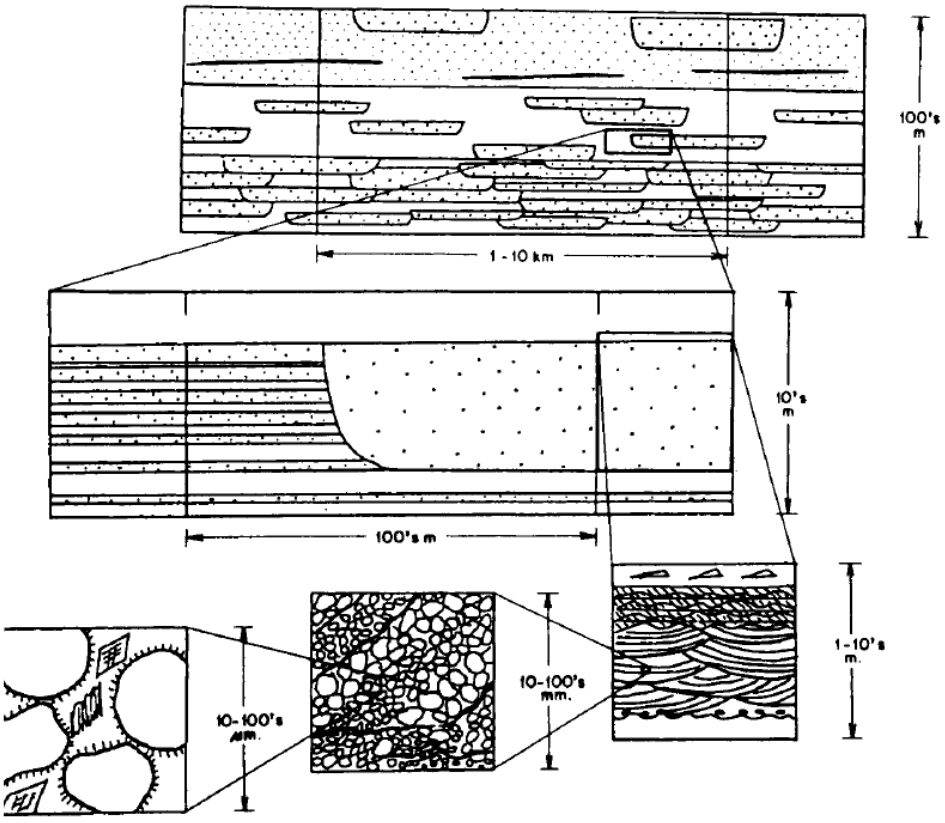

Figure 21. Iterative reduction in representative elementary volume (i.e., scale) of observation, from regional scale to pore scale (Weber, 1986).

At the largest scale, hydraulic conductivities are typically derived through inverse modelling involving matching groundwater flow model outputs to observation data, such as hydraulic heads (Laloy et al., 2013). At the next largest scale, pump tests may be applied (Bredehoeft et al., 1983). At the next scale, hydraulic conductivity may be derived from slug tests, single well tests with packers or drill stem tests (QWC, 2012). Core-scale measurements are typically used at the centimetre to decimetre scale (QGC, 2013). For micro- or even nano-meter scale hydraulic conductivities pore-scale modelling can be applied based on reconstructed 3-D pore models derived from micro-computed tomography images (Gerke et al., 2013).

Methods for obtaining hydraulic properties are summarised in Table 3. Hydraulic property observations are summarised in terms of increasing measurement scale, ranging from core scale to regional scale. A detailed discussion of the main three observation/measurement scales is provided in Sections 3.1.1 to 3.1.3 .

Table 3. Summary of methods available for the measurement of hydraulic parameters.

Method type	Test method		Measurement scale	Observation	Derived property
Hydraulic, laboratory based	Permeameter tests	Constant head	Core-scale. Point values conducted on small samples, often collected during drilling	Flux	Hydraulic conductivity
		Triaxial cell		Flux	
		Centrifuge		Flux	
		Gas		Flux	
	Air permeameter		Core-scale	Pressure	
	Pore-scale modelling based on micro-CT images or mercury porosimetry		Core-scale	Porosity	
Hydraulic, field based	Single well	Slug test	Bore-scale. Near the borehole; intervals when using packers	Pressure	Hydraulic conductivity
		Drill stem test	Bore-scale. Near the borehole; intervals when using packers	Pressure	Hydraulic conductivity, storage
		Flow meters	Bore-scale	Heat flux, EM current, acoustic	Hydraulic conductivity
		Pump test	Bore-scale. Larger than the borehole; intervals when using packers	Pressure	Hydraulic conductivity
	Multiple wells		Bore-scale. Averaged over a large aquifer volume, identify anisotropy	Pressure	Hydraulic conductivity, storage
	Passive test		Bore-scale. Averaged over entire aquitard	Pressure	Hydraulic conductivity
	Time series analysis		Bore-scale. Averaged over entire aquitard	Pressure	Hydraulic conductivity
Geophysical	Gamma ray, neutron density, and/or sonic logs		Bore-scale. Near the borehole	Porosity	Hydraulic conductivity

Tracer, field/regional-based	Artificial tracers	Bore-scale	Tracer concentration	Hydraulic conductivity

3.1.1. Core scale observations

Here we refer to observations of hydraulic properties that are integrated over a representative elementary volume that corresponds to a typical core volume of ~100 – 1000 cm^3 or a characteristic length of 0.1 - 1 metres (Dagan, 1986). Multiple observations from a single hydrostratigraphic unit are required to estimate the statistical distribution of facies present.

Undisturbed cores obtained from stratigraphic units can be tested to obtain an estimate of permeability. Permeability testing is typically undertaken using either a fluid or gas permeameter (Corey, 1986; Klinkenberg, 1941; Springer et al., 1998). The latter approach includes hand-held air permeameters, typically used to sample outcrop permeability (Eijpe and Weber, 1971; Rogiers et al., 2013), and laboratory methods using inert gases such as nitrogen. More recently, centrifuge methods have been developed (Conca and Wright, 1998; Wright et al., 2002; Timms et al., 2015). For cores obtained at significant depth, pressure can be artificially applied during permeameter testing in order to represent the overburden pressure present under in-situ conditions. Failure to account for in-situ pressure can lead to overestimation of hydraulic conductivity (Enever et al., 1994).

In addition to permeametry-based techniques, hydrochemical and isotopic analyses provide additional means of constraining estimates of hydraulic properties. For example, the helium-4 content of pore water can be measured from cores obtained along a vertical profile within a given stratigraphic unit (i.e. aquitard). The concentration profile observed along the vertical profile can then be used to derive a formation scale vertical hydraulic conductivity (Gardner et al., 2012; Harrington et al., 2013), as further discussed in Section 3.1.2. A similar method involves analysis of the helium-4 content of quartz grains contained in a given low-permeability stratigraphic unit (Smith et al., 2013). Although the initial measurements of tracer concentrations are made on typical core volumes of ~100 cm^3, the derived hydraulic conductivities represent an average value across an entire profile potentially spanning hundreds of meters. In this way the indirectly measured hydraulic conductivity itself is an upscaled value as it is an average or equivalent value that captures the integral effect of small-scale variability across a formation.

Core scale values of hydraulic properties have been used for upscaling to allow both groundwater flow and solute transport simulations. For example, Bianchi et al. (2011) upscaled core scale observations in order to investigate the degree of spatial connectivity in a small portion of highly heterogeneous aquifer at the Macrodispersion Experiment site in Columbus, Mississippi, on the migration of a tracer. Rogiers et al. (2014a) obtained an improved groundwater model performance when a geostatistical approach to generate spatially variable *K* values was compared with a previously developed groundwater model with spatially uniform *K* values for the different hydrogeological units. The geostatistical approach involved generating 3-D realisations of K_H and K_V values (using ordinary kriging and sequential Gaussian simulation) that were conditioned to core scale and cone penetration test-based *K* observations, which were then upscaled using arithmetic mean for K_H and harmonic mean for K_V.

The upscaling of hydraulic properties from core scale observations is subject to a number of sources of uncertainty. Where properties vary with depth within a given stratigraphic unit, values obtained from core testing may vary accordingly, either randomly or according to an underlying structure. A summary of various sources of uncertainty associated with geostatistically-based methods of parameter upscaling, including mean values and variogram parameters, is available from Khan and Deutsch (2015).

3.1.2. Bore scale observations

Here we refer to observations of hydraulic properties that are integrated over a representative elementary volume that corresponds to the volume of subsurface sampled by bore-based observations. The bore (i.e., formation or local) scale is

defined as being of the order of formation thickness (i.e., ~10^1-10^2 m) in the vertical direction and of the same order in the horizontal plane (Dagan, 1986). A range of bore scale methods for determining the hydraulic properties of aquitards were reviewed by van der Kamp (2001). Such observations often sample the full vertical extent of a hydrostratigraphic unit, or portions thereof using hydraulic packers that isolate sections of a borehole. This allows for the identification of multiple facies within a given hydrostratigraphic unit (HSU). For hydraulic testing methods, the sample volume (while primarily a function of the hydraulic parameters themselves) will typically be proportional to the duration of the test. The measurement volume can be easily several tens to hundreds of m^3. For petrophysical observations that may be used to indirectly estimate hydraulic conductivity (Rubin and Hubbard, 2006; Vereecken et al., 2006; Yand and Aplin, 2010), the sample volume will be only slightly greater than the circumference of the bore sampled, as geophysical wireline logging tools do not typically sample far beyond the bore casing.

Estimates of hydraulic properties at the bore scale typically involve hydraulic testing. This may involve the removal (i.e., pump test) or addition (i.e., slug test) of a known volume of water from or to a bore. Pump testing may be performed once or many times (i.e., step testing – using increasing pumping rates). Hydraulic properties are subsequently estimated from the transient hydraulic response observed. Alternatively, drill stem testing may be undertaken to estimate hydraulic properties during bore installation. This typically involves isolating a hydrostratigraphic unit of interest using inflatable packers and circulating fluids through the drill bit. Hydraulic properties are subsequently estimated from the rate of fluid circulation observed (Kruseman and de Ridder, 1990).

The hydraulic response of a bore (that is, the time and amount of groundwater level recovery or decline required to achieve equilibrium conditions) is interpreted using analytical solutions of the one-dimensional diffusion equation [Kruseman and de Ridder (1990): e.g., Theis (1935), Cooper and Jacob (1946), Hantush (1966), Bouwer and Rice (1976)]. These solutions provide estimates of hydraulic conductivity and storativity (*S*). For pump tests, the length of time over which the test is undertaken is generally considered to correlate with the volume of aquifer sampled. Because hydraulic tests sample relatively large regions of an aquifer, zones of both high and low conductivity contribute to flow, although the contribution from the former generally exceeds that of the latter. For this reason, they produce hydraulic conductivity estimates that effectively average the response from high-conductivity and low-conductivity zones. As such, they can be considered as large-scale equivalent conductivities.

A second approach to obtaining bore scale observations of hydraulic properties is the use of downhole geophysical logging tools (Balan et al., 1995; Jorgensen, 1989; Van der Baan and Jutten, 2000). For example, the dual density and neutron porosity logs plus the gamma ray log can be used to determine in-situ porosity and to qualitatively define lithology. Using empirical relationships, preferably calibrated at the site of interest, porosity values can then be used to estimate hydraulic conductivity (Table 4; Figure 22). Importantly, data obtained from downhole geophysics can be used to examine the variability of hydraulic properties in the vertical plane, within a given stratigraphic unit. For example, an upward fining trend is often observed in sedimentary units, owing to the decreasing level of energy involved in deposition. Where a stratigraphic unit is discretised into a number of model layers, such information could be used to inform parameter variability either directly or via an ensemble of stochastic realisations.

Table 4. Summary of empirical models for estimating porosity (η_d and η_s) and permeability (k) from geophysical measurements

Hydraulic property	Reference	Empirical model	Model parameters
permeability	Jorgensen (1989)	$k = \frac{C}{{S_s}^2}\frac{\eta^{m+2}}{1-\eta^2} = \frac{C}{{S_s}^2}P$ $\cong 1.828\ P^{1.1}$	C = Kozeny coefficient (-); S_s: specific surface area of the solids per unit volume of solids (m^2); η = porosity (-); m: cementation factor (-); P: porosity factor (-)
	Bourbie et al., (1987)	$k = d^2\eta^m$	d = grain diameter (m); η = porosity (-); m = exponent (-); ≥7 for porosities below 5% to ≤2 for porosities above 30%
	Timur equation (Schlumberger, 1991):	$k = 10000\frac{\eta^{4.5}}{{S_{wi}}^2}$ or $k = 8581\frac{\eta^{4.4}}{{S_{wi}}^2}$	S_{wi} = irreducible water saturation (-); η: porosity (-)
	Tixier equation (Schlumberger, 1991):	$k = 63500\frac{\eta^6}{{S_{wi}}^2}$	S_{wi} = irreducible water saturation (-); η = porosity (-)
	Coates equation (Schlumberger, 1991):	$k = 4900\eta^4\frac{(1-S_{wi})^2}{{S_{wi}}^2}$	S_{wi} = irreducible water saturation (-); η = porosity (-)
	Coates-Dumanoir equation (Schlumberger, 1991):	$k = 90000\frac{\eta^{2m}}{m^4{S_{wi}}^2}$	S_{wi} = irreducible water saturation (-); η = porosity (-); m = exponent (-)
porosity (bulk density log)	Bassiouni (1994)	$\eta_d = \frac{\rho_g - \rho_b}{\rho_g - \rho_f}$	ρ_b = wireline bulk density ($g.cm^{-3}$); ρ_f = fluid density ($g.cm^{-3}$); 0.2 for gas, 0.85 for oil and 1.0–1.2 for water; ρ_g = grain density ($g.cm^{-3}$); often taken as 2.65 (sandstone), 2.87 (dolomite), 1.2 (coal)
porosity (sonic log)	Raymer-Hunt-Gardner (1980)	$\eta_s = \frac{5}{8}\left(\frac{\Delta t_{log} - \Delta t_{matrix}}{\Delta t_{log}}\right)$	Δt_{log}= sonic log transit time ($\mu sec.m^{-1}$); Δt_{matrix}= formation matrix transit time ($\mu sec.m^{-1}$), 167-182 (sandstone), 143 (dolomite)

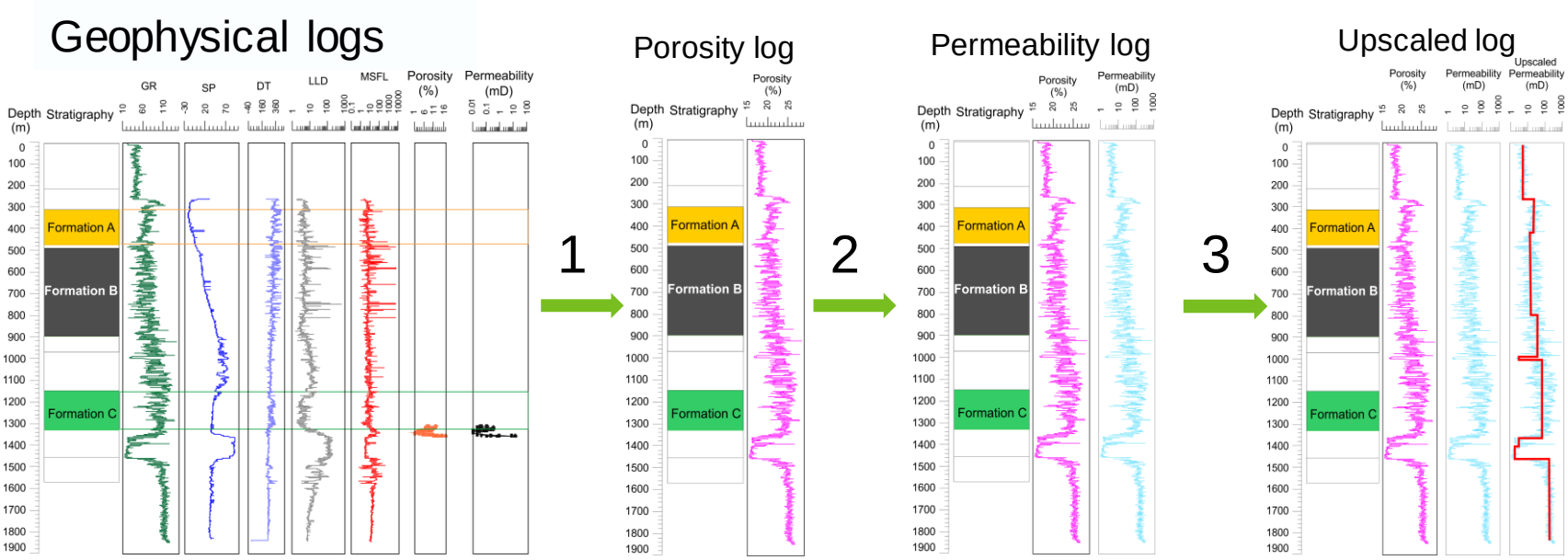

Figure 22. Workflow for developing permeability estimates from geophysical wireline logs (GR = gamma ray; SP = sonic potential; DT = sonic log travel time; LLD = Laterolog Deep (resistivity); MSFL = Microspherically Focused Log (resistivity)). Step 1 = applying physical model to estimate porosity. Step 2 = applying empirical model to estimate permeability. Step 3 = vertical upscaling of permeability (Ricard et al., 2014).

The combination of petrophysical logs (e.g., sonic, density and neutron) may be used to interpret complex matrix and fluid mixtures, thereby providing a more accurate determination of porosity. The combination of neutron and density logs is the most common of all porosity estimation tool pairs. Figure 23 shows an example application where five different methods for estimating porosity were compared. Generally, the minimum and maximum porosity at any depth differed by no more than 10 %. This provides an indication of the uncertainty associated with estimates of porosity, which can then be used to derive uncertainty about related permeability predictions. In addition to uncertainties related to predicting hydrogeological properties such as porosity and permeability from the signal there are intrinsic uncertainties associated with the measurements themselves (Fournier et al. 2013; e.g. Wessling et al. 2013).

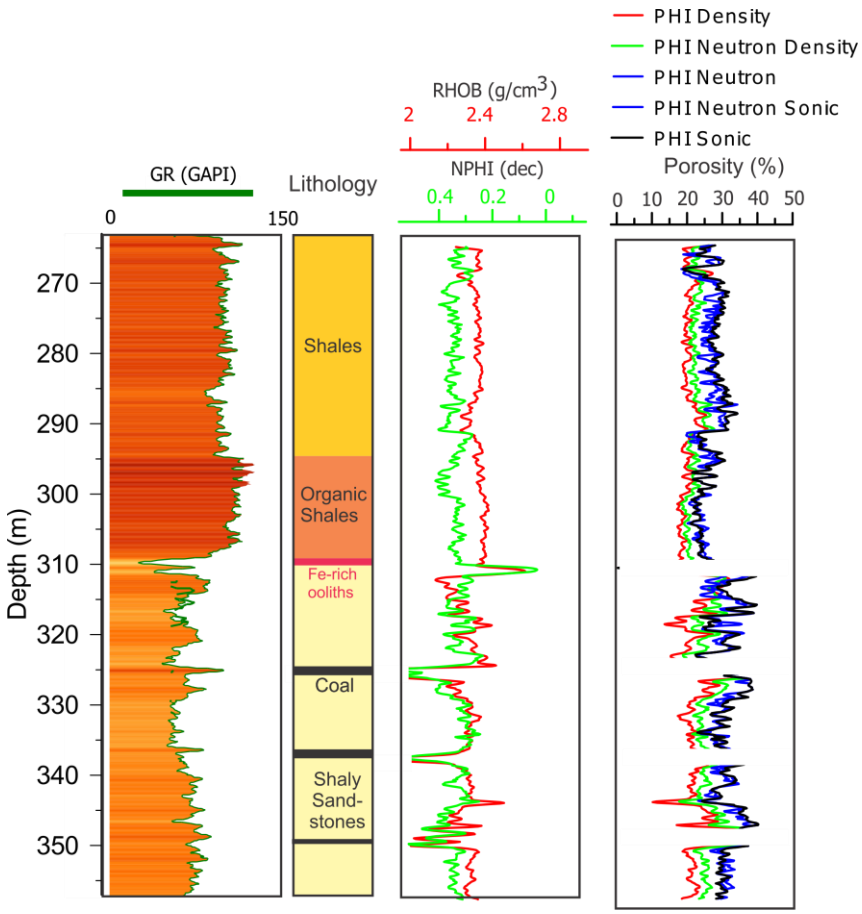

Figure 23. Geophysical wireline logs for porosity estimation. From left to right: natural Gamma ray log (API = American Petroleum Institute units), lithology, bulk density log (RHOB) and neutron porosity log (NPHI), five different estimates of porosity. PHI density = porosity derived from bulk density log; PHI neutron density = porosity derived from both bulk density and neutron log; PHI neutron = porosity derived from both bulk density and neutron log; PHI neutron sonic = porosity derived from both neutron and sonic log; PHI sonic = porosity derived from sonic log (Ricard et al., 2014).

A third approach to obtaining bore scale observations of hydraulic properties is the use of time series analysis techniques. Such methods involve calculating the delay or attenuation observed between a source signal and a response signal. Source signal types include fluctuations in barometric pressure, earth tides, ocean tides, or the time varying pressure load of an overlying HSU. The hydraulic response is observed as time series observations of groundwater levels, hydraulic heads or pore pressures in the HSU of interest. For example, Smith et al. (2013) analysed the pore pressure response to barometric fluctuations in order to estimate storage properties of a claystone aquitard in Saskatchewan, Canada. Aquitard observations were obtained from vibrating wire piezometers that were installed during observation well installation. Pore pressure observations were recorded every 30 minutes for a three month period. Specific storage values obtained were found to be comparable to in-situ estimates and were up to an order of magnitude smaller than laboratory-based estimates of specific storage. The latter result is consistent with the historical overestimation of compressibility (and therefore specific storage) by laboratory-based methods. Smerdon et al. (2014) used a similar approach to estimate the

storage properties of a shale aquitard in the Great Artesian Basin. In addition, the pore pressure response to initial well installation was used to estimate aquitard hydraulic conductivity. Rates of hydraulic conductivity were found to be within one order of magnitude of estimates obtained from laboratory-based methods and inverse modelling.

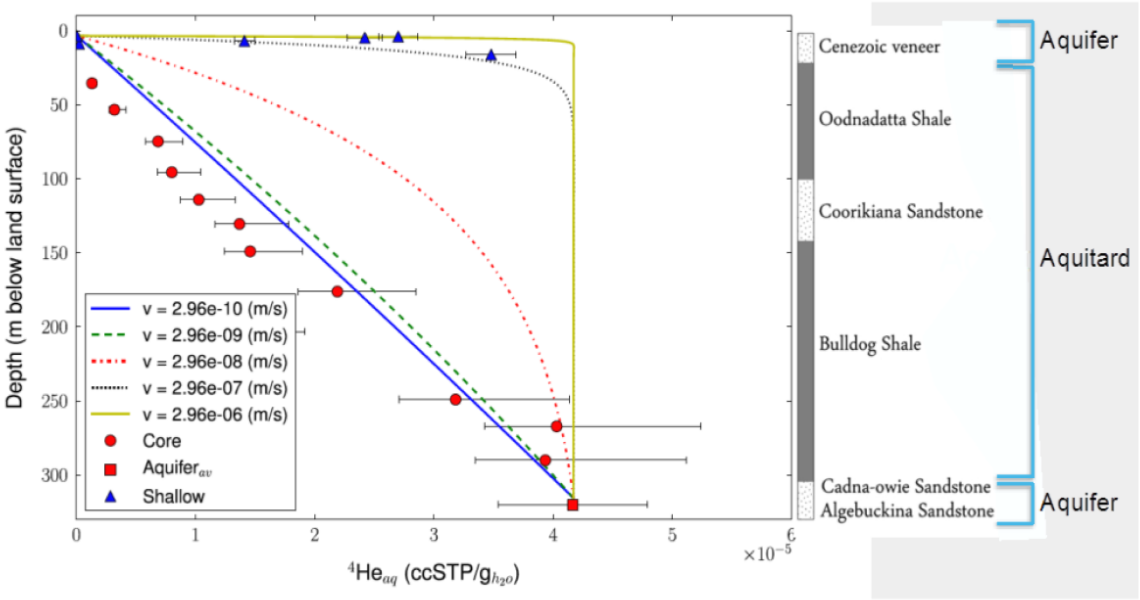

Figure 24. Derivation of formation scale vertical hydraulic conductivity using ⁴He concentration profile (Gardner et al., 2012).

A fourth approach to obtaining bore scale observations of hydraulic properties is the use of environmental tracer techniques. These include analyses of the occurrence of natural and anthropogenic compounds or isotopes in groundwater, which may be used to estimate pathways and timescales of subsurface processes (Cook and Herczeg, 2000). In the present context, tracer techniques may be used to estimate vertical fluxes within and between hydrostratigraphic units. Commonly used tracers include the element chloride and the isotopes deuterium, oxygen-18 and helium-4. For example, Harrington et al. (2012) used observations of chloride, deuterium and oxygen-18 to estimate the vertical flux through a shale aquitard in the Great Artesian Basin. As previously discussed, Gardner et al. (2012) derived a formation scale K_v of 5×10^{-11} m.s^{-1} for the Bulldog and Oodnadatta shale based on helium-4 analysis (Figure 24).

The upscaling of hydraulic properties from bore scale observations to regional scale models is subject to several sources of uncertainty. Properties obtained from downhole geophysical observations are subject to the empirical relationships used to convert neutron, density or sonic logs to porosity values. The uncertainty of porosity values obtained will be a function of the uncertainty of the coefficients used in such relationships (see Figure 23). Similarly, an additional source of uncertainty will be the coefficients in the empirical relationships used to relate porosity to permeability. When uncalibrated relationships such as those from Table 4 are used, uncertainties are expected to be larger than when site-specific relationships are established.

Vidstrand (2001) compared bore scale observations of hydraulic conductivity in fractured granite derived from pump testing to values calculated using a number of analytical upscaling approaches, including arithmetic, geometric and harmonic means (see Table 5, Section 3.1.4 for a discussion of analytical upscaling approaches). Calculated effective hydraulic conductivity values were consistent between the different analytical upscaling approaches. Echoing previous work by Neuman (1988), the authors proposed that, for a given subsurface medium, there exists a minimum REV size below which its hydraulic properties cannot be characterised using an averaged value (Figure 28). Subsequently, they proposed that field investigations should aim to characterise hydraulic properties at an REV size greater than a site-specific threshold. For example, in practice this could involve undertaking a pump test for a duration sufficient to sample the appropriate REV size.

3.1.3. Regional scale observations

Here we refer to observations of hydraulic properties that are integrated over a representative elementary volume that is consistent with a groundwater flow path that may be many kilometres in length. Regional scale is defined as being in the order of 10^4–10^5 metres in the horizontal plane (Dagan, 1986). As demonstrated in Figure 25, data measured in crystalline rock increase by several orders of magnitude from the laboratory to the regional scales. This scale effect has been observed in all kinds of geologic media. Derivation of regional scale hydraulic properties generally involves groundwater flow (and solute transport) inverse modelling based on local scale observations of head, fluxes and solute concentration (Bredehoeft et al., 1983; Clauser, 1992; Laloy et al., 2013).

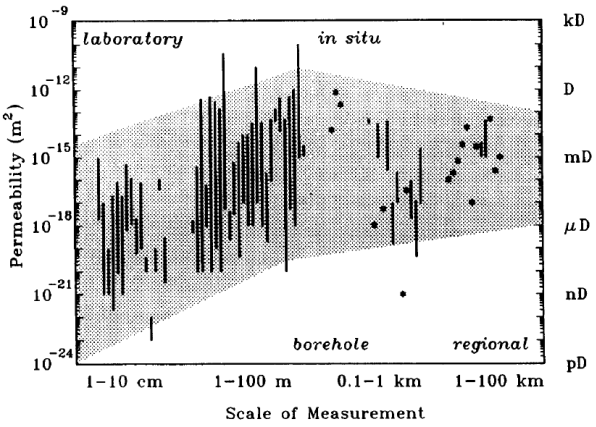

Figure 25. Permeability of crystalline rocks and characteristic scale of measurement (Clauser, 1992).

Groundwater flow paths typically originate in recharge areas (such as topographic highs) and terminate in discharge areas (such as alluvial planes, coastal lakes or as submarine discharge). When groundwater is sampled for environmental tracers at a point located along a flow path, and when the source (i.e., recharge) location is well characterised, the tracer composition of the sample can indicate the time taken to travel from source location to sample location (Bethke et al., 1999; Cook and Bölke, 1999; Taylor et al., 2015). In turn, interpretation of this travel time can provide an estimate of subsurface hydraulic properties, including hydraulic conductivity and aquitard diffusion coefficient (Figure 26). These estimates will be effective properties that are integrated over the entire length of the flow path (Castro et al., 1998b). Typical tracers studied for this purpose are the radioactive isotopes of naturally occurring elements (e.g., carbon-14, helium-4 and tritium) and anthropogenically-produced compounds (e.g., sulphur hexafluoride – SF_6 – and chlorofluorocarbons – CFC).

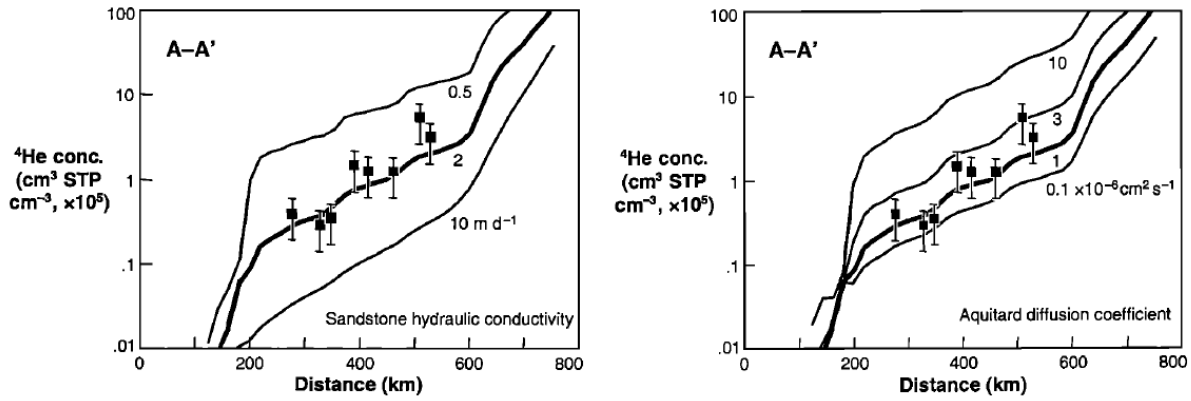

Figure 26. Left: Effect of sandstone hydraulic conductivity on ^{4}He concentration at top of Jurassic aquifer along a flow line. Bold line shows reference model (conductivity 2 m.d^{-1}); fine lines show calculation results for conductivity of 0.5 and 10 m.d^{-1}. Right: Effect of aquitard diffusion coefficient on ^{4}He concentration at top of Jurassic aquifer along flow line. Bold lines show reference model (diffusion coefficient 10^{-6} cm^2.s^{-1}); fine lines show calculation results for coefficient of 0.1x10^{-6}, 3x10^{-6}, and 10x10^{-6} cm^2.s^{-1} (Bethke et al., 1999).

Some geological formations, however, have favourable characteristics (relatively homogeneous clay content, plastic clay, absence of fractures and faults) that produce a much less pronounced scale effect of hydraulic conductivity. For instance, hydraulic conductivities of a plastic clay near Boom, Belgium, measured through various testing techniques in the laboratory (i.e., tracer percolation experiments, constant head permeameter experiments and isostatic experiments) exhibit similar *K* values in the order of 10^{-12} m.s^{-1} (Yu et al., 2013). In situ measurements obtained from both several-centimetre long piezometer filters and percolation into a 7-metre long gallery and 21-metre long shaft at the HADES underground research facility yield *K* values that are very similar to values measured in the laboratory on samples of a few centimetres. A model-based analysis of profiles of the environmental tracer helium-4 measured across the Boom Clay aquitard revealed similarly low *K* values (on the order of 10^{-12} m.s^{-1}). This indicates that the *K* measurements for the Boom Clay Formation obtained through various techniques across a range of scales are very consistent (Figure 27). Note that the Boom clay features hardly any secondary porosity and is fairly homogeneous.

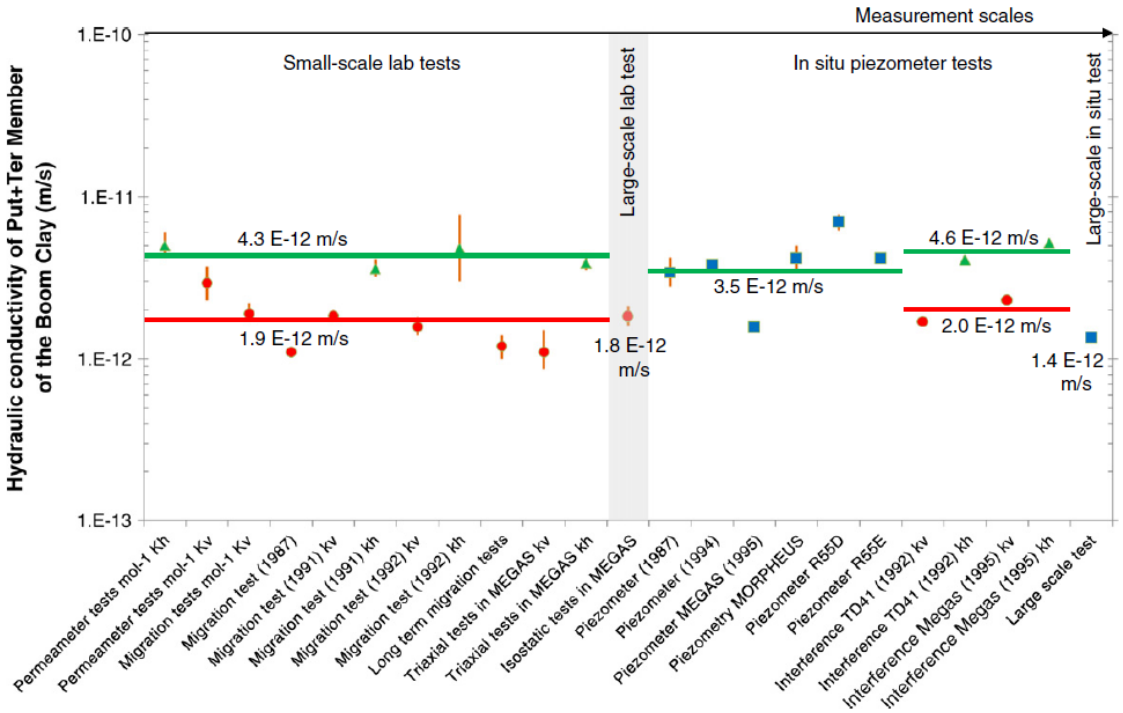

Figure 27. Overview of hydraulic conductivity values (m/s) for the Boom Clay aquitard (Putte and Terhagen Members at the Mol site). Vertical bars represent the 95% confidence interval (Yu et al., 2013).

In addition to tracer-based estimates of hydraulic properties, inverse modelling based on hydraulic head observations is often used to estimate values appropriate at regional scales. The conceptual basis for deriving hydraulic properties in this manner is similar to that used for tracer interpretation; i.e., it is assumed that the locations of boundary conditions are well-known and their properties well-characterised. Model outputs of state variables (i.e., hydraulic heads) are then matched to observations by iteratively adjusting model parameters. The metric used to quantify the degree of fit is typically the sum of squared residuals, each of which can be weighted by the inverse of the measurement uncertainty associated with the relevant observation. For many numerical groundwater flow models, the number of model parameters will exceed the number of observations used for calibration; this is a condition known variously as model ill-posedness (Hadamard, 1902), non-uniqueness (Refsgaard and Henriksen, 2004), or equifinality (Beven, 2006). As a result of model ill-posedness, many parameter sets will each produce an equally well calibrated or equally probable model. In the context of regional scale groundwater flow modelling, parameter value uncertainty is often dominated by poorly constrained boundary conditions. In such cases, unphysical model parameter values may be estimated which compensate for the absence or mis-specification of boundary conditions (Doherty and Christensen, 2011). In the context of simulating CSG

groundwater impacts, global inversion-based upscaling was undertaken with single phase models where hydraulic conductivities in three directions in all upscaled model cells were estimated (Moore et al., 2013). Although the inversion based upscaling performed much better than analytical upscaling methods, a perfect replication of both near-well and far-field drawdown could not be obtained at the same time. Furthermore, these authors highlight that the inversion "forces" the upscaled parameters to take on surrogate roles that compensate for dual phase and other local processes not represented in the model.

In addition to the use of hydraulic head observations alone, environmental tracer observations may also be used to constrain inverse modelling-based estimates of hydraulic properties. Tracer observations can be related to lateral rates of groundwater flow either through analytical (i.e., convolution-based) models, or through numerical solute transport modelling (Turnadge and Smerdon, 2014). Example applications are available from Castro et al. (1998a), Castro and Goblet (2003), and Castro et al. (2000).

3.2. Parameter upscaling

In the context of groundwater flow modelling, parameter upscaling involves the transformation of a detailed description of the spatial variability of geologic and hydrogeological properties at a relatively small measurement or support scale to a simpler description commensurate with the size of grid cells used in groundwater flow models (Durlofsky, 2005). More specifically, the objective of the upscaling processes discussed here is to obtain a description of hydraulic properties at the regional model scale that is consistent with either hydraulic property or flow velocity observations obtained at the measurement scale (for further discussions see Section 3.2.2) within limits for a computational load.

The upscaling of hydraulic properties is a key consideration when informing the parameterisation of numerical groundwater flow models. Observations at scales smaller than the regional scale potentially result in the underestimation of hydraulic conductivity (Figure 25). This is due to the inability of such samples to capture large scale preferential flow features, whether sedimentary (e.g., palaeochannels) or structural (e.g., geological faults) in nature. For example, Hart et al. (2006) compared observations of vertical hydraulic conductivity obtained from pore scale water permeametry and regional scale inverse modelling. Significant discrepancies between estimated values were attributed to the influence of fractures as preferential flow paths at regional scales. For fractures that penetrated the entire thickness of a shale aquitard, the authors estimated the aperture and spatial distribution required to match the vertical hydraulic conductivity estimated from inverse modelling. These observations relate to the principle of the representative elementary volume (REV), which is shown to be scale-dependent. Small-scale samples (pore-scale and bed-scale) are not able to capture heterogeneities due to large-scale features at the body scale (Figure 28). Because the measurement support of the small-scale observations is too small compared to an REV inclusive of large-scale preferential flow paths, upscaling of such small-scale values will produce values that underestimate those obtained through inverse modelling based on large-scale effective flow properties that implicitly include effects of large-scale preferential flow paths. Often only a few high-conductivity zones transmit most of the water, yet they control the large-scale behaviour of the system. Therefore, because connectivity controls large-scale conductivity, it is essential to define it.

Bredehoeft et al. (1983) reported the effective hydraulic conductivity of the Pierre Shale, estimated from regional mass balance, to be 1000 times larger than that derived from laboratory core tests. Similar findings were reported by Schulze-Makuch and Cherkauer (1998), who analysed hydraulic conductivity measurements made with different methods in porous carbonate rocks. They showed that the increase in hydraulic conductivity with scale of measurement occurs until an upper bound is reached, after which the geological formation behaves as a homogeneous medium and hydraulic conductivity remains constant with scale.

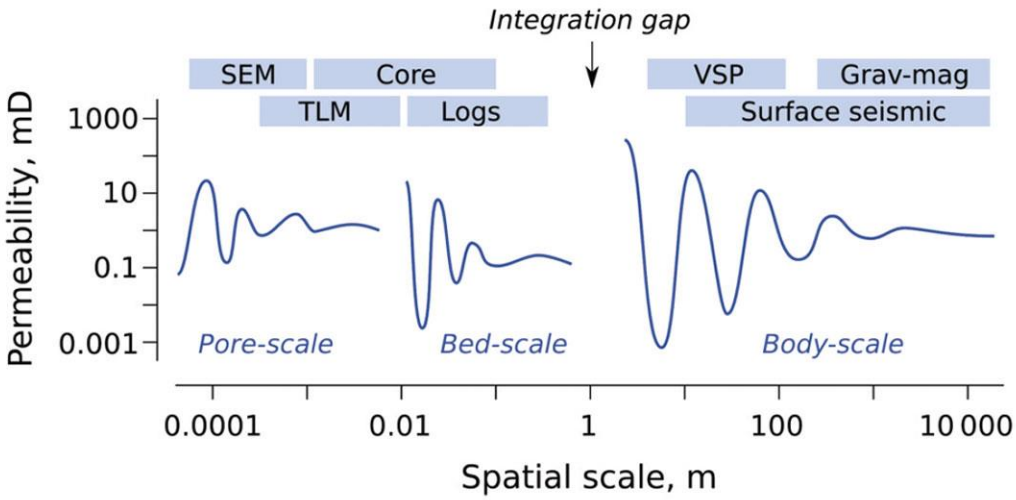

Figure 28. Representative Elementary Volumes at various spatial scales (Hall 2012, modified from Ringrose et al. 2008); SEM = Scanning Electron Microscopy, TLM = Time-Lapse Magnetic resonance sounding; VSP = Vertical Seismic Profiling; Grav-Mag = gravity and magnetic data.

Parameter upscaling typically involves the calculation of effective or equivalent properties, either using closed form, parametric analytical solutions or estimation from stochastic sampling of numerical realisations. Distinctions between equivalent and effective parameters were discussed by Neuman and Di Federico (1998) and Sanchez-Vila et al. (1996). Neuman and Di Federico (1998) defined effective parameters as those parameters that are used in ensemble-averaged Darcy equations (e.g., effective hydraulic conductivity relating the ensemble average flux to the ensemble mean gradient). In contrast, the authors defined equivalent parameters as those that are derived from spatial averaging methods (Darcy-based). Practically speaking, effective parameters are an intrinsic property of the homogenised domain (not a function of the particular boundary conditions imposed on the domain), while equivalent parameters are based on numerical modelling and are therefore valid only for a specific set of imposed groundwater flow boundary conditions. The effective conductivity is mathematically the easiest to derive, hence many analytical expressions exist. However, the concept of equivalent parameters is better suited to solving the problem of upscaling, i.e. for a given *K* distribution over a fine grid, finding the *K* representative for larger blocks.

The upscaled parameters are known to compensate for larger scale features and also for dual phase, dual porosity and other processes not represented in a coarse scale model. For example, Doherty and Christensen (2011) and Watson and Doherty (2012) discuss why some parameters can attain supposedly out-of-range values as a result of global upscaling. They demonstrate this arises from the need for upscaled parameters to adopt “surrogate roles” to compensate for processes and parameter details omitted from a coarser scale model. They further show that this may induce bias in a model’s predictions. For instance, if the flow field under which predictions are required is similar to that which occurs during the upscaling process, the use of unrealistic upscaled parameter values will not necessarily lead to erroneous predictions. In contrast, where upscaled parameter values are used under another set of flow conditions, this may lead to large predictive errors. As part of a study on groundwater impacts from CSG extraction, Moore et al. (2013) quantified simulation errors in a coarse scale regional groundwater model that used upscaled parameters. When inversion-based upscaling was used, parameters were shown to play surrogate roles to compensate for simplification-induced model inadequacies in order to obtain a good fit between drawdowns calculated by the upscaled coarse scale model and drawdowns calculated by the fine-scale model.

3.2.1. Hard and soft data

Subsurface characterisation for building geological and hydrogeological models was originally based on information extracted from drilling holes (cuttings, more or less undisturbed rock material contained in cores) and borehole-based geophysical wireline logging tools (US EPA 1993a, b). Since the 1980s increasingly the subsurface architecture (thicknesses of strata and the topography of the bedrock surface) and some aquifer properties (salinity, groundwater balance or

moisture storage) are being mapped by means of non-invasive methods (US EPA 1993a, b). These include methods applied either at the land surface (e.g., electrical, electromagnetic and seismic refraction tests, ground penetrating radar) or derived from airborne sensors on conventional aircraft (e.g., low frequency airborne electromagnetic methods - AEM) and satellites (e.g., gravity based detection of the groundwater storage using GRACE (Forootan et al., 2012) or soil-moisture detection using SMOS (van der Schalie et al., 2015)). Because geophysical methods cover more area spatially and volumetrically, and require less time and cost than drilling wells, preliminary site characterization by geophysical methods is typically verified by subsequent direct observation and analysis of sediment and rock material from drilled wells.

The well-based data are plentiful in the vertical plane, but sparse in the horizontal plane, making determination of horizontal spatial correlation of so-called hard data (i.e. direct observations of physical properties used in modelling with negligible uncertainty, e.g., hydraulic conductivity, porosity or observations of lithology) difficult. This problem can be resolved by using soft data (used to estimate the hard data and possibly its spatial correlation), which can be plentiful in the horizontal dimension (e.g., geophysical data collected in surface or cross-hole surveys, Freeze et al. 1992). Such soft data are mostly of a qualitative nature (Zhu and Journel, 1993), have a non-negligible uncertainty (McKenna and Poeter, 1995), and have been categorised as type A soft data (values based on an imprecise measurement), type B soft data (recognized bounds on a value without information on the distribution of values between the bound), and type C soft data (prior probability distribution on the variable) (McKenna and Poeter, 1995). Examples of soft data include categorical variables (e.g., lithological facies based on a measurement of seismic velocity - type A soft data – see e.g. Weissmann et al., 2002) or the indication of a trend (e.g., changes in hydraulic properties within a hydrostratigraphic unit). Geophysical methods, in particular, are often unable to measure hydraulic properties directly but can provide insights into spatial trends and/or lithological facies can be spatially correlated to hydraulic properties. Liu et al. (2004) demonstrated how the integration of seismic data reduces the uncertainty in geofacies simulation. Along the same lines He et al. (2014) used high-resolution airborne electromagnetic (AEM) data in multiple-point geostatistical simulations to improve the geological structure and groundwater flow simulations (AEM data were used as the training image as well as secondary data for soft conditioning). Similarly, some environmental tracer (such as helium-4) observations can be used to estimate the vertical groundwater velocity across an aquitard from which vertical hydraulic conductivity can be inferred (Gardner et al., 2012).

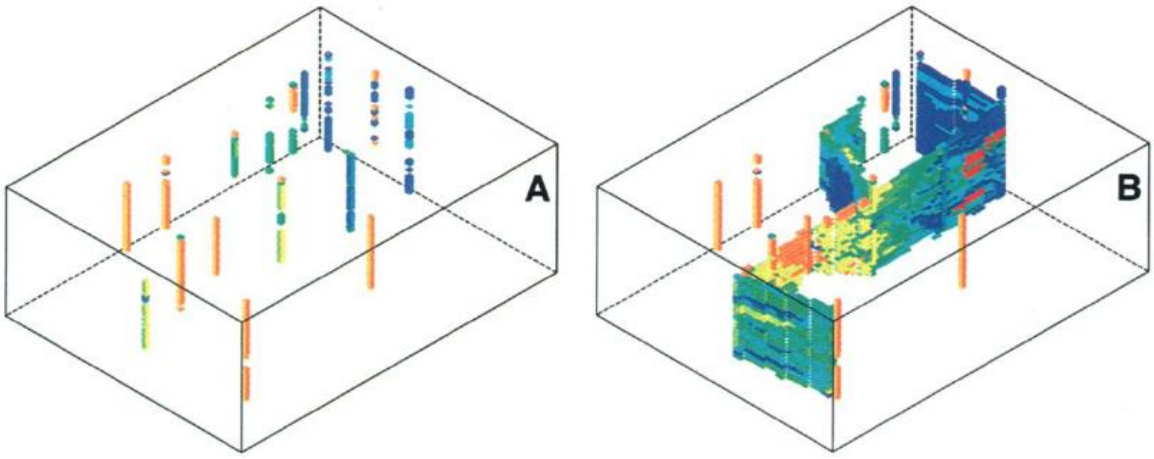

Figure 29. Three-dimensional distribution of (a) hard data (hydrofacies 1 through 7 are dark blue through orange) and (b) hard data with soft data included (hydrofacies 1 through 8 are dark blue through red) (McKenna and Poeter, 1995).

In mathematical terms, the true hard data covariance is estimated as a linear combination of the sample hard data auto-covariance, the soft-hard cross-covariance, and the soft data auto-covariance (e.g. McKenna and Poeter, 1995). A convincing example of the power of fusing hard and soft data to improve the predictive capacity of a groundwater flow model was provided by McKenna and Poeter (1995). By incorporating geologic knowledge, geophysical log data, cross-hole seismic tomography, hydraulic test data, and observations of head, they were able to significantly reduce uncertainty associated with subsurface heterogeneity interpretation (Figure 29). Hard data hydrofacies were derived at wells from the

combination of hydrologic, geologic and geophysical data, while soft data hydrofacies between wells were derived from cross-borehole tomography.

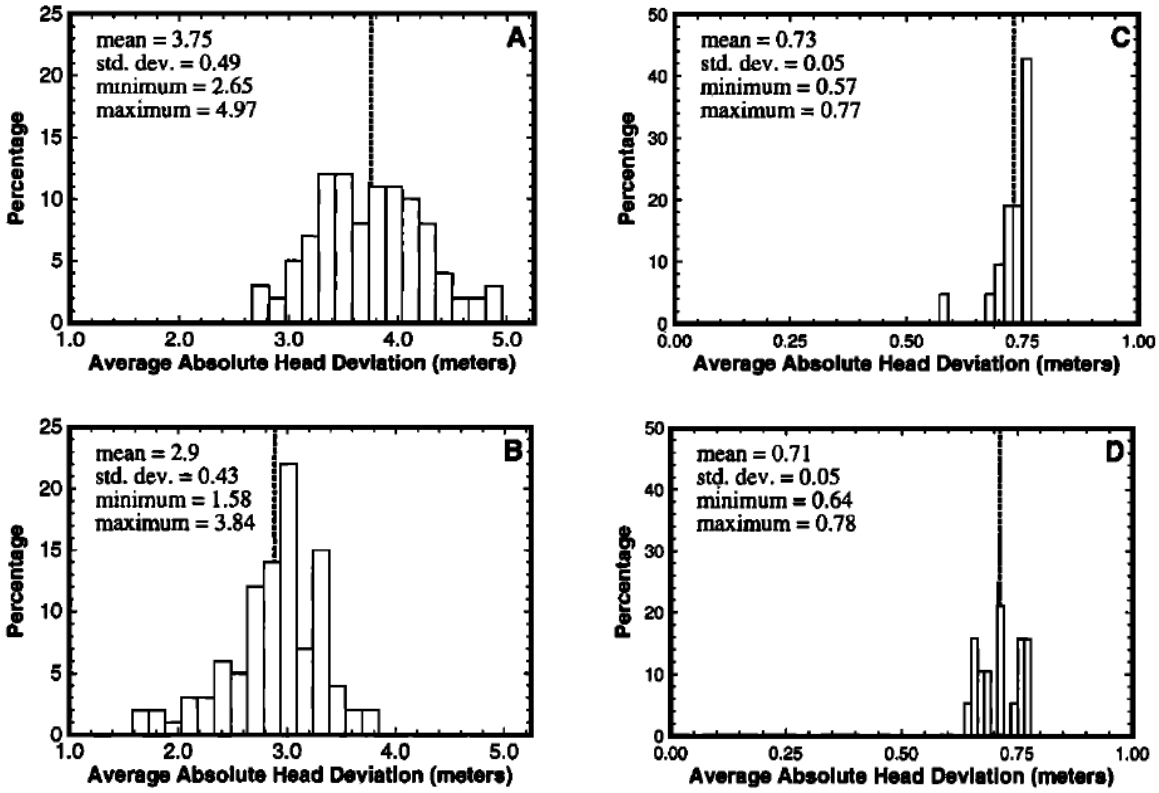

Figure 30. Groundwater model performance expressed as Average Absolute (Hydraulic) Head Deviation; i.e. the absolute difference between modelled and observed hydraulic head values. Distributions of average absolute head deviations for (a) the hard data and (b) the hard/soft data realizations resulting from forward groundwater flow modelling using field estimates of K and distributions of average absolute head deviation after inverse parameter estimation for (c) the hard data and (d) the hard/soft data realization (McKenna and Poeter, 1995).

McKenna and Poeter (1995) demonstrated that forward groundwater flow modelling using estimates of hydraulic conductivity from field testing yielded smaller hydraulic head residuals for realisations that include soft data (Figure 30). Inverse modelling was then used to eliminate hydrofacies realizations that do not honour hydraulic data and to estimate hydrofacies hydraulic conductivity ranges for the hard and hard/soft data ensembles. Inverse parameter estimation substantially decreased head residuals for both ensembles (Figure 31). Standard deviations of hydraulic conductivities estimated through inverse modelling were shown to be smaller when both hard and soft data are used to generate the simulations.

While a powerful example, in reality many, especially large-scale site characterisations will have much less data; in this case a careful selection has to be made prior to any data collection efforts about what the best combination of hard and soft data will be. Value of information or data worth analysis studies then become very useful to ensure the limited resources are used to provide data most suitable to resolve a particular question (Engelhardt et al., 2013; Freeze et al. 1992; Moore, 2005; Wallis et al., 2014). However, the value of information is not absolute; instead, it is always dependent on the management or research question of interest. Indeed, there is no intrinsic value in collecting data unless it can influence a specific decision goal.

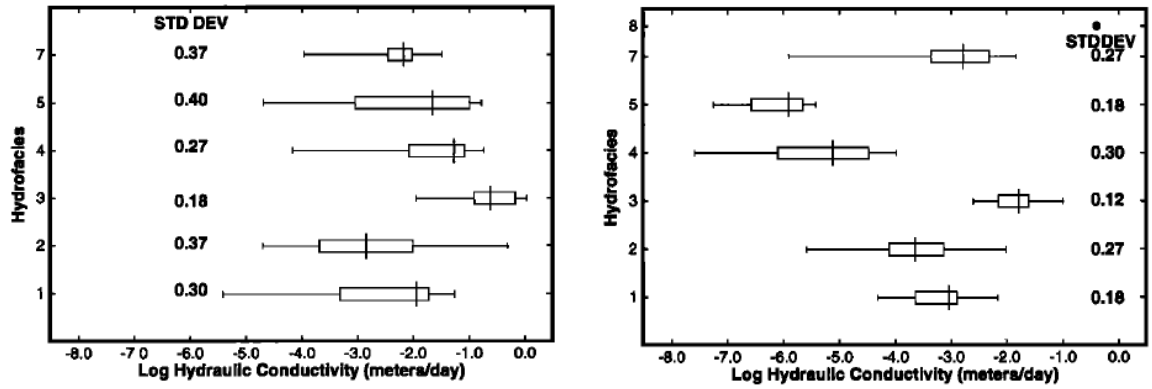

Figure 31. Box and whisker plots of hydraulic conductivity estimates for (a) the 21 hard data and (b) the 19 hard/soft data realizations. The dashed lines indicate the median, the ends of the box are the 25th and 75th quartiles, and the ends of the whiskers are the minimum and maximum of the distribution. Values next to the whiskers are the standard deviations (McKenna and Poeter, 1995).

3.2.2. Upscaling methods

Despite significant recent increases in computation power, there remains a need for upscaling hydrogeological parameters and processes from the typically small measurement scale to a coarser scale for numerical modelling. Likewise, upscaling is also needed to derive a parameter field for a coarse-gridded model that allows replication of quantities calculated by a fine-gridded model, albeit at a fraction of the computational resources. This need is driven by the requirement to minimise numerical model run times, in order for models to remain computationally tractable for regional scale CSG related assessments. The need for upscaling becomes even more important when undertaking Monte Carlo type sensitivity and uncertainty analyses. The coarse-gridded flow model itself should adequately represent key behaviours, such as the overall flow rate for given boundary conditions or critical connected flow paths (Gerritsen and Lambers, 2008).

Upscaling methods can be classified as local or global methods, depending on the type of flow problem that is solved to determine the coarse scale parameters (Moore et al., 2013). Local upscaling methods solve a fine scale flow problem over each coarse block under some assumed local boundary conditions. These methods include use of analytical averaging methods and flux-based approaches (see below for further discussion). Global upscaling methods solve the global fine scale flow problem directly for the determination of coarse scale parameters. In other words, the entire fine scale model is simulated for the calculation of the coarse scale parameters. This is typically implemented using inversion-based methodologies. Chen and Durlowsky (2006) developed a coupled local-global upscaling approach, in which the local boundary conditions used to compute upscaled properties are determined from global coarse scale flows. Gerritsen and Lambers (2008) developed a multilevel local–global upscaling method for generating accurate upscaled models of permeabilities or transmissibilities for flow simulation on adapted grids in heterogeneous subsurface formations (e.g. channel-like structures).

There are several advantages of using global upscaling methods compared to local scale methods (Moore et al., 2013): (i) they provide the ability to simultaneously satisfy upscaling metrics over large parts of the model domain, (ii) they readily allow imposition of a stress regime during the upscaling process which is similar to that for which predictions will be made using the upscaled model, and (iii) they are superior to local methods where reservoirs contain important heterogeneities such as high permeability flow paths, see e.g. Gerritsen and Lambers (2008). Disadvantages of global methods include (Moore et al., 2013): (i) their implementation is often numerically intensive, (ii) they can lead to locally higher-than-expected or lower-than-expected upscaled parameter values (e.g. Chen and Durlofsky, 2006).

In cases where flow of multiple phases is simulated, such as in CSG target formations, upscaling must address both hydraulic properties and their desaturation relationships. This is known to be an inherently complex process (Barker and Thibeau (1997), Lohne et al., 2006), which is further complicated because the shape of the “true” relative permeability curve for coal is uncertain anyway (Ham and Kantzas (2008), and Clarkson et al., 2010).

Comprehensive reviews of upscaling approaches, including discussions on equivalent and effective hydraulic conductivity, were published by Sanchez-Vila et al., (1996), Wen and Gomez-Hernandez (1996), Renard and de Marsily (1997) and Sanchez-Vila et al., (2006). Sanchez-Vila et al. (1995) reviewed several analytical approaches to parameter upscaling, including those by Rubin and Gomez-Hernandez (1990), Durlofsky (1991; 1992), Desbarats (1992) and Indelman and Dagan (1993a; 1993b; 1993c), and provided comparisons to numerical results. In addition, stochastic approaches to the upscaling of hydraulic properties have been summarised in numerous monographs [e.g., Gelhar (1993); Rubin (2003)]. Here we discuss three broad categories of upscaling methods: statistical approaches, flux-based approaches, and connectivity-based approaches.

Upscaling that is undertaken in contexts such as that of the present study must thus be considered as specific to a particular purpose, and not assumed to be fit for general use. It follows from the specificity of parameter fields thus sought, that the metric through which they are judged must be clearly defined. In particular, an upscaled parameter field must be sought which maximizes the ability of a coarse-gridded model to simulate certain aspects of the behaviour of the studied system under a specific stress regime. In the present case this regime is the extraction of water and gas from multiple coal seams comprising a coal measure formation. It cannot therefore be guaranteed that an upscaled parameter field which performs well under these conditions will perform well under an alternative stress regime.

Statistical or analytical approaches

Approaches to parameter upscaling vary in complexity. The simplest, local approach involves calculating the arithmetic, geometric, harmonic, power or volume-weighted mean of a given sample volume (Table 5). Li et al. (2011) summarised upscaling methods based on mean-based approaches. For one-dimensional flow in a heterogeneous aquifer, the equivalent hydraulic conductivity is calculated as the harmonic mean of the hydraulic conductivities (Freeze and Cherry, 1979). In two-dimensional heterogeneous media characterised by isotropic spatial correlation and a lognormal probability distribution of hydraulic conductivity, it has been shown that the geometric mean is an appropriate means of parameter upscaling (Gomez-Hernandez and Wen, 1998; Sanchez-Vila et al., 1996).

Table 5. Summary of averaging methods commonly used in the upscaling of hydraulic properties.

Averaging method	Equation
Arithmetic	$\mu = \frac{1}{n}\sum_{i=1}^{n} x_i$
weighted arithmetic	$\mu = \frac{\sum_{i=1}^{n} w_i x_i}{\sum_{i=1}^{n} w_i}$
Harmonic	$\mu = \frac{1}{n}\sum_{i=1}^{n} \frac{1}{x_i}$
Geometric	$\mu = \left(\prod_{i=1}^{n} x_i\right)^{1/n}$
Power	$\mu = \left(\frac{1}{n}\sum_{i=1}^{n} x_i^{\omega}\right)^{1/\omega}$

In three-dimensional heterogeneous media, Cardwell and Parsons (1945) showed that the effective conductivity of a given upscaled volume should lie between the arithmetic mean and the harmonic mean. Journel et al. (1986) proposed the use of power averages (also referred to as ω-norms) to estimate upscaled conductivities (Table 5); i.e., the integral of all hydraulic conductivities, each raised to the power ω, divided by the volume of observation, raised to the power $1/\omega$. When ω=–1 the expression simplifies to the harmonic mean; when ω=0 the expression simplifies to the geometric mean; and when ω=1 the expression simplifies to the arithmetic mean. In other words, the suitability of these averaging approaches is

direction-dependent. Desbarats (1992) demonstrated that ω=1/3 for isotropic and mildly heterogeneous formations in three dimensions. For highly heterogeneous environments, ω is typically estimated from numerical experiments using stochastically-generated parameter fields (Li et al., 2011). Essentially, the statistical approaches aim to preserve a mean value when the scale of interest is increased. These methods vary primarily in the type of mean value used.

The limitations of geometrical upscaling methods (such as those listed in Table 5) were clearly illustrated by Moore et al. (2014a) when coal layers and interburden were lumped into single upscaled cells in an attempt to derive upscaled relative permeability functions with a single-phase flow model. The homogenization in a single upscaled cell of two very different lithologies, one of which produces gas and undergoes desaturation while the other does not, results in failure to represent the relative permeability curves for both coal and interburden.

Flux-based approaches

Flux-based approaches aim to preserve the hydraulic mass balance (and therefore groundwater flow rates) when the scale of interest is increased. In other words, if the behaviour of a system is to be valid both at the fine scale and at the coarse scale, the underlying physical laws should remain the same. These methods vary primarily in the method of calculation employed (i.e., analytical or numerical) and in the type of parameter tensor that is generated (i.e., diagonal or full-rank). Li et al. (2011) summarised flux-based upscaling methods; specifically, solutions to the Laplace equation for groundwater flow. By rearranging Darcy's Law, the upscaled hydraulic conductivity in any given direction can be calculated as the ratio of the flow rate to the cross-sectional thickness divided by the hydraulic gradient (Figure 32). In practice, this expression is evaluated for each model grid cell through numerical experiments. Laplace equation-based methods have been widely used to calculate upscaled hydraulic conductivities in petroleum engineering and hydrogeology [e.g., Warren and Price (1961); Journel et al., (1986); Desbarats (1987); Deutsch (1989)]. Sanchez-Vila et al. (1996) used the approach to upscale transmissivity values; Jourde et al. (2002) used it to calculate equivalent hydraulic conductivity values for fault zones; and Flodin et al. (2004) used this method to illustrate the impact of boundary conditions on upscaling (Li et al., 2011). Zhou et al. (2010) used numerical experiments to estimate the individual components of a full rank hydraulic conductivity tensor. In comparison, most numerical groundwater flow models use only a diagonal tensor (i.e., containing components K_{xx}, K_{yy}, K_{zz}) with all off-diagonal components (e.g., K_{xy}, K_{xz}) set to zero. Other studies [e.g., Li et al., (2011)] have examined the importance of neighbouring cells when calculating upscaled parameters.

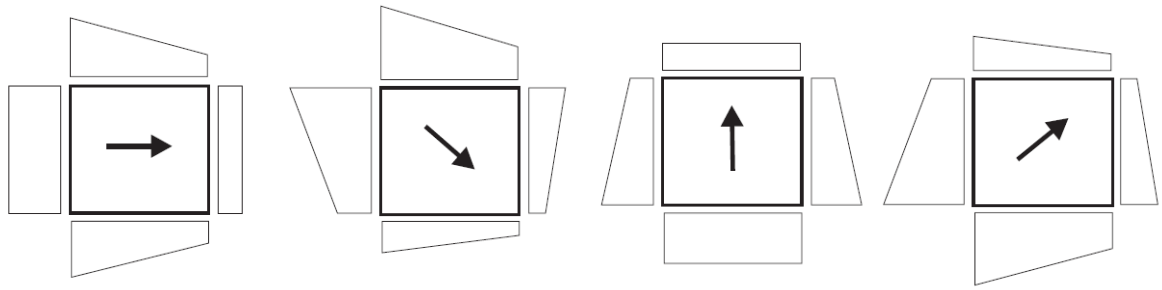

Figure 32. Four typical boundary conditions used to estimate block conductivity in 2-D. Arrows indicate the (negative) mean head gradient induced by the prescribed head boundary conditions, and the shapes on the sides of the block indicate the magnitude of the prescribed heads given by tilting planes with gradients opposite to the arrows (Zhou et al., 2010).

Because flux based approaches at the local scale require solving a small scale inversion problem for all cells in the upscaled grid block to derive the upscaled permeability tensor, these approaches are computationally intensive. This becomes exacerbated if multiple calculations are required based on stochastic Monte Carlo realisations.

Connectivity-based approaches

Methods by which to represent subsurface heterogeneity (including upscaling) were reviewed by Koltermann and Gorelick (1996), de Marsily et al., (2005; 1998) and Szymkiewicz (2013). An alternative to traditional approaches to the

characterisation of subsurface heterogeneity (see Section 3.2.3) is the use of connectivity metrics (Renard, 2011; Renard and Allard, 2011; Trinchero et al., 2008). These metrics can be used to indicate the connectivity of high hydraulic conductivity regions. In upscaled subsurface media, these regions can account for a significant proportion of the total groundwater flow. Knudby and Carrera (2005) proposed and evaluated three metrics by which to quantify flow connectivity in porous media, which characterises the degree of flow channeling, i.e. to what extent a small fraction of the medium provides a large fraction of the flux. These metrics were found to be superior to metrics based on two point geostatistics. Knudby and Carerra (2006) found the use of the hydraulic diffusivity (i.e., the ratio of transmissivity to storativity) a particularly useful metric for flow and transport related connectivity. An analytical approach to upscaling binary porous media that accounts for metrics of connectivity is available from Knudby et al. (2006).

Essentially, connectivity-based approaches aim to preserve a specified metric of connectivity when the scale of interest is increased. These methods vary primarily in the type of connectivity metric specified. While applications have mainly been in aquifers, connectivity-based approaches are probably equally useful in aquitards (de Marsily et al. 2005).

3.2.3. Simulation-based spatial interpolation methods

In the study of groundwater flow systems, hydraulic conductivity is the most heterogeneous hydraulic property required for flow simulation. The hydraulic conductivity of a given hydrostratigraphic unit is typically log-normally distributed and may range over orders of magnitude. The primary cause of heterogeneity is variations in geological facies. Following the deposition and lithification of facies, their variability may subsequently be altered by secondary processes, such as diagenesis by silicification, or by the development of structural features, such as geological faults. The parameterisation of hydraulic properties in groundwater flow models often involves the use of scalar values to represent the bulk properties of a given hydrostratigraphic unit. This approach neglects (often due to data paucity) the existence of multiple facies within a HSU. Alternative approaches use explicit representations of multiple facies types to subsequently calculate equivalent hydraulic properties. Whilst requiring a higher level of data support, these approaches provide a more rigorous basis for determining hydraulic property values. Falivene et al. (2007) summarised the range of numerical approaches to parameter upscaling based on facies reconstruction. At the highest level, methods were categorised as either deterministic or stochastic. In the present work we focus only on stochastic approaches, as deterministic approaches are, by definition, unable to characterise the uncertainties associated with upscaling and spatial interpolation. Stochastic approaches were classified into pixel-based methods and object-based methods (Figure 33). Pixel-based methods refer to approaches where upscaling and interpolation are undertaken using a discrete grid or mesh. In comparison, object-based (or Boolean) approaches use a combination of predefined shapes (often simple geometric or curvilinear shapes) to represent heterogeneity. The two approaches may also be used in combination, which can enable stochastic parameterisation of geologically realistic heterogeneous features (e.g., Michael et al., 2010). We subsequently discuss the following methods: Monte Carlo sampling, two-point statistics, multi-points statistics and transition probability statistics.

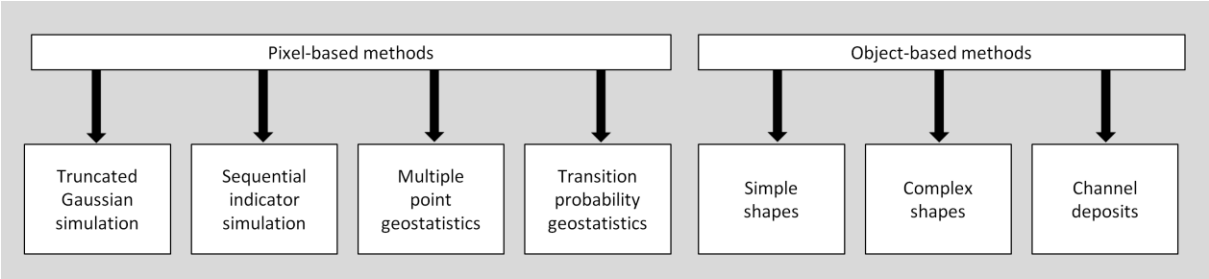

Figure 33. Categorisation of numerical upscaling approaches [after Falivene et al., (2007)]

Monte Carlo sampling

The simplest approach to generate spatially continuous facies and/or hydraulic conductivity models involves defining, for a given hydrostratigraphic unit (HSU), probability density functions (PDFs) for the facies located within the HSU, and for the properties within each facies. Using a Monte Carlo (MC) sampling approach, a regional scale REV composed of many spatially uncorrelated core or bore scale REVs can be populated stochastically according to these PDFs. The effective hydraulic properties of the regional scale REV can then be calculated using analytical/empirical solutions or by numerical sampling methods.

Two-point statistics

More complex approaches are based on the same procedure of MC sampling of parameter PDFs, but preserve a given spatial structure identified a priori. Traditionally, spatial structure (i.e., correlation) was specified using two point geostatistics (Chilès and Delfiner, 1999; Isaaks and Srivastava, 1989; Journel and Huijbregts, 1978; Wackernagel, 2003; Rogiers et al., 2014b). This typically involves fitting a spatial correlation function (i.e., a variogram or semivariogram) to a set of data points located within a given region (Figure 34). This function may be continuous, as used by simple or ordinary kriging approaches, or discrete (i.e., categorical), as used in indicator kriging methods. Essentially, these approaches are based on identifying spatial correlations between pairs of points separated by a given distance drawn sequentially from a given set, hence the name, "two point" methods. These methods generally assume a stationary mean and spatial correlation that decreases (usually exponentially) with distance. If a variogram rather than a correlogram is used, the semi-variance reaches a constant value (the sill, or the variance of the random field) when the spatial dependency (autocorrelation) becomes insignificant (the range).

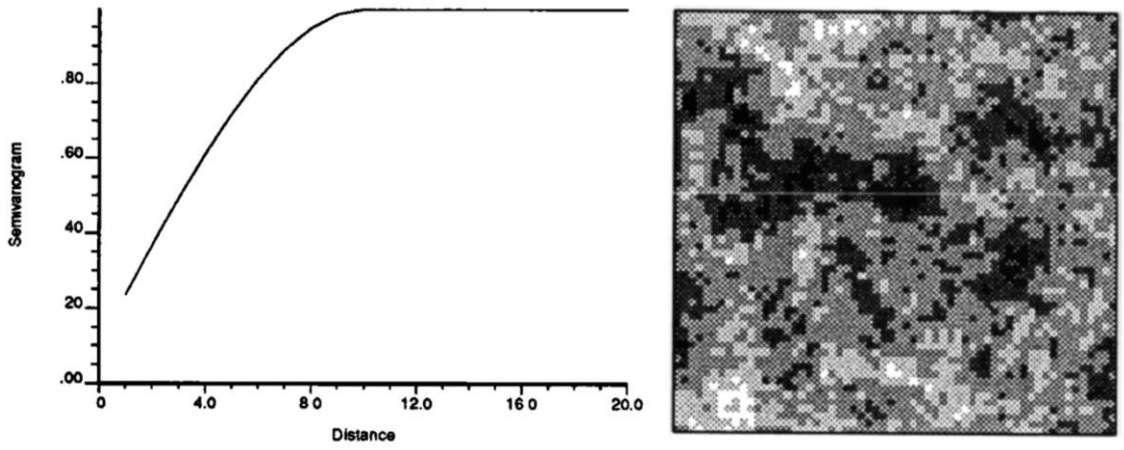

Figure 34. (left) Example semivariogram used in two-point geostatistical approaches to characterise the structure of spatial variability. (right) Example of a spatially distributed parameter field generated stochastically using the variogram from the left panel (Koltermann and Gorelick, 1996).

While geostatistically-based spatial interpolation can be undertaken using geographic information system applications, such results are deterministic in nature. Conversely, stochastic spatial interpolation tools use the uncertainty associated with variogram-based descriptions to generate a given number of equally likely realisations of a parameter field. This process, known as sequential simulation, involves the cell-by-cell population of values based on those of neighbouring cells. Publicly available implementations of sequential field simulators based on the two point geostatistical approach include GSLIB (Deutsch, 1999) and GCOSIM3D (Gómez-Hernández and Journel, 1993).

The limitations of Gaussian fields generated using two point geostatistics in groundwater flow studies have been discussed at length in peer reviewed literature. Wen and Gomez-Hernandez (1996) highlighted the tendency of multiGaussian approaches to generate smooth continuous parameter fields which are unable to represent preferential flow features such

as high hydraulic conductivity channel deposits, faults or fractures. Zinn and Harvey (2003) demonstrated a method by which to enhance the connectivity of multiGaussian fields whilst preserving the specified probability density and isotropic covariance functions. Kerrou et al. (2008) demonstrated the inability of multiGaussian simulation to accurately characterise a synthetic braided aquifer featuring a bimodal transmissivity probability density function. They attributed their results to the inability of multiGaussian fields to represent hydraulic connectivity. Meerschaert et al. (2013) found that, for a highly heterogeneous aquifer, the combination of various facies with unique mean and variance values results in significantly non-Gaussian parameter fields. However, they noted that it is reasonable to characterise the variability of values within a facies using a Gaussian model.

Continuous and categorical methods of sequential simulation can be combined in what is known as truncated Gaussian simulation. While this approach uses traditional variograms for spatial interpolation, the value at interpolated points is also used concurrently to determine which facies is present.

Reducing uncertainty and improving representativeness of stochastic groundwater flow simulations may be achieved by so-called conditional stochastic simulations. In conditional simulation the measured values at a limited number of points are kept fixed and uncertainty exists only at all other points. In case of hydraulic conductivity conditioned simulations, both the spatial correlation information and the actual hydraulic conductivity values at their measurement locations are taken into account (Varljen and Shafer, 1991). Furthermore, this method requires that each single member also preserves the observed conductivity values at their measurement locations; the measurement uncertainties at these locations is disregarded. This method can be extended to also include conditioning on flow variables (head, fluxes, or even solute concentrations in case a solute transport model is used).

Multiple-point statistics

More recently (i.e., post–2000) an alternative approach known as multiple point statistics (MPS) has seen widespread application, although its development goes back to the early 1990s (e.g. Journel, 1993; Guardiano and Srivastava, 1993). This approach is based on the use of training images developed *a priori*, rather than two-point geostatistical models (variograms) to describe spatial variability (Table 6). Such images can be developed from rock outcrops (see Figure 35 for an example of an outcrop used to develop training images), from continuous areal geophysical observations (Dickson et al., 2015; He et al., 2014), or from geomorphological expertise (Alcolea and Renard, 2010). Summaries of the theoretical development of the MPS concept are available from Hu and Chugunova (2008) and Wu et al. (2008).

Table 6 Comparison of two-point and multiple point statistics.

Feature	Two-point statistics	Multiple point statistics
Measure	Statistical realisation of two points $z(u)$ and $z(u+h)$, where h is separation distance	Structures and patterns beyond two-point correlation
Conditional probability	Variogram model	Training image
Parameterisation	Sill, range, nugget, shape of variogram	Proportions, scale, anisotropy

MPS has produced some exciting developments since its introduction, since it allows reconstruction of much more realistic geological structures (e.g. where areas of high and low permeability coexist, or to preserve connectivity of facies via channel-like structures) than the traditional two-point statistics. The implementation described by Guardiano and Srivastava (1993) was computationally intensive, as it required re-sampling of an entire training image for the generation of each pixel value. Strebelle (2000; 2002) reduced the computational burden by replacing repeated re-sampling with a search tree (i.e., frequency tree). The MPS concept was extended to continuous variables by Arpat and Caers (2007). The efficiency of the approach was subsequently improved through pre-filtering of training image data by Wu et al. (2008).

Mariethoz et al. (2010) extended the MPS concept to multivariable parameter field generation. Comunian et al. (2012) developed methods by which to generate 3-D realisations from 2-D training images. Mariethoz and Lefebvre (2014) identified methods used in texture synthesis, such as principal components analysis, that may be used to accelerate the performance of MPS algorithms. Silva and Deutsch (2014) used a linear opinion pool method to generate MPS-based realisations from multiple training images. Li et al. (2015) demonstrated the use of an ensemble Kalman Filter in combination with the Direct Sampling MPS approach of Mariethoz et al. (2010) to characterise parameter heterogeneity. Most recently, Mahmud et al. (2015) applied an existing method named 'image quilting' (Efros and Freeman, 2001) to generate parameter realisations that were conditioned to multiple training images derived at different observation scales.

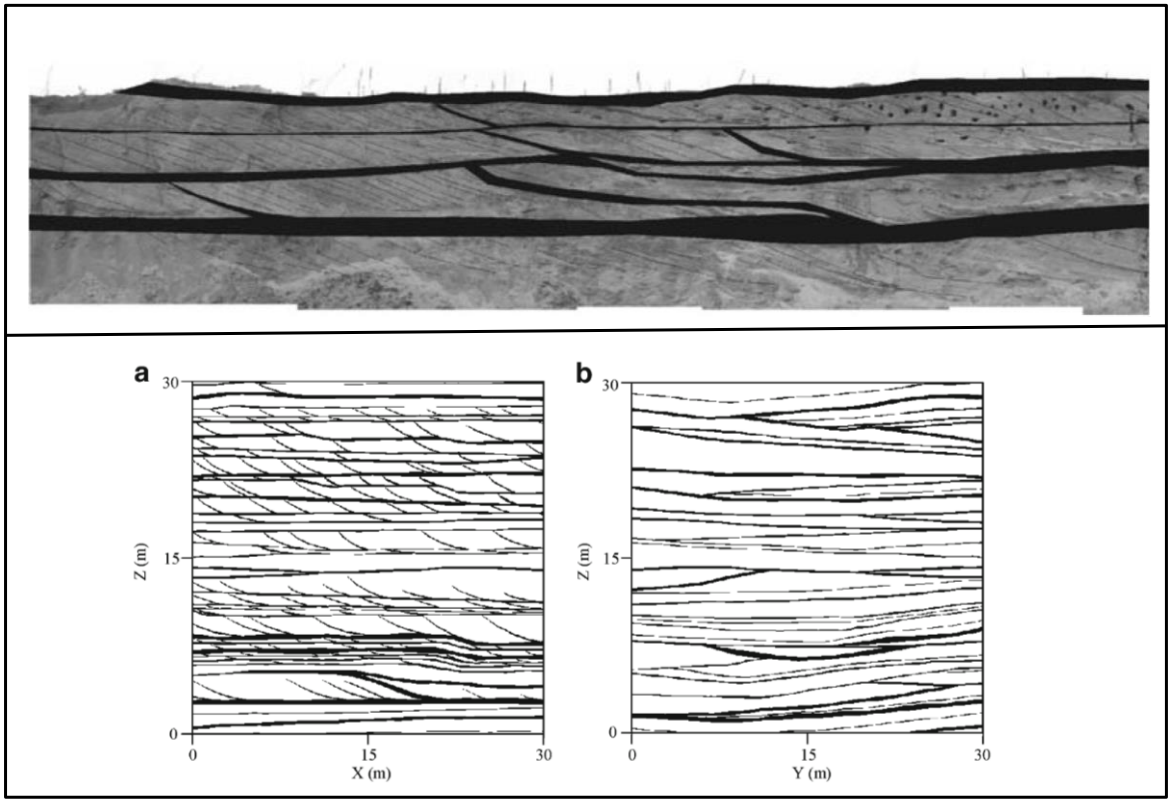

Figure 35. (top) Interpreted photomosaic of a quarry wall of Brussels Sands showing silt facies consisting of clay-rich bottomsets and distinct mud drapes in black; grey background consists of sand facies. Height of quarry wall is approximately 4–5 m. (bottom) Training images of 30 × 30 m (360,000 grid nodes each 0.05 × 0.05 m) used in a multiple point statistics simulation of silt and sand facies (white refers to sand facies, black refers to silt facies) (Huysmans and Dassargues, 2009).

Numerous applications of MPS can be found in reservoir modelling, hydrogeology and groundwater flow and solute transport modelling. For example, Liu et al. (2009) used MPS to simulate groundwater flow in fractured rock at the Yucca Mountain test site in Nevada, USA. Stochastic realisations of a matrix–fracture network dual medium were generated from a training image and incorporated in a groundwater flow model. Jung et al. (2013) combined MPS with the discrete fracture network model FRACMAN (Dershowitz et al., 1999) to simulate oil production from a 19 × 16 km fractured carbonate rock reservoir, representative of those typically found in the Middle East.

Multiple point statistics has also been successfully combined with other approaches to generate stochastic realisations of sedimentary groundwater flow environments. For example, Huysmans and Dassargues et al. (2009) presented a workflow that uses MPS to investigate the effect of complex small-scale sedimentary heterogeneity on the short-term migration of a contaminant plume. Training images of highly heterogeneous and anisotropic sandy sediments were constructed based on geological and hydrogeological field data collected from outcrops (Figure 36). Characteristics of the sediments are typical for tidal deposits, and include important grain size variations, cross-bedding, bottomsets, foresets, mud drapes and unidirectional reactivation surfaces. Permeability variability within the sand and silt facies (i.e. intrafacies variability) was simulated using direct sequential simulation with histogram reproduction based on histograms and variograms obtained

from in situ air permeability measurements. Simulation was performed separately for each facies after which the simulated sand and silt facies realisations are assembled (Figure 36). This approach enabled the stochastic parameterisation of geologically realistic features. Similarly, Comunian et al. (2014) used a process-based approach to generate training images for MPS-based realisations of the Lower Namoi alluvial aquifer in the Murray Darling Basin.

Publicly available implementations of the MPS approach include SGEMS (Remy et al., 2009) and SNESIM (Strebelle, 2000; Strebelle, 2002). Liu (2006) demonstrated the use of SNESIM software to characterise a synthetic 250 × 250 pixel reservoir featuring a mixture of sand and shale facies. A description of the *TiGenerator* software for the generation of training images from parametric and rasterised shapes is available from Maharaja (2008).

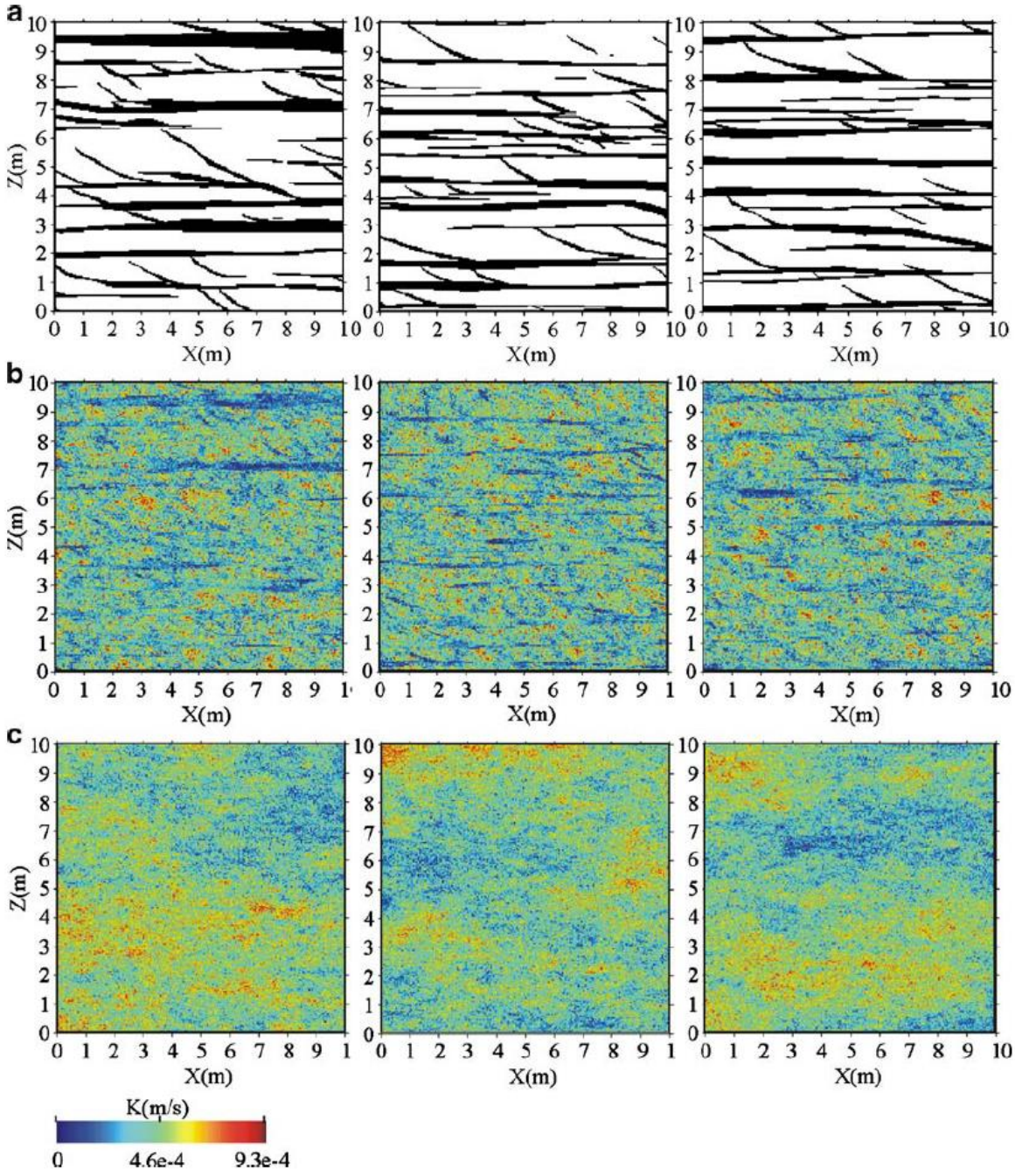

Figure 36. (a) Example SNESIM facies realisations consisting of 40,000 cells of 0.05 × 0.05 m (white refers to sand facies, black refers to silt facies); (b) corresponding hydraulic conductivity K (m.s^{-1}) realisations based on K histograms and variograms for both facies; (c) SGSIM hydraulic conductivity K (m.s^{-1}) realisations based on standard variograms without accounting for facies (Huysmans and Dassargues, 2009).

Transition probability geostatistics

Another approach involves the use of transition probabilities when stochastically populating a regional scale REV with smaller scale components (Carle and Fogg, 1996). Transition probabilities are commonly used in Markov Chain Monte Carlo (MCMC) sampling methods. Rather than employing a training image to qualitatively condition a stochastic realisation, quantitative measures are instead used (Dell'Arciprete et al., 2011). For a given feature (i.e., facies), these metrics typically include mean volumes, lengths and thicknesses, as well as descriptions of anisotropy and spatial variability. The commonly-used implementation of the transition probability geostatistics approach is T-PROGS (Carle, 1999). For example, Fleckenstein and Fogg (2008) used T-PROGS to generate hydrofacies distributions to represent geologic heterogeneity of a sedimentary fan system. *K*-values were subsequently assigned to each of the four hydrofacies (gravel and coarse sand, sand, muddy sand, and mud), resulting in a high-resolution *K*-models (comprising 1,244,000 cells, Figure 37). Upscaling was performed on realisations of the geostatistical models using the arithmetic and harmonic means of the high-resolution *K*-values within vertical grid columns (Figure 38). A logarithmic increase in model domain equivalent *K* was observed with increasing degree of upscaling.

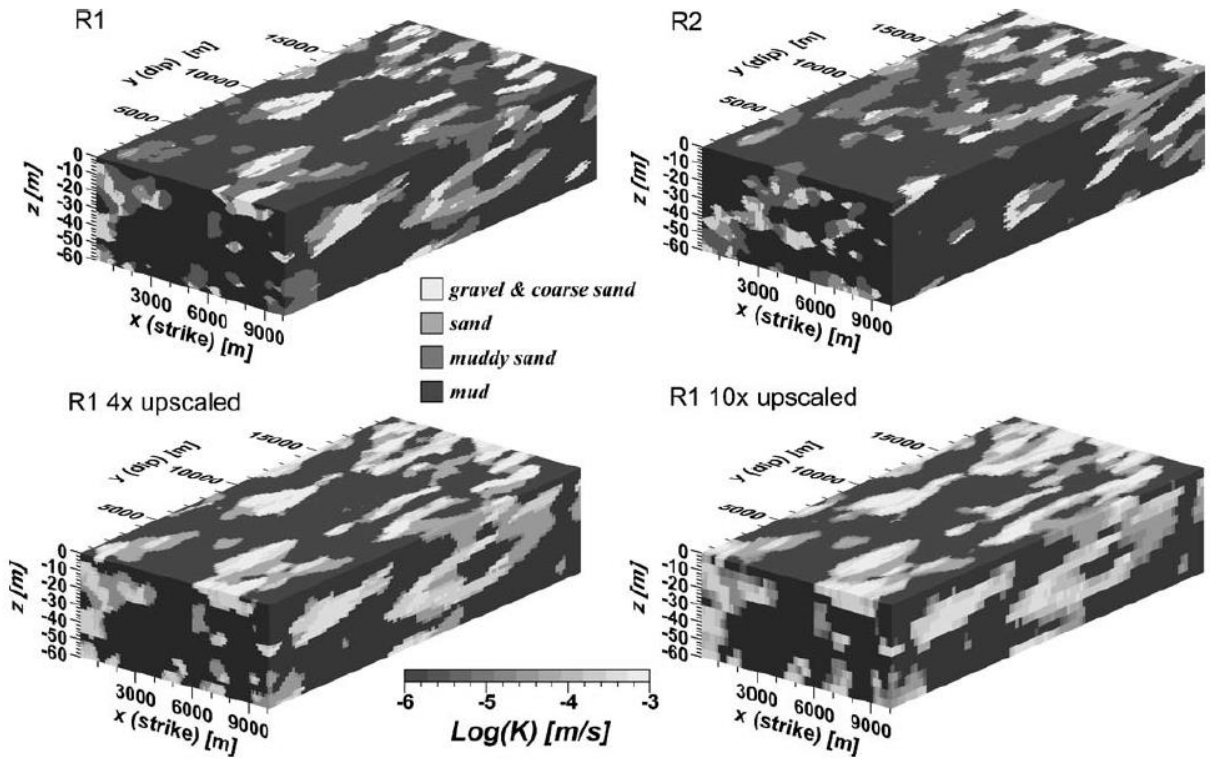

Figure 37. Two realizations R1 and R2 of the geostatistical model of hydrofacies distributions (top) and their upscaled 4x and 10x equivalents (bottom). The original model has 120 layers (1,224,000 cells) and the upscaled models 30 layers (30,6000 cells) and 12 layers (122,400 cells) respectively (Fleckenstein and Fogg , 2008).

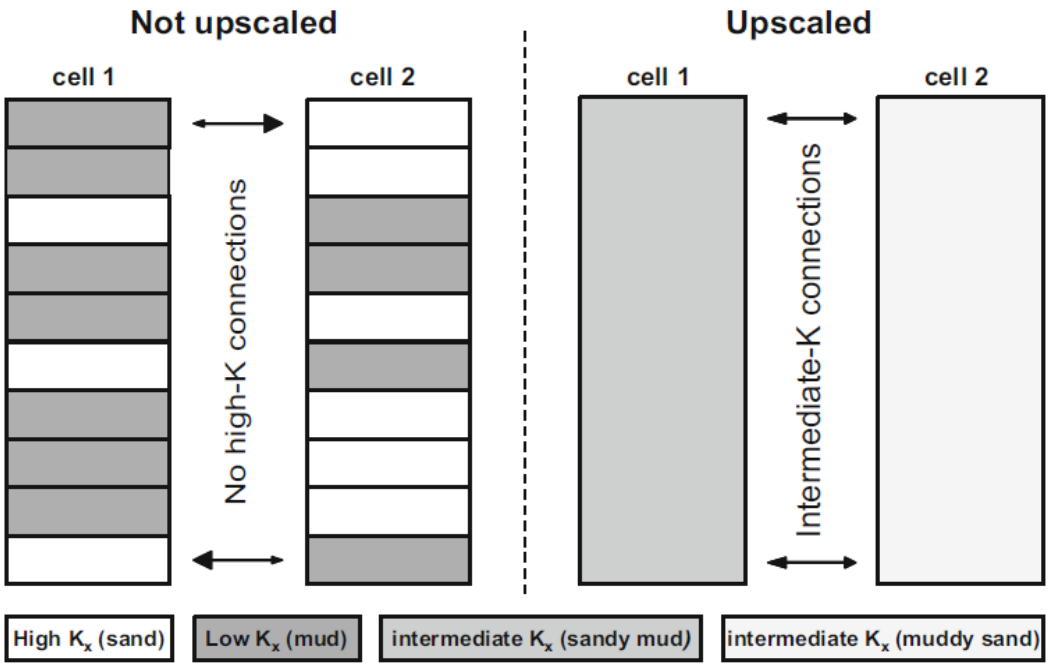

Figure 38. Effects of upscaling on flow connections between model blocks. Arrows indicate flow between cells, size of the arrow heads indicates the ease at which water can flow into the adjacent cell. Equivalent horizontal K was upscaled using the volume weighted arithmetic mean; equivalent vertical K was upscaled using the volume weighted harmonic mean (Fleckenstein and Fogg , 2008).

3.3. Structural features

As discussed in the previous sections, facies heterogeneity is one contributor to hydraulic conductivity heterogeneity and thus of groundwater flow variability. Another cause of hydraulic conductivity heterogeneity is the presence of structural features. Structural features include faults and fractured zones, both of which can serve as preferential flow paths. While fracturing of consolidated media may occur in faulted environments, the study of fracture flow constitutes a distinct field of research; therefore, these two types of structural features are discussed separately in the following sections.

3.3.1. Geological faults

Geological faults may act as a barrier or a conduit for groundwater flow, or a combination of the two (Aydin, 2000). More specifically, the hydraulic properties of faults are commonly highly anisotropic; i.e. a fault may simultaneously act as a conduit for flow parallel to the fault whilst acting as a barrier to flow perpendicular to the fault (Fachri et al., 2013). The hydrogeology of fault zones was summarised by Bense et al. (2013). Published studies of the effects of faults on local-scale groundwater flow include Person et al. (2000); regional groundwater flow studies have been reported by Bense et al. (2003), Bense and Person (2006), and Castro et al. (1998a). Published studies of the effects of faults on groundwater flow in reservoir models include Manzocchi et al. (2010; 2008; 2002; 1999). Recent examinations of the representation of faults in groundwater flow models include Islam and Manzocchi (2014a) and (2014b). In order to understand their influence on groundwater flow, the characterisation of geological faults in terms of architecture, spatial distribution and hydraulic properties is required. Here, we describe the architecture of faults in both crystalline (i.e. deep) and poorly lithified (i.e. shallow) environments. The alteration of host rock hydraulic properties by faulting is then discussed. We subsequently summarise existing representations of faults in numerical groundwater flow models.

Characterisation of fault architecture

The architecture of fault geology is context-specific and therefore varies considerably (Loveless et al., 2011). A primary distinction is made between faults that occur in (typically deep) crystalline media and those that occur in (typically shallow) unconsolidated environments. The classic conceptualisation of fault architecture in crystalline rocks was described by Caine et al. (1996). More recently, Loveless et al. (2011) presented two dimensional conceptualisations of fault zones in (a) crystalline rock and (b) unconsolidated media (Figure 39).

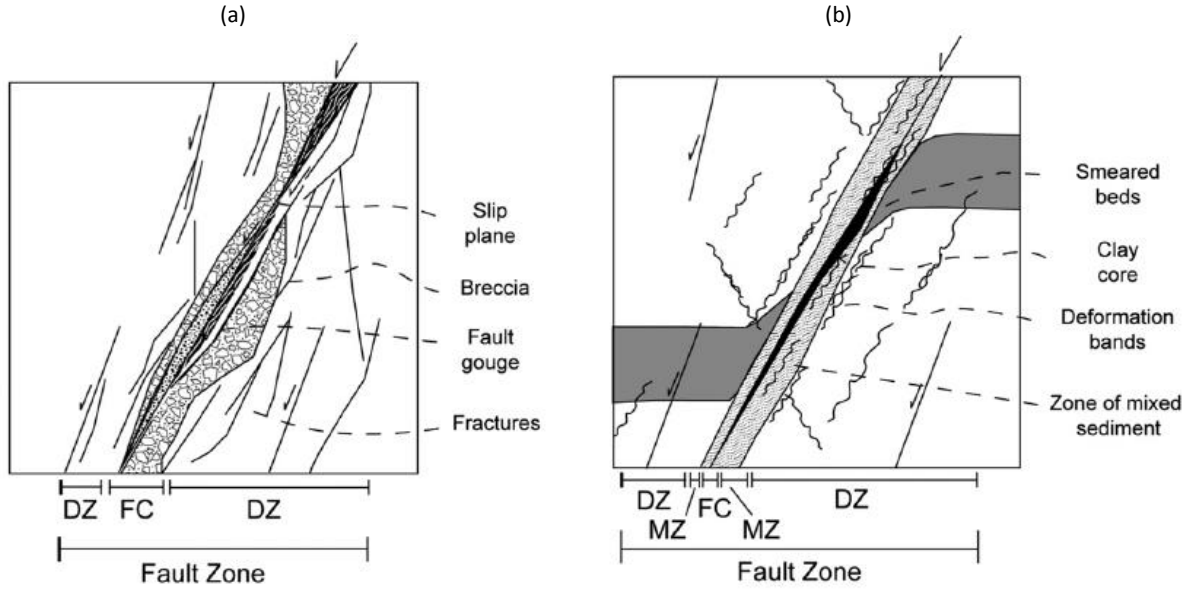

Figure 39. Conceptualisations of fault zone architecture in (a) crystalline (deep) media and (b) unconsolidated (shallow) media, showing fault core (FC), damage zone (DZ), and mixed zone (MZ) (Loveless et al., 2011).

Fault cores in crystalline rock occur as relatively narrow, localized zones containing modified media including breccias, and cataclasites. In this case, the permeability of the fault core will be higher than that of the host rock. In unconsolidated media, however, fault cores can act as barriers to groundwater flow, while the surrounding damage zones typically feature the presence of fractures which may provide conduits for fluid flow. Fractures in the damage zone are generally oriented parallel to the fault core (i.e. are mostly vertical), with hydraulic conductivity subsequently enhanced in both vertical and along-fault directions.

The combined width of the fault core and damage zone is collectively known as the fault zone. This represents the complete volume of rock deformed when lithospheric stresses cause two tectonic blocks to move in relation to one another (Loveless et al., 2011). Caine et al. (1996) proposed a number of fluid flow conceptualisations based on this fault characterisation (Table 7) including both conduits and barriers to flow, as well as mixed conceptualisations. More recent conceptualisations of fault zones in crystalline rock consider the presence of multiple fault cores as well as the geometric architecture of faults in three dimensions, in addition to heterogeneity in the permeability of fault rocks and fractures (Faulkner et al., 2010). A three-dimensional conceptualisation (Figure 40) illustrates the additional complexity of fault architecture in groundwater flow and hence the necessity for the development of 3-D (rather than 2-D) groundwater flow models.

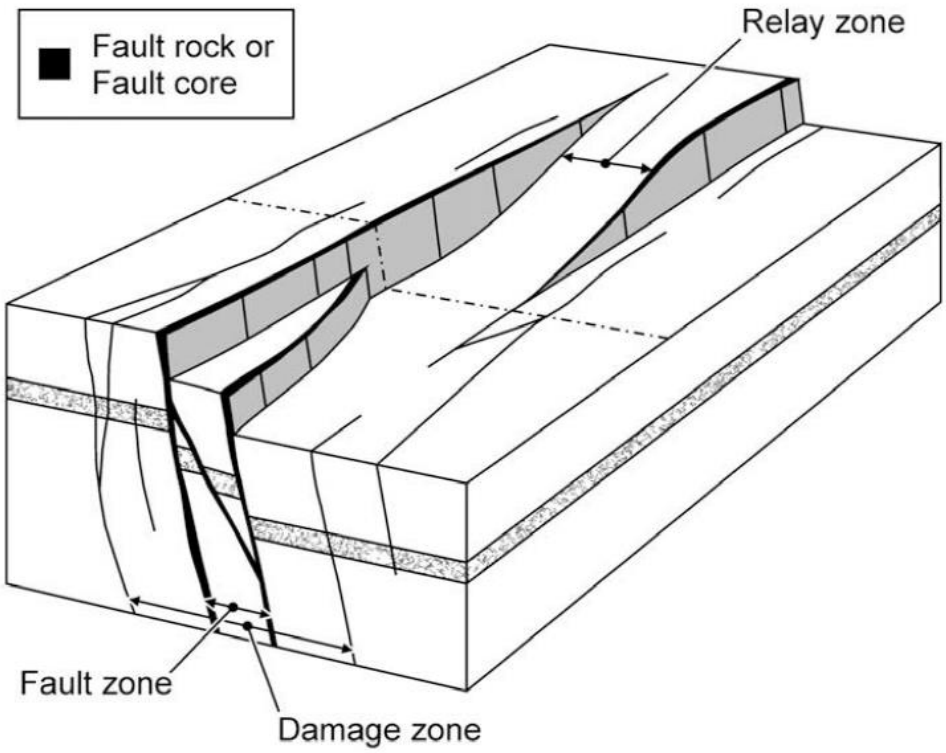

Figure 40. Three-dimensional conceptualisation of fault zone geometry, including fault, damage and relay zones, and showing the locations of multiple fault cores (Childs et al., 2009).

While the characterisation of faults has historically been focused on deep crystalline media (Loveless et al., 2011), a handful of studies have also considered shallow unconsolidated environments (Caine and Minor, 2009; Heynekamp et al., 1999; Rawling et al., 2001). In these publications shallow faults are characterised as consisting of a fault core, a damage zone and a third 'mixed' zone. The latter zone can consist of variably deformed, entrained and attenuated beds that are rotated parallel to the fault zone, forming smears along the fault trace with a continuous displacement geometry (Loveless et al., 2011). Other studies have examined shallow faults for which the fault core is entirely absent (Balsamo and Storti, 2010; Loveless et al., 2011). The absence of low permeability clay fault cores (or shear deformation bands) is potentially of hydrological significance, since these typically act as barriers to cross-fault fluid flow (Loveless et al., 2011). However, the presence of mixed zones may also impact fluid flow. Depending upon sediment content, mixed zones may act as either as barriers or conduits to cross-fault fluid flow (Loveless et al., 2011).

Table 7. Fault zone architectural styles and permeability structures (after Caine et al., 1996)

Permeability structure	Example architectural style	Fault core development	Damage zone development	Suggested flow model representation
Localised conduit	Localised slip fault along a single surface or multiple planes	Low	Low	Discrete fracture networks simulated as parallel conduits
Distributed conduit	Distributed slip fault accommodated along multiple surfaces	Low	High	Equivalent porous medium
Localised barrier	Localised slip fault accommodated within a cataclastic zone	High	Low	Aquitard within an aquifer
Combined conduit–barrier	Deformation accommodated within a localised cataclastic zone	High	High	Aquitard within two aquifers

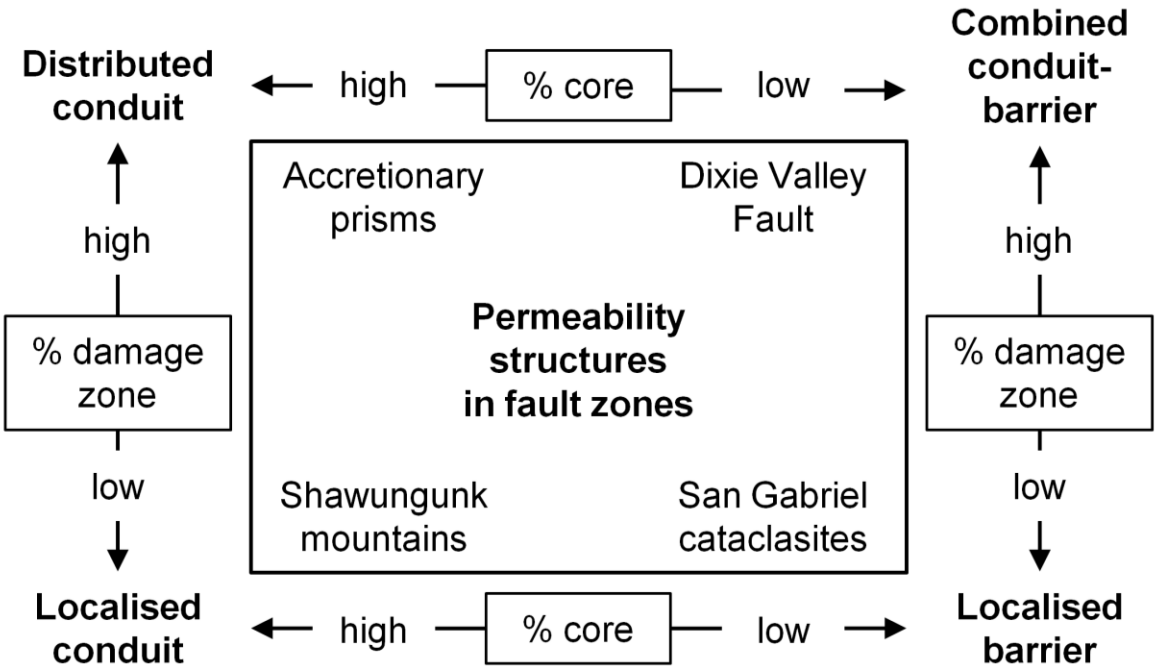

Figure 41. Conceptualisation of permeability structures in fault zones based on the relative composition of fault core and damage zones present (after Caine et al. 1996)

Characterisation of fault distributions

Torabi and Berg (2011) discussed empirical relationships typically used to characterise the dimensions (fault length versus fault displacement) and frequency of occurrence (frequency of fault displacements) of faults. A power-law relationship between fault displacement *D* [L], and length *L* [L] is often used:

$$D = cL^n \tag{4}$$

where *c* is a constant relating to material properties and the value of the exponent *n*, which typically ranges from 0.5 to 2.0, is informed by observational data. Figure 42 presents data from Kim and Sanderson (2005) who reviewed 15 studies of fault architecture in various locations and geological settings.

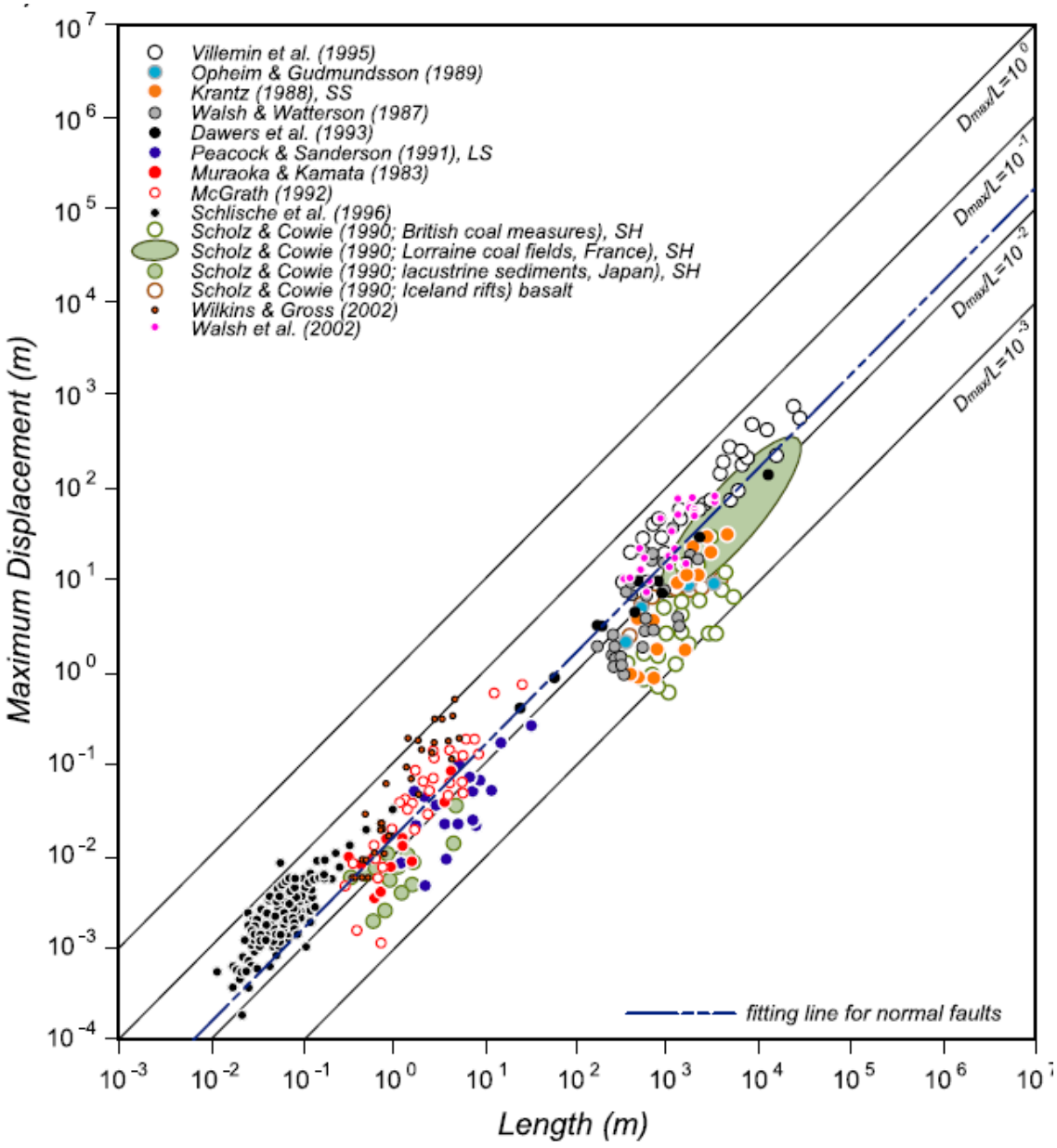

Figure 42. Fault displacement and length data from 15 studies collated by Kim and Sanderson (2005).

The validity of power-law relationships between fault displacement and length was reviewed by Kim and Sanderson (2005), based on a large number of faulted environments. Differences in such relationships could be related to errors in measurements of fault length and displacement, as well as to the history of fault growth. The number of faults (*N*) that are greater than or equal to *D* [L] located in a given region may be described by the power law:

$$N \propto D^{-m} \tag{5}$$

where the power law exponent *m* is informed by observational data. In the Australian context, Frery et al. (2014) presented observations of fault displacement and spatial distribution for the Stratford area of the Gloucester Basin, New South Wales (Figure 43).

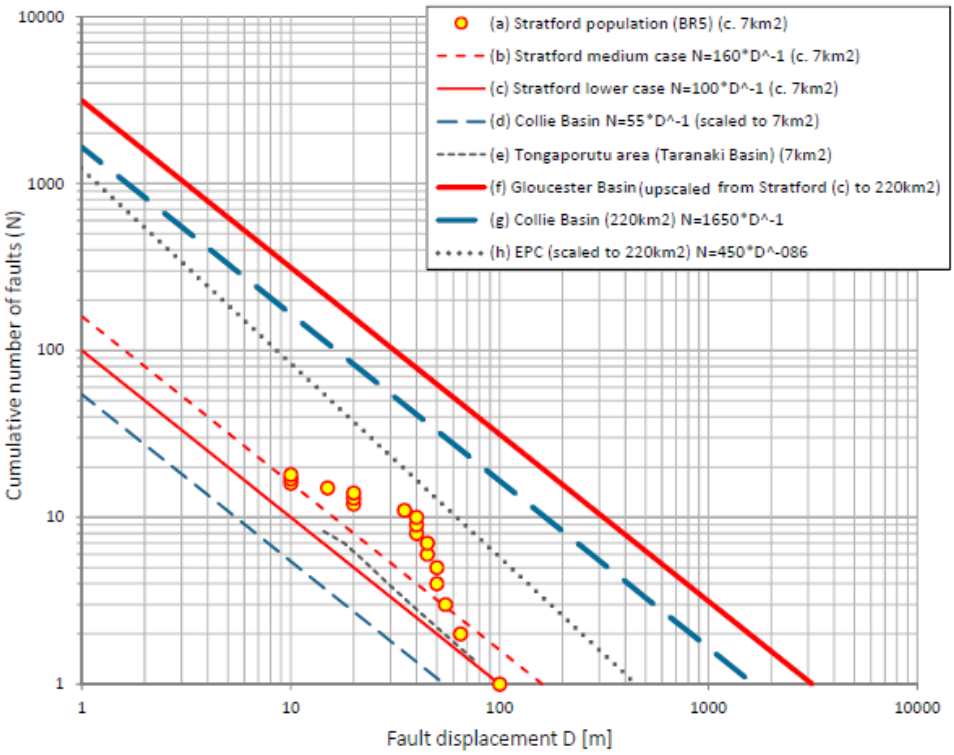

Figure 43.Observations of fault displacement and spatial distribution for the Stratford area of the Gloucester Basin, New South Wales (red circles with yellow fill); also shown are fault displacement–spatial distribution relationships derived in previous studies of the Gloucester Basin and other basins (Frery et al., 2014).

Relationships between fault displacement and fault core and/or damage zone thickness have been hypothesised by many authors (Childs et al., 2009; Knott et al., 1996; Sperrevik et al., 2002; Torabi and Berg, 2011). Sperrevik et al. (2002) derived a method for estimating fault zone thickness from fault throw based on outcrop data. The relationship, which was lithology-dependent, was related to the clay content of the fault zone. Faulkner et al. (2010) summarised relationships between microfracture density and distance from faults to estimate damage zone width from three published studies [Anders and Wiltschko (1994); Shipton and Cowie (2001); Vermilye and Scholz (1998); Figure 44]. A maximum damage zone width of 1000 m was observed and exponential models (black lines) were proposed to describe observed spatial variations.

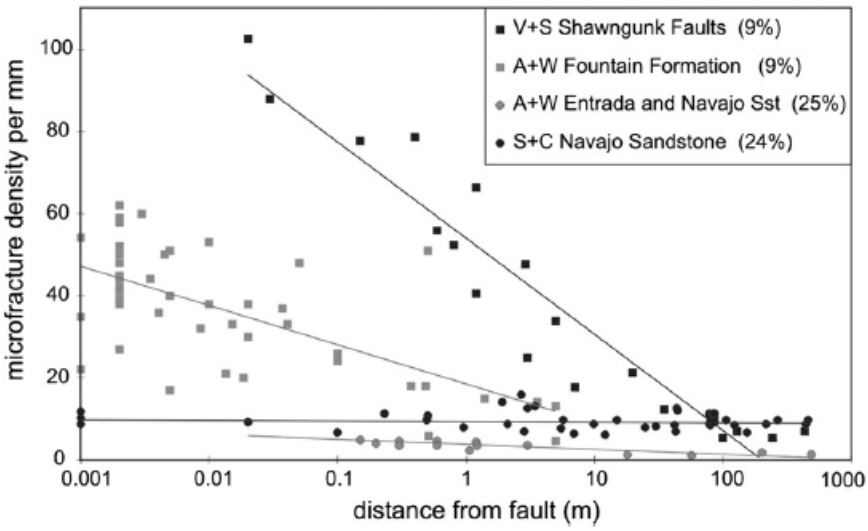

Figure 44. Damage zone width (as defined by microfracture density) data as a function of distance from fault, as summarised by Faulkner et al. (2010), using data from Anders and Wiltschko (1994), Shipton and Cowie (2001) and Vermilye and Scholz (1998).

Alteration of hydraulic properties

Processes that enhance or reduce the permeability of rocks and sediments in the vicinity of faults were summarised by Bense et al. (2013). Simplified versions of their findings (excluding references to field studies) are presented here. Key processes that may enhance fault zone permeability include particulate flow, fracturing and brecciation (Table 8). Particulate flow, which only occurs in unlithified rock, refers to the process of grains moving past one another. This process leads to rearrangement of the pore network and, depending upon the host rock type, either an increase or decrease in permeability. Fracturing, which may occur in all rock types, results from geomechanical stresses imposed by faulting; this is discussed in detail in Section 3.2.2. Brecciation, which may occur in all rock types, refers to the development of angular, coarse-grained fragments (i.e., clasts) from high-density fracturing. These clasts are typically embedded in a fine-grained matrix that accounts for less than 30% of the total rock volume (Bense et al., 2013).

Table 8. Primary fault processes that enhance permeability [after Bense et al., (2013)].

Process	Product	Unlithified to poorly lithified rock	Siliciclastic sedimentary rock	Carbonate sedimentary rock	Crystalline rock	Volcanic rock
Particulate flow	Deformation bands, sand smear	**common**				
Fracturing	Shear fractures, joints	possible	possible	**common**	**common**	**common**
Brecciation	Breccias	possible	possible	**common**	**common**	**common**

Key processes that may reduce fault zone permeability include particulate flow, phyllosilicate smearing, cataclasis and brecciation. Cataclasis refers to the fracturing and breakage of grains, resulting in a reduction in grain size (i.e., comminution). This results in a commensurate reduction in permeability. Phylosilicate (i.e., clay) smearing refers to the movement of clay grains due to shear stresses. This process typically occurs in unlithified and siliciclastic rocks and clay smears often develop along fault zones that intersect clay units (Bense and Person, 2006). A range of metrics exist by which to quantify the degree of smear, which include the shale gouge (Yielding et al., 1997), clay shear potential (Fulljames et al., 1997) and shale smear factor (Lindsay et al., 1993) (Figure 45). Recently Pei et al. (2015) summarised these approaches, each of which are based on a ratio involving a combination of fault displacements and clay unit thicknesses.

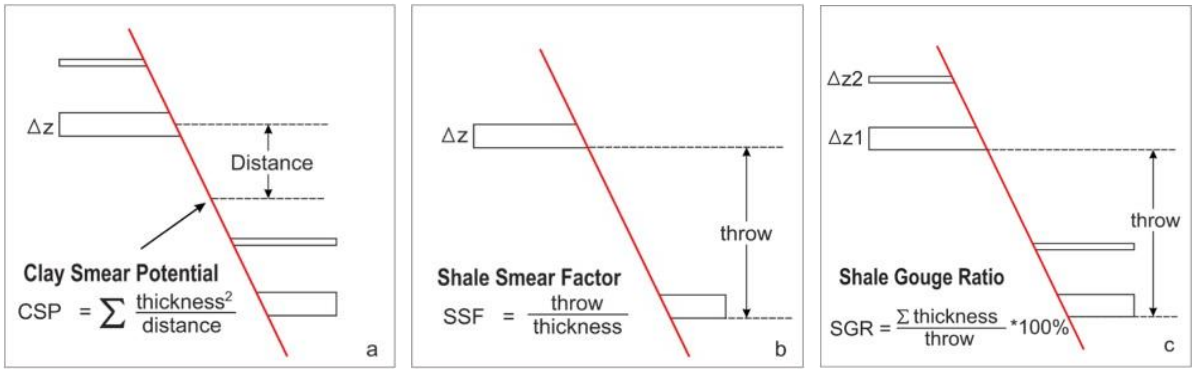

Figure 45. Common approaches to the estimation of fault zone clay content and permeability, including (a) clay shear potential (Fulljames et al., 1997), (b) shale smear factor (Lindsay et al., 1993) and (c) shale gouge ratio (Yielding et al., 1997) (Pei et al., 2015).

Table 9. Primary fault processes that reduce permeability [after Bense et al., (2013)].

Process	Product	Unlithified to poorly lithified rock	Siliciclastic sedimentary rock	Carbonate sedimentary rock	Crystalline rock	Volcanic rock
Particulate flow	Sediment mixing, dilation	**common**				
Phyllosilicate smearing	Phylosilicate bands	possible	**common**			
	Clay smearing	**common**	**common**	possible		
Cataclasis	Deformation bands	possible	**common**	possible		
	Cataclasite, ultracataclasite		**common**	**common**	**common**	possible
Brecciation, cataclasis	Fault gouges		**common**	**common**	**common**	**common**

Secondary processes that alter fault zone permeability include dissolution and cementation, pressure solution, sediment infilling and fault in-growth. Fluid flow in carbonate sedimentary rocks can lead to the formation of dissolution features. Subsequent precipitation of minerals results in the cementation of such features, which can reduce rock permeability. Pressure solution refers to the enhanced dissolution of minerals by external (e.g., geomechanical) stresses. This can result in the presence of insoluble clay minerals in the absence of calcite, thus reducing rock permeability.

Table 10. Secondary fault processes that either enhance or reduce permeability [after Bense et al., (2013)].

Process	Product	Unlithified to poorly lithified rock	Siliciclastic sedimentary rock	Carbonate sedimentary rock	Crystalline rock	Volcanic rock
Dissolution and cementation	Solution cavities, incomplete precipitation			common		
	Crack-seal veins or breccias			common	common	
	Veins, concretions and localised precipitation	possible	common	common	common	common
Pressure solution	Solution bands		possible	common		
	Stylolites			common		
Sediment infilling	Sediment infill			common		

Bense et al. (2003) characterised the hydraulic properties of a shallow fault zone in unconsolidated sediments of the Roer Valley Rift System, The Netherlands. Outcrop, core and image analysis techniques were used to estimate the spatial distribution of hydraulic conductivity in the fault core and damage zone respectively. Constant head permeameter testing of core samples indicated that hydraulic conductivity increased linearly from 16 $m.d^{-1}$ at the fault core to 19 $m.d^{-1}$ in the damage zone (Figure 38). Hydraulic conductivity then decreased with distance from the fault, with protolith values ranging from 5–12 $m.d^{-1}$. From independent image analysis, clay smearing, grain-scale mixing, and iron-oxide precipitation were identified as mechanisms by which hydraulic conductivity may be reduced in the fault core. Conversely, particulate flows were identified as hydraulic conductivity–enhancing mechanisms.

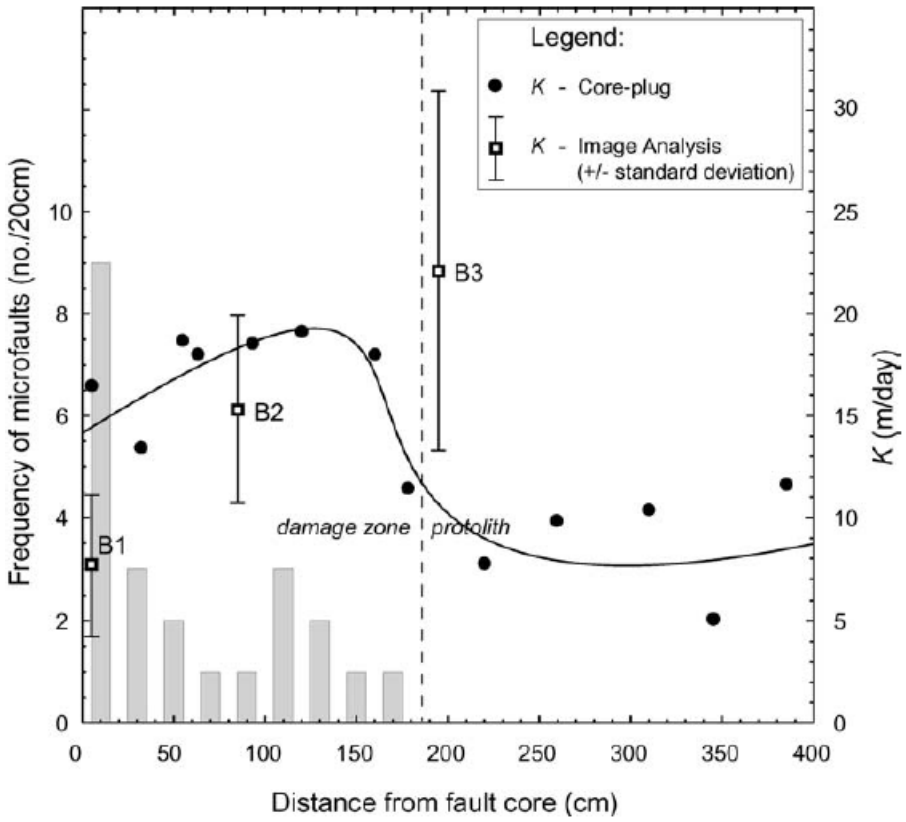

Figure 46. Constant head permeameter-based estimates of hydraulic conductivity of fault core, damage and protolith zones of the Geleen Fault Zone, part of the Roer Valley Rift System, The Netherlands (Bense et al., 2003).

Bense and Person (2006) presented an algorithm to predict fault zone width, lithological heterogeneity and hydraulic anisotropy in siliciclastic sediments, based upon the degree of fault throw and the clay content of the host lithology. The vertical permeability of the fault zone was calculated using a harmonic mean while horizontal permeability was calculated using an arithmetic mean. Using numerical groundwater flow models, they showed that strong hydraulic anisotropy in a fault zone can cause a fault to form a barrier to cross-fault flow while simultaneously acting as a conduit for along-fault flow, including vertical flow.

Myers (1999) first considered the use of power averaging methods (Deutsch, 1989) to characterise faulted permeability averaged over a given volume (Flodin et al., 2004). In this approach, the faulted permeability is calculated as the sum of the volume–permeability products for host rock, fault rock and joints, all raised to the power $1/\omega$.

Representation of faults in models

The representation of faults in groundwater flow models for CSG-related impact assessments is rare; for example, only three out of the 10 case studies reviewed herein (Section 4) featured representations of faults. Further exceptions include the study of Janardhanan and Moore (2015) who used the FAULTSIM utility of PEST to simulate the effect of faults on the groundwater head change and dilution impacts associated with injection of reverse osmosis-treated CSG produced water. Conversely, the simulation and parameterisation of faults in reservoir models has been an active research topic since 1990 [e.g., Bentley and Barry (1991); Acharya et al., (1997); Fisher and Knipe (1998, 2001), Knai and Knipe (1998); Manzocchi et al., (1998); Walsh et al., (1998)]. Manzocchi et al. (1999) derived an analytical approach incorporating the shale gauge ratio (Yielding et al., 1997) (Figure 45a) to derive transmissibility multipliers for use in reservoir simulation models. Manzocchi et al. (2002) further developed this approach to represent dual phase (i.e., water and oil) properties for both faults and host rock. Use of transmissibility multipliers is now the industry standard approach to representing faults in reservoir models (Manzocchi et al., 2010).

In addition to considering the single phase permeability of faults when calculating transmissibility multipliers, Fisher and Jolley (2007) suggested that the capillary pressure and relative permeability of fault rocks may also be significant. Examples of this approach include Fisher and Knipe (2001), Manzocchi et al. (2002), Rivenaes and Dart (2002), Al-Busafi et al. (2005), Al-Hinai et al. (2006), and Ziljstra et al. (2007). The effects of fault reactivation on shear stress, and therefore fluid flow, in the context of hydrocarbon reservoirs were examined using numerical models by Zhang et al. (2009; 2011). TerHeege et al. (2013) examined the sealing capacity of faults in siliciclastic sediments using a two-dimensional discrete element model informed by laboratory sandbox experimentation. A vertical clay smear structure representing a fault zone was vertically displaced by applying normal and/or shear stresses. The fault host rock simulated was a layered combination of sandstone and mudstone. A reduction in integrity of the smear structure was observed with increasing shear magnitude. Their results suggest that the sealing capacity of clay smears persist even where large fault displacements occur. This may be due to other permeability-reducing processes such as cataclasis. In such cases, shale gouge ratio approaches are well-suited, as these are able to account implicitly for the effects of such processes.

An alternative three-dimensional approach to fault representation in reservoir models was proposed by Tveranger et al. (2005) and Braathen et al. (2009) and subsequently demonstrated by Fredman et al. (2007, 2008), Soleng et al. (2007) and Fachri et al. (2011, 2013). In this approach, the fault zone is represented explicitly and is discretised to allow for heterogeneity in hydraulic properties (Fachri et al., 2013). A similar approach was undertaken by Wellmann et al. (2014), who developed 2-D vertical cross-sectional models of a CO_2 reservoir featuring a seal that had been breached by a geological fault. Uncertainties associated with various aspects of the groundwater flow system conceptualisation were quantified, including the location and thickness of the fault zone as well as the dimensions of both the reservoir and seal. Numerous numerical models were then created in order to test the sensitivity of predictions of CO_2 leakage via the fault. Predictions were found to be most sensitive to the location of the top of the fault and to the dimensions of the CO_2 reservoir top. Other modelling studies of CO_2 flow across geological faults were summarised recently by Celia et al. (2015), including works by Pruess (2005; 2008) and Kang et al. (2014).

In addition to representations of fault core permeability (which are primarily a function of damaged siliciclastic sediments), fault damage zones are often extensively fractured and require alternative approaches. For example, Caine and Forster (1999) developed numerical geological models of each permeability structure in order to simulate groundwater flow dynamics. Fault damage zones were represented by fracture sets and were generated stochastically using FRACMAN (Dershowitz et al., 1999).

Implementations

TransGen was the first commercial reservoir modelling software to include the calculation of transmissibility multipliers for all model cells located adjacent to faults. Since then, industry standard software packages such as TrapTester, PETREL, TEMPEST RMS and ECLIPSE (Schlumberger, 2011) have added the ability to calculate transmissibility multipliers from fault zone thickness, permeability and clay distribution (Fisher and Jolley, 2007). FAULTSIM (Doherty, unpublished; Janardhanan and Moore, 2015) implemented the approach of Bense and Person (2006) to calculate the permeability of fault zones based on throw, fault core thickness, damage zone thickness, and two anisotropic power coefficients. FAULTSIM was recently used by the Queensland Office of Groundwater Impact Assessment to investigate the effects of faults on groundwater flow in the Surat Basin (See Section 4.1.1 for details). FAULTSIM was previously used by Janardhanan and Moore (2015) in an assessment of risks associated with a large-scale CSG reinjection scheme.

3.3.2. Fractured media

Fractures are defined as the geometric planes in lithified media along which stress has caused partial loss of cohesion, resulting in a void space (Cook, 2003). Fractures may occur in impermeable rock (i.e., a single domain system) or in permeable rock (i.e., a dual domain system). Background reviews on groundwater flow through fractured porous media are available from Ababou (1991), Berkowitz (2002), Cook (2003) and Hsieh et al. (2001). Diodato (1994) provides an overview of fracture flow models. A review of permeability evolution (as a result of mechanical, chemical or thermal

processes) models for fractured porous media is available from Ma (2015). Approximations of groundwater flow in fractured media usually assume that fractures are planar and parallel. Many approaches also assume that fracture characteristics are identical. While these assumptions are unlikely to be true in the real world, they do provide a useful starting point for understanding the dynamics of groundwater flow through fractured rocks (Cook, 2003).

The hydraulic conductivity (K_f) [$L.T^{-1}$] of a single fracture located in impervious rock can be calculated as: [for a derivation of the equation from first principles, see (Bear et al., 1993)]

$$K_f = \frac{b^2}{12}\frac{\rho g}{\mu} \tag{6}$$

where b = fracture aperture [L], ρ = density of water [$M.L^{-3}$], g = gravitational acceleration [$L.T^{-2}$] and μ = viscosity of water [$M.L^{-1}.T^{-1}$]. Similarly, the transmissivity (T_f) a single fracture located in impervious rock can be calculated as (Bear et al., 1993):

$$T_f = \frac{b^3}{12}\frac{\rho g}{\mu} \tag{7}$$

In order to estimate a specific discharge rate (q) [$L.T^{-1}$], a network of fractures can be conceived as a parallel set of identical single fractures. Therefore, the latter equation can be scaled linearly by the number of fractures (N) and by the hydraulic gradient (i) (Bear et al., 1993):

$$q = N\frac{b^3}{12}\frac{\rho g}{\mu}i \tag{8}$$

This approach can be further developed for a network of fractures of varying apertures and spacings (Ababou, 1991):

$$\hat{q} = \frac{\sum {b_k}^3}{\sum l_k}\frac{1}{12}\frac{\rho g}{\mu}i \tag{9}$$

where $\hat{q}$ is the mean specific discharge rate [$L.T^{-1}$], and for a network of k=1...N fractures, each with aperture b_k and spacing l_k. Based on principles of superposition, additional expressions can be derived for orthogonal fracture networks. Similarly, expressions can be derived for networks featuring fractures of arbitrary orientation. It has been shown that the latter formulation is a generalisation of the Kozeny-Carman relationship.

Approaches to characterising fluid flow and solute transport in fractured media have often been grouped into three categories: (1) equivalent porous media approaches; (2) dual domain approaches; (3) discrete fracture networks. Altman et al. (1996) further divided each category into two sub-categories (Figure 11). The three key categories are now described.

Equivalent porous media approaches

Equivalent porous media approaches involve the representation of combined matrix and fracture flow using a single representative medium. This is the simplest approach and features the lowest data requirements; therefore, it is most suitable for regional-scale applications of steady-state flow (Cook, 2003). More highly fractured zones can be simulated using model cells featuring increased hydraulic conductivity and porosity. The primary limitation of the approach is the difficulty in defining the size of the REV used for simulation. Example applications of equivalent porous media approaches include Long et al. (1982), who used a stochastic approach to generate two dimensional fracture set realisations, from which effective parameters were estimated using numerical groundwater flow simulations. Andersson and Dverstorp (1987) used the same methodology to generate three-dimensional realisations and examined the effects of fracture radii and density on flow through a discrete fracture network. Dverstorp and Andersson (1989) continued this approach to simulate water inflow to a mine tunnel in Stripa, Sweden and compared modelled results to observed mine water inflows.

Dual domain approaches

Dual domain approaches involve the discretisation of the rock matrix and fractures as two separate flow domains (Figure 12). Within each of the two domains, bulk groundwater flow is simulated using equivalent hydraulic properties. The interaction between the matrix and fracture domains is typically implemented using a transfer rate coefficient. Gerke and van Genuchten (1993a; 1993b) derived a physically-based transfer rate coefficient for dual porosity models, based on rock

geometry and hydraulic conductivity. While the primary limitation of this approach is the difficulty in defining the rate coefficient, this approach is also limited by the ability to define the REV for both the matrix and fracture domains (Cook, 2003). Examples of dual domain approaches include Dershowitz and Miller (1995), who derived a dual porosity, single permeability approach to groundwater water flow and solute transport in fractured rock. Flow from the rock matrix to fractures was represented by an equivalent flux, calculated as a Darcian flux scaled by a geometric shape factor. Therrien and Sudicky (1996) developed a numerical solution to unsaturated flow and solute transport through fractured rock in which the rock matrix was represented in three dimensions while fractures were represented in two dimensions. Sarda et al. (2002) used a dual porosity approach to simulate fracture networks and matrix–fracture exchanges using a minimum number of model cells. Matrix geometry was determined using a training image approach featuring an image processing algorithm.

Discrete fracture networks

Discrete fracture network (DFN) approaches involve the explicit simulation of fracture networks, typically using stochastic realisations featuring simplified geometries. This is the most complex approach and requires a high level of fracture set characterisation. Image log testing is an available technique for assessing near wellbore fracture density, fracture aperture, and fracture orientation. Examples of image log techniques include borehole video camera (Overbey et al., 1988), acoustic formation image technology (McLean and McNamara, 2010), and resistivity image or formation micro-image logs (Kalathingal P and Kuchinski R, 2010). DFN approaches have been applied to nuclear waste disposal (Herbert, 1996), multiphase flow (Kim and Deo, 2000) and gas flow (Basquet et al., 2003). Recent developments include the generation of DFNs using connectivity metrics (Xu et al., 2006) and multiple point simulation (Liu et al., 2009), the use of Monte Carlo sampling to parameterise DFNs (Erhel et al., 2009), as well as the representation of heterogeneous fractures within DFNs (de Dreuzy et al., 2012). Elmouttie and Poropat (2012) presented a new method based on Monte-Carlo simulations of DFN geometry using more realistic and general representations of fractures combined with a robust polyhedral modelling algorithm.

3.4. Summary

With regards to the upscaling of hydraulic properties for use in groundwater flow models, a range of approaches have been identified. These may be classified into methods that involve reconstruction of geological heterogeneity (facies) followed by assigning representative hydraulic properties to the different facies [e.g., de Marsily et al., 2005 ; Falivene et al., (2007)] and those that reconstruct the heterogeneity of the flow property of interest directly [e.g., Renard and de Marsily (1997)]. The latter category includes conceptually simpler approaches which, through the upscaling process, attempt to preserve either a statistical characterisation or a rate of groundwater flow. Statistical characterisation typically involves the use of an appropriate mean type. Darcy Law-based approaches involve the imposition of a steady state groundwater flow problem on a sample volume, which is typically solved numerically. A third, less commonly used approach involves the preservation of connectivity metrics through the upscaling process.

Methods of spatial interpolation vary in complexity, depending upon how spatial variability is described. The simplest approach involves random sampling of a probability distribution to generate a spatial distribution of facies. This approach requires the identification of an appropriate statistical distribution; e.g., from expert elicitation. Traditional two-point geostatistical approaches use the first two statistical moments (i.e. mean and variance) and variogram models to characterise spatial variability. This approach requires a sufficient spatial distribution of observations to fit a variogram model. Two-point geostatistical approaches are typically used to generate multiGaussian parameter fields, which are appropriate for the characterisation of smoothly varying properties. Multiple-point statistical methods use training images as a basis from which to generate stochastic realisations. Training images are typically informed by outcrop exposures, geophysical data, or depositional modelling. This approach requires the identification of an appropriate training image and allows reconstruction of much more realistic geological structures such as channel-like features or discrete changes in hydraulic properties. Transition probability-based methods use probability distributions in a sequential Markov chain

approach to generate spatial distributions of multiple facies. These approaches require a sufficient spatial distribution of observations to identify the transition probability distributions.

The representation of geological faults in groundwater flow models is not commonly undertaken. Representations are typically limited to the simulation of faults as barriers to cross-fault groundwater flow. This is achieved by reducing inter-cell hydraulic conductivity parameters. In comparison, the effects of geological faults on groundwater flow are commonly simulated in reservoir models using the transmissibility multiplier approach first derived by Manzocchi et al. (1999). This approach requires quantification of the degree of fault displacement and the shale gauge ratio. The latter metric is commonly used to characterise the alteration of fault zone hydraulic properties. More complex approaches to the representation of faults include the consideration of the effects of multiphase flow on fault hydraulic properties or the explicit simulation of fault zone heterogeneity. Discrete fracture network models have also been used to represent the damage zone beyond the fault core. In a CSG impact assessment context, very few published studies have implemented faults in their groundwater models; to date only the FAULTSIM utility of PEST has seem some applications (Janardhanan and Moore, 2015; Moore et al., 2014b).

Groundwater flow through fractured porous media has commonly been simulated using three approaches. The simplest method represents combined fracture and matrix flow using an equivalent porous medium. This approach requires the characterisation of bulk flow properties, which may be estimated from hydraulic or environmental tracer testing. Of moderate complexity are dual domain approaches, which simulate flow in fractured and matrix domains separately. Flow between the two domains is typically simulated using a transfer rate coefficient. This approach requires the characterisation of the two flow domains. The parameterisation of rate transfer coefficient requires characterisation of fracture geometry, either from outcrop or core data. The most complex approach to representing groundwater flow in fractured porous media is the use of discrete fracture networks. These require the characterisation of fractures at the REV scale in order to generate stochastic realisations of fracture sets. Observations include fracture geometry, orientation, and spatial density.

4. Groundwater flow modelling of coal seam gas-related activities in Australia

Reservoir and groundwater flow models have been used in Australia to estimate the impacts of coal seam gas production in a number of published studies, primarily Environmental Impact Statements. These publications have informed our analysis of the current commonly used approaches to upscaling parameters, to performing spatial interpolation, and to representing faults and fractures. Model features salient to these approaches include model spatial extent and discretisation resolution. Processes by which geological layers are converted to hydrostratigraphic units (HSUs) and by which HSUs are subsequently converted to numerical model layers will also be discussed in the subsequent sections; published studies have been arranged per major basin, i.e. Surat Basin (Section 4.1), Bowen Basin (Section 4.2), Gunnedah Basin (Section 4.3), and Gippsland Basin (Section 4.4). The data sources for hydraulic property values and ranges will be highlighted, including the scale of support. Methods used to represent CSG extraction from the coal resource and how such models are linked with regional scale groundwater flow models will also be examined. The representation of geological faults is discussed only in those cases where these were explicitly included in groundwater flow modelling. A final summary of the analysis of ten CSG impact studies involving groundwater flow models is provided in Section 4.5.

4.1. Surat Basin

4.1.1. QWC / OGIA

In 2011 the Queensland Water Commission (QWC) commissioned GHD and Watermark Numerical Computing to develop a numerical model of groundwater flow in the Surat Cumulative Management Area (CMA) in order to estimate the potential cumulative impacts of multiple coal seam gas operation applications. Initial model development was undertaken and reported by GHD (2011) with further uncertainty analysis and predictive model runs undertaken and reported by Watermark Numerical Computing (2012). Summaries of the model design and main outputs were presented in the Surat Cumulative Management Area (CMA) Underground Water Impact Report (QWC, 2012). A transient MODFLOW-2005 finite difference model was developed in which a spatial extent of approximately 660 × 550 km was discretised into 441 rows and 365 columns using uniform cell dimensions of 1500 m × 1500 m. The model featured 19 layers and a mixture of specified flux and hydraulic head-dependent boundary conditions. Model layer geometries were developed from a hydrostratigraphic model developed using the geological modelling package MINEX.

Model layers were assigned on a one-to-one basis (i.e., direct translation from geological unit to hydrostratigraphic unit), with the exception of the uppermost layer and layers 7 to 11 (Table 11). This approach allows impacts from a single aquitard or from a series of aquitards to be analysed in detail. The uppermost layer was used to represent either the Condamine Alluvium, other alluvial deposits, or Main Range Volcanics, depending upon cell location. A minimum thickness of five metres was specified for layer 1. The Springbok Sandstone was sub-discretised into two layers (7–8) according to a 67:33 ratio. This was in accordance with field observations that the lower third of the Springbok Sandstone is characterised by markedly lower permeability than in the upper two thirds of the unit. The Walloon Coal Measures were sub-discretised using three model layers (9–11). The middle of these three layers represented the productive portion of the Walloon Coal Measures while the overlying and underlying layers represent mudstone aquitards (QWC, 2012).

Table 11. Summary of geological units, hydrostratigraphic units and groundwater flow model layers represented in OGIA Surat Basin groundwater flow model.

Geological unit	Hydrostratigraphic unit		Model layer
	aquifer	aquitard	
Condamine Alluvium / Main Range Volcanics	✓		1
Rolling Downs Group		✓	2
Bungil Formation / Mooga Sandstone	✓		3
Orallo Formation		✓	4
Gubberamunda Sandstone	✓		5
Westbourne Formation		✓	6
Springbok Sandstone (upper)	✓		7
Springbok Sandstone (lower)	✓		8
Walloon Coal Measures (upper aquitard)		interburden	9
Walloon Coal Measures (coal seams)	CSG reservoir		10
Walloon Coal Measures (lower aquitard)		interburden	11
Hutton Sandstone / Marburg Sandstone	✓		12
Evergreen Formation		✓	13
Precipice Sandstone	✓		14
Moolayember Formation		✓	15
Clematis Sandstone / Showgrounds Sandstone	✓		16
Rewan Group		✓	17
Bandanna Formation	CSG reservoir		18
Permian sediments	✓		19

GHD (2011) reported hydraulic conductivity (*K*) values separately for assigned aquifer and aquitard model layers. Horizontal hydraulic conductivity (K_h) values were reported for the former while vertical hydraulic conductivity (K_v) values were reported for the latter. "Secondary" *K* values (e.g., K_h values for aquitard layers) were calculated using anisotropy scalars.

Initial pre-calibration K_h values were obtained from a number of sources. For the majority of model aquifer layers (i.e., 3, 5, 7, 8, 12), single values were derived from a review of previous Surat Basin models (USQ, 2011). For the productive seam of the Walloon Coal Measures and for all aquifer layers underlying the Hutton Sandstone (i.e., model layers 10 and 14, 16, 18), values were assigned on a cell-by-cell basis using empirical functions of depth in order to account for overburden pressure effects. For the horizontal *K* of the Main Range Volcanics (model layer 2), a median value obtained from all available hydraulic pumping test results for this unit was used. For the Condamine Alluvium and for other alluvial units (model layers 1 and 3), hydraulic conductivities were obtained from a prior model of the Condamine Alluvium aquifer.

Similarly, initial pre-calibration K_v values were also obtained from a number of sources. For the majority of model aquitard layers (2, 4, 6, 13, 15), values were derived from a review of Surat Basin models (USQ, 2011). For the aquitard units of the Walloon Coal Measures, values were assigned on a cell-by-cell basis using empirical functions of depth in order to account for overburden pressure effects. K_v values of the Rewan Group (17) and pre-Bandanna units (19) were obtained from prior modelling of the Bowen Basin by Santos (2010).

Acceptable hydraulic conductivity ranges for model inversion purposes were defined based on the 5^{th} and 95^{th} percentiles of the available observed data. Results from over 13 000 drill stem tests were obtained from the Queensland Petroleum Exploration Database and more than 1000 pump test records were obtained from the DNRM groundwater database (QWC, 2012). Aquifer K_h values and aquitard K_v values were adjusted through inverse modelling and were typically allowed to vary over three to five orders of magnitude. Anisotropy scalars were also calculated through inverse modelling, during which they were typically allowed to vary over three or four orders of magnitude.

Specific storage and specific yield values for the Walloon Coal Measures only were estimated through calibration of a transient sub-model of the operational Kogan North / Daandine CSG borefield. Storage values were allowed to vary across a wide range of values between the minimum anticipated specific storage (i.e., 5×10^{-6} m^{-1} for most layers) and the maximum anticipated specific yield (i.e., 0.01 – 0.1 in most layers). This reflects the fact that semi-confined conditions can occur in units that are not present at outcrop. Available time series data of hydraulic head were considered to be insufficient to reliably estimate storage parameters through inverse modelling. Storage parameters for the remaining model layers excluding the Walloon Coal Measures were therefore unconstrained for predictive modelling purposes. The effects of this assumption on predictions were tested via the subsequent uncertainty analysis work (Watermark Numerical Computing, 2012).

Structural features such as geological faults were not explicitly represented in the model or subsequent uncertainty analyses; hence, it is not possible to differentiate the impacts of faults from other contributors to regional scale parameter uncertainty.

Coal seam gas extraction was simulated using a hydraulic head-dependent (i.e., Cauchy) boundary condition, implemented using the MODFLOW Evapotranspiration package. For a given model cell, this approach removes water at a specified maximum rate when the hydraulic head in the cell is at or above a specified (upper) elevation. When the hydraulic head is below a second specified (lower) elevation then zero flux is applied. When the cell hydraulic head is located between the two nominated elevations then the extraction flux is calculated as a linear function of position between the two specified elevations. Maximum extraction fluxes were obtained from each of the four coal seam gas development applicants. Lower specified elevations (i.e., target hydraulic heads) were specified as 20 – 40 m above the productive portion of the Walloon Coal Measures (i.e., model layer 10) depending on the depth to the top of coal measures, based on advice received from the relevant CSG companies.

From 2012 onward, OGIA has continued to develop the Surat CMA groundwater flow model and other related models through a range of research projects (OGIA, 2013; 2014). A new geological model of the Surat CMA has been developed based on reinterpretation of existing data as well as the inclusion of lithological and downhole geophysical data from over 3500 CSG bores. This revised geological model includes explicit representation of major fault systems present within the basin.

The Surat CMA groundwater flow model itself is in the process of being extensively revised based on the revised geological model but also incorporating a number of other improvements which are briefly described below. One significant change has been the conversion of the model from the MODFLOW–2005 platform to MODFLOW–USG. While the former code used a finite difference scheme to solve the groundwater flow equation on a rectilinear grid, the latter code uses a control volume finite difference formulation on unstructured grids (Panday et al., 2013). The latter approach enables greater flexibility in local grid refinement and is well suited to the simulation of discontinuous hydrostratigraphic units.

Significant effort is also being expended to more accurately represent the local scale physics of CSG extraction in the Surat CMA model (OGIA 2015, pers. comm.) including, but not limited to, the following four points.

- Changes in coal seam permeability and storage coefficients due to desaturation during CSG extraction will be approximated using a modified Richards equation framework that employs a CSG-specific van Genuchten (1980) function that can reflect saturation–pressure relationships observed in detailed CSG reservoir simulations (Herckenrath et al., 2015). The efficacy of this approach has been validated through comparison to hydraulic responses calculated using an ECLIPSE reservoir model.
- Distinction will be made between coal and non-coal lithology within CSG reservoirs. This is achieved through lithological segregation in which coal and non-coal reservoir units are lumped together, after which these portions of the CSG reservoir are represented in a dual-porosity framework where coal acts as the mobile domain and the non-coal units as the immobile domain. This is an implementation of the general theory discussed in section 2.1.
- Increases in the apparent permeability of upscaled coal measures immediately adjacent to CSG production bores will also be considered. At a regional scale, coal formations such as the Walloon Coal Measures are typically considered as low permeability units, as a result of limited lateral connectivity between coal seams. CSG production wells are

located in order to access coal seams preferentially. For this reason, hydraulic properties will be enhanced on a cell-by-cell basis. Similarly, once wells are decommissioned, de-enhancement of such properties will be implemented.

- The representation of CSG extraction using hydraulic head–dependent boundary conditions has been further developed. Rather than the MODFLOW Evaporation package used in the previous model, CSG extraction will be simulated using the Drain package parameterised using bottom-hole pressure information provided by the gas companies. Furthermore three MODFLOW layers will also be used to represent the Walloon Coal Measure to accommodate large vertical gradients induced within the CSG reservoir due to the gas-filled nature of CSG wells. Vertical offsets of cell-centred nodes will also be applied that facilitate the representation of these vertical gradients more accurately while ensuring correct calculation of inter-layer conductances.

Further improvements will also be applied in terms of the initial parameterisation of the model. In particular, the transition probability-based stochastic parameter field generator T-PROGS (Carle, 1999) has been used to generate multiple realisations of lithology for individual stratigraphic units for over 350 sub-areas within the Surat Basin. Local models were developed for each of these sub-areas and for each stratigraphic unit present from the Gubberamunda Sandstone down to the Precipice Sandstone. A fine vertical discretization ranging from 0.1 m to 1.0 m was adopted to ensure the accurate simulation of the local connected-network generated by T-PROGS. For areas with borehole data lithological realisations were generated honouring local lithology proportions, empirical transition probabilities and local borehole lithologies. For areas without borehole data local proportions were generated stochastically based on the regional lithology dataset. These lithological realisations were subsequently populated by permeabilities obtained through stochastic permeability modelling that integrates all available data at all available scales, including petrophysical, core, drill stem test and pumping test data. The lithological realisations populated with permeability (referred to as numerical permeameters) are then subject to flow calculations which enable back-calculation of effective permeability in both the horizontal and vertical direction at a stratigraphic unit or formation scale. In addition to providing robust estimates of expected formation scale hydraulic conductivity values for all units present at the location of each of 350 permeameters this process also provides information on the stochasticity of these upscaled properties for use in subsequent model calibration and uncertainty analysis calculations. One or more papers describing the parameterisation of the next generation of the OGIA regional groundwater model are currently in preparation.

The effects of structural features on the propagation of CSG impacts at a regional scale will be examined through the inclusion of geological faults in the MODFLOW–USG model. Major faults, which are also represented in the geological model, will be represented explicitly in the model geometry and parameterisation (Keith Phillipson, OGIA, pers. comm. June 2015). Minor sub-seismic faults will be represented stochastically as part of a calibration constrained uncertainty analysis. Parameterisation of faults will be implemented using a customised FORTRAN code ('FAULTSIM'; Doherty, unpublished; Janardhanan and Moore, 2015) to modify hydraulic properties on a cell-by-cell basis based on anticipated fault throw magnitudes, the thicknesses of the fault core and damage zone, the scalar effect on both horizontal and vertical hydraulic conductivity, and the proportion of each model cell affected by faulting.

Many of the improvements outlined above have resulted from and are under-pinned by results from a number of detailed local scale research models. One such model has been developed for the Talinga CSG borefield area. An ECLIPSE model was used to simulate fluid flow processes in 294 layers spanning the vertical interval from the top of the Springbok Sandstone to the bottom of the Hutton Formation. Conditioned lithological realisations for the static Talinga model were generated using T-PROGS. Dual phase flow equations were solved using the ECLIPSE reservoir simulator. The model was history matched against water and gas production as well as observed drawdowns in the Springbok and Hutton sandstones before a detailed sensitivity analysis was undertaken. Model parameters that were investigated in the parametric sensitivity analysis include horizontal and vertical permeabilities, porosity and compressibility as well as diffusion coefficients, relative permeabilities and Langmuir isotherm coefficients. The sensitivity of CSG impacts to the presence of structural features was also examined. Features tested included: (a) a normal fault; (b) an abandoned well that connected aquifers with CSG-producing coal seams; and (c) a CSG bore with sections screened in aquifer units, such as the Springbok Sandstone. Further studies are planned involving the Talinga reservoir model, including simulation of various normal fault settings (i.e., different fault throws and lengths) and stochastic parameterisation of fault core and damage zones. A detailed 158 layer MODFLOW-USG model of part of the Condamine Alluvium and adjacent QGC and Arrow CSG bore fields has also been

developed. This model was built to explore details of the effect of CSG extraction on the Condamine Alluvium that the regional scale OGIA Surat CMA model cannot explore. One or more papers describing the Talinga sensitivity analysis work are currently in preparation.

4.1.2. Arrow Energy

As part of EIS requirements for the Surat Gas Project, Arrow Energy commissioned Schlumberger Water Services to develop a numerical groundwater flow model to provide estimates of CSG extraction impacts (SWS, 2012). Based on a PETREL geological model, a MODFLOW–2000 model was developed, covering a total area of 453 × 270 km. This was discretised using 1000 m × 1000 m cells into 453 rows and 270 columns. The model featured 15 layers and a mixture of Neumann (or flow) and Cauchy (or head-dependent) flow boundary conditions. The discretisation of model layers is shown in Table 12. For this model, the Westbourne Formation represents the key aquitard that will affect the upward vertical propagation of hydraulic stresses, induced in the underlying coal seams by CSG production, to the Gubberamunda Sandstone and other overlying aquifers. Conversely, the combined Eurombah–Durabilla Formation represents the key aquitard that will affect the downward vertical propagation of hydraulic impacts to the underlying Hutton Sandstone aquifer.

Model layers were assigned on a one-to-one basis, with the exception of the Lower Cretaceous sequence (2) and the Durabilla and Eurombah formations (12), which were both amalgamated as single model layers. Hydraulic property ranges were informed by literature review of numerous published EIS and state agency documents. Horizontal to vertical hydraulic conductivity ratios based on rock type were obtained from literature. Neither spatial variability nor depth-dependency of hydraulic properties was considered; all model layers featured homogeneous hydraulic conductivity and specific storage values. The former parameters were anisotropic. Horizontal hydraulic conductivity values, K_h : K_v ratios and specific storage values were estimated within specified ranges during model inversion.

Table 12. Summary of geological units, hydrostratigraphic units and groundwater flow model layers represented in Arrow Energy Surat Basin groundwater flow model.

Geological unit	Hydrostratigraphic unit		Model layer
	aquifer	aquitard	
Condamine Alluvium	✓		1
Lower Cretaceous sequence		✓	2
Mooga Sandstone	✓		3
Orallo Formation	✓		4
Gubberamunda Sandstone	✓		5
Westbourne Formation		✓	6
Springbok Sandstone	✓		7
10 m thick shale		interburden	8
Juandah Coal Measures	CSG reservoir		9
Tangalooma Sandstone		interburden	10
Taroom Coal Measures	CSG reservoir		11
Durabilla Formation / Eurombah Formation		✓	12
Hutton Sandstone	✓		13
Evergreen Formation		✓	14
Precipice Sandstone	✓		15

CSG production was simulated using the Multi-Node Well (MNW) package (Halford and Hanson 2002), which allows for extraction fluxes to be partitioned across model layers. This approach is commonly used for water bores that are screened across multiple hydrostratigraphic units. The proportion of extracted volume is calculated as a function of the transmissivity and hydraulic head in each HSU. In the present case, the MNW package was used to distribute CSG fluxes across the Juandah Coal Measures, Tangalooma Sandstone and Taroom Coal Measures (i.e., model layers 10–12).

4.1.3. Origin Energy

As part of EIS requirements for the Australia Pacific Liquefied Natural Gas Project, Origin Energy commissioned Worley Parsons to develop a numerical groundwater flow model to provide estimates of CSG extraction impacts (APLNG, 2010a; 2010b). Based on a PETREL geological model, a FEFLOW model was developed, covering a total area of 172 740 km^2. This was discretised using approximately 12 km–sized triangular cells. The solution mesh was refined using 6 km–sized cells within a 70 km buffer around CSG tenement areas. The solution mesh was further refined using 3 × 3 km^2–sized cells within CSG tenement areas. The model featured 23 layers and a mixture of Neumann and Cauchy boundary conditions. The discretisation of model layers is shown in Table 13. For this model, the Westbourne Formation represents the key aquitard that will affect the upward vertical propagation of hydraulic stresses induced in the underlying coal seams by CSG production to the Gubberamunda Sandstone and other overlying aquifers. Conversely, the Eurombah Formation represents the key aquitard that will affect the downward vertical propagation of hydraulic impacts to the underlying Hutton Sandstone aquifer.

Model layers were assigned on a one-to-one basis, with the exception of the combined Bungil Formation / Mooga Sandstone / Orallo Formation (3) and the Walloon Coal Measures (7–17) (Table 13). The latter unit, composed of an alternating sequence of coal seams and interburden layers, was discretised using 11 model layers. Horizontal hydraulic conductivity (K_h) values were obtained through inverse modelling, based on the matching of model outputs to pre-development hydraulic heads, as well as to estimates of water production from reservoir modelling. Vertical hydraulic conductivity values were subsequently calculated by assuming anisotropy ratios of 1:30 and 1:300 for aquifers and aquitards respectively. A quantitative basis for this assumption was not described by APLNG (2010a; 2010b). Initial K_h values (minima and maxima) used in model inversion were based on a range of sources. Initial values were calculated using the geometric mean of each range identified. Data sources included drill stem tests (for coal seams only), an aquifer test conducted in the Precipice Sandstone, and previous numerical groundwater models, as well as the interpretation of downhole geophysical logs. For the latter case, the following relationship between K_h (m.d^{-1}) and gamma ray counts (γ; API units) was established, based on data obtained from up to fifteen locations:

$$K_h = \exp\left(-\frac{\gamma+39.891}{3.6771}\right) \quad (10)$$

While multiple downhole geophysical logs were used to estimate the statistical variability of hydraulic conductivity for each hydrostratigraphic unit, they were not used to characterise spatial variability. Instead, homogeneous hydraulic conductivity values were specified for all model layers. Similarly, uniform storage parameters (specific storage = 4.0 × 10^{-6} m^{-1}; specific yield = 0.03) were specified in all layers of the model. The specific storage value was based on a single hydraulic test conducted on the Precipice Sandstone at the Kogan Creek power station, as reported by AGE (1999). The source of the specific yield value used was not described by APLNG (2010a; 2010b).

Table 13. Summary of geological units, hydrostratigraphic units and groundwater flow model layers represented in Origin Energy Surat Basin groundwater flow model.

Geological unit	Hydrostratigraphic unit type		Model layer
	aquifer	aquitard	
Cenozoic alluvium	✓		1
Rolling Downs Group		✓	2
Bungil Formation / Mooga Sandstone / Orallo Formation	✓		3
Gubberamunda Sandstone	✓		4
Westbourne Formation		✓	5
Springbok Sandstone	✓		6
WCM (upper unit)		interburden	7
WCM (Macalister coal seam)	CSG reservoir		8
WCM (Macalister mudstone)		interburden	9
WCM (upper Juandah sandstone)	✓		10
WCM (lower Juandah mudstone)		interburden	11
WCM (lower Juandah coal seam)	CSG reservoir		12
WCM (lower Juandah mudstone)		interburden	13
WCM (Tangalooma Sandstone)	✓		14
WCM (upper Taroom mudstone)		interburden	15
WCM (Taroom Coal Measures)	CSG reservoir		16
WCM (lower Taroom mudstone)		interburden	17
Eurombah Formation		✓	18
Upper Hutton Sandstone	✓		19
Lower Hutton Sandstone	✓		20
Evergreen Formation		✓	21
Precipice Sandstone	✓		22
Moolayember Formation		✓	23

CSG production was represented using a time-varying specified hydraulic head (i.e., Dirichlet) boundary condition. Transient hydraulic head values were calculated *a priori* using the Theis (1935) analytical solution for radial 1-D drawdown in an isotropic homogeneous infinite aquifer. Calculated solutions were consistent with a final target pressure head of 35 metres above the top of coal seams (at which it is assumed that gas flow commences). Transient hydraulic head values were applied in the Macalister coal seam, lower Juandah coal seam and Taroom Coal Measures (i.e., model layers 8, 12 and 16).

4.1.4. Queensland Gas Company

As part of EIS requirements for the Queensland Curtis Liquefied Natural Gas Project, the Queensland Gas Company commissioned Golder Associates to develop three numerical groundwater flow models to provide estimates of CSG extraction impacts (QGC, 2013). The first two models (i.e., GEN1 and GEN2) were developed in 2009 and 2011 respectively using the MODFLOW single phase flow simulation code. The most recent model (GEN3) was developed in 2013 using the multi-phase flow simulation code ECLIPSE and incorporated improvements derived from prior modelling as well as from the Queensland Water Commission Surat Cumulative Management Area model. This work was complemented by a study undertaken by the CSIRO and Queensland Gas Company to look at the issue of predictive simulation errors arising from the

combination of upscaling of hydraulic properties, and representation of dual phase processes - occurring under conditions of CSG extraction - with a single phase model (Moore et al., 2013).

Based on a PETREL geological model, the GEN3 model covered a total area of 172 740 km^2. This was discretised using 1500 m × 1500 m cells into 243 rows and 245 columns. The model featured 21 layers and a mixture of Neumann and Cauchy boundary conditions. The discretisation of model layers is shown in Table 14. The Westbourne Formation represents the key aquitard that will affect the upward vertical propagation of hydraulic stresses induced in the underlying coal seams by CSG production to the Gubberamunda Sandstone and other overlying aquifers. Conversely, the Eurombah Formation represents the key aquitard that will affect the downward vertical propagation of hydraulic impacts to the Hutton Sandstone aquifer.

Table 14. Summary of geological units, hydrostratigraphic units and groundwater flow model layers represented in QGC Surat Basin GEN3 groundwater flow model.

Geological unit	Hydrostratigraphic unit		Single porosity model layer	Dual porosity model layer
	aquifer	aquitard		
Cretaceous sediments	✓		1	22
	✓		2	23
	✓		3	24
Gubberamunda Sandstone	✓		4	25
Westbourne Formation		✓	5	26
Springbok Sandstone	✓		6	27
	✓		7	28
	✓		8	29
	✓		9	30
Juandah Coal Measures (upper)	CSG reservoir		10	31
interburden		interburden	11	32
Juandah Coal Measures (lower)	CSG reservoir		12	33
interburden		interburden	13	34
Tangalooma Sandstone / Taroom Coal Measures	CSG reservoir		14	35
Eurombah Formation		✓	15	36
		✓	16	37
Hutton Sandstone	✓		17	38
Evergreen Formation		✓	18	39
Precipice Sandstone	✓		19	40
Bowen Basin			20	41
			21	42

For the Gubberamunda Sandstone, Westbourne Formation, Hutton Sandstone, Evergreen Formation and Precipice Sandstone units, model layers were assigned on a one-to-one basis. Cretaceous sediments were discretised using three layers (1–3) and the Springbok Sandstone was discretised using four layers (6–9). The Walloon Coal Measures were discretised using five layers of alternating coal seams and interburden (10–14). The Eurombah Formation was discretised into two layers (15–16), as were the unidentified Bowen Basin units underlying the Precipice Sandstone. Using a dual porosity approach, all model layers were assigned a second layer in order to simultaneously account for fractured (i.e., not matrix) flow in all hydrostratigraphic units.

Hydraulic property values were informed by analysis of downhole geophysical logs. Eleven locations were used to estimate properties for the Precipice Sandstone and all deeper geological units, while 118 locations were used to estimate properties for the Gubberamunda Sandstone, Westbourne Formation and Springbok Sandstone. Hydraulic conductivity values were estimated from downhole petrophysical observations using the following approach. First, effective porosities were estimated from shale volumes identified in neutron- density and resistivity logs. Anomalous porosity values resulting from borehole casing and "coal shoulder" effects were subsequently removed, as were values judged to be unreasonably low. Using data from core analyses, exponential porosity-permeability relationships were identified for each formation. These relationships were subsequently used to convert the statistical distributions of porosities obtained from petrophysical logs to distributions of permeabilities, and then of hydraulic conductivities. A single representative horizontal permeability value for each layer was then calculated as the arithmetic mean of the relevant statistical distribution. Vertical permeability values were calculated using anisotropy ratios based on observed data (Figure 47).

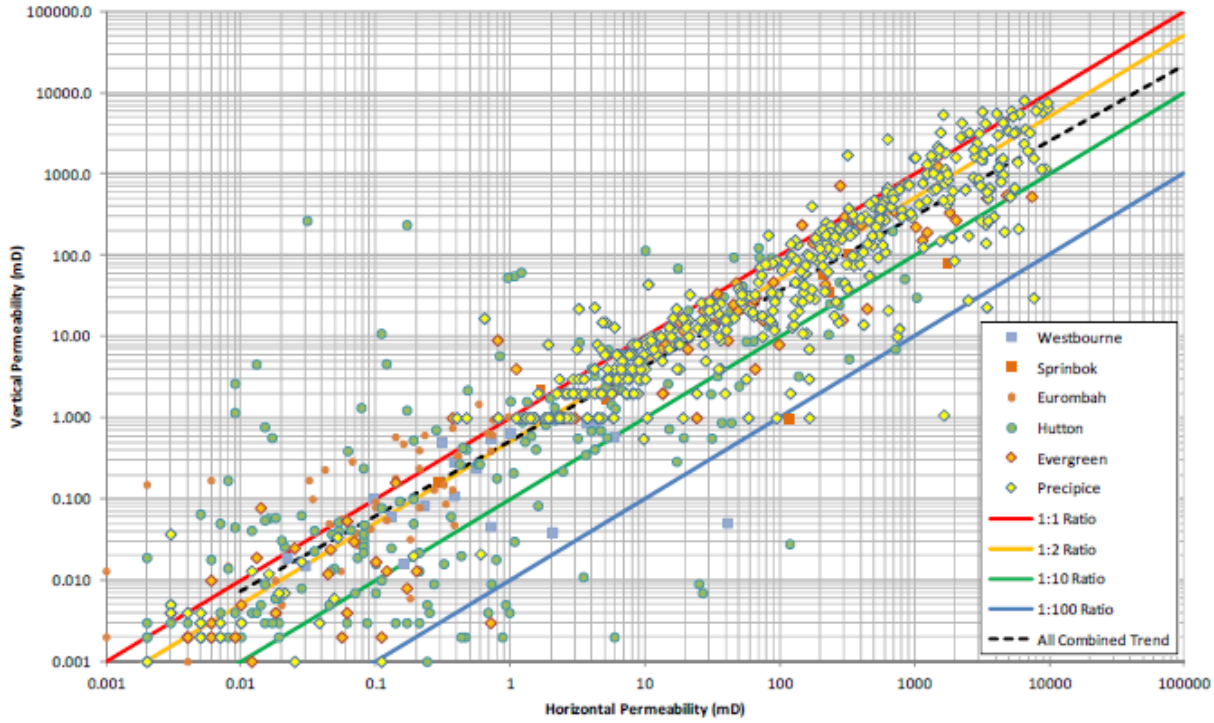

Figure 47. Core scale horizontal and vertical permeability for various Surat Basin geological units (QGC 2013). Coloured lines indicate various anisotropy ratios.

Hydraulic conductivity and storage parameter values were subsequently adjusted during model inversion. As the GEN3 model was a steady state model of hydraulic equilibrium prior to CSG development, CSG extraction was not simulated in the model. Similarly, storage parameters were not required; however these are described by QGC (2013), since the GEN3 model is intended to be used in future in a predictive (i.e. transient) context. Confined and unconfined storage parameter values were sourced from QWC (2012) and GABCC (1998). It is also noted that, under confined conditions, specific storage values cannot be specified directly when using the ECLIPSE modelling code; instead, these are calculated from rock and fluid compressibility and rock porosity values.

4.1.5. Santos

As part of EIS requirements for the Gladstone Liquefied Natural Gas Project, Santos commissioned Matrix Plus Consulting to develop a numerical groundwater flow model to provide estimates of CSG extraction impacts (Matrix Plus, 2009). A

MODFLOW-96 model was developed for the Comet Ridge gas field, covering a total area of 289 × 289 km. This was discretised using minimum cell widths of 1350 m^2. The model featured three layers and a mixture of Neumann and Cauchy boundary conditions. The discretisation of model layers is shown in Table 15. A uniform thickness of 100 m was specified for model layers 1 and 3. For this model the Triassic sequence, which contains the Rewan Formation, represents the key aquitard that will affect the upward vertical propagation of hydraulic stresses induced in the underlying coal seams by CSG production to the overlying Precipice Sandstone aquifer.

Table 15. Summary of geological units, hydrostratigraphic units and groundwater flow model layers represented in Santos Surat Basin groundwater flow model.

Geological unit	Hydrostratigraphic unit		Model layer
	aquifer	aquitard	
Precipice Sandstone	✓		1
Rewan Group		✓	2
Bandanna Formation	CSG reservoir		3

Model layers 1 (Precipice Sandstone) and 3 (Bandanna Formation) were assigned on a one-to-one basis. Conversely, model layer 2 collectively represents the Moolayember Formation, Clematis Sandstone and Rewan Formation of the Triassic age Rewan Group.

The origin of the hydraulic property values used (i.e., transmissivity and storativity) in the Comet Ridge model is not documented. Model layers 1 and 2 featured uniform values. Transmissivity values in layer 3 were spatially interpolated from an unknown number of observations. Spatial interpolation was undertaken using the tool PMDIS, which is part of the PMWIN graphical user interface for MODFLOW. The interpolation algorithm used is not documented; however, algorithms available in PMDIS include inverse distance weighting and ordinary kriging. Hydraulic property values were subsequently adjusted during model inversion.

Time-varying hydraulic head (i.e., Dirichlet) boundary conditions were used to represent CSG extraction from the Comet Ridge borefield. Matrix Plus (2009) state that hydraulic heads at each CSG bore were reduced "gradually" over a nominated 10 year period to a final pressure head of 70 m above the top of the Bandanna Formation (i.e., model layer 3). As no further information is provided with regards to the method used to calculate time-varying hydraulic head values, it is assumed that "gradually" is equivalent to "linearly".

As part of further EIS considerations for the Gladstone Liquefied Natural Gas project, Santos later employed the first iteration of the Surat CMA numerical groundwater flow model (Section 4.1.1) developed by QWC to provide estimates of cumulative CSG extraction impacts.

4.2. Bowen Basin

4.2.1. Arrow Energy

As part of EIS requirements for the Bowen Gas Project, Arrow Energy commissioned Ausenco and Norwest Corporation to develop a numerical groundwater flow model to provide estimates of CSG extraction impacts (Ausenco-Norwest Corporation, 2012). Based on a PETREL geological model, a MODFLOW–SURFACT model was developed, covering a total area of 402 × 165 km. This was discretised using 1500 × 1500 m cells into 268 rows and 11 columns. The model featured 18 layers and a mixture of specified flux (i.e., Neumann) and hydraulic head-dependent (i.e., Cauchy) boundary conditions. The discretisation of model layers is shown in Table 16. For this model, the Rewan Formation represents the key aquitard that will affect the vertical propagation of hydraulic stresses induced in the underlying coal seams by CSG production.

Model layers 1–4 were assigned on a one-to-one basis (Table 16). The Rangal Coal Measures and the Fort Cooper Sandstone were both discretised using three model layers (5–7 and 8–10). The Moranbah Coal Measures was discretised using five model layers (11-17).

Table 16. Summary of geological units, hydrostratigraphic units and groundwater flow model layers represented in Arrow Energy Bowen Basin groundwater flow model.

Geological unit	Hydrostratigraphic unit		Model layer
	aquifer	aquitard	
Quaternary Alluvium	✓		1
Tertiary sediments	✓		2
Clematis Sandstone	✓		3
Rewan Formation		✓	4
Rangal Coal Measures	CSG reservoir		5
		interburden	6
	CSG reservoir		7
Fort Cooper Sandstone	non-target CSG reservoir		8
	non-target CSG reservoir		9
	non-target CSG reservoir		10
Moranbah Coal Measures	CSG reservoir		11
		interburden	12
	CSG reservoir		13
		interburden	14
	CSG reservoir		15
		interburden	16
	CSG reservoir		17
Collinsville Coal Measures		interburden	18
Back Creek Group		impermeable basement	18

Hydraulic conductivity values were informed by literature review and from field observations. The permeability (and therefore hydraulic conductivity) of modelled coal layers was calculated using exponential functions of depth. The vertical hydraulic conductivity of coal model layers was assumed to be one-fifth of horizontal hydraulic conductivity. Isotropy was assumed for all other model layers. Specific storage values were obtained from literature review and from laboratory testing of coal cores. The spatial variability of hydraulic properties was not considered; all model layers featured homogeneous hydraulic conductivity and specific storage values. In order to test the sensitivity of modelled impacts the presence of geological faults, these were included in the model using the Horizontal Flow Barrier package (Hsieh and Freckleton, 1993). A one metre fault zone thickness was assumed, as was an isotropic hydraulic conductivity of 1×10^{-9} (units not specified). Faults were represented in consolidated formations only.

CSG extraction was simulated using time-varying specified flux (i.e., Neumann) boundary conditions, based on yearly production estimates acquired from Arrow Energy. Using past observations of water and gas production obtained from Arrow Energy, continuous functions were developed to describe the volumes of water extracted over time at various depths. These were used to parameterise time-varying flux boundary conditions. Where a CSG bore intersected multiple coal seams, the extraction flux was partitioned equally across each seam.

4.3. Gunnedah Basin

4.3.1. Santos

As part of EIS requirements for the Narrabri Gas project, Santos commissioned CDM Smith to develop a numerical groundwater flow model to provide estimates of CSG extraction impacts (CDM Smith, 2014). Based on a LeapfrogHydro geological model, a MODFLOW–SURFACT model was developed, covering a total area of 53 219 km^2. The spatial interpolation of geological data was undertaken using a proprietary approach based on radial basis functions (Beatson and Newsam 1992). For groundwater flow simulation, the geological domain was discretised using a combination of 1 km^2 and 5 km^2 cells into 238 rows and 126 columns. The model featured 24 layers and a mixture of specified flux (i.e., Neumann) and hydraulic head-dependent (i.e., Cauchy) boundary conditions. The discretisation of model layers is shown in Table 17. For this model, the aquitard sequence overlying the Hoskisson Coal represents the key aquitard that will affect the vertical propagation of hydraulic stresses induced in the underlying coal seams by CSG production to the overlying Pilliga Sandstone aquifer.

Geological model layers represented either a single geological unit (e.g., Pilliga Sandstone) or a combination of multiple units (e.g., layer 9) (Table 17). Before the numerical discretisation of the geological layers (column 2) was undertaken, further aggregation was applied (column 3). For example, geological layers 5 to 9 (representing 11 geological units) were combined as a single aquitard. Numerical discretisation of the resulting hydrostratigraphic units was subsequently undertaken (column 4). For example, the single aggregated aquitard between the Pilliga Sandstone and the Hoskissons Coal was divided into six groundwater model layers. The thickness of model layers used to represent aquitards adjacent to CSG reservoirs was increased exponentially with increasing vertical distance from the reservoir units.

CDM Smith (2014) described the rationale for discretising aquitards in this manner as follows. The sudden decrease of hydraulic heads in the CSG reservoir due to water extraction leads to nonlinear hydraulic gradients in aquitards adjacent to the CSG reservoir, particularly near the interfaces of both units. Therefore, the representation of nonlinear aquitard gradients in groundwater flow models and the associated releases of water from aquitards requires appropriate vertical discretisation. The use of a single model layer per aquitard unit would be inappropriate, as it implies a linear hydraulic gradient across the aquitard and a near-instantaneous release of water from storage throughout the entire thickness of the aquitard in response to water extraction. Instead, aquitard units adjacent to CSG reservoirs were represented using multiple model layers with an exponentially increasing model layer thickness when moving away from the coal seam–aquitard interfaces. This ensures that a relatively fine discretisation was applied where the hydraulic gradients are likely to be largest (CDM Smith, 2014).

Hydraulic property values were informed by an extensive literature review of numerous published EIS investigations and state agency and consultant reports. Values were selected from the ranges defined by these publications on a qualitative basis, rather than by use of a mean-based calculation. Vertical-to-horizontal hydraulic conductivity anisotropy ratios of 0.01–0.1 were observed. Storage parameter values were also informed by the compressibility of rock types (Kruseman and de Ridder, 1990). The spatial variability of hydraulic properties was not considered; all model layers featured homogeneous hydraulic conductivity and storage parameter values.

CDM Smith (2014) stated that “current geological evidence indicates that Permian to Triassic age faulting in the Gunnedah Basin is unlikely to provide conduits for preferential flow of water and hydrocarbons between the target coal seams and shallow groundwater sources in the overlying Surat Basin and Namoi alluvium”. Geologial evidence includes core sample analysis that shows no signs of extensional faulting and an analysis of the stress regime in the Bohena Trough indicating a predominantly compressional regime. The Bohena Trough defines the structure of the Gunnedah Basin Permian sediments. For this reason, geological faults were not represented in the model.

CSG production was simulated using time-varying specified flux (i.e., Neumann) boundary conditions. In an extensive discussion [CDM Smith(2014); Section 6.8.2], the authors summarise the relative advantages of simulating CSG extraction

using either time-varying Dirichlet or Neumann boundary conditions. Dirichlet boundary conditions ensure consistency in calculated drawdowns between reservoir and regional scale groundwater models. However, this approach leads to the overestimation of CSG extraction fluxes since, in order to reach bore target pressures, the hydraulic head of an entire model cell is reduced, rather than the hydraulic head at the bore alone. Conversely, Neumann boundary conditions ensure consistency in calculated fluxes between reservoir and regional scale groundwater models. This approach, however, leads to the underestimation of drawdown as hydraulic heads reflect spatial averages over the area of model cells, rather than at a point location (i.e., CSG bore). CDM Smith (2014) argue that Neumann boundary condition-based representations of CSG extraction are most appropriate for regional scale modelling of CSG impacts. Such approaches ensure that CSG contributions to regional groundwater balances are accurate while the underestimation of drawdown is limited to local scale effects.

Table 17. Summary of geological units, hydrostratigraphic units and groundwater flow model layers represented in Santos Gunnedah Basin groundwater flow model.

Geological unit	Geological model layer	Hydrostratigraphic unit	Groundwater model layer(s)
Cenozoic Alluvium	1	aquifer	1
Liverpool Range Volcanics	2	aquitard	2
Wallumbilla Formation			3
Bungil Formation	3		4
Mooga Sandstone Orallo Formation			5
Pilliga Sandstone	4	aquifer	6
Purlawaugh Formation	5	aquitard	7
Garrawilla Volcanics	6		8
Deriah Formation Napperby Formation	7		9
Digby Formation	8		
Trinkey Formation Wallala Formation	9		10
Breeza Coal Member Clare Sandstone			11
Howes Hill Coal Member Benelabri Formation			12
Hoskissons Coal	10	CSG reservoir	13
Brigalow Formation	11	aquitard	14
Arkarula Formation			15
Melvilles Coal Member			16
Pamboola Formation			17
Watermark Formation	12		18
Porcupine Formation			19
Maules Creek Formation (upper)		interburden	20, 21
Maules Creek Formation (coal measures)	13	CSG reservoir	22
Maules Creek Formation (lower)		interburden	23, 24

4.3.2. Schlumberger Water Services

In response to community concerns, in 2010 the New South Wales State Government commissioned a study into the potential effects of coal resource development activities on catchment water resources in the Namoi surface water catchment (SWS, 2012). The study included the development of a numerical groundwater flow model to provide estimates of CSG extraction impacts. Based on a PETREL geological model, a MODFLOW–2000 model was developed, covering a total area of approximately 30 380 km^2. This was discretised using 1 km × 1 km cells into 310 rows and 180 columns. The model

featured 20 layers and a mixture of specified flow (i.e., Neumann) and hydraulic head-dependent flow (i.e., Cauchy) boundary conditions. The discretisation of model layers is shown in Table 18. For this model, the aquitard sequence overlying the Hoskisson Coal represents the key aquitard that will affect the vertical propagation of hydraulic stresses induced in the underlying coal seams by CSG production to the overlying Pilliga Sandstone aquifer.

Model layers 1, 6, 7, 8, 10, 15 and 16 were assigned on a one-to-one basis (Table 18). Elsewhere, many model layers represent a combination of geological units; i.e., layers 2, 9 and 20. It is not clearly stated which geological units that model layers 3, 4 and 5 represent. The two coal bearing formations included in the model are discretised using multiple model layers of alternating coal seams and interburden. The Black Jack Formation is discretised using five layers while the Maules Creek Formation is discretised using three layers.

Table 18. Summary of geological units, hydrostratigraphic units and groundwater flow model layers represented in Schlumberger Water Services Gunnedah Basin groundwater flow model.

Geological unit	aquifer	aquitard	Model layer
Narrabri Formation	✓		1
Gunnedah Formation / Cubbaroo Formation	✓		2
Regolith zone	✓		3
Fractured New England Fold Belt rocks	✓		4
Great Artesian Basin	✓		5
Pilliga Sandstone	✓		6
Purlawaugh Formation		✓	7
Garrawilla Volcanics		✓	8
Deriah Formation / Napperby Formation		✓	9
Digby Formation		✓	10
Black Jack Formation (upper)		interburden	11
Hoskissons Coal	CSG reservoir		12
Black Jack Formation (middle)		interburden	13
Melvilles Coal Member	CSG reservoir		14
Black Jack Formation (lower)		interburden	15
Watermark Formation		✓	15
Porcupine Formation		✓	16
Maules Creek Formation (upper)		interburden	17
Maules Creek Formation (middle)	CSG reservoir		18
Maules Creek Formation (lower)		interburden	19
Goonbri Formation / Leard Formation		✓	20

Hydraulic property ranges were informed by a literature review of four EISs (Aquaterra 2009; Golder Associates 2008, 2010; GeoTerra 2008), a Great Artesian Basin resource assessment (GABCC 2010), the NSW groundwater database (NSW Office of Water 2010), and a textbook (Freeze and Cherry 1979). Parameter values were subsequently estimated during model inversion. The spatial variability of hydraulic properties was not considered; all model layers featured homogeneous hydraulic conductivity and specific storage values. CSG production was simulated using time-varying specified flux (i.e., Neumann) boundary conditions. Extraction was simulated from the Hoskissons Seam, the Melvilles Coal Member and the Maules Creek Formation (model layers 12, 14 and 18 respectively).

4.4. Gippsland Basin

4.4.1. CSIRO (Strand et al., 2012)

Strand et al. (2012) developed a numerical groundwater flow model of CSG production in the Gippsland Basin. The aim of the study was to determine the volume of extracted water required for economically viable methane production and to estimate the impact of CSG extraction on aquifers underlying a target coal seam. Based on a Victorian State government geological model, a MODFLOW–2000 model (Harbaugh et al., 2000) was developed, covering a total area of approximately 40 km × 20 km. This was discretised using 100 m × 100 m cells into 310 rows and 180 columns. The model featured 17 layers and specified hydraulic head (i.e., Dirichlet) boundary conditions. The discretisation of model layers was not described by Strand et al. (2012). For this model, the Yallourn Formation aquitard overlying the Morwell Formation coal seams was assumed to limit the upward vertical propagation of hydraulic stresses induced by CSG production. Hence, the focus of the modelling was on the downward propagation of hydraulic stresses to aquifers in the underlying Traralgon Formation.

Homogeneous hydraulic properties were specified by Strand et al. (2012). Hydraulic property values were specified according to a previous study by Schaeffer (2008). As geological faults are not present in the Oligocene–Miocene age geological units simulated, faults were not represented in the model. Volumetric rates of groundwater extraction for CSG production were obtained from a COMET3 reservoir model (Sawyer et al., 1990). CSG production was simulated over a 30 year period, during which individual bore extraction rates varied from 0.5 $ML.d^{-1}$ to 0.01 $ML.d^{-1}$. All extraction was simulated from the uppermost coal seam in the Morwell Formation. Time-varying specified flux (i.e., Neumann) boundary conditions were used to represent CSG extraction. After one year of time elapsed, drawdowns of up to 100 m were predicted in the receptor Traralgon Formation aquifer indirectly underlying the target coal seam in the Morwell Formation.

4.4.2. CSIRO (Varma and Michael 2012)

Varma and Michael (2012) developed a numerical groundwater flow model of the Gippsland Basin which included groundwater extraction for coal mine dewatering. The aim of the study was simulate the cumulative impacts of groundwater production for agricultural and municipal use, offshore petroleum production, and mine dewatering on the Latrobe Group aquifer. A single layer transient MODFLOW–2000 model was developed, covering a total area of approximately 40 x 20 km. This was discretised using 95 rows and 143 columns with uniform cell dimensions of 2 km x 2 km. The model featured a combination of specified flow (i.e., Neumann) boundary conditions and hydraulic head-dependent flow (i.e., Cauchy) boundary conditions. Predicted drawdowns of up to 30 m were reported.

The model featured heterogeneous hydraulic properties that were interpolated from point estimates using the nearest neighbour algorithm. Point scale estimates of horizontal hydraulic conductivity, specific yield and specific storage were calculated from formation shale volumes which, in turn, were estimated from downhole geophysical logs. Vertical hydraulic conductivity was initially assumed to be one order of magnitude lower than horizontal hydraulic conductivity. This ratio was subsequently estimated during model inversion, as were scalars that were applied to interpolated spatial distributions of horizontal hydraulic conductivity and storage parameters. Three geological faults, representing the Rosedale and Foster fault systems, were simulated as flow barriers using the Horizontal Flow Barrier package (Hsieh and Freckleton, 1993). However, no details are provided of the parameterisation of these faults. While not described by Varma and Michael (2012), the parameterisation of these faults was based on prior characterisation by Ciftci et al. (2014)

4.5. Summary

In total, ten CSG impact studies involving groundwater flow models were discussed, including eight models developed for EIS studies and two developed by CSIRO researchers for hypothesis testing (Table 19). These models are now summarised with respect to the key regional scale considerations identified in this report, namely parameter upscaling and regionalisation, and representations of faults and fracture zones. Also discussed are the approaches taken to (i) obtain hydraulic property values, (i) the discretisation of geological and/or hydrostratigraphic units, and (iii) develop the linkage between coal formations and aquifer/aquitards (i.e. linkage between reservoir model and regional groundwater flow model)

For the majority of the impact studies discussed, the model geometry was based on a single geological model. It should be noted that a common oil industry approach to reservoir modelling is to have several geological models that represent a range of plausible geologcial scenarios and then run multiple stochastic permeability parameterisations on each of a these geological models. The use of multiple conceptual models in a groundwater context has also been explored by Rojas et al. (2010). These approaches aim to capture the uncertainty associated with conceptualisation, e.g. geometry, deposition, secondary processes. The translation of information from a geological model to a numerical groundwater flow model is typically a two-step process. In the first step, the hydrogeological characteristics of geological units are assessed, resulting in their classification as either aquifers or aquitards. This may involve the aggregation of multiple geological layers into a single hydrostratigraphic unit. For example, CDM Smith (2014) aggregated the Purlawaugh Formation to Benalabri Formation sequence (comprising a total of 11 geological units) as a single aquitard, which was discretised using six model layers. In other models, the aggregation of geological units was generally restricted to the representation of surficial alluvial units. In the second step, vertical discretisation of the hydrostratigraphic units identified should be undertaken on the basis of expected groundwater flow dynamics. Variable model layer thicknesses were specified to assist calculations of steep hydraulic gradients between target coal seams and adjacent aquitard sequences. Model layer thicknesses were increased exponentially with distance from the target coal seams. In general, the discretisation of thick aquitard units is often necessary to capture the nonlinear propagation of vertical hydraulic gradients. Most models included vertical discretisation of the target coal measures and the OGIA and QGC models also included discretisation of the aquifer overlying the upper coal measure.

The majority of the impact studies simulated groundwater flow using a version of the standard finite difference groundwater flow code MODFLOW. Other groundwater flow codes used were FEFLOW (Origin Energy) and MODFLOW–USG (OGIA); these two codes allow use of an unstructured grid (allows grids other than the standard orthogonal structured grids). Only one impact study used a reservoir simulation code for both the coal formation and the overlying aquitards and aquifers: the QGC Surat Basin model, which used ECLIPSE. As such only two models simulated dual domain flow: the Surat Basin models developed by QGC and OGIA. (While the current release of MODFLOW–USG does not include dual domain flow, the OGIA model was based on a pre-release update to the code which allowed for dual domain flow). Model cell dimensions used were typically around 1 km × 1 km, with the exception of the Origin and CDM Smith models, which featured coarse cell discretisation in far field areas (i.e., distant from areas of predictive interest). Kilometre-scale discretisation is consistent with regional scale groundwater flow modelling. An advantage of finite element (e.g., FEFLOW) and finite volume (e.g., MODFLOW–USG) solution schemes is the ability to refine solution grids around areas of interest (Figure 48). Grid refinement may also be used to better represent geological complexity, including discontinuous geological units and structural discontinuities, such as geological faults.

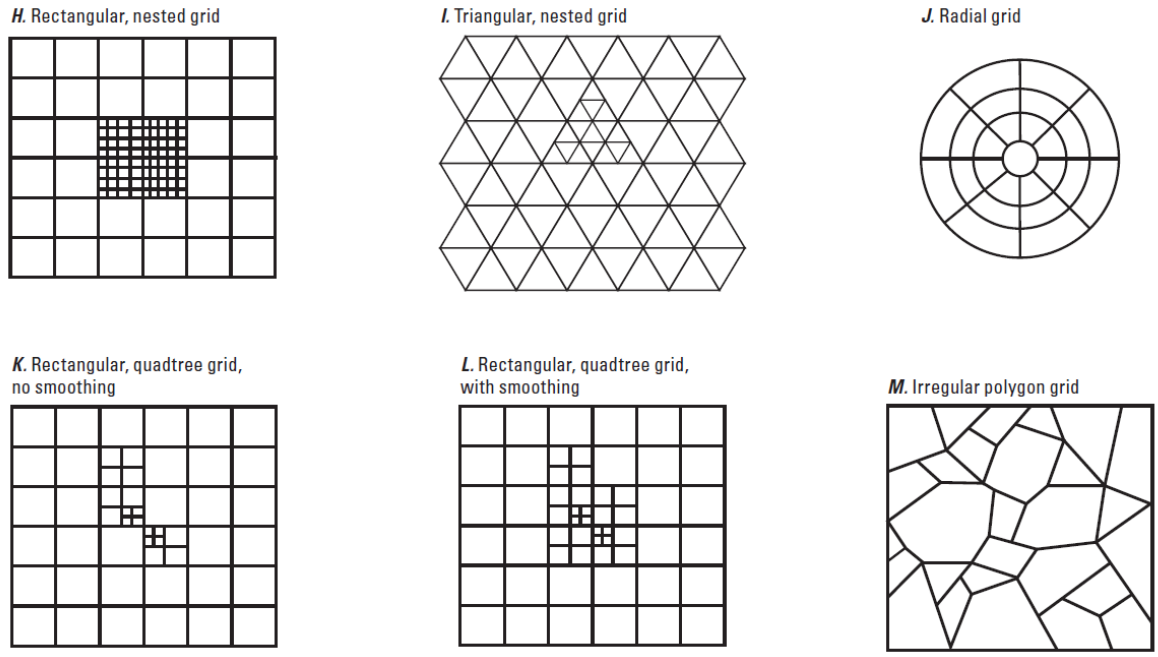

Figure 48 Examples of different types of unstructured grids implemented in MODFLOW-USG (Panday et al., 2013)).

Hydraulic property values were primarily obtained from literature reviews; in some cases this included textbook values (e.g., SWS). Hydraulic property values for the Origin Energy and Arrow Energy (Bowen Basin) models were also informed by unspecified field testing. For the QGC model, hydraulic property values were also informed by downhole geophysical observations. The hydraulic property values used in the OGIA model were the most comprehensively informed. Hydraulic conductivity values were based on over 13 000 drill stem test records and more than 1000 pump test records obtained from State government groundwater databases. Storage parameter values were based, in part, on finer-scale groundwater modelling. In all cases, spatially homogeneous values were used. While this represents a gross simplification, it can be justified to some extent by the regional scale of modelling and where there are insufficient data to support representations of spatial variability. However, the use of uniform parameter values should ideally have a rigorous theoretical basis; for example, they should be derived using an appropriate averaging method, or from Darcy's Law-based approaches.

In the context of CSG impact estimation, vertical hydraulic conductivity (K) is a key hydraulic property, as the K_v of aquitards can significantly retard the vertical propagation of hydraulic gradients. However, for most models reviewed, K_v was not estimated directly. Instead, the ratio of vertical to horizontal hydraulic conductivity was estimated, typically through inverse modelling. Improved representations of vertical hydraulic conductivity could be based on core-scale observations, drill stem testing, and/or time series analyses of aquitard pressure head [e.g., Smerdon et al., (2014)].

Formal averaging methods were generally not applied for the determination of homogeneous values. Instead, the majority of models used parameter estimation procedures to estimate hydraulic property values, based on ranges determined from literature review and other sources. This leads to a more general discussion of modelling methodology. It is often assumed that a model that can represent past observations is a good predictor of future conditions. The deterministic calibration of groundwater models (as used in most examples discussed here) is an example of this type of approach. However, for complex and/or large scale systems, such as regional groundwater flow systems, this assumption has been proven conclusively to be false (Konikow and Bredehoeft, 1992; Oreskes et al., 1994). Alternative approaches involve quantifying the uncertainties associated with all model inputs; models are then run stochastically, resulting in probabilistic model outputs. This type of model output is particularly valuable for hypothesis testing (i.e., rejection) analyses as part of risk–based studies such as assessments of CSG impacts.

Two of the groundwater flow systems investigated featured significant faulting: the Bowen and Gippsland Basins. Faults were simulated in two of the models: the Arrow (Bowen Basin) model and the Varma and Michael (2012) Gippsland Basin

model. Both models used the MODFLOW simulation code in which faults were represented using the Horizontal Flow Barrier package (Hsieh and Freckleton, 1993). This approach modifies the conductance between neighbouring model cells in order to represent barriers or conduits to flow. As such, this approach cannot be used to represent complex anisotropic fault conceptualisations; e.g., a cross-fault barrier/along-fault (including vertical) conduit structure. Fracture zones were not simulated in any of the models.

For five of the ten case studies, rates of groundwater extraction for coal seam depressurisation were obtained from prior reservoir modelling. Other studies obtained extraction rates from the Theis equation (Origin Energy Surat Basin), from an unspecified source (Arrow Energy Surat Basin, Santos Surat Basin, Varma and Michael, 2012), or did not simulate extraction (QGC Surat Basin). Groundwater extraction was represented using a Neumann–type boundary condition in six of the ten case study models. As described by CDM Smith (2014), this approach ensures that the CSG contribution to the calculated regional groundwater balance will be correct, while drawdown in the vicinity of CSG bores will be underestimated. For three of the models, groundwater extraction occurred from a single model layer. Conversely, the Arrow (Surat Basin) MODFLOW model represented simultaneous extraction from multiple model layers using the Multi-Node Well package (Halford and Hanson, 2002; Konikow et al., 2009). The OGIA Surat Basin model features the most advanced approach to the representation of CSG extraction. Cauchy-type boundary conditions were represented using standard MODFLOW Evapotranspiration or Drain packages. This method allows for the specification of a maximum extraction flux when a cell hydraulic head is above a given elevation. Zero flux is specified when cell hydraulic heads are equal to or lower than a nominated target elevation (e.g., 30 metres above the top of a target coal seam). Linear interpolation of extraction fluxes is undertaken when hydraulic heads are calculated between the two specified elevations. This approach ensures (a) that a physically-based upper limit on extraction is imposed and (b) that extraction ceases when the target pressure is achieved.

Table 19. Summary of modelling case studies, including approaches to upscaling, regionalisation and structural features.

#	1	2	3	4	5	6	7	8	9	10
Basin	**Surat**					**Bowen**	**Gunnedah**		**Gippsland**	
Author	**OGIA (iteration 3)**	**Arrow**	**Origin**	**QGC (GEN3)**	**Santos**	**Arrow**	**Santos**	**SWS**	**Strand**	**Varma**
Geological basis?	MINEX model	PETREL model	PETREL model	PETREL model	Georeferenced data	PETREL model	Leapfrog Hydro model	PETREL model	Georeferenced data	Not specified
Aggregation of geological units?	No	Cretaceous sediments, one aquitard	One aquifer/aquitard sequence	No	No	Quaternary alluvium, Tertiary sediments	Numerous aquitards	One aquifer, two aquitards	Not specified	N/A (single layer model)
Subdivision of geological units into multiple model layers?	Yes: coal measures and overlying sandstone unit	Yes: coal measures	Yes: coal measures	Yes: Cretaceous sediments, coal measures, overlying sandstone unit	No	Yes: coal measures	Yes: coal measures	Yes: coal measures	Not specified	N/A (single layer model)
Single phase or multi-phase model?	Single phase (MODFLOW-2005, MODFLOW-USG)	Single phase (MODFLOW-2000)	Single phase (FEFLOW)	Multi-phase (ECLIPSE)	Single phase (MODFLOW-1996)	Single phase (MODFLOW-SURFACT)	Single phase (MODFLOW-SURFACT)	Single phase (MODFLOW-2000)	Single phase (MODFLOW, version not specified)	Single phase (MODFLOW-2000)
Numerical solution scheme?	Finite difference, Control volume finite difference	Finite difference	Finite element	Finite volume	Finite difference	Finite difference	Finite difference	Finite difference	Finite difference	Finite difference
Dual domain flow?	Yes (MODFLOW-USG)	No	No	Yes	No	No	No	No	No	No
Cell / element dimensions?	1.5 km x 1.5 km	1k m x 1 km	3, 6 and 12 km	1.5 km x 1.5 km	1.35 km x 1.35 km	1.5 km x 1.5 km	1 km x 1 km and 5 km x 5 km	1k m x 1 km	100 m x 100 m	Not specified; likely 2 km x 2 km
Parameter value source(s)?	Literature review, database records, pump tests, modelling	Literature review	Literature review, unspecified field observations	Downhole geophysics	Not documented	Literature review, core testing, unspecified field observations	Literature review	Literature review	Not specified	Not specified
Parameter value averaging used?	No	No	Not documented	Arithmetic	Not documented	Not documented	No	No	Not specified	Not specified
Homogeneous parameters used?	Yes	Yes	Not documented; likely no	Not documented; likely yes	Yes, except coal measures	Yes	Yes	Yes	Yes	Yes
K_h : K_v ratio used ?	Yes	Yes	Not documented	Yes	Not documented	Yes	No	Not specified	Not specified	Not specified
Parameter estimation used?	Yes	Yes	Not documented	Yes	Yes	No	No	Yes	No	Yes
Faults or fractures represented?	No	No, in progress	No	No	No	Faults (Horizontal Flow Barrier package)	No	No	No	Faults (Horizontal Flow Barrier package)
BC type used to represent source term?	Cauchy	Neumann (Multi-Node Well package)	Dirichlet	Not implemented	Dirichlet	Neumann, though poorly documented	Neumann	Neumann	Not specified; likely Neumann	Not specified; likely Neumann

5. Summary

Unconventional gas production occurs at the site scale and is governed by local physical processes in the vicinity of each coal seam gas well. However, unconventional gas plays typically occur over large areas and their exploitation can cause regional scale impacts, hence a single modelling approach is rarely suitable to describe the physical processes operating at both scales. Complex geological models are typically built as precursors to groundwater flow models. However, the geological models require fine discretisation and are computationally prohibitive when directly used for flow simulation. This is particularly true in the context of sensitivity studies involving Monte-Carlo simulations. Upscaling of both small-scale heterogeneity, multi-phase flow and boundary conditions is needed during development of regional scale groundwater flow models, and the associated uncertainty must be quantified. The appropriateness of upscaling methodologies, whether focussed on property heterogeneity or physical processes or a combination of these, needs robust testing for the appropriate flow boundary conditions (i.e. reflecting the water management questions the model needs to address).

This report provides an overview of recent national and international literature and Environmental Impact Statements undertaken in Australian coal basins as relates to groundwater impacts from coal seam gas extraction, which allows current upscaling practices and trends to be identified. In particular, the analysis centres on three key considerations involving upscaling and spatial interpolation when developing a regional scale groundwater flow model with initial parameter estimates being obtained at a range of scales, including the bore and regional observations. First, estimates of local or point scale hydraulic properties must be upscaled to the scale of numerical groundwater model cells (typically 1 km^2 in the horizontal plane). Second, the effect of structural features (e.g. faults) must be adequately represented in numerical groundwater flow models. Third, spatial interpolation is most effective (in terms of minimising predictive uncertainty) if spatial correlation of key hydrogeological parameters such as hydraulic conductivity is determined and represented in the model.

The current, commonly used approaches to upscaling and regionalisation of heterogeneity in Australia are examined. The present analysis indicates that while there is a substantial body of academic literature regarding parameter upscaling and related uncertainty analysis, relatively few regional groundwater models featuring CSG extraction explicitly address upscaling of hydraulic properties, or incorporate structural features such as faults that are known or inferred to exist in the model areas. Examples of leading practice in Australia have, however, been identified. These may be considered as benchmark approaches in regards to testing the representation of dual-phase flow characteristics and small-scale heterogeneity in hydraulic properties in upscaled models.

Knowledge of current and leading practice with respect to upscaling methods used in regional scale groundwater models may inform the assessment and evaluation of models and their predictive uncertainty. This is especially important when groundwater modelling is used to underpin regulatory decisions.

The key findings presented in this overview report include the following:

- Representations of aquitards and geological faults in groundwater flow models used to estimate potential impacts of coal seam gas production in Australian coal basins are often highly simplified. A small number of exceptions prove the rule. While simplifications cannot be avoided, there is an urgent need for robust testing of simplifying assumptions to gain confidence that models are fit-for-purpose, uncertainties are quantified and can be attributed to conceptual model uncertainty, parameter uncertainty, or boundary condition uncertainty. Categorisation of uncertainties helps in allocating resources for collecting those data and developing those model components that will have largest impact on reducing model uncertainty.
- For aquitards, simplification typically involves neglecting the spatial heterogeneity of hydraulic conductivity and storativity by adopting spatially uniform values. The use of large scale uniform values may be justified when equivalent properties are derived from robust upscaling methods, or when the support volume used to derive flow properties is large enough to produce scale-independent values. Probably the best example of the latter is the use of global inverse modelling approaches, where grid scale parameters are derived by iteratively matching

predicted to observed system behaviour (typically groundwater heads and fluxes, although increasingly tracer-derived metrics are incorporated) until model bias is minimised. Often, however, there are insufficient data to derive meaningful equivalent properties in the first place. While global inversion-based upscaling methods have been identified to be superior over analytical upscaling (arithmetic and harmonic averaging) when coal layers and interburden were upscaled, inversion-based upscaling methods are less likely to be useful when applied to aquitards because the available (head) data do not carry sufficient information. To identify what type of observations carry sufficient information for derivation of regional-scale aquitard flow properties, a more systematic implementation of data worth analysis is warranted.

- Structural geological features including faults and fractured zones surrounding fault cores can serve as preferential flow paths and or barriers to flow; they are another cause of hydraulic conductivity heterogeneity and thus of groundwater flow variability. While the simulation and parameterisation of faults in reservoir models has been an active research topic since the early nineties, with the use of transmissibility multipliers (estimated from fault zone thickness, permeability and clay distribution) now being the industry standard approach to representing faults in reservoir models, application in regional scale groundwater flow models has been limited. Recent attempts to improve fault modelling capability in standard groundwater flow simulators such as MODFLOW include the FAULTSIM utility for calculating the permeability of fault zones based on throw, fault core thickness, damage zone thickness, and two anisotropic power coefficients. If such approaches are implemented more systematically in coal seam gas groundwater impact studies, then at least the potential influence (small or large) of faults on regional groundwater flow can be tested. Also, regardless of whether the predicted impact on the groundwater system is small or large, the mere fact of developing improved conceptualisation and representation of faults in groundwater models will increase confidence in model predictions.
- Regardless of whether the key uncertainty of the groundwater model relates to representation of aquitards or faults, there is a need for better data integration across multiple scales to maximise subsurface data coverage; this will require better linkages between geological, geophysical, hydrological and hydrochemical information, thereby encompassing several spatial scales of heterogeneity. Several methodologies have been discussed where representation of geological heterogeneity and its relationship with hydraulic properties resulted in improved groundwater flow simulations. Examples include multi-point statistics (employing a training image developed from rock outcrops or geomorphological expertise to qualitatively condition a stochastic realisation) and transition probability geostatistics (quantitative measures such as hydrofacies distribution are used to condition realisations).
- As far as the characterisation of geological faults and fault networks is concerned, there exists a paucity of data with regards to both fault architecture (e.g. orientation, location, size and frequency) and to the flow properties of faults. In addition, due to a lack of numerical capability in standard groundwater flow models, the implementation of faults is often not trivial. As for aquitards, the improved integration of different sources of information on the geometry and flow properties of fault zones is required to better conceptualise and represent faults in groundwater flow models. This conceptualisation, and the testing of the role of faults on local and regional groundwater flow systems, will benefit from improved numerical schemes that seamlessly merge fine-scale fault meshes with coarse-scale numerical grid blocks, while not being computationally prohibitive.
- Coal seam gas extraction invokes a number of physical processes that are not normally simulated in regional scale groundwater models: dual domain flow, gas desorption, dual phase flow, and geomechanical deformation. While considerable knowledge resides with the reservoir engineering community, uptake of this knowledge into groundwater models for simulating coal seam gas groundwater impacts is rare. A further complication arises when such processes have to be upscaled from their small scale lithology-specific behaviour into large-scale cellular groundwater models where different lithologies may be combined into a supposedly homogenous hydrogeoligical unit. The few studies that have been undertaken to date indicate i) incorporating dual phase processes has a large effect on the groundwater system when compared to a single phase model, ii) use of different upscaling methods applied to dual phase features yields markedly different effects on the groundwater system, and iii) further work is needed to test if upscaling of other processes such as gas desorption and coal

deformation is required, and if so, what then the most appropriate upscaling methods are (e.g. analytical averaging or inversion-based).

6. References

Ababou R (1991) Approaches to large scale unsaturated flow in heterogeneous, stratified, and fractured geologic media, U.S. Nuclear Regulatory Commission, Office of Nuclear Regulatory Research, Washington, DC, USA.

Abdallah W, Buckley JS, Carnegie A, Edwards J, Herold B, Fordham E, Graue A, Habashy T, Seleznev N, Signer C, Hussain H, Montaron B, and Ziauddin M (2007) Fundamentals of wettability, Oilfield Review 19(2): 44-61.

Adhikary DP and Guo H (2005) A coupled Cosserat two-phase double porosity flow model, in: MODSIM 2005 International Congress on Modelling and Simulation, pp. 1189-1195.

Advanced Resources International (2015) "COMET3 Reservoir Simulator", URL=<http://www.adv-res.com/COMET3_reservoir_simulator_for_gas_shale_and_coalbed_methane_CBM_reservoirs.php>, viewed 16 November 2015.

Ahmed U, Crary S and Coates G (1991) Permeability estimation: The various sources and their interrelationships, Journal of Petroleum Technology 43(5): 578-587.

Alcolea A and Renard P (2010) Blocking Moving Window algorithm: Conditioning multiple-point simulations to hydrogeological data, Water Resources Research 46(W08511): 1-18.

Al-Jubori A, Johnston S, Boyer C, Lambert SW, Bustos OA, Pashin JC and Wray A (2009) Coalbed methane: clean energy for the world, Oilfield Review 21(2): 4-13.

Almeida AS and Frykman P (1994) Geostatistical modeling of chalk reservoir properties in the Dan field, Danish North Sea, in: Yarus JM and Chambers RL (eds) Stochastic Modeling and Geostatistics : Principles, Methods and Case Studies, American Association of Petroleum Geologists,Tulsa, OK, USA, 379p.

Altman SJ, Arnold B, Barnard R, Barr G, Ho C, McKenna S and Eaton R (1996) Flow calculations for Yucca Mountain groundwater travel time, report no. GWTT-95, Sandia National Labs, Albuquerque, NM, USA.

Amankwah K and Schwarz J (1995) A modified approach for estimating pseudo-vapour pressures in the application of the Dubinin-Astakhov equation, Carbon 33(9): 1313-1319.

Aminian K, Ameri S, Bhavsar A, Sanchez M and Garcia A (2004) Type curves for coalbed methane production prediction, in: Society of Petroleum Engineers Eastern Regional Meeting, document # SPE-91482-MS, http://dx.doi.org/10.2118/91482-MS.

Amyx JW, Bass DM, Whiting RL (1960) Petroleum reservoir engineering physical properties. New York, McGraw.

Anders MH and Wiltschko DV (1994) Microfracturing, paleostress and the growth of faults, Journal of Structural Geology 16(6): 795-815.

Andersson J and Dverstorp B (1987) Conditional simulations on fluid-flow in 3-dimensional networks of discrete fractures. Water Resources Research 23(10): 1876-1886.

Aquaterra (2009) Narrabri Coal Mine Stage 2 Longwall Project Hydrogeological Assessment.

Arpat G and Caers J (2007) Conditional simulation with patterns. Mathematical Geology 39(2): 177-203. doi:10.1007/s11004-006-9075-3.

Ausenco-Norwest Corporation (2012) Groundwater model, northern Bowen Basin regional model impact predictions, Queensland, Australia.

Australasian Groundwater and Environmental Consultants (1999) Pumping test analysis for Kogan Creek Power Station.

Australia Pacific Liquefied Natural Gas (2010a) Australia Pacific LNG Project: environmental impact statement, Australia Pacific LNG, Brisbane, Queensland, URL=<http://www.aplng.com.au/eis>.

Australia Pacific Liquefied Natural Gas (2010b) Surat Basin regional numerical groundwater flow model for the Australia Pacific LNG environmental impacts assessment methodology.

Aydin A (2000) Fractures, faults, and hydrocarbon entrapment, migration and flow, Marine and Petroleum Geology 17(7): 797-814.

Bakker M (2013) Semi-analytic modeling of transient multi-layer flow with TTim, Hydrogeology Journal 21(4): 935-943.

Balan B, Mohaghegh S and Ameri S (1995) State-of-the-art in permeability determination from well log data: Part 1-A comparative study, model development, SPE Eastern Regional Meeting, Society of Petroleum Engineers.

Balsamo F and Storti F (2010) Grain size and permeability evolution of soft-sediment extensional sub-seismic and seismic fault zones in high-porosity sediments from the Crotone basin, southern Apennines, Italy, Marine and Petroleum Geology 27(4): 822-837.

Bandilla KW, Celia MA, Birkholzer JT, Cihan A and Leister EC (2015) Multiphase modeling of geologic carbon sequestration in saline aquifers, Ground Water 53(3): 362-377.

Barker JW and Thibeau S (1997) A critical review of the use of pseudorelative permeabilities for upscaling. SPE Reservoir Engineering, May 1997: 138 - 143.

Barrett DJ, Couch CA, Metcalfe DJ, Lytton L, Adhikary DP, and Schmidt BK (2013). Methodology for bioregional assessments of the impacts of coal seam gas and coal mining development on water resources. A report prepared for the Independent Expert Scientific Committee on Coal Seam Gas and Large Coal Mining Development through the Department of the Environment.

Basquet R, Jeannin L, Lange A, Bourbiaux B and Sarda S (2003) Gas flow simulation in discrete fracture network models, Society of Petroleum Engineers.

Bassiouni Z (1994) Theory, measurement, and interpretation of well logs, Henry L. Doherty Memorial Fund of AIME, Society of Petroleum Engineers.

Bastian P, Chen Z, Ewing RE, Helmig R, Jakobs H and Reichenberger V (2000) Numerical simulation of multiphase flow in fractured porous media, in: Numerical Treatment of Multiphase Flows in Porous Media, pp. 50-68, Springer Berlin Heidelberg.

Bear J (1972) Dynamics of Fluids in Porous Media, Elsevier, New York, NY, USA.

Bear J, Tsang C-F and de Marsily G (1993) Flow and Contaminant Transport in Fractured Rock, Academic Press, London, UK.

Beerten K, Wemaere I, Gedeon M, Rogiers D, Mallants D, and Salah S (2010) Geological, hydrogeological, and hydrological data for the Dessel disposal site, report no. NIROND-TR 2009-05 V1, 261p.

Bense V, and Person MA (2006) Faults as conduit-barrier systems to fluid flow in siliciclastic sedimentary aquifers. Water Resources Research 42, W05421, doi:10.1029/2005WR004480.

Bense V, Gleeson T, Loveless S, Bour O and Scibek J (2013) Fault zone hydrogeology, Earth-Science Reviews 127: 171-192. Bense V and Person M (2006) Faults as conduit-barrier systems to fluid flow in siliciclastic sedimentary aquifers, Water Resources Research 42(5).

Bense V, Van den Berg E and Van Balen R (2003) Deformation mechanisms and hydraulic properties of fault zones in unconsolidated sediments; The Roer Valley Rift System, The Netherlands, Hydrogeology Journal 11(3): 319-332. Bethke CM, Zhao X and Torgersen T (1999) Groundwater flow and the ^{4}He distribution in the Great Artesian Basin of Australia, Journal of Geophysical Research 104(B6): 12999-13011.

Beven K (2006) A manifesto for the equifinality thesis, Journal of Hydrology 320(1): 18-36.

Bianchi M, Zheng C, Wilson C, Tick G, Liu G and Gorelick S (2011) Spatial connectivity in a highly heterogeneous aquifer: From cores to preferential flow paths, Water Resources Research 47.

Bissell E and Aichele S (2004) Geostatistical analysis of effective vertical hydraulic conductivity and presence of confining layers in the shallow glacial drift aquifer, Oakland County, Michigan. U.S. Geological Survey.

Bourbié T, Coussy O and Zinszner B (1987) Acoustics of Porous Media, Gulf Publishing Co., Houston, TX, USA.

Bouwer H and Rice R (1976) Slug test for determining hydraulic conductivity of unconfined aquifers with completely or partially penetrating wells, Water Resources Research 12(3): 423-428.

Bredehoeft JD (2005). The conceptualization model problem—surprise. Hydrogeology Journal 13: 37–46.

Bredehoeft JD, Neuzil CE and Milly PCD (1983) Regional flow in the Dakota aquifer: A study of the role of confining layers, U.S. Geological Survey Water Supply Paper 2237, pp.1–45.

Bromhal GS, Sams WN, Jikich S, Ertekin T, Smith DH (2005) Simulation of CO_2 sequestration in coal beds: The effects of sorption isotherms, Chemical Geology 217(3), 201-211.

BURGEAP (2015) "SIMUSCOPP: SIMUlation des Sites COntaminés par des Produits Pétroliers", URL=<http://www.burgeap.fr/index.php/fr/innovations/logiciels-et-bases-de-donnees/simuscopp>, viewed 16 November 2015.

Caine J, Evans J and Forster C (1996) Fault zone architecture and permeability structure, Geology 24(11): 1025-1028.

Caine JS and Forster CB (1999) Fault zone architecture and fluid flow: Insights from field data and numerical modeling, in: Haneberg WC (ed.) Faults and Subsurface Fluid Flow in the Shallow Crust, American Geophysical Union, Washington, DC, USA, pp.101-127.

Caine JS and Minor SA (2009) Structural and geochemical characteristics of faulted sediments and inferences on the role of water in deformation, Rio Grande Rift, New Mexico, Geological Society of America Bulletin 121(9-10):1325-1340.

Cao H (2002) Development of techniques for general purpose simulators, PhD thesis, Stanford University, Stanford, CA, USA.

Carle SF (1999) T-PROGS: Transition probability geostatistical software, University of California, Davis, California, USA.

Carle SF and Fogg GE (1996) Transition probability-based indicator geostatistics, Mathematical Geology 28(4): 453-476.

Castro MC and Goblet P (2003) Calibration of regional groundwater flow models: Working toward a better understanding of site-specific systems, Water Resources Research 39 (6).

Castro MC, Stute M and Schlosser P (2000) Comparison of ^{4}He ages and ^{14}C ages in simple aquifer systems: Implications for groundwater flow and chronologies, Applied Geochemistry 15: 1137–1167.

Castro MC, Goblet P, Ledoux E, Violette S and de Marsily G (1998a) Noble gases as natural tracers of water circulation in the Paris Basin: 2. Calibration of a groundwater flow model using noble gas isotope data, Water Resources Research 34(10): 2467-2483.

Castro MC, Jambon A, de Marsily G and Schlosser P (1998b) Noble gases as natural tracers of water circulation in the Paris Basin: 1. Measurements and discussion of their origin and mechanisms of vertical transport in the basin, Water Resources Research 34(10): 2443-2466.

CDM Smith (2014) Santos Narrabri Gas Project Groundwater Impact Assessment, Subiaco, Western Australia.

Celia M, Bachu S, Nordbotten J and Bandilla K (2015) Status of CO_2 storage in deep saline aquifers with emphasis on modeling approaches and practical simulations, Water Resources Research 51(9): 6846-6892.

Center for Subsurface Modeling (2015) [IPARS] Simulator Characteristics, URL=<http://csm.ices.utexas.edu/IparsWeb/iparsintro-characteristics.html>, viewed 16 November 2015.

CGS Europe (2015), 3.2.7 Coores™, URL=<http://repository.cgseurope.net/eng/cgseurope/knowledge-repository/key-reports/evaluation/3/2/7.aspx>, viewed 16 November 2015.

Clarkson CR, Rahmanian MR, Kantzas A and Morad K (2010) Relative permeability of CBM reservoirs: controls on curve shape. Canadian Society for Unconventional Gas. CSUG/SPE 137404. Presented at the Canadian Unconventional Resources and International Petroleum Conference held in Calgary, Alberta, Canada, 19-21 October, 2010.

Childs C, Manzocchi T, Walsh J, Bonson C, Nicol A and Schopfer M (2009) A geometric model of fault zone and fault rock thickness variations, Journal of Structural Geology 31(2): 117-127.

Chilès J and Delfiner P (1999) Geostatistics: Modeling Spatial Uncertainty, Wiley, New York, NY, USA.

Çiftçi NB, Langhi L, Strand J and Divko LG (2014) Efficiency of a faulted regional top seal, Lakes Entrance Formation, Gippsland Basin, SE Australia, Petroleum Geoscience 20(3): 241-256.

Class H, Ebigbo A, Helmig R, Dahle HK, Nordbotten JM, Celia MA, Audigane P, Darcis M, Ennis-King J, Fan Y, Flemisch B, Gasda SE, Jin M, Krug S, Labregere D, Beni AN, Pawar RJ, Sbai A, Thomas SG, Trenty L and Wei L (2009) A benchmark study on problems related to CO_2 storage in geologic formations, Computational Geosciences, 13(4): 409-434.

Clauser C (1992) Permeability of crystalline rocks, Eos: Transactions of the American Geophysical Union 73(21): 233-238.

Commonwealth of Australia (2008) Risk assessment and management, in: Australia Co (ed.), Department of Resources, Energy and Tourism.

Commonwealth of Australia (2014a) Coal seam gas extraction modelling groundwater impacts, Canberra, Australian Capital Territory, URL=<http://iesc.environment.gov.au/index.html>.

Commonwealth of Australia (2014b) Subsidence from coal seam gas extraction in Australia, in: Australia Co (ed.), Department of the Environment, Canberra, ACT, Australia.

Computer Modeling Group (2003) Generalized Equation of State Model (GEM), Calgary, Alberta, Canada.

Computer Modelling Group (2014) "Compositional & Unconventional Reservoir Simulator", URL=<http://www.cmgl.ca/uploads/files/pdf/SOFTWARE/2014%20Product%20Sheets/14-GE-02_GEM_Technical_Specs_Oct2014-A4.pdf>, viewed 16 November 2015.

COMSOL Inc. (2015) Multiphysics Software Product Suite, URL=<http://www.comsol.com/products>, viewed 16 November 2015.

Comunian A, Jha S, Giambastiani B, Mariethoz G and Kelly B (2014) Training Images from process-imitating methods, Mathematical Geosciences 46(2): 241-260.

Comunian A, Renard P and Straubhaar J (2012) 3D multiple-point statistics simulation using 2D training images, Computers and Geosciences 40: 49-65.

Conca JL and Wright J (1998) The UFA method for rapid, direct measurements of unsaturated transport properties in soil, sediment, and rock, Australian Journal of Soil Research 36(2): 291-315.

Connell LD, Detournay C (2009) Coupled flow and geomechanical processes during enhanced coal seam methane recovery through CO_2 sequestration, International Journal of Coal Geology 77(1): 222-233.

Cook PG (2003) A guide to regional groundwater flow in fractured rock aquifers, Seaview Press, Henley Beach, South Australia.

Cook PG and Böhlke J-K (1999) Determining timescales for groundwater flow and solute transport, in: PG Cook and AL Herczeg (ed.s) Environmental Tracers in Subsurface Hydrology, Kluwer Academic Press, Boston, MA, USA, pp. 1-30.

Cook PG and Herczeg AL (2000) Environmental Tracers in Subsurface Hydrology, Kluwer Academic Press, Boston, MA, USA.

Cooper HH and Jacob C (1946) A generalized graphical method for evaluating formation constants and summarizing well-field history, Eos: Transactions of the American Geophysical Union 27(4): 526-534.

Corey A (1986) Air permeability: Methods of Soil Analysis: Part 1—Physical and Mineralogical Methods, pp.1121-1136.

Court B, Bandilla KW, Celia MA, Janzen A, Dobossy M and Nordbotten JM (2012) Applicability of vertical-equilibrium and sharp-interface assumptions in CO_2 sequestration modeling, International Journal of Greenhouse Gas Control 10: 134-147.

Cronican AE and Gribb MM (2004) Literature review: Equations for predicting hydraulic conductivity based on grain-size data, Supplement to technical note entitled: Hydraulic conductivity prediction for sandy soils, Ground Water 42(3): 459-464.

Dagan G (1986) Statistical theory of groundwater flow and transport: Pore to laboratory, laboratory to formation, and formation to regional scale, Water Resources Research 22(9S), 120S-134S.

de Dreuzy J, Meheust Y and Pichot G (2012) Influence of fracture scale heterogeneity on the flow properties of three-dimensional discrete fracture networks (DFN), Journal of Geophysical Research-Solid Earth 117.

Dell'Arciprete D, Bersezio R, Felletti F, Giudici M, Comunian A, and Renard P (2011) Comparison of three geostatistical methods for hydrofacies simulation: a test on alluvial sediments, Hydrogeology Journal 20: 299-311.

Delshad M, Kong X, Tavakoli R, Hosseini SA and Wheeler MF (2013) Modeling and simulation of carbon sequestration at Cranfield incorporating new physical models, International Journal of Greenhouse Gas Control 18: 463-473.

de Marsily G, Delay F, Goncalves J, Renard P, Teles V and Violette S (2005) Dealing with spatial heterogeneity, Hydrogeology Journal 13(1): 161-183.

de Marsily G, Delay F, Teles V and Schafmeister M (1998) Some current methods to represent the heterogeneity of natural media in hydrogeology, Hydrogeology Journal 6(1): 115-130.

Der Kiureghian A, Ditlevsen O (2007). Aleatory or epistemic? Does it matter? Special Workshop on Risk Acceptance and Risk Communication March 26-27, 2007, Stanford University: 13 pp.

Dershowitz W, Lee G, Geier J, Foxford T, LaPointe P and Thomas A (1999) User documentation for FracMan, Golder Associates, Seattle, WA, USA.

Dershowitz W and Miller I (1995) Dual porosity fracture flow and transport, Geophysical Research Letters 22(11): 1441-1444.

Desbarats A (1987) Numerical estimation of effective permeability in sand-shale formations, Water Resources Research 23(2): 273-286.

Desbarats A (1992) Spatial averaging of hydraulic conductivity in 3-dimensional heterogeneous porous media, Mathematical Geology 24(3): 249-267.

Deutsch C (1989) Calculating effective absolute permeability in sandstone/shale sequences, SPE Formation Evaluation 4(3).

Deutsch C (1999) Reservoir modeling with publicly available software, Computers and Geosciences 25(4): 355-363.

Dickson NEM, Comte JC, Renard P, Straubhaar JA, McKinley JM and Ofterdinger U (2015) Integrating aerial geophysical data in multiple-point statistics simulations to assist groundwater flow models, Hydrogeology Journal.

Diersch H (2005) FEFLOW finite element subsurface flow and transport simulation system reference manual, WASY GmbH, Berlin, Germany, 20-102.

Doherty JE and Christensen S (2011). Use of paired simple and complex models in reducing predictive bias and quantifying uncertainty. Water Resources Research doi:10.1029/2011WR010763.

Doherty JE, Hunt RJ, and Tonkin MJ (2010) Approaches to Highly Parameterized Inversion: A Guide to Using PEST for Model-Parameter and Predictive-Uncertainty Analysis: U.S. Geological Survey Scientific Investigations Report 2010–5211, 71 pp.

Durlofsky L (1991) Numerical calculation of equivalent grid block permeability tensors for heterogeneous porous media, Water Resources Research 27(5): 699-708.

Durlofsky L (1992) Representation of grid block permeability in coarse scale models of randomly heterogeneous porous media, Water Resources Research 28(7): 1791-1800.

Durlofsky L (2005) Upsaling and gridding of fine scale geological models for flow simulation, Proceedings of the 8th International Forum on Reservoir Simulation, Iles Borromees, Stressa, Italy, June 20-24 2005, 59p.

Dverstorp B and Andersson J (1989) Application of the Discrete Fracture Network concept with field data - Possibilities of model calibration and validation, Water Resources Research 25(3): 540-550.

Efros AA and Freeman WT (2001) Image quilting for texture synthesis and transfer, Proceedings of the 28th Annual Conference on Computer Graphics and Interactive Techniques.

Elmouttie MK, Poropat GV and Krahenbuhl G (2012 A method to estimate in situ block size distribution. Rock Mechanics and Rock Engineering 45: 401-407

Engelhardt I, Prommer H, Moore C, Schulz M, Scheuth C, and Ternes TA (2013) Suitability of temperature, hydraulic heads, and acesulfame to quantify wastewater-related fluxes in the hyporheic and riparian zone. Water Resources Research 49: 426–440.

Eijpe R and Weber K (1971) Mini-permeameters for consolidated rock and unconsolidated sand: Geological note, AAPG Bulletin 55(2): 307-309.

Emerson Electric Co. (2015) Tempest MORE Reservoir Simulation, URL=<http://www2.emersonprocess.com/en-us/brands/roxar/reservoirmanagement/reservoirsimulation/pages/tempestmore.aspx>, viewed 16 November 2015.

Enever J, Bocking M and Clark I (1994) The application of in-situ stress measurement and numerical stress analysis to coalbed methane exploration in Australia, SPE Asia Pacific Oil and Gas Conference, Society of Petroleum Engineers.

Enever J and Henning A (1997) The relationship between permeability and effective stress for Australian coal and its implications with respect to coalbed methane exploration and reservoir model, Proceedings of the 1997 International Coalbed Methane Symposium, Tuscaloosa, AL, USA

Erhel J, De Dreuzy J and Poirriez B (2009) Flow simulation in three-dimensional discrete fracture networks, SIAM Journal on Scientific Computing 31(4): 2688-2705.

Fachri M, Rotevatn A and Tveranger J (2013) Fluid flow in relay zones revisited: Towards an improved representation of small-scale structural heterogeneities in flow models, Marine and Petroleum Geology 46: 144-164.

Falivene O, Cabrera L, Munoz J, Arbues P, Fernandez O and Saez A (2007) Statistical grid-based facies reconstruction and modelling for sedimentary bodies, Alluvial-palustrine and turbiditic examples, Geologica Acta 5(3): 199-230.

Faulkner D, Jackson C, Lunn R, Schlische R, Shipton Z, Wibberley C and Withjack M (2010) A review of recent developments concerning the structure, mechanics and fluid flow properties of fault zones, Journal of Structural Geology 32(11): 1557-1575.

Fegh A, Riahi MA and Norouzi GH (2013) Permeability prediction and construction of 3D geological model: Application of neural networks and stochastic approaches in an Iranian gas reservoir, Neural Computing and Applications 23(6): 1763-1770.

Fisher Q and Jolley S (2007) Treatment of faults in production simulation models, Geological Society of London Special Publications 292(1): 219-233.

Fleckenstein J and Fogg G (2008) Efficient upscaling of hydraulic conductivity in heterogeneous alluvial aquifers, Hydrogeology Journal 16(7): 1239-1250.

Flemisch B, Fritz J, Helmig R, Niessner J, Wohlmuth B (2007) DUMUX: A multi-scale multi-physics toolbox for flow and transport processes in porous media, in: ECCOMAS: Thematic conference on multi-scale computational methods for solids and fluids, Cachan, France, pp. 82–87.

Flodin E, Durlofsky L and Aydin A (2004) Upscaled models of flow and transport in faulted sandstone: boundary condition effects and explicit fracture modelling, Petroleum Geoscience 10(2): 173-181.

Forootan E, Awange J, Kusche J, Heck B, and Eicker A (2012) Independent patterns of water mass anomalies over Australia from satellite data and models, Remote Sensing of Environment 124: 427-443

Fournier A, Mosegaard K, Omre H, Sambridge M and Tenorio L (2013) Assessing uncertainty in geophysical problems - Introduction, Geophysics 78(3): WB1-WB2.

Freeze RA and Cherry JA (1979) Groundwater, Prentice Hall, Englewood Cliffs, NJ, USA, 604p.

Freeze RA, James B, Massmann J, Sperling T and Smith L (1992) Hydrogeological decision analysis: 4. The concept of data worth and its use in the development of site investigation strategies, Groundwater 30(4): 574-588.

Frery E, Langhi L, Rohead-O'Brien H and Strand J (2014) 3-D modelling of complex coal bed methane basins, Gloucester Basin case study, NSW, proceedings of the Australian Earth Sciences Convention 7-10 July 2014, Geological Society of Australia.

Fulljames JR, Zijerveld LJJ and Franssen RCMW (1997) Fault seal processes- Systematic analysis of fault seals over geological and production time scales, in: Møller-Pedersen P and Koestler AG (eds) Hydrocarbon Seals: Importance for Exploration and Production, Elsevier Science, New York, NY, USA, pp.51-59.

Great Artesian Basin Consultative Council (1998) Great Artesian Basin Resource Study, Cox R and Barron A (eds.), 237p.

Great Artesian Basin Consultative Council (2010), Great Artesian Basin Resource Study Update, 138p, URL=<http://www.gabcc.gov.au/system/files/resources/66540f98-c828-4268-8b8b-b37f8193cde7/files/resource-study-2010-update.pdf>, viewed 16 November 2015.

Gardner WP, Harrington GA and Smerdon BD (2012) Using excess ^{4}He to quantify variability in aquitard leakage, Journal of Hydrology 468: 63-75.

Gasda SE, Nordbotten JM and Celia MA (2009) Vertical equilibrium with sub-scale analytical methods for geological CO_2 sequestration, Computational Geosciences, 13(4): 469–481.

Gelhar L (1993) Stochastic Subsurface Hydrology, Prentice-Hall, Englewood Cliffs, NJ, USA.

Geoterra (2008) Groundwater Assessment of the Sunnyside Coal Project via Gunnedah, NSW.

Gerke H and van Genuchten M (1993a) A dual-porosity model for simulating the preferential movement of water and solutes in structured porous media, Water Resources Research 29(2): 305-319.

Gerke H and van Genuchten M (1993b) Evaluation of a 1st-order water transfer term for variably saturated dual-porosity flow models, Water Resources Research 29(4): 1225-1238.

Gerke K, Vasilyev R, Korost D, Karsanina M, Balushkina N, Khamildullin R, Mallants D (2013) Determining physical properties of unconventional reservoir rocks: From laboratory methods to pore-scale modeling, SPE Unconventional Resources Conference and Exhibition-Asia Pacific, Society of Petroleum Engineers.

GHD (2011) Report for QWC17-10 Stage 2: Surat Cumulative Management Area Groundwater Model Report (Draft). Brisbane, Queensland.

Golder Associates (2008) Report on groundwater modelling for Sunnyside open pit coal mine, Gunnedah, NSW, in: Geoterra (2008) Groundwater assessment of the Sunnyside Coal Project via Gunnedah.

Golder Associates (2010) Santos Gunnedah Basin CSG Project Groundwater Impact Study – Kahlua Pilot Test, report no. 107626100-005-Rev1.

Golder Associates (2015), FracMan Reservoir Edition, URL=<http://www.golder.com/us/modules.php?name=Services&op=viewbrochure&sp_id=1139&brochure_id=82> , viewed 16 November 2015.

Gómez-Hernández J and Wen X (1998) To be or not to be multi-Gaussian? A reflection on stochastic hydrogeology, Advances in Water Resources 21(1): 47-61.

Gómez-Hernández J and Journel A (1993) Joint simulation of multiGaussian random variables, Geostatistics Tróia 92(1): 85-94.

Green T and Selby T (1994) Pyridine sorption isotherms of Argonne premium coals - Dual-model sorption and coal microporosity, Energy and Fuels 8(1): 213-218.

Guardiano FB and Srivastava RM (1993) Multivariate geostatistics: Beyond bivariate moments, Geostatistics Troia 92, Springer, 133-144.

Guo H, Adhikary DP, and Craig MS (2009) Simulation of mine water inflow and gas emission during longwall mining, Rock Mechanics and Rock Engineering, 42(1): 25-51.

Hadamard J (1902) Sur les problèmes aux dérivées partielles et leur signification physique, Princeton University Bulletin 13(49-52), 28.

Halford KJ and Hanson RT (2002) User guide for the drawdown-limited, multi-node well (MNW) package for the US Geological Survey's modular three-dimensional finite-difference ground-water flow model, versions MODFLOW-96 and MODFLOW-2000, US Department of the Interior, US Geological Survey.

Hall M (2012) Do you know what you think you know? CSEG Recorder 37(2): 30-34.

Hantush M (1960) Modification of the theory of leaky aquifers, Journal of Geophysical Research 65(11): 3713-3725.

Hantush M (1966) Analysis of data from pumping tests in anisotropic aquifers. Journal of Geophysical Research 71(2).

Hao Y, Sun Y and Nitao JJ (2012) Overview of NUFT: A versatile numerical model for simulating flow and reactive transport in porous media, in: Zhang et al. (ed.s), Groundwater Reactive Transport Models, pp. 212-239.

Harbaugh A, Banta E, Hill M and McDonald M (2000) MODFLOW-2000, the US Geological Survey modular ground-water model: User guide to modularization concepts and the ground-water flow process, U.S. Geological Survey.

Harbaugh AW (2005) MODFLOW-2005, the US Geological Survey modular ground-water model: The ground-water flow process, US Department of the Interior, US Geological Survey Reston, VA, USA.

Harrington G, Gardner W, Smerdon B and Hendry M (2013) Palaeohydrogeological insights from natural tracer profiles in aquitard porewater, Great Artesian Basin, Australia, Water Resources Research 49(7): 4054-4070.

Hart D, Bradbury K and Feinstein D (2006) The vertical hydraulic conductivity of an aquitard at two spatial scales, Ground Water 44(2): 201-211.

He XL, Sonnenberg TO, Jørgensen F and Jensen KH (2014) The effect of training image and secondary data integration with multiple-point geostatistics in groundwater modelling, Hydrology and Earth System Sciences 18: 2943-2954.

Helton JC, Johnson JD, Oberkampf WL (2004) An exploration of alternative approaches to the representation of uncertainty in model predictions. Reliability Engineering and System Safety 85: 39–71.

Helton JC, Johnson JD, Oberkampf WL, Sallaberry CJ (2008) Representation of Analysis Results Involving Aleatory and Epistemic Uncertainty. SAND2008-4379. Sandia National Laboratories, Albuquerque, New Mexico, 60 pp.

Herbert AW (1996) Modelling approaches for discrete fracture network flow analysis, in: Stephansson O, Jing L and Tsang C-F (ed.s) Coupled Thermo-Hydro-Mechanical Processes of Fractured Media, Elsevier, New York, NY, USA, 213-229.

Herckenrath D, Doherty J and Panday S (2015) Incorporating the effect of gas in modelling the impact of CBM extraction on regional groundwater systems, Journal of Hydrology 523: 587-601.

Heynekamp MR, Goodwin LB, Mozley PS and Haneberg WC (1999) Controls on fault-zone architecture in poorly lithified sediments, Rio Grande Rift, New Mexico: Implications for fault-zone permeability and fluid flow, Faults and Subsurface Fluid Flow in the Shallow Crust, 27-49.

Hird KB and Dubrule O (1998) Quantification of reservoir connectivity for reservoir description applications, SPE Reservoir Evaluation and Engineering, 1(1): 12-17.

Hsieh P, Bahr J, Doe T, Flint A, Gee G, Gelhar L, Solomon D, van Genuchten M and Wheatcraft S (2001) Conceptual Models of Flow and Transport in the Fractured Vadose Zone, National Academy Press, Washington, DC, USA.

Hsieh PA and Freckleton JR (1993) Documentation of a computer program to simulate horizontal-flow barriers using the US Geological Survey's modular three-dimensional finite-difference ground-water flow model, US Department of the Interior, US Geological Survey.

Højberg AL, Refsgaard JC (2005). Model uncertainty – parameter uncertainty versus conceptual models. Water Science Technology 52(6): 177–86.

Hu L and Chugunova T (2008) Multiple-point geostatistics for modeling subsurface heterogeneity: A comprehensive review, Water Resources Research 44(11).

Huang X, Bandilla KW, Celia MA and Bachu S (2014) Basin-scale modeling of CO_2 storage using models of varying complexity, International Journal of Greenhouse Gas Control 20: 73-86.

Hussen C, Amin R, Madden G and Evans B (2012) Reservoir simulation for enhanced gas recovery: An economic evaluation, Journal of Natural Gas Science and Engineering 5: 42-50.

Huysmans M and Dassargues (2009) Application of multiple-point geostatistics on modelling groundwater flow and transport in a cross-bedded aquifer (Belgium), Hydrogeology Journal 17: 1901-11.

Iglauer S, Pentland CH, and Busch A (2014). CO2 wettability of seal and reservoir rocks and the implications for carbon geo-sequestration. Water Resources Research 51: 729–774.

Institute of Hydraulic Engineering (2015) MUFTE-UG: Structure, Applications and Numerical Methods, Department of Hydromechanics and Modeling of Hydrosystems, Institute of Hydraulic Engineering, Universität Stuttgart, URL=<http://www.hydrosys.uni-stuttgart.de/institut/hydrosys/publikationen/paper/IGWMC_newsletter_MUFTE.pdf>, viewed 16 November 2015.

IHS (2015) IHS CBM - Coalbed Methane Reservoir Analysis, URL=<https://www.ihs.com/pdf/b-cbm_169589110913044932.pdf>, viewed 16 November 2015.

Indelman P and Dagan G (1993a) Upscaling of conductivity of heterogeneous formations: General approach and application to isotropic media, Transport in Porous Media 12(2): 161-183.

Indelman P and Dagan G (1993b) Upscaling of permeability of anisotropic heterogeneous formations: 1. The general framework, Water Resources Research 29(4): 917-923.

Indelman P and Dagan G (1993c) Upscaling of permeability of anisotropic heterogeneous formations: 2.General structure and small perturbation analysis, Water Resources Research 29(4): 925-933.

International Energy Agency Greenhouse Gas (IEAGHG) Programme (2011) Caprock systems for CO_2 geological storage, report no. 2011/01, Cheltenham, UK, 149 pp., URL=<http://hub.globalccsinstitute.com/sites/default/files/publications/100471/caprock-systems-co2-geological-storage.pdf>.

Isaaks EH and Srivastava RM (1989) Applied Geostatistics, Oxford University Press, New York, NY, USA.

Islam M and Manzocchi T (2014a) New approaches to upscaling fault zones for flow simulation, 76th EAGE Conference and Exhibition 2014.

Islam M and Manzocchi T (2014b) The transmissibility of partially connected cells, ECMOR XIV-14th European Conference on the Mathematics of Oil Recovery.

Jansen JD, Fonseca RM, Kahrobaei S, Siraj MM, Van Essen GM and Van den Hof PMJ (2014) The egg model–A geological ensemble for reservoir simulation, Geoscience Data Journal 1(2): 192-195.

Jarvis N (1998) Modeling the impact of preferential flow on nonpoint source pollution, in: Physical Non-equilibrium in Soils: Modeling and Application, Ann Arbor Press, Chelsea, MI, USA, 195-221.

Jiang X (2011) A review of physical modelling and numerical simulation of long-term geological storage of CO_2, Applied Energy 88(11): 3557-3566.

Jorgensen DG (1989) Using geophysical logs to estimate porosity, water resistivity, and intrinsic permeability, USGPO.

Journel AG (1993) Geostatistics: Roadblocks and challenges, Geostatistics Troia 92, Springer, 213-224.

Journel AG, Deutsch C and Desbarats AJ (1986) Power averaging for block effective permeability, SPE California Regional Meeting, Society of Petroleum Engineers.

Journel AG and Huijbregts CJ (1978) Mining Geostatistics, Academic Press.

Jung A, Fenwick D and Caers J (2013) Training image-based scenario modeling of fractured reservoirs for flow uncertainty quantification, Computational Geosciences 17(6): 1015-1031.

Kalathingal P and Kuchinski R (2010). The role of resistivity image logs in deep natural gas reservoirs, SPE paper no. 131721 presented at the SPE Deep Gas Conference and Exhibition, Manama, Bahrain, 24-26 January 2010.

Kang M, Nordbotten JM, Doster F and Celia MA (2014) Analytical solutions for two-phase subsurface flow to a leaky fault considering vertical flow effects and fault properties, Water Resources Research 50(4): 3536-3552.

Karacan CÖ and Olea RA (2015) Stochastic reservoir simulation for the modeling of uncertainty in coal seam degasification, Fuel 148: 87-97.

Kempka T, Class H, Görke UJ, Norden B, Kolditz O, Kühn M, Walter L, Wang W and Zehner B (2013) A dynamic flow simulation code intercomparison based on the revised static model of the Ketzin pilot site, Energy Procedia 40: 418-427.

Kerrou J, Renard P, Franssen H and Lunati I (2008) Issues in characterizing heterogeneity and connectivity in non-multiGaussian media, Advances in Water Resources 31(1): 147-159.

Khan KD and Deutsch C (2015) Practical incorporation of multivariate parameter uncertainty in geostatistical resource modeling, Natural Resources Research, 1-20.

Kim J and Deo M (2000) Finite element, discrete-fracture model for multiphase flow in porous media, American Institute of Chemical Engineers Journal 46(6): 1120-1130.

Kim YJ, Brooks SC, Zhang F, Parker JC, Moon JW and Roh Y (2015) Fate and transport of uranium (VI) in weathered saprolite, Journal of Environmental Radioactivity 139: 154-162.

Kim Y and Sanderson D (2005) The relationship between displacement and length of faults: A review, Earth Science Reviews 68 (3-4): 317-334.

Klinkenberg L (1941) The permeability of porous media to liquids and gases, Drilling and Production Practice, American Petroleum Institute.

Knott S, Beach A, Brockbank P, Brown J, McCallum J and Welbon A (1996) Spatial and mechanical controls on normal fault populations, Journal of Structural Geology 18(2-3): 359-372.

Knudby C and Carrera J (2005) On the relationship between indicators of geostatistical, flow and transport connectivity, Advances in Water Resources 28(4): 405-421.

Knudby C and Carrera J (2006) On the use of apparent hydraulic diffusivity as an indicator of connectivity, Journal of Hydrology 329(3-4): 377-389.

Knudby C, Carrera J, Bumgardner J and Fogg G (2006) Binary upscaling - the role of connectivity and a new formula, Advances in Water Resources 29(4): 590-604.

Kolditz O (1995) Modelling flow and heat transfer in fractured rocks: conceptual model of a 3-D deterministic fracture network, Geothermics 24(3): 451-470.

Kolditz O, Ratke R, Diersch H-JG, Zielke W (1998) Coupled groundwater flow and transport: 1. Verification of variable density flow and transport models. Advances in Water Resources 21: 27-46

Kolditz O, Bauer S, Bilke L, Böttcher N, Delfs JO, Fischer T, Görke UJ, Kalbacher T, Kosakowski G, McDermott CI, Park CH, Radu F, Rink K, Shao H, Shao HB, Sun F, Sun YY, Singh AK, Taron J, Walther M, Wang W, Watanabe N, Wu Y, Xie M, Xu W and Zehner B (2012) OpenGeoSys: An open-source initiative for numerical simulation of thermo-hydro-mechanical/chemical (THM/C) processes in porous media, Environmental Earth Sciences 67(2): 589-599.

Koltermann C and Gorelick S (1996) Heterogeneity in sedimentary deposits: A review of structure-imitating, process-imitating, and descriptive approaches, Water Resources Research 32(9): 2617-2658.

Konikow L and Bredehoeft J (1992) Groundwater models cannot be validated, Advances in Water Resources 15(1): 75-83.

Konikow L, Hornberger G, Halford K and Hanson R (2009) Revised multi-node well (MNW2) package for MODFLOW ground-water flow model, U.S. Geological Survey.

Kröhn KP (2012) Qualifying a computer program for simulating fracture flow, Computing and Visualization in Science, 15(1): 29-37.

Kruseman G and de Ridder N (1990) Analysis and evaluation of pumping test data, International Institute for Land Reclamation and Improvement, Wageningen University, Wageningen, The Netherlands.

Laloy E, Rogiers B, Vrugt JA, Mallants D and Jacques D (2013) Efficient posterior exploration of a high-dimensional groundwater model from two-stage Markov chain Monte Carlo simulation and polynomial chaos expansion, Water Resources Research 49(5): 2664-2682.

Langmuir I (1918) The adsorption of gases on plane surfaces of glass, mica and platinum, Journal of the American Chemical Society 40: 1361-1403.

Law DHS, Van der Meer LGH and Gunter WD (2002) Numerical simulator comparison study for enhanced coalbed methane recovery processes, Part I: Pure carbon dioxide injection, in: Society of Petroleum Engineers Gas Technology Symposium, Calgary, Alberta, Canada, April 30–May 2, 2002.

Law DHS, Van der Meer LGH and Gunter WD (2003) Comparison of numerical simulators for greenhouse gas storage in coal beds, Part II: Flue gas injection, in: Proceedings of the 6th International Conference on Greenhouse Gas Control Technologies, Kyoto, Japan, October 1-4, 2002.

Law DHS, Van der Meer LGH and Gunter WD (2004) Comparison of numerical simulators for greenhouse gas sequestration in coalbeds, Part III: More complex problems, 2nd Annual Conference on Carbon Sequestration, Alexandria, VA, USA, May 5–8, 2003.

Law DHS, Van der Meer LGH and Gunter WD (2005) Comparison of numerical simulators for greenhouse gas sequestration in coalbeds, Part IV: History match of field micro-pilot test data, in: Proceedings of the 7th International Conference on Greenhouse Gas Control Technologies, Vancouver, BC, Canada, September 5-9, pp. 2239-2242.

Li X and Fang ZM (2014) Current status and technical challenges of CO_2 storage in coal seams and enhanced coalbed methane recovery: An overview, International Journal of Coal Science and Technology, 1(1): 93-102.

Li L, Srinivasan S, Zhou H and Gómez-Hernández JJ (2015) Two-point or multiple-point statistics? A comparison between the ensemble Kalman filtering and the ensemble pattern matching inverse methods, Advances in Water Resources 86(B): 297-310.

Li L, Zhou H and Gomez-Hernandez J (2011) A comparative study of three-dimensional hydraulic conductivity upscaling at the macro-dispersion experiment (MADE) site, Columbus Air Force Base, Mississippi (USA), Journal of Hydrology 404(3-4): 278-293.

Lichtner PC, Hammond GE, Lu C, Karra S, Bisht G, Andre B, Mills R, Kumar J (2015) PFLOTRAN User Manual: A Massively Parallel Reactive Flow and Transport Model for Describing Surface and Subsurface Processes, Los Alamos National Laboratory, Los Alamos, NM, USA, 195p.

Lindsay N, Murphy F, Walsh J and Watterson J (1993) Outcrop studies of shale smears on fault surfaces, The Geological Modelling of Hydrocarbon Reservoirs and Outcrop Analogues, pp. 113-123.

Liu H, Doughty C and Bodvarsson G (1998) An active fracture model for unsaturated flow and transport in fractured rocks, Water Resources Research 34(10): 2633-2646.

Liu H, Zhang G and Bodvarsson G (2003) The active fracture model: Its relation to fractal flow patterns and an evaluation using field observations, Vadose Zone Journal 2(2): 259-269.

Liu Y, Harding A, Abriel W and Strebelle S (2014). Multiple-point simulation integrating wells, three-dimensional seismic data, and geology. AAPG Bulletin 88: 905–921.

Liu X, Zhang C, Liu Q and Birkholzer J (2009) Multiple-point statistical prediction on fracture networks at Yucca Mountain, Environmental Geology 57(6): 1361-1370.

Liu Y (2006) Using the Snesim program for multiple-point statistical simulation, Computers and Geosciences 32(10): 1544-1563.

Lohne A, Vimovsky G and Durlofsky LJ (2006) Two-stage upscaling of two-phase flow: from core to simulation scale. SPE Journal, September 2006: 304-316.

Long J, Remer J, Wilson C and Witherspoon P (1982) Porous media equivalents for networks of discontinuous fractures, Water Resources Research 18(3): 645-658.

Loveless S, Bense V and Turner J (2011) Fault architecture and deformation processes within poorly lithified rift sediments, Central Greece, Journal of Structural Geology 33(11): 1554-1568.

MacQuarrie KT, Mayer KU (2005) Reactive transport modeling in fractured rock: A state-of-the-science review, Earth Science Reviews 72(3): 189-227.

Maharaja A (2008) TiGenerator: Object-based training image generator, Computers and Geosciences 34(12): 1753-1761.

Mahmud K, Mariethoz G, Baker A and Sharma A (2015) Integrating multiple scales of hydraulic conductivity measurements in training image-based stochastic models, Water Resources Research 51(1): 465-480.

Mallants D, Jacques D and Perko J (2007) Modelling multi-phase flow phenomena in concrete barriers used for geological disposal of radioactive waste, The 11th International Conference on Environmental Remediation and Radioactive Waste Management, American Society of Mechanical Engineers.

Mallants D, Vanclooster M, Diels J, and Feyen J (1996) A stochastic approach to simulate water flow in a macroporous soil, Geoderma 70: 299-324.

Mallants D, Vermariën E, Perko J, Gedeon M and Olyslaegers G (2009) Overview of qualification file for conceptual models and codes for long-term radiological safety assessments, ONDRAF/NIRAS (Belgian Agency for Radioactive Waste and Enriched Fissile Materials).

Manik J, Ertekin T, Kohler T (2002) Development and validation of a compositional coalbed simulator, Journal of Canadian Petroleum Technology, 41 (2002): 39–45.

Manzocchi T, Childs C and Walsh J (2010) Faults and fault properties in hydrocarbon flow models, Geofluids 10(1-2): 94-113.

Manzocchi T, Heath A, Palananthakumar B, Childs C and Walsh J (2008) Faults in conventional flow simulation models: A consideration of representational assumptions and geological uncertainties, Petroleum Geoscience 14(1): 91-110.

Manzocchi T, Heath A, Walsh J and Childs C (2002) The representation of two phase fault-rock properties in flow simulation models, Petroleum Geoscience 8(2): 119-132.

Manzocchi T, Walsh J, Nell P and Yielding G (1999) Fault transmissibility multipliers for flow simulation models, Petroleum Geoscience 5(1): 53-63.

Mariethoz G and Lefebvre S (2014) Bridges between multiple-point geostatistics and texture synthesis: Review and guidelines for future research, Computers and Geosciences 66: 66-80.

Mariethoz G, Renard P and Straubhaar J (2010) The Direct Sampling method to perform multiple-point geostatistical simulations, Water Resources Research 46(11).

Matrix Plus (2009) Groundwater (Deep Aquifer Modelling) for SANTOS GLNG Environmental Impact Statement, Brisbane, Queensland.

Mayer KU, Alt-Epping P, Jacques D, Arora B and Steefel CI (2015) Benchmark problems for reactive transport modeling of the generation and attenuation of acid rock drainage, Computational Geosciences, pp. 1-13.

McLean K and McNamara D (2010) Fractures interpreted from acoustic formation imaging technology: Correlation to permeability, Proceedings of the 36th Workshop on Geothermal Reservoir Engineering, California, USA, 31 January – 2 February 2011.

McKenna EP and Poeter SA (1995) Field example of data fusion in site characterization, Water Resources Research 31(12): 3229-3240.

Meerschaert MM, Dogan M, Dam RL, Hyndman DW and Benson DA (2013) Hydraulic conductivity fields: Gaussian or not? Water Resources Research 49(8): 4730-4737.

Michael H, Li H, Boucher A, Sun T, Caers J and Gorelick S (2010) Combining geologic-process models and geostatistics for conditional simulation of 3-D subsurface heterogeneity, Water Resources Research 46(5).

Middleton RS, Keating GN, Stauffer PH, Jordan AB, Viswanathan HS, Kang QJ, Carey JW, Mulkey ML, Sullivan EJ, Chu SP, Esposito R and Meckel TA (2012) The cross-scale science of CO_2 capture and storage: From pore scale to regional scale, Energy and Environmental Science, 5(6): 7328-7345.

Middleton RS, Carey JW, Currier RP, Hyman JD, Kang Q, Karra S, Jiménez-Martínez J, Porter ML and Viswanathan HS (2015) Shale gas and non-aqueous fracturing fluids: Opportunities and challenges for supercritical CO2, Applied Energy 147: 500-509.

Moore C (2005) The Use of Regularized Inversion in Groundwater Model Calibration and Prediction Uncertainty Analysis, PhD thesis, University of Queensland, St. Lucia, Australia.

Moore C, Wohling T and Wolf L (2011) Optimisation of monitoring data for increased predictive reliability of regional water allocation models, 19th International Congress on Modelling and Simulation, Perth, Australia, 12–16 December 2011 .

Moore C, Doherty J, Howell S and Erriah L (2013). Upscaling hydraulic properties and processes in the Coal Seam Gas Context - Heterogeneity and dual phase flow challenges in lithologically segregated upscaling. CSIRO Client Report: 129 pp.

Moore C, Doherty J, Howell S and Erriah L (2014a) Some challenges posed by coal bed methane regional assessment modeling, Ground Water 53(5): 737-747.

Moore C, Cui T, Doherty J, Turnadge C, Pagendam D, and Peeters L (2014b) Uncertainty analysis, data worth analysis and hypothesis testing: Assessments to support Environmental impact Assessments related to cumulative impacts of Coal Seam Gas extraction in the Surat Basin, Queensland. CSIRO, Australia.

Moore T (2012) Coalbed methane: A review, International Journal of Coal Geology 101: 36-81.

Morad K, Mireault R and Dean L (2008) Reservoir Engineering for Geologists: Coalbed Methane Fundamentals.

Morris JP, Hao Y, Foxall W and McNab W (2011) A study of injection-induced mechanical deformation at the In Salah CO2 storage project, International Journal of Greenhouse Gas Control 5(2): 270-280.

Motz LH (1992) Salt-water upconing in an aquifer overlain by a leaky confining bed. Ground Water 30: 192-198.

Mukhopadhyay S, Birkholzer JT, Nicot JP and Hosseini SA (2012) A model comparison initiative for a CO2 injection field test: An introduction to Sim-SEQ, Environmental Earth Sciences 67(2): 601-611.

Myers RD (1999) Structure and hydraulics of brittle faults in sandstone, PhD thesis, Stanford University, Palo Alto, CA, USA.

Neuman S and Witherspoon PA (1969) Applicability of current theories of flow in leaky aquifers, Water Resources Research 5(4): 817-829.

Neuman SP (1988) Stochastic continuum representation of fractured rock permeability as an alternative to the REV and fracture network concepts, in: Custodio E, Gurgui A and Ferreira JPL (ed.s) Groundwater Flow and Quality Modelling, Springer Netherlands, pp. 331-362.

Neuman SP and Di Federico V (1998) Correlation, flow, and transport in multiscale permeability fields, in: Scale Dependence and Scale Invariance in Hydrology, Cambridge University Press, Cambridge, UK, pp. 354-397.

Neuman SP and Wierenga PJ (2003) A Comprehensive Strategy of Hydrogeologic Modeling and Uncertainty Analysis for Nuclear Facilities and Sites. NUREG/CR-6805 U.S. Nuclear Regulatory Commission, Office of Nuclear Regulatory Research, Washington, DC.

New South Wales Chief Scientist and Engineer (2014) Independent review of coal seam gas activity in NSW – Information paper: Abandoned wells.

New South Wales Office of Water (2010) PINNEENA 3.2 Continuous Monitoring – Users Guide, New South Wales groundwater data archive.

New South Wales Office of Water (2012) NSW Aquifer Interference Policy.

Nordbotten JM, Kavetski D, Celia MA, Bachu S (2009) Model for CO_2 leakage including multiple geological layers and multiple leaky wells, Environmental Science and Technology 43(3): 743-749.

Office of Groundwater Impact Assessment (2013) Annual Report 2013 for the Surat Underground Water Impact Report, Office of Groundwater Impact Assessment, Department of Natural Resources and Mines, Brisbane, Queensland.

Office of Groundwater Impact Assessment (2014) Annual Report 2014 for the Surat Underground Water Impact Report, Office of Groundwater Impact Assessment, Department of Natural Resources and Mines, Brisbane.

Olivella S, Gens A, Carrera J and Alonso EE (1996) Numerical formulation for a simulator (CODE_BRIGHT) for the coupled analysis of saline media, Engineering Computations 13(7): 87-112.

Oreskes N, Shraderfrechette K and Belitz K (1994) Verification, validation, and confirmation of numerical models in the earth sciences, Science 263(5147): 641-646.

Overbey WK, Yost LE, and Yost II AB (1988) Analysis of natural fractures observed by borehole video camera in a horizontal well, in: SPE Gas Technology Symposium, Society of Petroleum Engineers.

Pan Z and Connell L (2012) Modelling permeability for coal reservoirs: A review of analytical models and testing data, International Journal of Coal Geology 92: 1-44.

Panday S, Langevin CD, Niswonger RG, Ibaraki M and Hughes JD (2013) MODFLOW–USG version 1: An unstructured grid version of MODFLOW for simulating groundwater flow and tightly coupled processes using a control volume finite-difference formulation, U.S. Geological Survey.

Pei Y, Paton DA, Knipe RJ and Wu K (2015) A review of fault sealing behaviour and its evaluation in siliciclastic rocks, Earth Science Reviews 150: 121-138.

Pettersen O (2006) Basics of Reservoir Simulation With the ECLIPSE Reservoir Simulator, Lecture Notes, Department of Mathematics, University of Bergen, Norway, 114p., URL=<http://folk.uib.no/fciop/index_htm_files/ResSimNotes.pdf>, viewed 16 November 2015.

PHH Engineering Software (2014) GCOMP, URL=<http://www.phhpc.com/simulation/gcomp.php>, viewed 16 November 2015.

Poeter SA and McKenna EP (1995) Reducing uncertainty associated with groundwater flow and transport predictions, Ground Water 33(6): 899-904.

Post V, Kooi H, and Simmons C (2007). Using Hydraulic Head Measurements in Variable-Density Ground Water Flow Analyses. Ground Water 45: 664-671.

Preisig M and Prévost JH (2011) Coupled multi-phase thermo-poromechanical effects, case study: CO_2 injection at In Salah, Algeria, International Journal of Greenhouse Gas Control, 5(4): 1055-1064.

Prevost JH (1983) DYNA-FLOW: A nonlinear transient finite element analysis program, Princeton University, Department of Civil Engineering, School of Engineering and Applied Science, Princeton, NJ, USA, 516p.

Pruess K (1991) TOUGH2: A general-purpose numerical simulator for multiphase fluid and heat flow, Lawrence Berkeley Laboratory, Berkeley, CA, USA.

Pruess K (2005) Numerical studies of fluid leakage from a geologic disposal reservoir for CO_2 show self-limiting feedback between fluid flow and heat transfer, Geophysical Research Letters 32(14).

Pruess K (2008) On CO_2 fluid flow and heat transfer behavior in the subsurface, following leakage from a geologic storage reservoir, Environmental Geology 54(8): 1677-1686.

Pruess K, Oldenburg C and Moridis D (1999) TOUGH2 User's Guide, Version 2.0, report no. LBNL-43134, Lawrence Berkeley National Laboratory, Berkeley, CA, USA, 212p.

Pruess K, García J, Kovscek T, Oldenburg C, Rutqvist J, Steefel C and Xu T (2004) Code intercomparison builds confidence in numerical simulation models for geologic disposal of CO_2, Energy 29(9): 1431-1444.

Pucci AA and Murashige JAE (1987) Applications of universal kriging to an aquifer study in New Jersey, Ground Water 25(6): 672-678.

Queensland Gas Company (2013) Approval Conditions 49 to 64 Stage 3 CSG Water Monitoring and Management Plan. Brisbane, Queensland, URL=<http://www.qgc.com.au/ebooks/201409_QGC_Stage_3_WMMP/index.html#/1/>.

Queensland Water Commission (2012) Underground water impact report for the Surat cumulative management area, Brisbane, Queensland, URL=<https://www.dnrm.qld.gov.au/ogia/surat-underground-water-impact-report>.

Rawling GC, Goodwin LB and Wilson JL (2001) Internal architecture, permeability structure, and hydrologic significance of contrasting fault-zone types, Geology 29(1): 43-46.

Raymer L, Hunt E and Gardner JS (1980) An improved sonic transit time-to-porosity transform, SPWLA 21st Annual Logging Symposium, Society of Petrophysicists and Well-Log Analysts.

Raza SH, Treiber LE and Archer DL (1968) Wettability of reservoir rocks and its evaluation, Production Monthly 37(4): 82-87.

Refsgaard JC and Henriksen HJ (2004) Modelling guidelines—terminology and guiding principles, Advances in Water Resources 27(1): 71-82.

Refsgaard JC, Christensen S, Sonnenborg TO, Seifert D, Højberg AL, Troldborg L (2012) Review of strategies for handling geological uncertainty in groundwater flow and transport modeling. Advances in Water Resources 36: 36-50.

Remy N, Boucher A and Wu J (2009) Applied Geostatistics with SGeMS: A User's Guide, Cambridge University Press, Cambridge, UK.

Renard P, Straubhaar J, Caers J, Mariethoz G (2011) Conditioning facies simulations with connectivity data. Mathematical geosciences, 43: 879-903.

Renard P and Allard D (2011) Connectivity metrics for subsurface flow and transport. Advances in Water Resources 51: 168-196.

Renard P and de Marsily G (1997) Calculating equivalent permeability: A review, Advances in Water Resources 20 (5-6): 253-278.

Ricard L, Godel B, Smerdon B and Esteban L (2014) Aquitard hydraulic properties estimation from wireline logs analysis: An application to the Surat Basin, Queensland, Australian Earth Science Convention.

Ringrose P, Nordahl K and Wen R (2005) Vertical permeability estimation in heterolithic tidal deltaic sandstones, Petroleum Geoscience 11(1): 29-36.

Rogiers B, Mallants D, Batelaan O, Gedeon M, Huysmans M and Dassargues A (2012) Estimation of hydraulic conductivity and its uncertainty from grain-size data using GLUE and artificial neural networks, Mathematical Geosciences 44(6): 739-763.

Rogiers B, Beerten K, Smekens T, Mallants D, Gedeon M, Huysmans M, Batelaan O, and Dassargues A (2013) The usefulness of outcrop-analogue air-permeameter measurements for analysing aquifer heterogeneity: Testing outcrop hydrogeological parameters with independent borehole data, Hydrology and Earth System Sciences 17: 5155–5166.

Rogiers B, Vienken T, Gedeon M, Batelaan O, Mallants D, Huysmans M and Dassargues A (2014a) Multi-scale aquifer characterization and groundwater flow model parameterization using direct push technologies, Environmental Earth Sciences 72 (5): 1303–1324.

Rogiers B, Winters P, Huysmans M, Beerten K, Mallants D, Gedeon M, Batelaan O, and Dassargues A (2014b) High resolution saturated hydraulic conductivity logging of borehole cores using air permeability measurements, Hydrogeology Journal 22(6): 1345-1358.

Rojas R, Kahunde S, Peeters L, Batelaan O, Feyen L, Dassargues A (2010) Application of a multimodel approach to account for conceptual model and scenario uncertainties in groundwater modelling. Journal of Hydrology 394: 416-435.

Ross JL, Ozbek MM, and Pinder GF (2009) Aleatoric and epistemic uncertainty in groundwater flow and transport simulation. Water Resources Research 45: W00B15.

Rubin Y (2003) Applied Stochastic Hydrogeology, Oxford University Press, Oxford, UK.

Rubin Y and Gomez-Hernandez J (1990) A stochastic approach to the problem of upscaling of conductivity in disordered media - Theory and unconditional numerical simulations, Water Resources Research 26(4): 691-701.

Rubin Y and Hubbard SS (2006) Hydrogeophysics, Springer Science and Business Media.

Salmon SU, Rate AW, Rengel Z, Appleyard S, Prommer H and Hinz C (2014) Reactive transport controls on sandy acid sulfate soils and impacts on shallow groundwater quality, Water Resources Research 50(6): 4924-4952.

Samper J, Moreira S, Alvares D, Montenegro L, Lu C, López C, Bonilla M, Ma H, Li Y, Pisani B, Arechaga F, Gil A, Menéndez JA, Lucas T and Valle-García R (2008) Model predictions of water chemistry for the future pit lake in As Pontes, A Coruña (Spain), in: K Vary, Rapantova N and Hrkal Z (ed.s) Mine Water and the Environment, X International Mine Water Association Congress.

Sanchez-Vila X, Carrera J and Girardi J (1996) Scale effects in transmissivity, Journal of Hydrology 183(1-2): 1-22.

Sanchez-Vila X, Girardi J and Carerra J (1995) A synthesis of approaches to upscaling of hydraulic conductivities, Water Resources Research 31(4): 867-882.

Sanchez-Vila X, Guadagnini A and Carrera J (2006) Representative hydraulic conductivities in saturated groundwater flow, Reviews of Geophysics 44(3).

Santos (2010) Bowen Basin groundwater modelling report.

Sarma P, Aziz K and Durlofsky LJ (2005) Implementation of adjoint solution for optimal control of smart wells, in: SPE Paper 92864, presented at the SPE Reservoir Simulation Symposium, Houston, TX, USA.

Sawyer WK, Paul GW and Schraufnagel RA (1990) Development and application of a 3-D coalbed simulator, Annual Technical Meeting, Petroleum Society of Canada.

Schaeffer J (2008) Scaling point based aquifer data for developing regional groundwater models: Application to the Gippsland groundwater system, PhD thesis, University of Melbourne, Melbourne, Victoria.

Schlumberger (1991) Log Interpretation Principles / Applications, Schlumberger Wireline and Testing, Houston, TX, USA.

Schlumberger (2011) Manual for ECLIPSE Reservoir Simulation Software, Houston, TX, USA.

Schulze-Makuch D and Cherkauer D (1998) Variations in hydraulic conductivity with scale of measurement during aquifer tests in heterogeneous, porous carbonate rocks, Hydrogeology Journal 6: 204–215.

Schneider A, Kröhn KP, Püschel A (2012) Developing a modelling tool for density-driven flow in complex hydrogeological structures, Computing and Visualization in Science 15(4): 163-168.

Shapiro SS and Wilk MB (1965) An analysis of variance test for normality (complete samples), Biometrika 52: 591-611.

Shipton Z and Cowie P (2001) Damage zone and slip-surface evolution over µm to km scales in high-porosity Navajo sandstone, Utah, Journal of Structural Geology 23(12): 1825-1844.

Silva D and Deutsch C (2014) A multiple training image approach for spatial modeling of geologic domains, Mathematical Geosciences 46 (7): 815-840.

Šimůnek J, Jarvis N, van Genuchten M and Gardenas A (2003) Review and comparison of models for describing non-equilibrium and preferential flow and transport in the vadose zone, Journal of Hydrology 272(1-4): 14-35.

Šimůnek J and van Genuchten MT (2006) Contaminant transport in the unsaturated zone theory and modeling, in: Delleur JW (ed.) The Handbook of Groundwater Engineering, CRC Press, 22-21-22-46.

Sinclair Knight Merz (2013) Monitoring and management of non-Lake Eyre bore integrity – Draft guidance for bore monitoring approaches, report prepared for the Australian Government Department of Sustainability, Environment, Water, Population and Communities.

Slater L (2007) Near surface electrical characterization of hydraulic conductivity: From petrophysical properties to aquifer geometries—A review, Surveys in Geophysics 28(2-3): 169-197.

Smerdon B, Smith L, Harrington G, Gardner W, Delle Piane C and Sarout J (2014) Estimating the hydraulic properties of an aquitard from in situ pore pressure measurements, Hydrogeology Journal 22(8): 1875-1887.

Smith SD, Solomon DK and Gardner WP (2013) Testing helium equilibrium between quartz and pore water as a method to determine pore water helium concentrations, Applied Geochemistry 35: 187-195.

Spencer SJ, Somers ML, Pinchewski WV, Doig ID (1987) Numerical simulation of gas drainage from coal seams, in: Proceedings of the 62nd SPE Annual Technical Conference and Exhibition, Dallas, TX, USA, pp. 217-229.

Sperrevik S, Gillespie PA, Fisher QJ, Halvorsen T and Knipe RJ (2002) Empirical estimation of fault rock properties, in: Koestler AG and Hunsdale R (ed.s) Hydrocarbon Seal Quantification, Elsevier Science, Amsterdam, The Netherlands, pp. 109-125.

Springer D, Loaiciga H, Cullen S and Everett L (1998) Air permeability of porous materials under controlled laboratory conditions, Ground Water 36(4): 558-565.

Srinivasan G, Tartakovsky DM, Robinson BA, and Aceves AB (2007) Quantification of uncertainty in geochemical reactions. Water Resources Research 43, W12415.

Stadler L, Hinkelmann R, Helmig R (2012) Modeling macroporous soils with a two-phase dual-permeability model, Transport in Porous Media 95(3): 585-601.

State of New South Wales (2015) Environmental Planning and Assessment Act 1979, in: Wales SoNS (ed.) 203.

State of Queensland (2014) State Development and Public Works Organisation Act 1971.

Steefel CI (2008) CrunchFlow Software for Modeling Multicomponent Reactive Flow and Transport: User's Manual, Earth Sciences Division, Lawrence Berkeley National Laboratory, Berkeley, CA, USA, 91p.

Steefel CI, Appelo CAJ, Arora B, Jacques D, Kalbacher T, Kolditz O, Lagneau V, Lichtner PC, Mayer KU, Meeussen JCL, Molins S, Moulton D, Shao H, Šimůnek J, Spycher N, Yabusaki SB and Yeh GT (2014) Reactive transport codes for subsurface environmental simulation, Computational Geosciences 19 (3): 445-478.

Strand J, Freij-Ayoub R and Ahmed S (2012) Simulating the impact of coal seam gas water production on aquifers, APPEA Journal and Conference Proceedings.

Strebelle S (2000) Sequential simulation drawing structures from training images, PhD thesis, Stanford University, Palo Alto, CA, USA.

Strebelle S (2002) Conditional simulation of complex geological structures using multiple-point statistics, Mathematical Geology 34(1): 1-21.

Schlumberger Water Services (2012) Namoi Catchment Water Study Independent Expert Final Study Report, Perth, Western Australia.

Swiler LP, Paez PT, Mayes RL (2009). Epistemic Uncertainty Quantification Tutorial. Proceedings of the IMAC-XXVII. February 9-12, 2009 Orlando, Florida USA. Society for Experimental Mechanics Inc.: 17 pp.

Szymkiewicz A (2013) Upscaling from Darcy scale to field scale, in: Modelling Water Flow in Unsaturated Porous Media, Springer, 139-175.

Taylor AR, Pichler MM, Olifent V, Thompson J, Bestland EA, Davies PJ, Lamontagne S, Suckow AO, Robinson NI and Love A (2015) Groundwater flow Systems of north eastern Eyre Peninsula: A multi-disciplinary approach: Hydrogeology, geophysics and environmental tracers, Facilitating Long Term Outback Water Solutions —Stage 2, Goyder Institute for Water Research, Adelaide, South Australia.

Tanikawa W and Shimamoto T (2006) Klinkenberg effect for gas permeability and its comparison to water permeability for porous sedimentary rocks. Hydrology and Earth System Sciences Discussion, 3: 1315-1338.

Teles V, Fornel A, Houel P, Delmas J, Mengus JM, Michel A and Maurand N (2014) Coupling basin and reservoir simulators for an improved co2 injection flow model, Energy Procedia 63: 3665-3675.

TerHeege J, Wassing B, Orlic B, Giger S and Clennell M (2013) Constraints on the sealing capacity of faults with clay smears from discrete element models validated by laboratory experiments, Rock Mechanics and Rock Engineering 46 (3): 465-478.

Thararoop P, Karpyn ZT and Ertekin T (2012) Development of a multi-mechanistic, dual-porosity, dual-permeability, numerical flow model for coalbed methane reservoirs, Journal of Natural Gas Science and Engineering 8: 121-131.

Theis C (1935) The relation between the lowering of the piezometric surface and the rate and duration of discharge of a well using ground water storage, EoS: Transactions of the American Geophysical Union 16: 519-524.

Therrien R and Sudicky E (1996) Three-dimensional analysis of variably-saturated flow and solute transport in discretely-fractured porous media, Journal of Contaminant Hydrology 23(1-2): 1-44.

Timms WA, Crane R, Anderson DJ, Bouzalakos S, Whelan M, McGeeney D, Rahman PF, Guinea A and Acworth RI (2015) Accelerated gravity testing of aquitard core permeability and implications at formation and regional scale, Hydrology and Earth System Sciences Discussions 12: 2799–2841.

Tonkin M and Doherty JE (2009) Calibration-constrained Monte Carlo analysis of highly parameterized models using subspace techniques. Water Resources Research 45, WOOB10, doi:10.1029/2007WR006678.

Torabi A and Berg S (2011) Scaling of fault attributes: A review, Marine and Petroleum Geology 28(8): 1444-1460.

Tran T (1996) The 'missing scale' and direct simulation of block effective properties, Journal of Hydrology 183: 37-56.

Trinchero P, Sanchez-Vila X, Fernandez-Garcia D, (2008) Point to point connectivity, an abstract concept of a key issue for risk assessment studies? Advances in water resources 31. 1742-1753.

Troldborg L, Refsgaard JC, Jensen KH, Engesgaard P (2007) The importance of alternative conceptual models for simulation of concentrations in multiaquifer system. Hydrogeology Journal 15:843–60.

Turnadge C and Smerdon BD (2014) A review of methods for modelling environmental tracers in groundwater: Advantages of tracer concentration simulation, Journal of Hydrology 519: 3674-3689.

Underschultz J, Esterle J, and Strand J (2018) Conceptual representation of fluid flow conditions associated with faults in sedimentary basins, report prepared for the Office of Water Science (OWS), Canberra, Australian Capital Territory.

United States Environmental Protection Agency (2003a) Use of airborne, borehole and surface geophysical techniques at contaminated sites: A reference guide, report no. EPA/625/R-92/007.

United States Environmental Protection Agency (2003b) Subsurface characterisation and monitoring techniques: A desk reference guide: Volume I: Solids and Groundwater, Appendices A and B, report no. EPA625/R-93/003a.

United States Environmental Protection Agency (2009) Statistical analysis of groundwater monitoring data at RCRA facilities – Unified Guidance, report no. EPA 530/R-09-007.

University of British Columbia (2015) The Reactive Transport Code MIN3P: Multicomponent reactive transport modeling in variably saturated porous media, URL=<http://www.eos.ubc.ca/research/hydro/research/min3p/reactive_tran_web.htm>, viewed 16 November 2015.

University of Southern Queensland (2011) Preliminary assessment of cumulative drawdown impacts in the Surat Basin associated with the coal seam gas industry: Investigation of parameters and features for a regional model of Surat Basin coal seam gas developments, Toowoomba, Queensland.

Van der Baan M and Jutten C (2000) Neural networks in geophysical applications, Geophysics 65(4): 1032-1047.

van der Kamp G (2001) Methods for determining the in situ hydraulic conductivity of shallow aquitards–An overview, Hydrogeology Journal 9(1): 5-16.

van der Schalie R, Parinussa RM, Renzullo LJ, van Dijk AIJM, Su CH and de Jeu RAM (2015) SMOS soil moisture retrievals using the Land Parameter Retrieval Model: Evaluation over the Murrumbidgee Catchment, southeast Australia, Remote Sensing of the Environment 163: 70-79.

van Genuchten MT (1980) A closed-form equation for predicting the hydraulic conductivity of unsaturated soils, Soil Science Society of America Journal 44(5): 892-898.

Varljen MD and Shafer JM (1991) Assessment of uncertainty in time-related capture zones using conditional simulation of hydraulic conductivity, Ground Water 29(5): 737-748.

Varma S and Michael K (2012) Impact of multi-purpose aquifer utilisation on a variable-density groundwater flow system in the Gippsland Basin, Australia, Hydrogeology Journal 20(1): 119-134.

Venkataramanan L, Hürlimann MD, Tarvin JA, Fellah K, Acero-Allard D, and Seleznev NV (2014). Experimental Study of the Effects of Wettability and Fluid Saturation on Nuclear Magnetic Resonance and Dielectric Measurements in Limestone. Petrophysics 55: 572–586.

Vereecken H, Binley A, Cassiani G, Revil A and Titov K (2006) Applied Hydrogeophysics, Springer.

Vermilye JM and Scholz CH (1998) The process zone: A microstructural view of fault growth, Journal of Geophysical Research: Solid Earth (1978–2012) 103(B6): 12223-12237.

Vidstrand P (2001) Comparison of upscaling methods to estimate hydraulic conductivity, Ground Water 39(3): 401-407.

Vienken T and Dietrich P (2011) Field evaluation of methods for determining hydraulic conductivity from grain size data, Journal of Hydrology 400(1): 58-71.

Vilarrasa V, Olivella S, Silva O, Carrera J (2012) Numerical simulation of non-isothermal CO_2 injection using the thermo-hydro-mechanical code CODE_BRIGHT, in: EGU General Assembly Conference Abstracts (vol. 14, p. 759).

Wackernagel H (2003) Multivariate Geostatistics, Springer Science and Business Media.

Wallis I, Moore C, Post V, Wolf L, Martens E, Prommer H (2014). Using predictive uncertainty analysis to optimise tracer test design and data acquisition. Journal of Hydrology 515: 191–204.

Wang K, Wang G, Ren T and Cheng Y (2014) Methane and CO_2 sorption hysteresis on coal: A critical review, International Journal of Coal Geology 132: 60-80.

Warren J and Price H (1961) Flow in heterogeneous porous media, Society of Petroleum Engineers Journal 1(3): 153-169.

Watanabe N, Kolditz O (2015) Numerical stability analysis of two-dimensional solute transport along a discrete fracture in a porous rock matrix, Water Resources Research 51(7): 5855-5868.

Watermark Numerical Computing (2012) Predictive uncertainty of the regional-scale groundwater flow model for the Surat Cumulative Management Area, report prepared by Watermark Numerical Computing for the Queensland Water Commission, Brisbane, Queensland.

Watson TA, Doherty JE and Christensen S (2012) Parameter and predictive outcomes of model simplification. Water Resources Research 49: 3952–3977.

Weber D and Englund E (1992) Evaluation and comparison of spatial interpolators, Mathematical Geology 24(4): 381-391.

Weber D and Englund E (1994) Evaluation and comparison of spatial interpolators II, Mathematical Geology 26(5): 589-603.

Weber K (1986) How heterogeneity affects oil recovery, Reservoir Characterization 487: 544.

Wellmann JF, Finsterle S and Croucher A (2014) Integrating structural geological data into the inverse modelling framework of iTOUGH2, Computers and Geosciences 65: 95-109.

Wen X and Gomez-Hernandez J (1996) Upscaling hydraulic conductivities in heterogeneous media: An overview, Journal of Hydrology 183(1-2): R9-R32.

Weissmann GS, Zhang Y, LaBolle EM, and Fogg GE (2002). Dispersion of groundwater age in an alluvial aquifer system. Water Resources Research 38(10): 1198, doi:1110.1029/2001WR000907.

Wessling S, Bartetzko A and Tesch P (2013) Quantification of uncertainty in a multistage/multiparameter modeling workflow: Pore pressure from geophysical well logs, Geophysics 78(3): WB101-WB112.

White MD and Oostrom M (2006) STOMP Subsurface Transport Over Multiple Phase: User's Guide, report no. PNNL-15782 (UC-2010), Pacific Northwest National Laboratory, Richland, WA, USA, 317p.

White JT, Doherty J, Hughes JD (2014). Quantifying the predictive consequences of model error with linear subspace analysis. Water Resources Research 50: 1152-1173.

Wright M, Dillon P, Pavelic P, Peter P and Nefiodovas A (2002) Measurement of 3-D hydraulic conductivity in aquifer cores at in situ effective stresses. Ground Water 40 (5): 509-517.

Wu J, Boucher A and Zhang T (2008) A SGeMS code for pattern simulation of continuous and categorical variables: FILTERSIM, Computers and Geosciences 34(12): 1863-1876.

Xu C, Dowd P, Mardia K and Fowell R (2006) A connectivity index for discrete fracture networks, Mathematical Geology 38(5): 611-634.

Xu W, Tran T, Srivastava R and Journel A (1992) Integrating seismic data in reservoir modeling: the collocated co-kriging alternative, SPE Annual Technical Conference and Exhibition, Society of Petroleum Engineers.

Yang Y and Apling AC (2010) A permeability–porosity relationship for mudstones, Marine and Petroleum Geology 27: 1692–1697.

Yeh GT and Tripathi VS (1991) A model for simulating transport of reactive multispecies components: Model development and demonstration, Water Resources Research 27(12): 3075-3094.

Yielding G, Freeman B and Needham D (1997) Quantitative fault seal prediction, AAPG Bulletin 81(6): 897-917, American Association of Petroleum Geologists.

Yu L, Rogiers B, Gedeon M, Marivoet J, De Craen M and Mallants D (2013) A critical review of laboratory and in-situ hydraulic conductivity measurements for the Boom clay in Belgium, Applied Clay Science 75: 1-12.

Zarrouk SJ, Moore TA (2009) Preliminary reservoir model of enhanced coalbed methane (ECBM) in a subbituminous coal seam, Huntly Coalfield, New Zealand, International Journal of Coal Geology 77(1): 153-161.

Zhang F, Yeh GT, Parker JC and Shi X (2012) Groundwater Reactive Transport Models, Bentham Science Publishers, Dubai, United Arab Emirates.

Zhang L, Soong Y, Dilmore R and Lopano C (2015) Numerical simulation of porosity and permeability evolution of Mount Simon sandstone under geological carbon sequestration conditions, Chemical Geology 403: 1-12.

Zhang Y, Gartrell A, Underschultz J and Dewhurst D (2009) Numerical modelling of strain localisation and fluid flow during extensional fault reactivation: Implications for hydrocarbon preservation, Journal of Structural Geology 31(3): 315-327.

Zhang Y, Underschultz J, Gartrell A, Dewhurst D and Langhi L (2011) Effects of regional fluid pressure gradients on strain localisation and fluid flow during extensional fault reactivation, Marine and Petroleum Geology 28(9): 1703-1713.

Zhou H, Li L and Gomez-Hernandez J (2010) Three-dimensional hydraulic conductivity upscaling in groundwater modeling, Computers and Geosciences 36(10): 1224-1235.

Zhu H and Journel AG (1993) Formatting and integrating soft data: Stochastic imaging via the Markov-Bayes algorithm, Geostatistics Tróia 92, Springer, pp. 1-12.

Zhu WC, Liu J, Sheng JC and Elsworth D (2007) Analysis of coupled gas flow and deformation process with desorption and Klinkenberg effects in coal seams, International Journal of Rock Mechanics and Mining Sciences, 44(7): 971-980.

Zinn B and Harvey CF (2003) When good statistical models of aquifer heterogeneity go bad: A comparison of flow, dispersion, and mass transfer in connected and multivariate Gaussian hydraulic conductivity fields, Water Resources Research 39(3).

Zyvoloski G, Dash Z and Kelkar S (1997) FEHM 1.0: Finite element heat and mass transfer code, report no. LA-12062, Los Alamos National Laboratory, Los Alamos, NM, USA, 59p.

7. Appendix 1

7.1. Multiphase flow models

Multiphase flow models capable of simulating the flow of water and gas resulting from CSG extraction are summarised in Table 20. To varying extents, these models are capable of representing local scale flow processes such as gas sorption and relative rock permeability; and fracture–matrix flow using dual domain and/or discrete fracture network approaches. Also indicated is the suitability of models to simulate the swelling or shrinkage of coal seams due to geomechanical stresses. An additional consideration is the ability of models to simulate reactive solute transport; i.e., of solutes used in CSG extraction. These models are suitable for the simulation of compounds used in CSG production, such as proppants and chemicals used in hydraulic fracturing processes. Notable published comparisons of models (tabulated here or otherwise) include:

- Law et al. (2002): GEM, ECLIPSE, COMET, SIMED II, GCOMP
- Law et al. (2003, 2004): GEM, ECLIPSE, COMET, SIMED II, GCOMP, METSIM
- Law et al. (2005): GEM, COMET, SIMED II, METSIM, PSU-COALCOMP
- Pruess et al. (2004): TOUGH2, MUFTE, SIMED, SIMSCOPP, GPRS, GEM, FLOTRAN, ECLIPSE, NUFT, STOMP
- MacQuarrie et al. (2005): ARASE, CORE2D, CRUNCH, DART, FLOTRAN, FRAC3DVS, HYTEC, HYDROGEOCHEM, MIN3P, NUFT, PHAST, PHT3D, RETRASO, TOUGH–REACT, TOUGH2–CHEM
- Class et al. (2009): COORES, DUMUX, ECLIPSE, FEHM, GEM, GPRS, IPARS, MORES, MUFTE, ROCKFLOW, RTAFF2, ELSA, TOUGH2, VESA
- Jiang (2011): CODE_BRIGHT, COORES, DUMUX, ECLIPSE, ELSA, FEHM, GEM, IPARS, MIN3P, MUFTE, PFLOTRAN, ROCKFLOW, RTAFF2
- Mukhopadhyay et al. (2012): GEM, TOUGH2, ECLIPSE, CCS_MULTIF, STOMP, VESA, DUMUX
- Thararoop et al. (2012): GEM, ECLIPSE, COMET, SIMED II, GCOMP, PSU-COALCOMP
- Kempka et al. (2013): ECLIPSE, TOUGH2, DUMUX, OPENGEOSYS
- Steefel et al. (2014): PHREEQC, HPX, PHT3D, OPENGEOSYS, HYTEC, ORCHESTRA, TOUGHREACT, STOMP, HYDROGEOCHEM, CRUNCHFLOW, MIN3P, PFLOTRAN
- Li and Fang (2014): GEM, ECLIPSE, COMET, SIMED II, GCOMP
- Jansen et al. (2014): MORES, ECLIPSE, GPRS, MATLAB Reservoir Simulation toolbox
- Mayer et al. (2015): CRUNCHFLOW, FLOWTRAN, HP1, MIN3P

In addition to numerical approaches, simplified solutions may also be used where appropriate. These include semi-analytical models such as ELSA (Nordbotten et al., 2009) and VESA (Gasada et al., 2009) as well as closed form analytical solutions. The applicability of simplified approaches in the context of carbon sequestration was discussed by Court et al. (2012) and Bandilla et al. (2015). Huang et al. (2014) compared ELSA and VESA models to single phase analytical solutions including the Theis (1935) solution.

Table 20. Comparison of multi-phase flow modelling codes

Model *	Source	Example	Availability	Dual domain flow	Gas desorption	Geomechanical effects	Discrete fracture networks	Reactive solute transport
CODE_BRIGHT	Olivella et al. (1996)	Vilarrasa et al. (2012)	Academic		✓	✓		
COMET [b]	ARI (2015)	Sawyer et al. (1990)	Commercial	✓	✓	✓		
COMSOL	COMSOL Inc. (2015)	Zhu et al. (2007)	Commercial	✓	✓	✓	✓	✓
COORES	CGS Europe (2015)	Teles et al. (2014)	Commercial		✓			✓
CORE2D	Zhang et al. (2012)	Samper et al. (2008)	Academic		✓			✓
COSFLOW [b]	Adhikary and Guo (2005)	Guo et al. (2009)	Academic	✓	✓	✓		
CRUNCHFLOW	Steefel (2009)	Zhang et al. (2015)	Academic					✓
D3F	Schneider et al. (2012)	Kroehn (2012)	Academic		✓		✓	R3T
DUMUX	Flemisch et al., (2007)	Stadler et al. (2012)	Academic	✓	✓			
DYNAFLOW	Prevost (2010)	Preisig and Prevost (2011)	Academic		✓	✓		
ECLIPSE [a]	Pettersen (2006)	Moore et al. (2014a)	Commercial	✓	✓			
FAST CBM	IHS (2015)	Karacan and Olea (2015)	Commercial		✓			
FEHM	Zyvoloski et al. (1991)	Middleton et al. (2012)	Public domain	✓	✓			
FRACMAN	Golder Associates (2015)	Kim and Deo (2000)	Commercial	✓	✓		✓	
GCOMP	PHH (2014)	Hird and Dubrule (1998)	Commercial	✓	✓			
GEM	CMG (2014)	Aminian et al. (2004)	Commercial	✓	✓		✓	
GPRS	Cao (2008)	Sarma et al. (2005)	Academic	✓	✓			
HYDROGEOCHEM	Yeh and Tripathi (1991)	Kim et al. (2015)	Academic					✓
IPARS	CSM (2015)	Delshad et al. (2013)	Public domain	✓	✓			
MIN3P	UBC (2015)	Salmon et al. (2014)	Academic	✓	✓			✓
MUFTE	IHE (2015)	Bastian et al. (2000)	Academic		✓		✓	
NUFT	Hao et al. (2012)	Morris et al. (2011)	Academic		✓			✓
OPENGEOSYS	Kolditz et al. (2012)	Watanabe and Kolditz (2015)	Public domain		✓	✓		OGS–CHEMAPP
PFLOTRAN	Lichtner et al. (2015)	Middleton et al. (2015)	Public domain	✓	✓	✓		✓
PSU-COALCOMP	Manik et al. (2000)	Bromhal et al. (2005)	Academic	✓	✓	✓		
ROCKFLOW	Kolditz (1995)	Class et al. (2009)	Academic				✓	
RTAFF2	Sbai (2007) in Class et al. (2009)	Class et al. (2009)	Academic			✓		✓
SIMED II [b]	Spencer et al. (1987)	Connell and Detournay (2009)	Academic	✓	✓	SIMED–FLAC3D		
SIMUSCOPP	BURGEAP (2015)	Pruess et al. (2004)	Academic		✓			✓
STOMP	White and Oostrom (2006)	Pruess et al. (2004)	Academic	✓	✓			STOMP–ECKECHEM
TEMPEST MORE [b]	Emerson Electric Co. (2015)	Hussen et al. (2012)	Commercial	✓	✓			
TOUGH2	Pruess et al. (1999)	Zarrouk and Moore (2009)	Academic	✓	✓	TOUGH–FLAC3D		TOUGH–REACT

* Superscript symbols indicate models that have been applied to the Australian context in published studies of (a) coal seam gas development or (b) other activities.

CONTACT US

t 1300 363 400
+61 3 9545 2176
e enquiries@csiro.au
w www.csiro.au

AT CSIRO WE SHAPE THE FUTURE

We do this by using science to solve real issues. Our research makes a difference to industry, people and the planet.

As Australia's national science agency we've been pushing the edge of what's possible for over 85 years. Today we have more than 5,000 talented people working out of 50-plus centres in Australia and internationally. Our people work closely with industry and communities to leave a lasting legacy. Collectively, our innovation and excellence places us in the top ten applied research agencies in the world.

WE ASK, WE SEEK AND WE SOLVE

FOR FURTHER INFORMATION

Land & Water
Chris Turnadge
t +61 08 303 8712
e Chris.Turnadge@csiro.au
w www.csiro.au/en/Research/LWF

Land & Water
Dirk Mallants
t +61 8 8303 8595
e Dirk.Mallants@csiro.au
w www.csiro.au/en/Research/LWF

Land & Water
Luk Peeters
t +61 8 8303 8405
e Luk.Peters@csiro.au
w www.csiro.au/en/Research/LWF